OCS Study
BOEM 2019-018

Determining Habitat Use by Marine Mammals and Ambient Noise Levels Using Passive Acoustic Monitoring Offshore of Maryland

US Department of the Interior
Bureau of Ocean Energy Management
Office of Renewable Energy Programs

BOEM
Bureau of Ocean Energy Management

OCS Study
BOEM 2019-018

Determining Habitat Use by Marine Mammals and Ambient Noise Levels Using Passive Acoustic Monitoring Offshore of Maryland

November 2018

Authors:
Helen Bailey, Aaron Rice, Jessica E. Wingfield, Kristin B. Hodge, Bobbi J. Estabrook, Dean Hawthorne, Aran Garrod, Amber D. Fandel, Leila Fouda, Elizabeth McDonald, Elizabeth Grzyb, William Fletcher, and Aimee L. Hoover

Prepared under BOEM Award M14AC00018 with the Maryland Department of Natural Resources (MDNR) and with the assistance of the Maryland Offshore Wind Development Fund via the Maryland Energy Administration
Through Cooperative Agreements with MDNR, numbers 14-14-1916 and 14-17-2241
By
University of Maryland Center for Environmental Science
Office of Research Administration and Advancement
P.O. Box 775
2020 Horns Point Road
Cambridge, MD 21613-0775

US Department of the Interior
Bureau of Ocean Energy Management
Office of Renewable Energy Programs

BOEM
Bureau of Ocean Energy Management

DISCLAIMER

Study collaboration and funding were provided by the US Department of the Interior, Bureau of Ocean Energy Management (BOEM), Environmental Studies Program, Washington, DC, under Agreement Numbers 14-14-1916 and 14-17-2241. This report has been technically reviewed by BOEM, and it has been approved for publication. The views and conclusions contained in this document are those of the authors and should not be interpreted as representing the opinions or policies of the US Government, nor does mention of trade names or commercial products constitute endorsement or recommendation for use.

REPORT AVAILABILITY

To download a PDF file of this report, go to the US Department of the Interior, Bureau of Ocean Energy Management Data and Information Systems webpage (http://www.boem.gov/Environmental-Studies-EnvData/), click on the link for the Environmental Studies Program Information System (ESPIS), and search on 2019-018. The report is also available at the National Technical Reports Library at https://ntrl.ntis.gov/NTRL/.

CITATION

Bailey H, Rice A, Wingfield JE, Hodge KB, Estabrook BJ, Hawthorne D, Garrod A, Fandel AD, Fouda L, McDonald E, Grzyb E, Fletcher W, Hoover AL. 2018. Determining habitat use by marine mammals and ambient noise levels using passive acoustic monitoring offshore of Maryland. Sterling (VA): US Department of the Interior, Bureau of Ocean Energy Management. OCS Study BOEM 2019-018. 232 p.

ABOUT THE COVER

Cover photos taken by Kristin Hodge, Sarah Brzezinski, and Helen Bailey.

ACKNOWLEDGMENTS

The following BOEM offices or programs contributed to this document: Office of Renewable Energy Programs.

Chesapeake Biological Laboratory, University of Maryland Center for Environmental Science

PI: Helen Bailey, Ph.D.

Data Collection, Analysis, and Report Authors: Helen Bailey, Amber Fandel, William Fletcher, Leila Fouda, Aran Garrod, Elizabeth Grzyb, Aimee Hoover, Elizabeth McDonald, and Jessica Wingfield.

Bioacoustics Research Program, Cornell Laboratory of Ornithology

Director: Holger Klinck, Ph.D.

Program Manager: Deborah Cipolla-Dennis

Science Director: Aaron N. Rice, Ph.D.

Senior Scientist: Christopher W. Clark, Ph.D.

Administration: Tish Klein, Linda Harris

Report Authors: Kristin B. Hodge, Bobbi J. Estabrook, Dean Hawthorne, Aaron N. Rice.

Data Analysis: Russ Charif, Bobbi Estabrook, Kristin B. Hodge, Ashakur Rahaman, Daniel Salisbury, Jamey Tielens

Deployment and Fabrication: Captain Fred Channell, David Doxey, Kristin B. Hodge, Derek Jaskula, Edward Moore, Christopher Tessaglia-Hymes

Hardware Engineering: Rob Koch, Raymond Mack, Jim Lowe

Software Engineering: Peter Dugan, Ph.D., Dean Hawthorne, Ph.D., Michael Pitzrick, Dimitri Ponirakis, Yu Shiu, Ph.D., John Zollweg, Ph.D.

Additional funding and staff support for various project components came from the Maryland Department of Natural Resources and the Maryland Energy Administration's Offshore Wind Development Fund. The statements, findings, conclusions, and recommendations expressed in this report are those of the author(s) and do not necessarily reflect the view of the Maryland Department of Natural Resources or the Maryland Energy Administration. Mention of trade names or commercial products does not constitute their endorsement by the State.

EXECUTIVE SUMMARY

As the focus of renewable energy in the United States turns to offshore wind facility development, there is an increasing need for an understanding of potential noise impacts from this development on marine mammals. Pile-driving of offshore wind turbines produces loud, low frequency sound that can travel great distances and could potentially harm or disturb marine mammals. As a result, a critical first step is to understand the current baseline ambient noise levels and the spatiotemporal distribution of marine species that could potentially be impacted. In this study, the project partners conducted passive acoustic monitoring for three years to characterize underwater ambient noise levels and identify vocalizing marine mammal species within and around the Maryland Wind Energy Area (WEA).

The project partners collected three years of baseline data 12 – 60 km offshore of Maryland prior to construction and operation of an offshore wind energy facility. Two main types of sound recording devices that encompassed a range of frequencies were used to detect vocalizations from baleen whales (low frequencies) and odontocetes (high frequencies): the Marine Autonomous Recording Unit (MARU, or pop-up) sampling at 2 kHz and the C-POD (cetacean click detector), which monitors the 20 – 160 kHz frequency range. These were supplemented by additional acoustic recorders during select periods of the study at five sites to provide further information on mid-frequency sounds, such as dolphin whistling behavior. The use of a grid array design for the acoustic detection devices within the Maryland WEA facilitated localization of vocalizing whales to further understand spatial patterns of habitat usage.

Key findings of this study were:

- Baleen whales (North Atlantic right whale, fin, humpback and minke whale) were mainly detected during the November to May timeframe.
- Fin whales were the most frequently detected baleen whale species, but detections were most common offshore of the WEA.
- Humpback whales mainly occurred within and offshore of the WEA. Minke whales were only occasionally detected within our passive acoustic array.
- North Atlantic right whales were detected during every month of the year, but were most common during the November to April timeframe.
- Localized North Atlantic right whale calls indicated they migrated through and offshore of the Maryland WEA.
- Bottlenose dolphins were frequently detected year-round within and inshore of the WEA, except in February, whereas offshore sightings were limited to summer and fall. Common dolphins were detected offshore of the WEA from December to May. Within the Maryland WEA, a minimum of 700 individual bottlenose dolphins occurred within the detection range of our acoustic recorders during Summer 2016 to Summer 2017 based on analysis of their signature whistle calls.
- Harbor porpoises were detected from November to June with the peak between January and May. During the first year of the study harbor porpoises were most common within and offshore of the WEA, whereas in the second and third years they were detected more commonly within and inshore of the WEA.
- Sites along the eastern edge and offshore of the WEA had the loudest ambient noise levels, particularly within low frequency bands, suggesting shipping noise is a major contributor to the noise environment.
- Elevated ambient noise levels were associated with higher dolphin whistle frequencies and a less complex whistle contour.

There is substantial overlap between marine mammals and the Maryland WEA, but this varies seasonally. While the risk to endangered whales is lowest during the summer, the risk to bottlenose dolphins may be highest at this time, as they are most abundant in the summer time. The year-round occurrence of marine mammals offshore of Maryland will require decision-makers to consider the trade-off of the potential impacts to different species and assess approaches that will minimize population-level impacts to marine mammals of offshore wind development and other activities. Mitigation measures that focus on real-time monitoring for whales and minimizing harm and disturbance to bottlenose dolphins would help to reduce any potential negative effects of offshore wind farm construction and operation activities. The results of this study will help to inform regulators and resource managers so that appropriate protection and mitigation measures can be developed for future anthropogenic activities. Our baseline data can also be compared with continued passive acoustic monitoring during construction and operation of an offshore wind facility to determine marine mammal responses.

Contents

List of Figures

List of Tables

List of Abbreviations and Acronyms

AIC	Akaike Information Criterion
AMAR	Autonomous Multichannel Acoustic Recorder
ANOVA	Analysis of Variance
ARS	Area-Restricted Search
BOEM	Bureau of Ocean Energy Management
BRP	Bioacoustics Research Program
COP	Construction and Operating Plan
C-POD	Cetacean click detector
Chl-a	Chlorophyll-a
CSE	Correlation Sum Estimator
DPH	Detection Positive Hour
DPM	Detection Positive Minute
DOI	US Department of the Interior
ERDDAP	Environmental Research Division Data Access Program
ESPIS	Environmental Studies Program Information System
dB	Decibel (referenced to 1 µPa in underwater acoustics)
FFT	Fast Fourier Transform
FN	False Negative
GAM	Generalized Additive Model
GARMA	Generalized Auto-regressive Moving Average
GEE	Generalized Estimating Equation
ICI	Inter-click Interval
IIR	Infinite Impulse Response
L_{eq}	Equivalent Continuous Sound Level
MANOVA	Multivariate Analysis of Variance
MARU	Marine Autonomous Recording Unit
MD	Maryland
MD	Missed Detections
NMFS	US National Marine Fisheries Service
NOAA	US National Oceanic and Atmospheric Administration
NPV	Negative Predictor Value
OCS	Outer Continental Shelf
P2P	Peak-Peak
PAM	Passive Acoustic Monitoring
PBR	Potential Biological Removal
PPV	Positive Predictor Value
P_{ref}	Reference Pressure of 1 µPa
PSD	Power Spectral Density
RL	Received Level
RMS	Root Mean Square
ROC	Receiver Operating Characteristic
SL	Source Level
SNR	Signal to Noise Ratio
SPL	Sound Pressure Level
SST	Sea Surface Temperature
SSTa	Sea Surface Temperature anomaly
TD	True Detections
TDOA	Time Difference of Arrival
TOL	Third Octave Level
TP	True Positive
T-POD	Timing Porpoise Detector
UMCES	University of Maryland Center for Environmental Science

VIF	Variance Inflation Factor
WEA	Wind Energy Area

1 Introduction

1.1 Statement of Purpose

Offshore wind farms provide a renewable energy source, but minimizing potential impacts on marine species, particularly protected species, requires evaluating species presence and distribution. The purpose of this report is to document the results of a 3-year passive acoustic monitoring study conducted in and around the Maryland Wind Energy Area (WEA). The two main objectives of this research were to determine the occurrence of marine mammals and to characterize the ambient noise levels. All marine mammals are protected under the Marine Mammal Protection Act and those that are known to occur in this region include large whale species listed as Endangered under the Endangered Species Act, such as the North Atlantic right whale and fin whale. There are also humpback and minke whales, and small cetacean species frequently present, such as bottlenose dolphins, short-beaked common dolphins, and harbor porpoises. The three years of passive acoustic monitoring allowed the study partners to determine seasonal and inter-annual variation in marine mammal occurrence and spatial patterns of habitat use by North Atlantic right whales. Spatial and temporal variations in ambient noise levels were also characterized. These data serve as a baseline that resource managers and regulators can use to inform mitigation measures and assess environmental responses and impacts of future activities, such as offshore wind energy developments.

2 Backgrounds

2.1 Maryland Wind Energy Area

Wind Energy Areas on the Atlantic Outer Continental Shelf (OCS) were identified by the Bureau of Ocean Energy Management (BOEM) in consultation with other agencies and state and local representatives. The WEA offshore of Maryland includes 9 whole OCS blocks and 11 partial blocks with an area of about 323 km^2. The edges of the Maryland WEA are approximately 20 – 50 km from Ocean City, Maryland (BOEM Office of Renewable Energy Programs 2012). The Maryland WEA was auctioned by BOEM as two leases, the North Lease Area (133 km^2) and the South Lease Area (190 km^2), in August 2014, and both leases were awarded to U.S. Wind Inc. for a total bid of $8,701,098 (details at https://www.boem.gov/state-activities-maryland). BOEM later consolidated the two separate leases into a single lease in 2018.

To facilitate offshore wind development, the Maryland Offshore Wind Energy Act of 2013 provided a mechanism of financial support through the Offshore Wind Renewable Energy Credit (OREC) program. Two projects applied for ORECs and both were awarded by the Maryland Public Service Commission in May 2017. One project proposed by U.S. Wind, Inc., was for a 248 MW wind facility in the Maryland WEA to be completed in 2020 and the second project was by Skipjack Offshore Energy, LLC for a 120 MW wind facility in the neighboring southern portion of the Delaware WEA to be completed in 2022.

Following lease issuance, site surveying to collect information on the wind and ocean conditions allow the feasibility and efficient design of a wind facility to be determined. U.S. Wind, Inc. submitted a Site Assessment Plan for the Maryland WEA to BOEM, which was approved in March 2018. U.S. Wind, Inc. proposed collection of meteorological and oceanographic data from a meteorological tower, which

will be installed near the center of the Maryland WEA. A detailed construction and operation plan (COP) will be required to be submitted by the developer and approved by BOEM prior to the construction of an offshore wind facility on the OCS.

2.2 Potential Impacts of Offshore Wind Energy on Marine Mammals

Offshore wind energy development allows the production of clean, homegrown renewable energy and has little risk of a catastrophic environmental impact as compared to conventional forms of energy extraction and production. However, there is still the potential to negatively impact marine species through habitat loss, collision or entanglement risk, and harmful effects from increased noise and electromagnetic fields (Wahlberg and Westerberg 2005; Madsen et al. 2006; Inger et al. 2009; Boehlert and Gill 2010). The process of pile-driving offshore wind turbines to secure the foundation to the seabed is of particular concern for marine species as it produces loud, low frequency sound that can travel great distances. The source level of this sound has been estimated to be 226 – 257 dB re 1 µPa at 1m (peak-to-peak) depending on the diameter of the pile and the method used to pile-drive with the peak energy below 1 kHz (OSPAR Commission 2009; Bailey et al. 2010). Marine mammals use sound to hunt, navigate and communicate and these loud sounds could potentially cause harm or disturbance. Ambient noise is the background noise in the environment (Hildebrand 2009) and marine mammals have evolved with ambient noise in their underwater environment (Clark et al. 2009), but it is unclear how additional noise from construction and operation of an offshore wind energy facility may affect marine mammals in U.S. waters (Bailey et al. 2014).

There is currently only one offshore wind facility in U.S. waters, the Block Island wind farm consisting of five 6MW turbines three miles off Block Island, RI, which became operational in December 2016. The majority of studies on the effects of offshore wind farms on marine species have occurred in Europe where offshore wind energy has been growing rapidly (Bailey et al. 2014). These studies have mainly focused on the most common cetacean species, the harbor porpoise (*Phocoena phocoena*). Harbor porpoises are considered to be more sensitive to high frequency sounds (Southall et al. 2007). However, avoidance responses of harbor porpoises to pile-driving have been reported up to 20 km or more and for a duration of up to three days (Tougaard, Carstensen, et al. 2009; Thompson et al. 2010; Brandt et al. 2011). There is a lack of information on the response of other cetacean species, including large whales that are considered more sensitive to low frequency sounds, because they occur less frequently in waters where offshore wind farms have currently been developed. Based on recorded sound levels, pile-driving may cause behavioral disturbance to large whales up to 40 km away and to bottlenose dolphins up to 50 km away (Bailey et al. 2010). Little is known about the cumulative effects of stressors, such as the construction of multiple wind farms within an animal's home range (National Academies of Sciences, Engineering, and Medicine 2017).

Responses of harbor porpoises and harbor seals (*Phoca vitulina*) to offshore wind farm construction have generally been short-term with animals returning to the area once pile-driving is completed and during operation (Scheidat et al. 2011; Russell et al. 2016).There has been one case of a slower recovery by harbor porpoises at the Nysted Offshore Wind Farm in the Baltic Sea where a vibrator was used in addition to a pile driver during construction, although echolocation activity by porpoises has since been increasing (Carstensen et al. 2006; Teilmann and Carstensen 2012). This indicates there may also be positive benefits with harbor porpoises increasing their occurrence and seals having been tracked concentrating their foraging near wind turbines, both of which may be a result of wind structures acting as artificial reefs and aggregating prey (Scheidat et al. 2011; Russell et al. 2014). Wind turbine noise during operation is mainly low frequency (< 500 kHz) with audibility to harbor porpoises and harbor seals expected to be within 70 m and a few kilometers, respectively, and a behavioral reaction only likely in the

immediate vicinity (Tougaard, Henriksen, et al. 2009). It is uncertain, however, how large whales sensitive to these low frequencies may respond to the operation of an offshore wind turbine.

2.3 Introduction to Marine Mammals of the Mid-Atlantic

Marine mammals that are known to occur in the Mid-Atlantic Bight region include large whale species that are listed as Endangered under the Endangered Species Act, such as the North Atlantic right whale (*Eubalaena glacialis*) and fin whale (*Balaenoptera physalus*). There are also humpback whale (*Megaptera novaeangliae*) and minke whale (*Balaenoptera acutorostrata*), as well as small cetacean species frequently present, such as bottlenose dolphins (*Tursiops truncatus*), short-beaked common dolphins (*Delphinus delphis*), and harbor porpoises, that are protected under the Marine Mammal Protection Act.

Despite their listing as endangered at both the State of Maryland and Federal levels, relatively little is known about the ecology of North Atlantic right whales and fin whales in the Maryland coastal waters. Little is also known about humpback whales and minke whales off the coast of Maryland. The waters offshore of Maryland are considered to be within the distribution area of all four baleen whale species, yet the seasonal residency and habitat use of baleen whales in this region remains unclear.

North Atlantic right whales are distributed along the eastern United States, and according to the generally accepted migratory paradigm, travel through the mid-Atlantic migratory corridor during the winter and spring to reach southern winter calving grounds (Florida, Georgia) and northern summer feeding grounds (Great South Channel, Cape Cod Bay, Gulf of Maine, Bay of Fundy) (Kraus et al. 1986; Winn et al. 1986; Kenney et al. 2001). However, since 2010, recent studies have elucidated a shift in North Atlantic right whale seasonal occurrence, with an increased presence in regions along the North Atlantic right whale migratory route including the mid-Atlantic migratory corridor (e.g. Morano, Rice, et al. 2012; Mussoline et al. 2012; Whitt et al. 2013; Hodge et al. 2015; Salisbury et al. 2016). There has also been a decrease in North Atlantic right whale distribution in northern aggregation sites, including the Bay of Fundy and the Gulf of Maine (Davis et al. 2017). Although it is unclear the cause of the change in distribution, it underlines the importance of continued investigation into the seasonal occurrence and distribution of North Atlantic right whales.

Fin whales in the North Atlantic are broadly distributed along the eastern United States, with a majority of aerial sightings, shipboard survey sightings, and acoustic survey detections occurring from Cape Hatteras northward to Nova Scotia and the southeastern coast of Newfoundland (Nieukirk et al. 2004; Edwards et al. 2015; Roberts et al. 2016; Hayes et al. 2017). Fin whales are one of the most common baleen whale species observed within this geographic range (Hain et al. 1992; Edwards et al. 2015; Hayes et al. 2017), and have also been acoustically detected in both coastal areas and offshore regions off the continental shelf (e.g. Clark 1995; Clark and Gagnon 2002; Nieukirk et al. 2004; Morano, Salisbury, et al. 2012; Muirhead et al. 2018). While it has been suggested the mid-Atlantic may be a calving area for fin whales (Hain et al. 1992), little is known about fin whale seasonal distribution, habitat use, and migratory movements in this region, particularly off the coast of Maryland, USA.

Humpback whales have a seasonal distribution in the western North Atlantic, aggregating in the calving and mating grounds in the West Indies during the winter, and migrating to northern feeding grounds during the spring, summer, and fall (Hayes et al. 2017). However, visual sightings and acoustic surveys have found the presence of humpback whales along the mid-Atlantic and northern latitudes during the winter and spring, suggesting not every individual whale follows the established migratory paradigm (Clapham et al. 1993; Swingle et al. 1993; Clark and Clapham 2004; Murray et al. 2014). Humpback whale song has also been acoustically detected in offshore regions (Clark and Gagnon 2002),

suggesting males are seasonally distributed in both coastal and deep-water habitats. Sightings and stranding data suggest the mid-Atlantic U.S. is occupied by humpback whales from multiple populations (although predominantly the Gulf of Maine Stock) and likely an important habitat for juvenile humpback whales (Swingle et al. 1993; Wiley et al. 1995; Barco et al. 2002).

Minke whales are widely distributed in the North Atlantic; recent acoustic surveys suggest minke whales undergo a seasonal migration between northern summer feeding grounds and low latitude wintering grounds (Risch et al. 2013; Risch et al. 2014; Hayes et al. 2017). Acoustic data also suggest minke whales occupy both coastal and deeper waters (Clark and Gagnon 2002; Risch et al. 2013; Risch et al. 2014). According to Risch (2014), minke whales likely migrate in a circuitous path, distributed further offshore during their southbound migration in autumn, and distributed near the shelf break during their northbound migration in the spring. While minke whale occurrence has been described in regions along their migratory route (Risch et al. 2013; Risch et al. 2014), little is understood about minke whale seasonal occurrence in the mid-Atlantic region, including off the coast of Maryland, USA.

The small cetaceans, dolphins and porpoises, produce high-frequency echolocation clicks to navigate and hunt. Dolphins also produce a variety of other sounds for communication. There are three stocks of dolphin likely to occur within our study area based on NOAA's Marine Mammal Stock Assessment Reports (Hayes et al. 2018). The two bottlenose dolphin stocks are the Western North Atlantic Northern Coastal Migratory Stock and the Western North Atlantic Offshore Stock. The coastal stocks are typically limited to waters less than 25 m deep (Kenney 1990). The Western North Atlantic Northern Coastal Migratory Stock consists of approximately 6,639 individuals and seasonally migrates northward during the summer and returns south in the winter (Hayes et al. 2018). The stock ranges from North Carolina to New Jersey in the summer and off central North Carolina in the winter. The stock is considered depleted and the potential biological removal (PBR) is 48 (Hayes et al. 2018). The Western North Atlantic Offshore Stock of bottlenose dolphins consists of 77,532 individuals and ranges from Georges Bank to the Florida Keys (Hayes et al. 2017). Very little is known about their seasonal movements. The status of this stock is unknown and the PBR is 561. They generally occur in water depths of greater than 40 m, typically concentrating along the shelf break (Kenney 1990). This overlaps with the distribution of common dolphins. The Western North Atlantic Stock of short-beaked common dolphins includes approximately 70,184 individuals and is mainly distributed from Cape Hatteras to Georges Bank from mid-January through May (Selzer and Payne 1988). In mid-summer to autumn they move north to Georges Bank, the Gulf of Maine, and the Scotian Shelf.

Harbor porpoises in the Western North Atlantic (Gulf of Maine/Bay of Fundy Stock) number approximately 79,883 individuals and mainly occur over the continental shelf. They seasonally migrate, although a temporally coordinated migration or specific migratory route has not been found (Hayes et al. 2018). They generally inhabit the Gulf of Maine to the southern Bay of Fundy from July through September, off New Jersey and Maine in the fall (October to December), between North Carolina and New Jersey in the winter (January to March), and move northwards back to between New Jersey and Maine in the spring (April to June). There have been very few reported sightings of harbor porpoises off Maryland although this region is within their range.

2.4 Rationale for Baseline Acoustic Monitoring Study

As a result of potential impacts from offshore wind energy construction and operation, particularly those from loud sound production, it is important to understand the baseline ambient noise levels and the spatiotemporal distribution of marine mammal species that could be affected. As marine mammals, particularly cetaceans (whales, dolphins and porpoises), produce identifiable vocalizations, passive acoustic monitoring (PAM) provides a non-invasive method for studying the occurrence of

marine mammals for long periods, including at all times of day and night and during adverse weather conditions. The deployment of multiple acoustic monitoring devices allows patterns of species occurrence to be tracked in space and time, and the ambient noises to which they are currently being exposed. These ambient noises will consist of a variety of natural (e.g. waves and rain) and anthropogenic sources (e.g. shipping traffic). This helps to inform how noise from other activities, such as offshore wind energy construction, may elevate noise levels and consequently how this could affect marine mammals.

2.5 Study Objectives and Hypotheses

In this study we collected passive acoustic data to characterize patterns of temporal and spatial occurrence of vocalizing marine mammal species, and characterize the existing ambient noise environment in and around the Maryland WEA. This information provides baseline information that can be used to assess potential influences of anthropogenic noises produced by the construction and operation of future offshore wind energy development. These data will also be shared with the National Oceanic and Atmospheric Administration's (NOAA's) Northeast Fisheries Science Center (NEFSC) Passive Acoustic Group to support broader scale studies of whale habitat use and migration along the Atlantic Coast.

The specific objectives of this project were within and around the Maryland WEA to:

1) Determine the temporal occurrence and spatial distributions of vocalizing marine mammals (including North Atlantic right whales, fin whales, humpback whales, minke whales, dolphins, and porpoises) identified using a combination of automated call detection software and expert human validation.
2) Estimate specific spatial locations and movements of North Atlantic right whales using an acoustic localization array.
3) Assess ambient sound levels and how these vary spatially and temporally.

3 Design and Methods

3.1 PAM Devices and Deployment Locations in the Maryland WEA

The PAM device array was designed as a hybrid to both, a) characterize seasonal occurrence of marine mammals across the shelf with a transect line of stations extending approximately 15 to 60 km offshore in an East-West direction, and b) estimate locations of calling whales in the Maryland WEA with a grid array that had overlapping detections ranges to allow call localization. The array was also designed to encompass the area of potential effect for offshore wind development plus an additional 10% of this total area according to BOEM's guidelines regarding information on marine mammals for renewable energy development on the Atlantic Outer Continental Shelf (version July 1, 2013). The sound produced during pile-driving could cause behavioral disturbance up to 40 km away for large whales (Bailey et al. 2010). We therefore defined the area of potential effect as up to 40 km from the boundaries of the proposed Maryland WEA and deployed devices within this area. We used multiple types of PAM devices to record continuously for up to 5 months at a time to encompass the broad range of frequencies over which different species of marine mammals vocalize. The two main devices were the Marine Autonomous Recording Unit (MARU, or pop-up) designed by Cornell University and the C-POD (cetacean click detector) by Chelonia Limited. This was supplemented by an Autonomous Multichannel Acoustic Recorder (AMAR), SM3M acoustic recorders by Wildlife Acoustics, and SoundTrap by Ocean Instruments NZ.

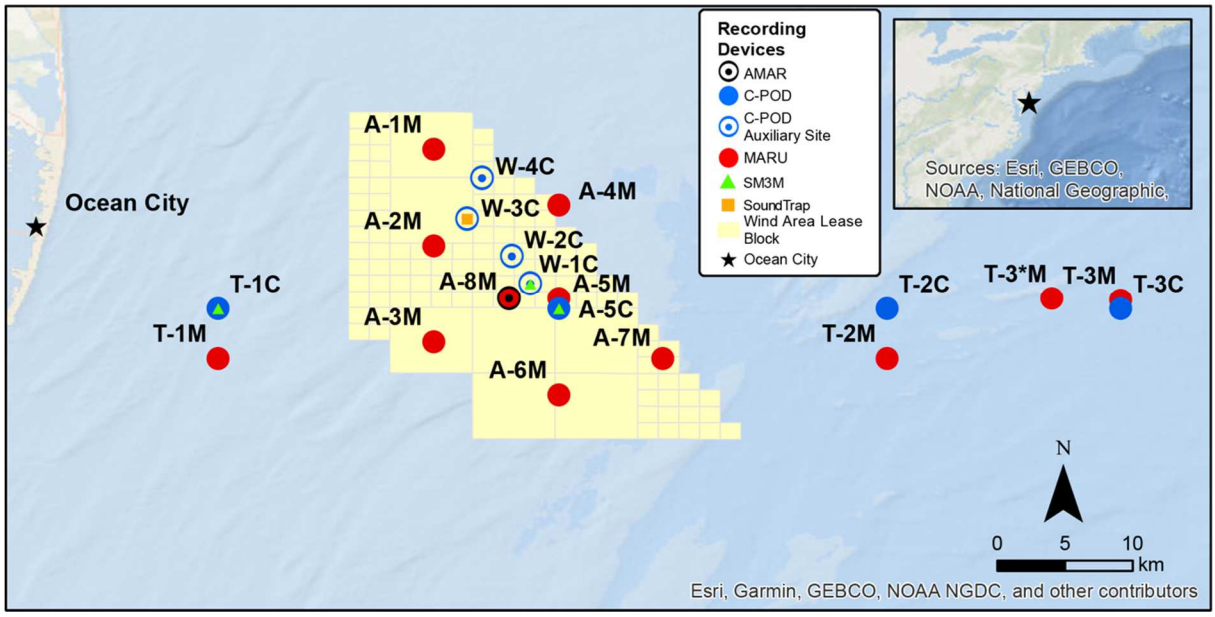

Figure 3.1a. Map of recording devices
All recording device deployment locations within and surrounding the Maryland WEA.

3.1.1 PAM Device Detection Attributes

Acoustic data were collected using Marine Autonomous Recording Units (MARUs; Calupca et al. 2000). A MARU is an archival digital audio recording system contained in a positively buoyant 0.4 m glass sphere that is deployed on the bottom of the ocean for periods of weeks to months (Figure 3.1.1a). MARUs were equipped with HTI-94-SSQ hydrophones, with a flat frequency response of 168 ± 2.0 dB (re: 1 V/µPa) between 2 – 30 kHz. The hydrophone is mounted outside the sphere in order to acquire sounds that are recorded and stored in a binary digital audio format on internal electronic storage media. At the conclusion of a deployment, the MARU is sent an acoustic command to release itself from its anchor and float to the surface for recovery. After the recovery, the MARU data are extracted, converted into lossless audio files and stored on a server for analysis. The unit is then refurbished (batteries and hard drive replaced, etc.) in preparation for a subsequent deployment. Data recorded by a MARU are thus accessible only after the device is retrieved.

Acoustic data at one location were also collected using Autonomous Multichannel Acoustic Recorders (AMARs), developed by JASCO Applied Sciences, in order to validate the noise level measurements from the MARUs. (Figure 3.1.1b). AMARs function similarly to MARUs, but have a higher sensitivity than the MARUs, as well as increased capacity for battery storage, which allows for collecting data for longer periods of time, or at higher sampling rates. AMARs are contained in a PVC tube measuring 16.5 cm in diameter and 57.2 cm in length (http://www.jasco.com/amar), and are equipped with an M8E-V35 dB hydrophone (24-bit, -163 dB re: 1 V/µPa at 1 kHz sensitivity). AMARs are attached to a weighted sled to anchor at the bottom of the ocean and are retrieved by attaching a tow line to a co-located MARU. An external mounted calibrated hydrophone sits approximately 1 m above the seafloor and records sound files to storage media. Because the AMAR records sound files directly in a .wav format, no additional post-processing of the data is needed.

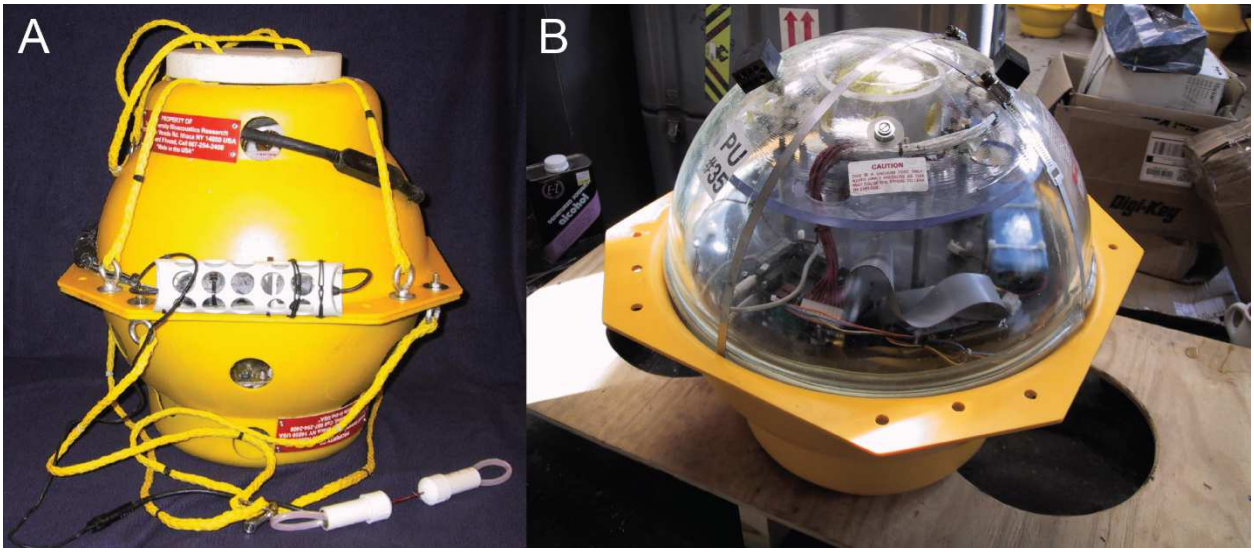

Figure 3.1.1a. Marine Autonomous Recording Unit (MARU)
The (a) external view and (b) internal view of the Marine Autonomous Recording Unit (MARU).

Figure 3.1.1b. Autonomous Multichannel Acoustic Recorder (AMAR)
External view of the Autonomous Multichannel Acoustic Recorder (AMAR).

To acoustically detect odontocete clicks, the T-POD (Timing Porpoise Detector) and its successor the C-POD, were developed by Chelonia Ltd. (Figure 3.1.1c; Cornwall, UK). C-PODs are the most commonly used passive acoustic data loggers for odontocetes in Europe (Carstensen et al. 2006; Tougaard, Carstensen, et al. 2009; Dähne et al. 2013), and they have been used to study many different odontocete species in diverse acoustic environments from the tropics to the Arctic (Chelonia Ltd.). The C-POD is not an archival acoustic recorder, as it does not store audio data; rather, it processes sound within certain frequencies, which requires less memory and is not as battery intensive as compared to storing high-frequency acoustic recordings. Tonal signals are identified from background noise through comparison of target and reference bands set by the manufacturer (Chelonia Ltd.). The C-POD digital processor measures amplitudes and times of waveform maxima and minima as well as zero-crossings. The data are processed by the accompanying CPOD.exe program (Chelonia Ltd.) and a proprietary algorithm called the KERNO classifier uses click train characteristics to indicate odontocete presence. The KERNO classifier defines a click train as five or more clicks between 20 – 160 kHz with decreasing inter-click intervals (ICIs).

Acoustic data were collected at three locations using an SM3M recorder (Wildlife Acoustics; Figure 3.1.1d). The SM3M's standard acoustic hydrophone (sensitivity: -165 dB re: 1 V/µPa) was deployed with a gain of 12 dB re 1 µPa, 48 kHz sampling rate, and peak-peak voltage range of 1.9997 V. The SM3M was duty-cycled to record 10 minutes on and 2 minutes off (T-1C February – April 2016 and T-1C and A-5C May – June 2016), 2 minutes on and 4 minutes off (A-5C and W-3C July – September 2016 and W-3C November 2016 – January 2017), or 5 minutes on and 10 minutes off (all sites from January 2017 onward), depending on the expected deployment duration and battery life. Once recovered, the data were downloaded in a .wav format, the file type directly recorded by SM3Ms.

Acoustic data at one location were also collected using a SoundTrap ST300 HF recorder (Figure 3.1.1e; Ocean Instruments NZ). The SoundTrap (sensitivity: -173 dB re: 1 V/µPa) was deployed with a gain setting of 'High', 48 kHz sampling rate, peak-peak voltage range of 2.0 V. An external battery pack was attached to increase battery life and, thus, allowing for a longer data collection period. The SoundTrap was duty cycled to record 5 minutes on and 10 minutes off for each deployment to increase the length of recordable days for the 128 gigabyte device. Once recovered, the data were downloaded and converted into .wav audio files using the SoundTrap Host 2.0.10.27427 software and stored for analysis.

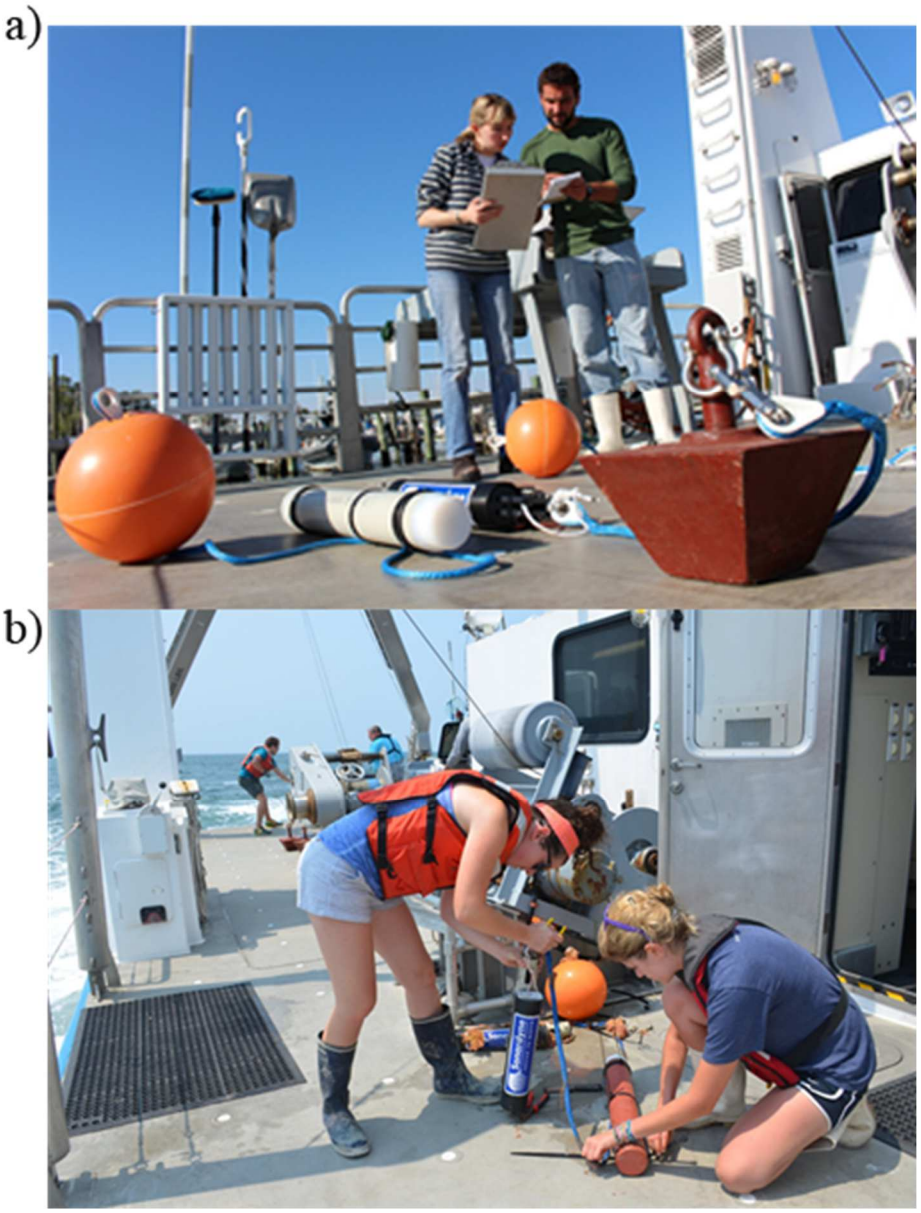

Figure 3.1.1c. Field images of the C-POD
a) Preparing a C-POD acoustic data logger (white) and its mooring and b) reattaching an anti-fouled C-POD for its deployment (red). Photos by Sarah Brzezinski (a) and Kristin Hodge (b) aboard the *R/V Rachel Carson*.

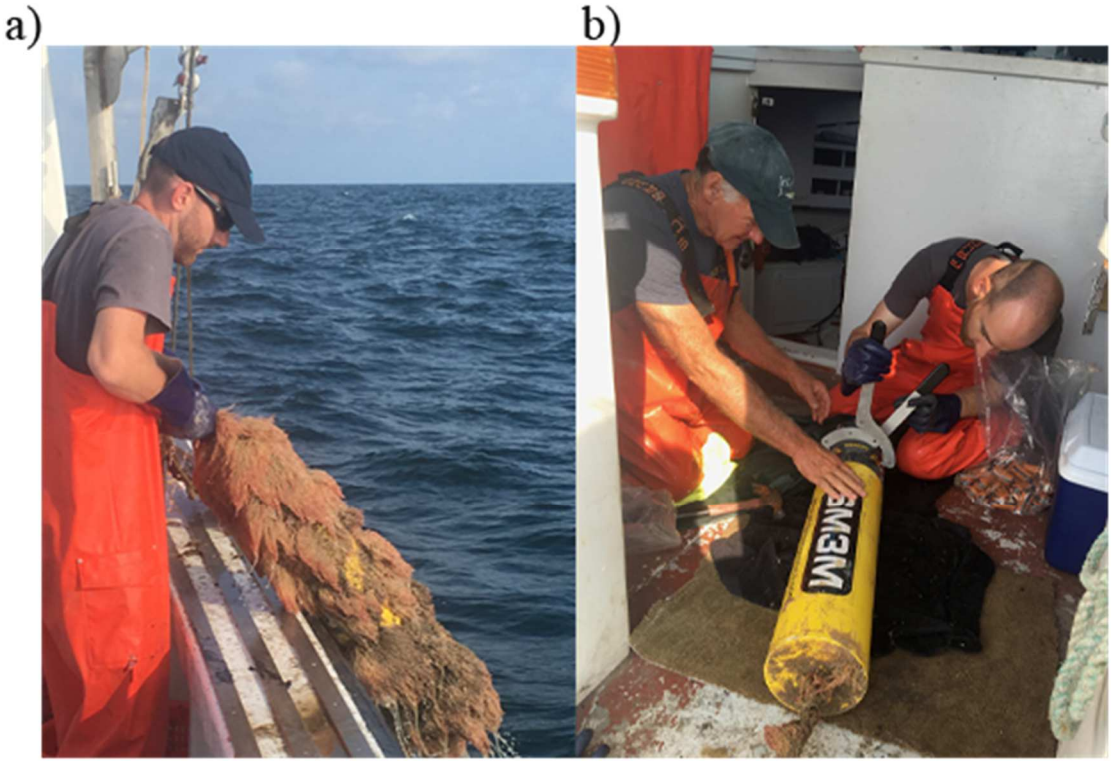

Figure 3.1.1d. Field images of the SM3M acoustic recorder
a) Recovered SM3M after a few months deployed in the Maryland WEA and b) opening the cleaned SM3M. Photos by Elizabeth McDonald (a) and Elizabeth Grzyb (b) aboard the *F/V Integrity*.

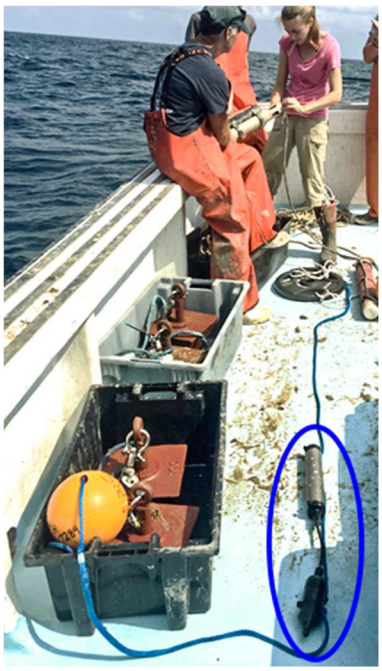

Figure 3.1.1e. Field image of the SoundTrap acoustic recorder
The SoundTrap acoustic recorder and its external battery pack (blue circle) attached to its mooring. The acoustic release and C-POD are in the background. Photo by Elizabeth Grzyb aboard the *F/V Integrity*.

The C-POD and acoustic recorder (SM3M or SoundTrap) were deployed in a tandem mooring attached to an anchor with five meters of ground line between them (Garrod et al. 2018). A Sonardyne acoustic release on the line holding the C-POD allowed retrieval of the entire mooring (Figure 3.1.1f). The C-POD and acoustic recorder were approximately 1 – 3 m above the seabed. C-PODs have a reported detection range for dolphins up to 1.8 km (Nuuttila, Thomas, et al. 2013).

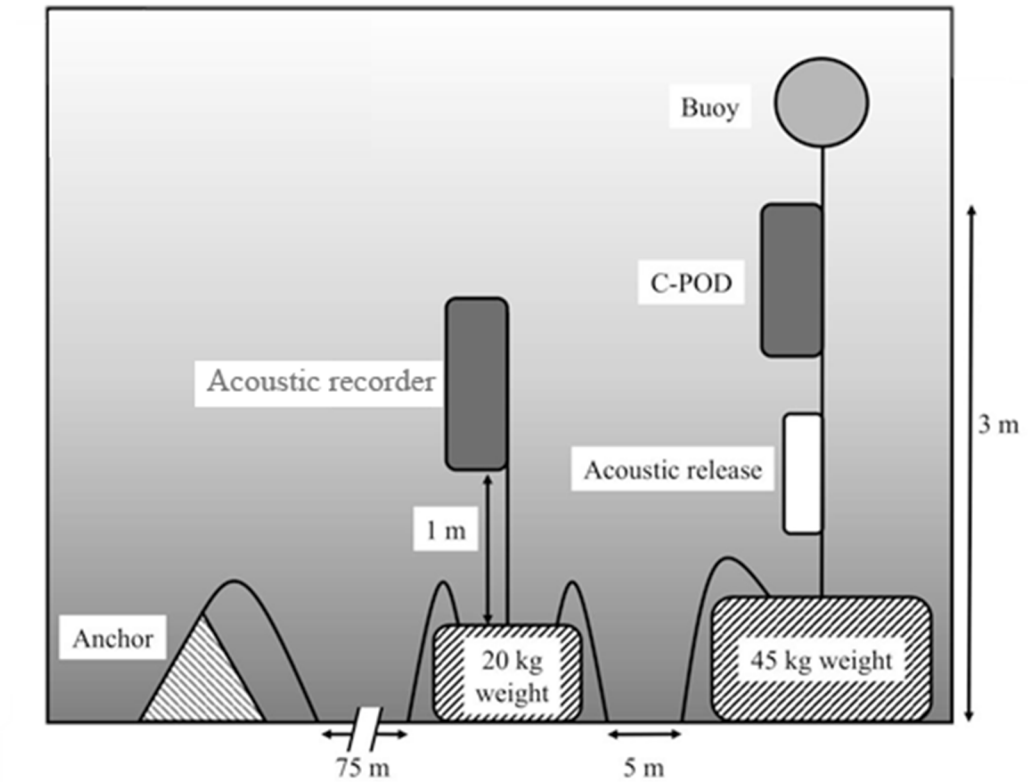

Figure 3.1.1f. Schematic of mooring design with both a C-POD and acoustic recorder (not to scale) C-PODs were attached to a mooring line connected to a 45 kg weight. The C-POD was approximately 3 m off the seafloor. For sites with an acoustic recorder, the instrument was on a separate mooring line connected to a 20 kg weight. This secondary mooring was attached to both the main anchor weight and a secondary anchor used to retrieve the equipment should the acoustic release fail. A Sonardyne acoustic release was used to bring the instruments to the surface for recovery.

3.2 PAM Deployments and Maintenance

In an effort to characterize baleen whale acoustic occurrence and ambient noise conditions within and surrounding the Maryland Wind Energy Area (WEA), MARUs were deployed at 12 survey sites in three spatial regions: inshore (1 site), offshore (3 sites, where site T-3M was moved to T-3*M due to high incidence of trawling at the original site) and within the Maryland WEA (8 sites) (Figure 3.2.a). Four MARUs were deployed in a transect line approximately 11 – 64 km offshore of Ocean City, Maryland (sites T-1M, T-2M, T-3*M, T-3M), and eight MARUs were deployed in a localization array centered on the Maryland WEA (sites A-1M to A-8M). MARUs were anchored at depths ranging between 20 – 42 m, and recording sites were 7 – 20 km apart within the entire array (Table 3.2a).

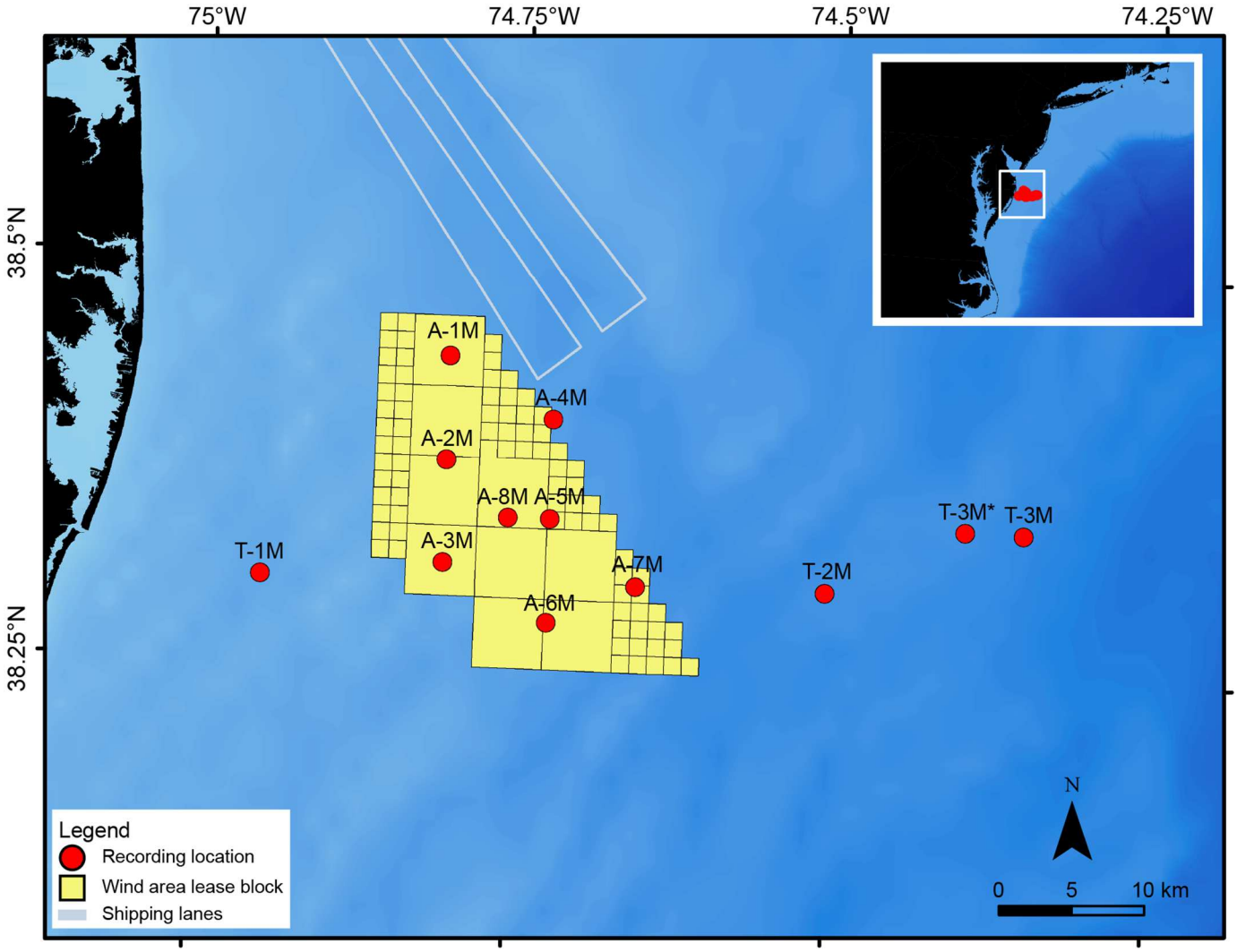

Figure 3.2a. Recording locations of the Marine Autonomous Recording Units (MARUs) within and surrounding the Maryland Wind Energy Area (WEA)

Recording locations of the MARUs located in three spatial regions: inshore (site T-1M), offshore (sites T-2M, T-3*M, T-3M) and within (sites A-1M through A-8M) the Maryland WEA.

Each MARU was deployed for approximately five months (across seven deployments) and was replaced with a refurbished unit upon recovery (Figure 3.2b). Each MARU had a gain setting of 23.5 dB (sensitivity of -145.5 dB re: 1 V/µPa), and recorded continuously at a 2 kHz sampling rate with a high-pass and low-pass filter (10 Hz and 800 Hz) to reduce electrical interference and aliasing. Synthetic time-referenced signals were played underwater during the beginning, midpoint, and end of each deployment to temporally align the acoustic data on all recording MARUs.

Table 3.2a Geographical coordinates and depths of Marine Autonomous Recording Units (MARUs) and Autonomous Multichannel Acoustic Recorder (AMAR) deployed within and surrounding the Maryland Wind Energy Area (WEA).

Sites	Latitude (°N)	Longitude (°W)	Depth (m)
T-1M	38.30	74.95	20
A-1M	38.44	74.81	23
A-2M	38.38	74.81	24
A-3M	38.31	74.81	21
A-4M	38.41	74.72	30
A-5M	38.34	74.72	29
A-6M	38.28	74.72	29
A-7M	38.30	74.65	35
A-8M	38.34	74.76	26
T-2M	38.30	74.51	37
T-3*M	38.34	74.40	42
T-3M	38.34	74.35	42
AMAR	38.30	74.76	26

Figure 3.2b. Field operations
Pictures of field operation aboard the *R/V Rachel Carson*. (a) Captain Fred Channell preparing to deploy a MARU; (b) Kristin Hodge placing a Lubell speaker into the water to time-synchronize the MARUs; (c) a MARU surfacing after being deployed for approximately 5 months; (d) Captain Fred Channell and Robert Nilsen retrieving a MARU. Photo credits: Kristin Hodge (a, c, d) and Captain Fred Channell (b).

Acoustic data were collected over an approximately 3-year study period, spanning 1,114 consecutive days during 5 November 2014 – 22 November 2017. Due to occasional incidents of trawling, instrumentation failure, and changes in a site location (moving site T-3M to site T-3*M), recording effort varied between survey sites (Figure 3.2c; Table 3.2b), ranging from 142 – 1114 total recording days. Significant efforts were made to mitigate the loss of acoustic data, although there were occasional data quality issues (Table 3.2b). MARUs were equipped with ARGOS satellite transmitters to determine their geospatial locations if they surfaced unexpectedly, and the local fishing fleet were recruited to assist in the recovery of units that surfaced prematurely. The MARUs, C-PODs and other acoustic recorders were also labeled with contact and recovery information in the event of trawling. Following multiple losses of MARUs at site T-3M, the site was moved 4 km westwards in December 2015 to reduce the risk of trawling based on discussions with local fishermen in Ocean City, MD, and fishing information from MD Department of Natural Resources. The locations of the MARU, C-PODs, and other acoustic recorders were given to the US Coast Guard and provided as a notification to mariners. The locations and device descriptions were also distributed to various fishing groups, and to US Wind and their surveying teams to help avoid any damage or loss of the devices.

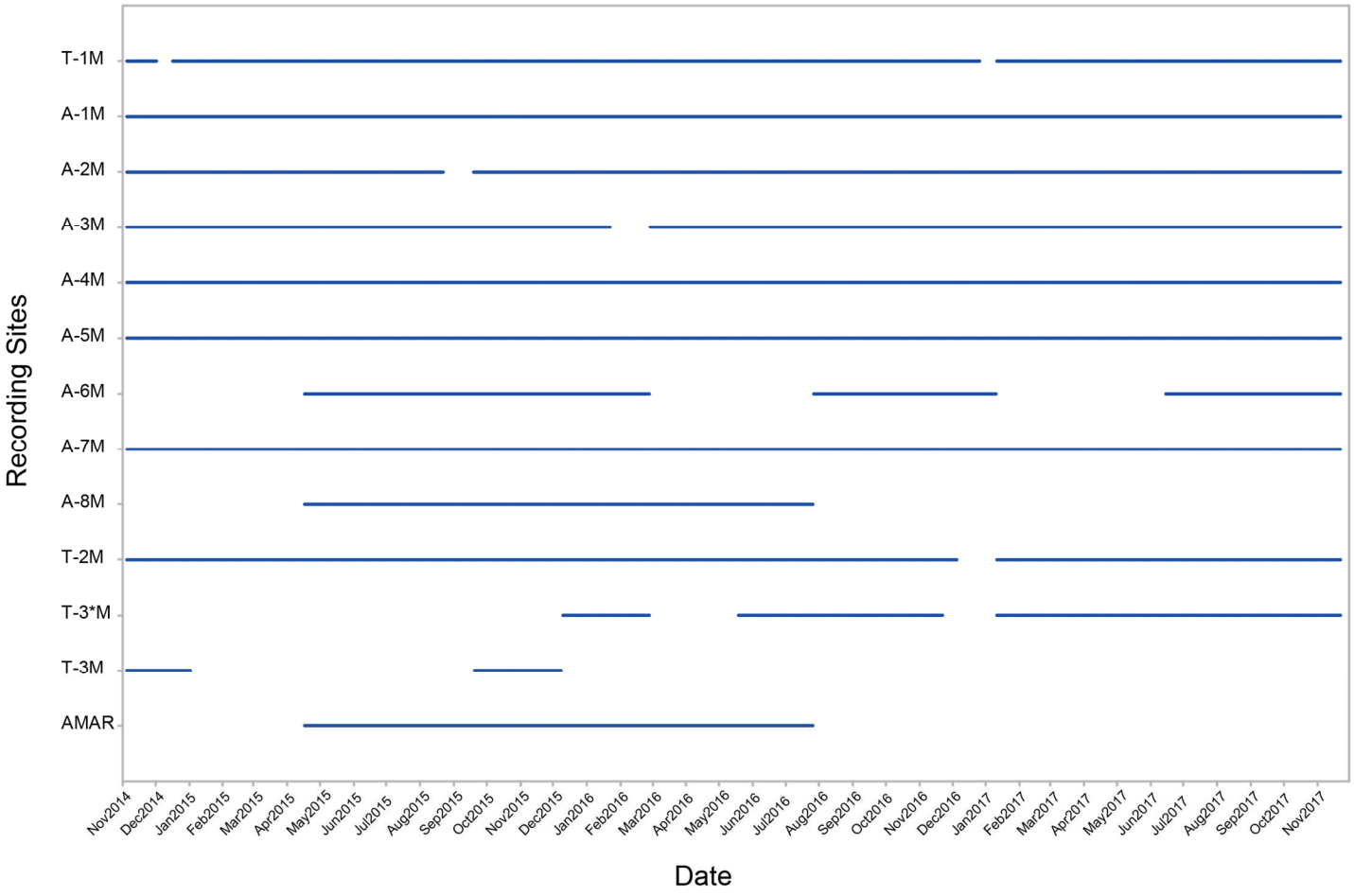

Figure 3.2c. Baleen whale recording effort
Recording effort for the Marine Autonomous Recording Units (MARUs) and the Autonomous Multichannel Acoustic Recorder (AMAR) during the 3-year survey period for each recorder. Spaces between horizontal lines for each sensor show acoustic data gaps due to occasional incidents of trawling, instrumentation failure, and changes in survey design (e.g. moving site T-3M to site T-3*M).

Table 3.2b Total number of recording days and total number of occurrence analysis days per recording site.

Sites	# Recording Days	# Occurrence Analysis Days	Data Quality Issues
T-1M	1085	266	No data during 3 December 2014 – 16 December 2014: MARU trawled. No data during 27 December 2014 – 10 January 2017: MARU trawled.
A-1M	1114	273	No data quality issues.
A-2M	1089	265	No data during 23 August 2015 – 18 September 2015: MARU malfunction.
A-3M	1078	264	No data during 23 January 2016 – 27 February 2016: MARU trawled.
A-4M	1114	273	No data quality issues.
A-5M	1114	273	No data quality issues.
A-6M	646	156	No data during 5 November 2014 – 16 April 2015: data corruption. No data during 28 February 2016 – 26 July 2016: MARU trawled. No data during 11 January 2017 – 14 June 2017: MARU trawled.
A-7M	1114	273	No data quality issues.
A-8M	467	116	No data during 5 November 2014 – 16 April 2015: MARU deployed 17 April 2015 as a drag line release for the co-located AMAR. No data during 27 July 2016 – 22 November 2017: MARU and co-located AMAR unit no longer deployed for remainder of acoustic survey.
T-2M	1079	267	No data during 7 December 2016 – 10 January 2017: MARU trawled.
T-3*M	586	105	No data during 5 November 2014 – 9 December 2015: site T-3M moved to site T-3*M as of 10 December 2015. No data during 28 February 2016 – 18 May 2016: data corruption. No data during 23 November 2016 – 10 January 2017: data corruption.
T-3M	142	36	No data during 3 January 2015 – 18 September 2015: MARU trawled No data during 9 December 2015 – 22 November 2017: MARU retrieved early, and deployment site consequently moved to T-3*M.

In an effort to validate ambient noise levels for the MARUs, the AMAR was deployed near the center of the WEA, at site A-8M (Table 3.2a). The AMAR recorded a total of 467 days during 17 April 2015 – 16 July 2016, and two different AMAR models were employed over the course of the study. The AMAR deployed during 17 April 2015 – 17 September 2015 recorded at a sampling rate of 128 kHz on a duty-cycle schedule of 84 s recording time repeated every 200 s. The AMAR deployed during 18 September 2015 – 16 July 2016 recorded on a duty-cycle schedule of 11 minutes at an 8 kHz sampling rate followed by 1.3 minutes at a 375 kHz sampling rate. The AMAR was equipped with an M8E-V35 dB hydrophone (24-bit, -163 dB re: 1 V/µPa at 1 kHz sensitivity).

To characterize odontocete occurrence within and surrounding the Maryland WEA, C-PODs were deployed in a transect line at 4 focal survey sites in three spatial regions: inshore (T-1C), offshore (T-2C, T-3C) and within the Maryland WEA (A-5C) (Table 3.2c; Figure 3.2d). Deployments at 4 auxiliary sites (W-1C, W-2C, W-3C, W-4C) occurred in the third year within the Maryland WEA in anticipation of the installation of a meteorological tower, but this installation was ultimately delayed beyond our study period. To record mid-frequency sounds at these sites, an acoustic recorder (SM3M or SoundTrap) was deployed with the C-POD at several sites (Figure 3.2d).

Table 3.2c Geographical coordinates and depths of C-PODs and SM3Ms deployed within and surrounding the Maryland Wind Energy Area (WEA).

Sites	Latitude (°N)	Longitude (°W)	Distance Offshore (from Ocean City, MD) (km)	Depth (m)
T-1C	38.34	74.95	11	20
A-5C	38.34	74.72	30	28
T-2C	38.34	74.51	49	45
T-3C	38.34	74.35	62	42
W-1C	38.35	74.74	28	28
W-2C	38.37	74.75	27	28
W-3C	38.40	74.78	24	27
W-4C	38.42	74.77	25	27

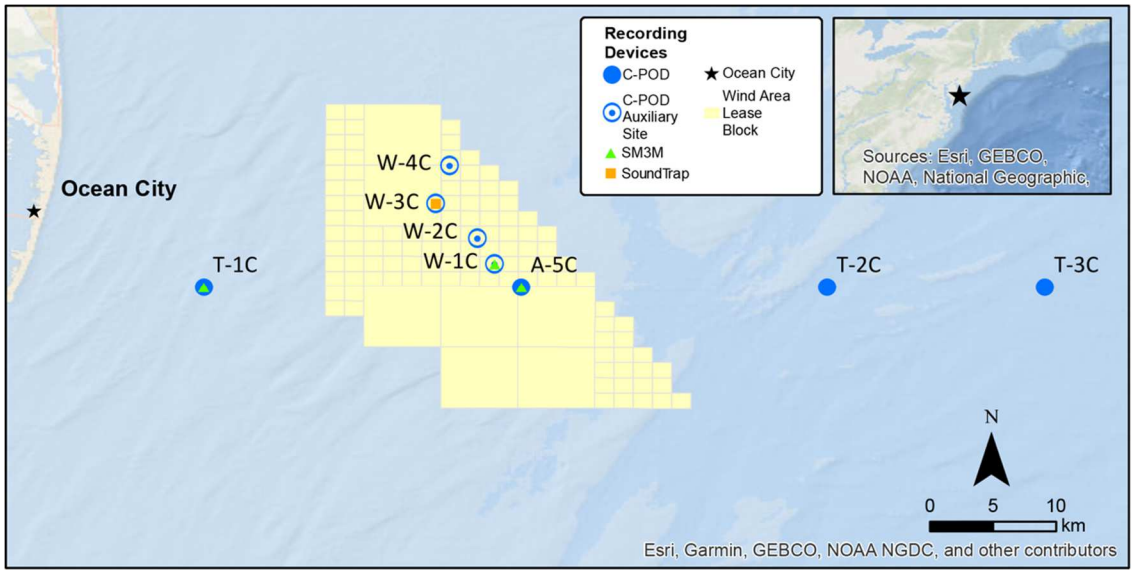

Figure 3.2d. Recording locations of the C-PODs and acoustic recorders within and surrounding the Maryland Wind Energy Area (WEA)

Recording locations of the C-PODs (filled blue circles) located in three spatial regions formed a transect line: inshore (site T-1C), offshore (sites T-2C, T-3C), and within (A-5C) the Maryland WEA. Additional C-POD sites within the Maryland WEA ("C-POD auxiliary sites", unfilled blue circles) were deployed during the third year of the study. Acoustic recorders were deployed during portions of the second and third years (SM3Ms, green triangle; SoundTrap, orange square).

The C-PODs and acoustic recorders were deployed for approximately three months for each deployment, with data downloaded upon recovery and equipment redeployed (Figure 3.2e). The 3-year study period included data collection across the four main locations for the majority of the study period, approximately 1,083 days between 5 November 2014 and 31 October 2017 (Figure 3.2f). Additional sites within the Maryland WEA were included later in the study period to obtain information during geophysical surveys and the installation of a meteorological tower within the Maryland WEA, although these activities were delayed and did not end up occurring within the study period. Gaps in the C-POD data were mainly caused by instrument loss, likely from trawling, and there was only one instance of data corruption. If a C-POD did not surface when the acoustic release was triggered, the acoustic release process was repeated at least three times. If this was not successful, then the process of grappling for the bottom mooring line was initiated and repeated at least three times before moving to the next site. If the C-POD had still not been retrieved, the process of grappling for the mooring line was repeated during the next cruise within a larger area and led to the successful recovery of a C-POD when the mooring had moved, mostly likely as a result of storms.

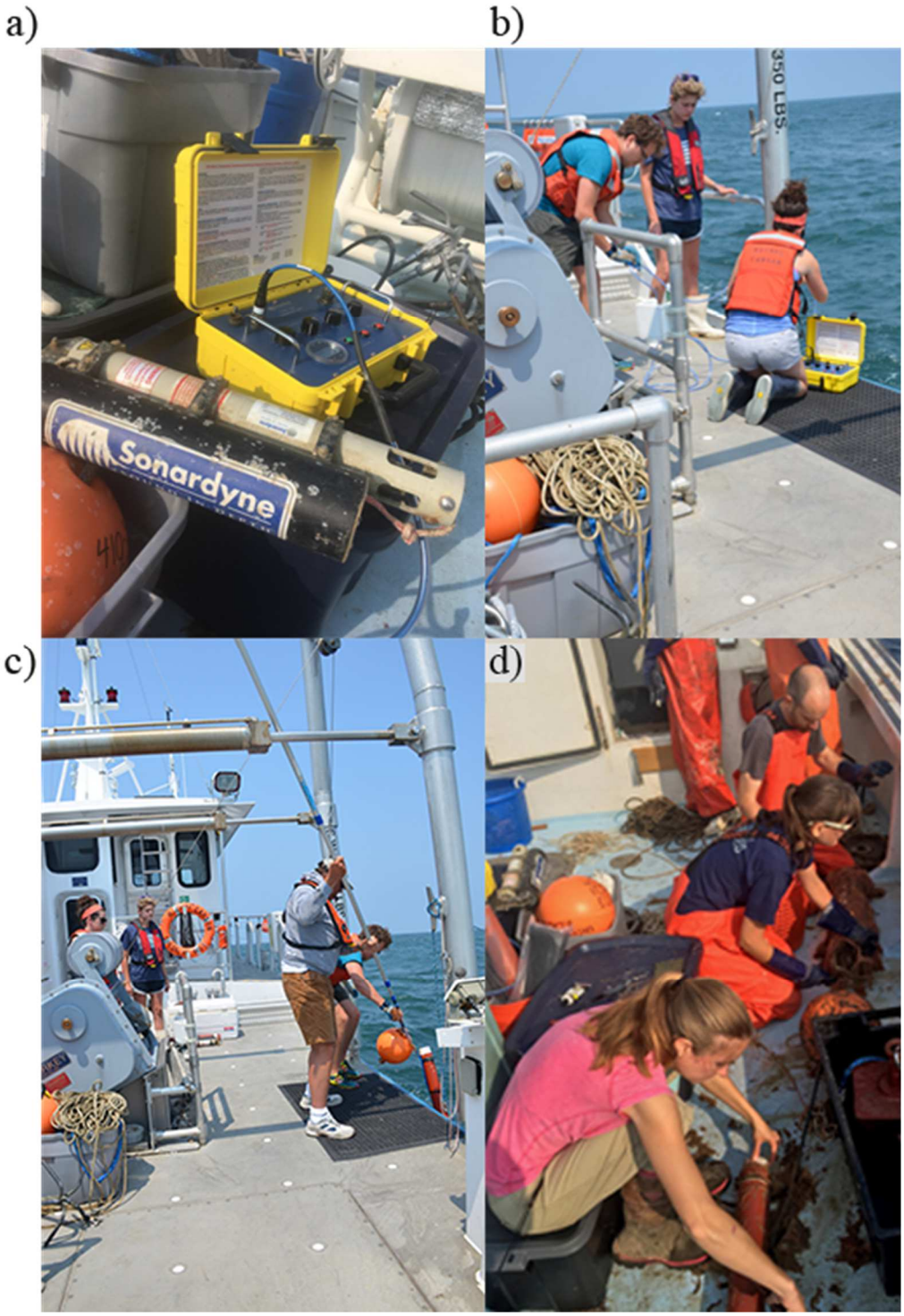

Figure 3.2e. Field operations for odontocetes
Pictures of field operations aboard the *R/V Rachel Carson* and *F/V Integrity*. a) Sonardyne acoustic release and deck unit with transponder attached; (b) Jessica Wingfield placing the Sonardyne transponder into the water to activate the acoustic release; (c) Aran Garrod recovering a C-POD aboard the *R/V Carson*; (d) Elizabeth McDonald cleaning a recovered C-POD (foreground) and Aimee Hoover cleaning a SM3M (background) after 3 months deployed. Photo credits: Elizabeth McDonald (a), Kristin Hodge (b,c) and Elizabeth Grzyb (d).

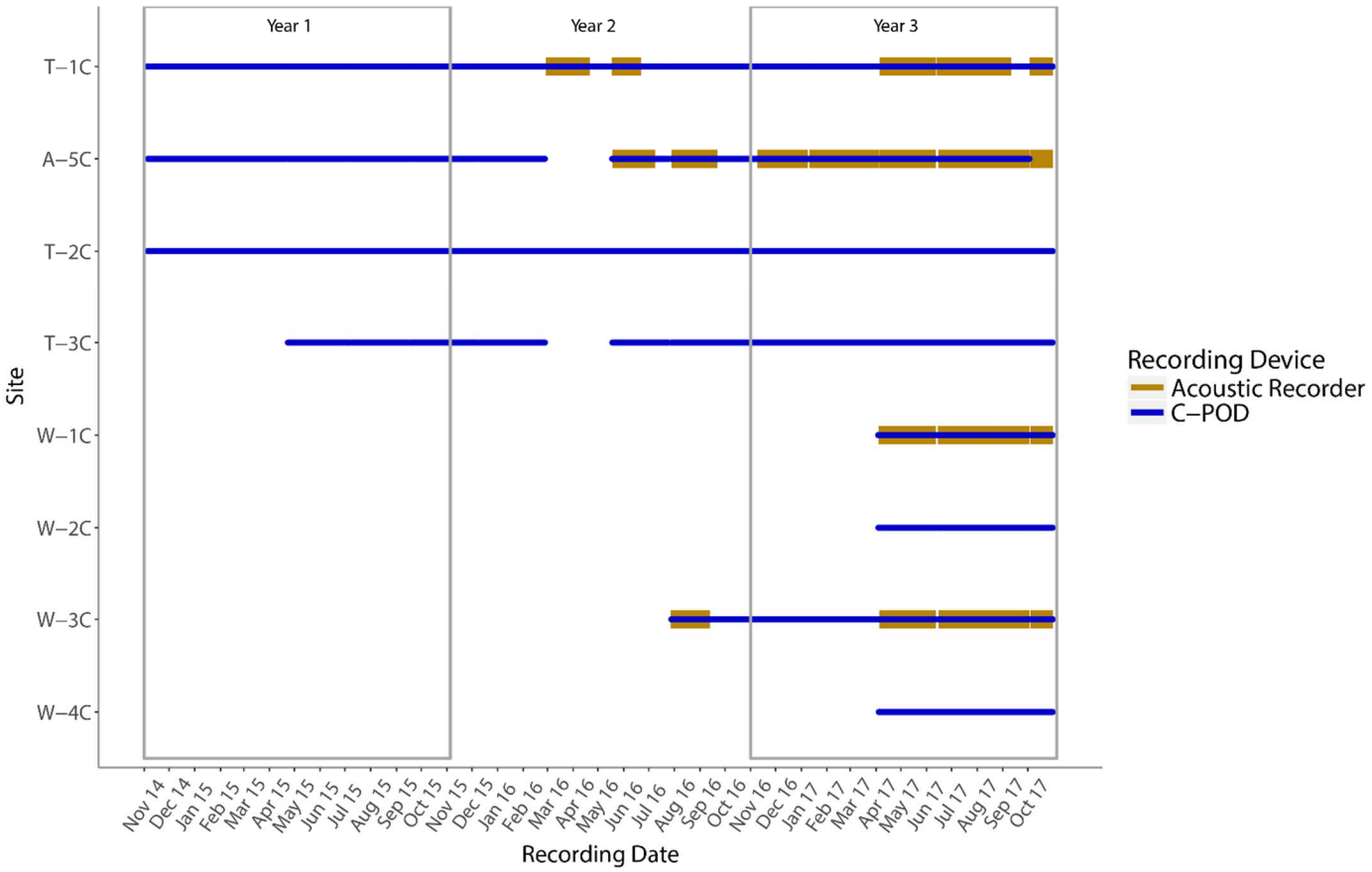

Figure 3.2f. Odontocete recording effort
Recording effort for the C-PODS (blue) and acoustic recorders (SM3M, SoundTrap; brown) during the 3-year survey period (gray boxes around Years 1 and 3). Spaces between horizontal lines show data gaps due to occasional incidents of possible trawling or instrumentation. T-1C, A-5C, T-2C, and T-3C represent our core study sites for odontocetes.

3.3 Data Analysis Methodology

3.3.1 Baleen Whale Acoustic Detection Range Estimates

In order to estimate how far away from the sensor network focal individuals were being recorded, acoustic detection ranges for the sounds of North Atlantic right whales, humpback whales, fin whales, and minke whales were modeled using the Acoustic Ecology Toolbox e, a MATLAB-based algorithm. In order to choose the appropriate transmission loss model for this shelf region (e.g. cylindrical versus spherical spreading), we conducted an empirical data transmission loss experiment using playback signals transmitted in the survey area during June 2017 (Figure 3.3.1a). Those data comprised 17 sequences of playbacks along two perpendicular transects at known distances to the array. Each sequence comprised eight sweep synthetic signals (each 1.5 seconds in duration and of constant amplitude) between 300 – 600 Hz, a frequency bandwidth that overlaps with the calls of North Atlantic right whales, minke whales and humpback whales. Since the transmit voltage response varied slightly between frequencies from 300 to 600 Hz, we chose to reference the median sensitivity of the frequency response curve (136 dB µPa/V @ 1 m), which occurred at 500 Hz. We measured the amplifier output to be 66 V pp; therefore, the source level (SL) root mean square (RMS) value was estimated as follows:

$$SL = 20log(66\,V/2) + 136\,dB\,re{:}\,1\mu Pa/V = 166\,dB\,re\,1\mu Pa\,@\,1m$$

We then measured the received level (RL) RMS value for each recorded signal and measured the distance from the source (Lubell LL9162T) to the recorder. A linear regression was used to model the relationship between received level and range for each site (Figure 3.3.1b). This model allowed us to determine sound attenuation at each site and to determine which transmission loss model best fit the empirical data. The transmission loss model that best fit the empirical data was then compared against the spherical spreading loss model ($20\log_{10}(R)$), cylindrical spreading loss model ($10\log_{10}(R)$), and a semi-empirical model. The semi-empirical model comprises the spherical spreading loss model (to account for near-source spreading) with an intermediate model based on the best fit to the empirical data (Richardson et al. 1995).

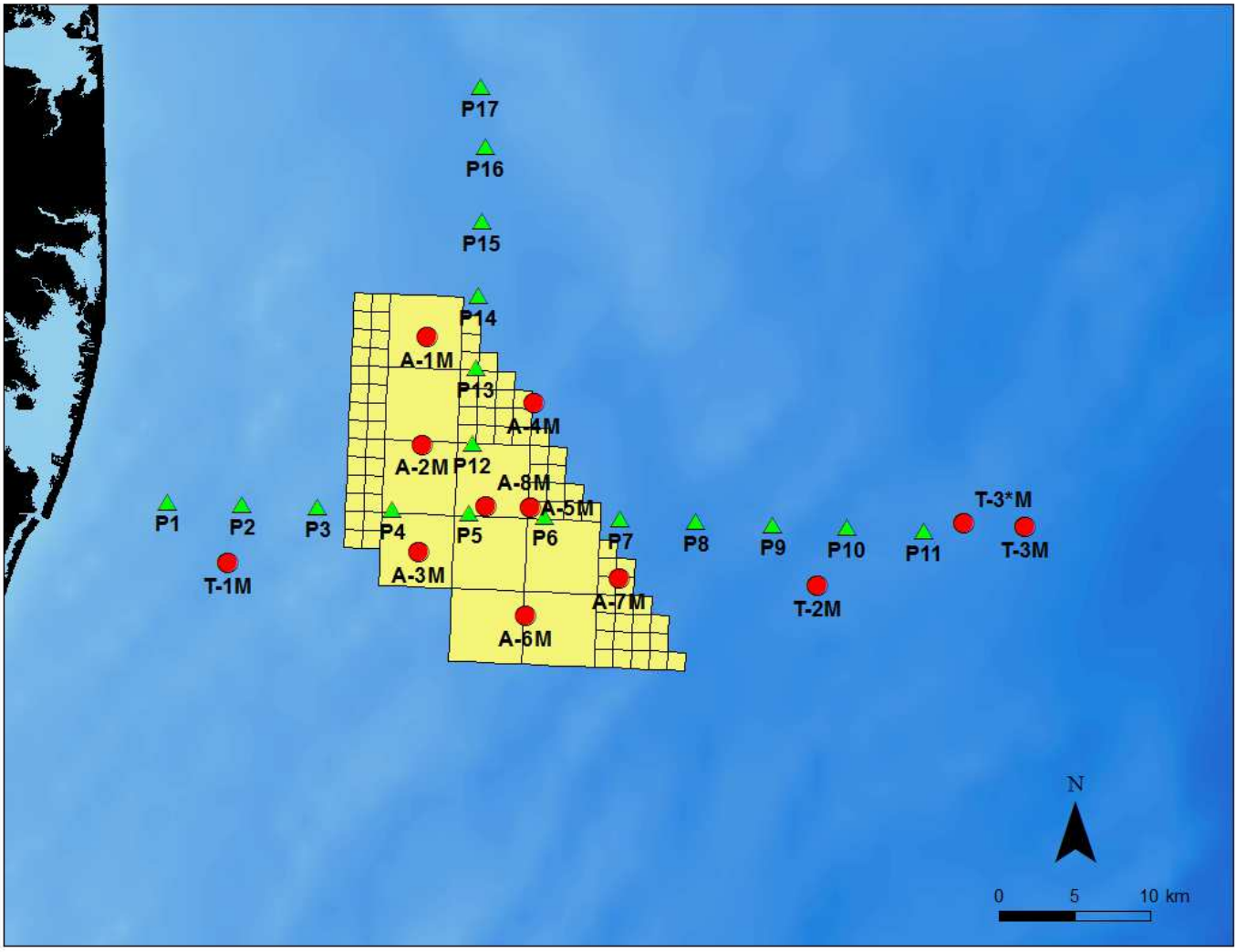

Figure 3.3.1a. Synthetic playback tone locations
The playback tone locations (green triangles P1 through P17) for the empirical data transmission loss experiment.

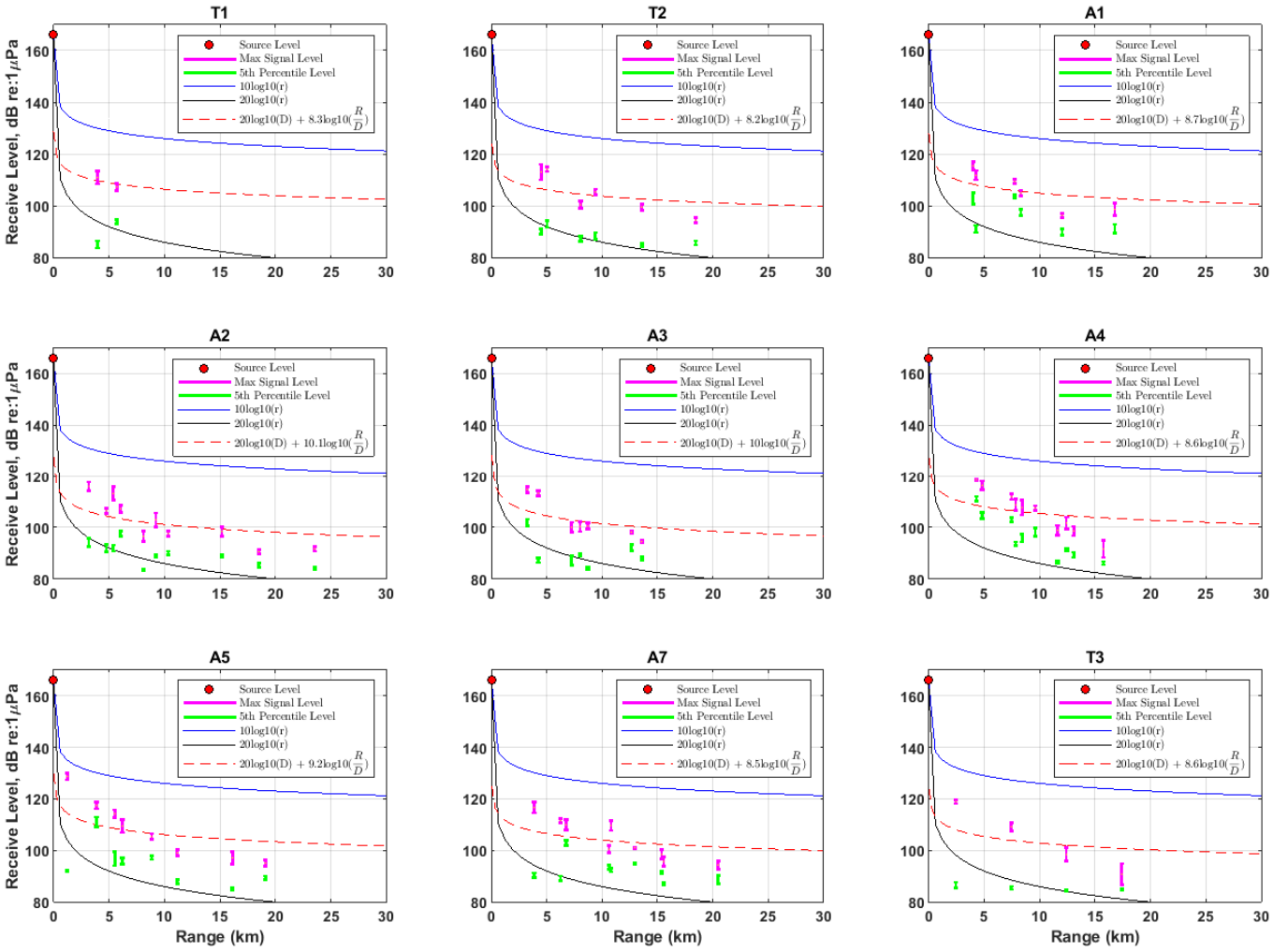

Figure 3.3.1b. Regression of modeled receive levels
Regression of max modeled receive levels for each playback sweep (300 – 600 Hz) at each site given range from the source. The dashed red line represents the model that best fits the empirical data. The blue line represents the $10\log_{10}(R)$ cylindrical spreading model and the black line represents the $20\log_{10}(R)$ spherical spreading model for comparison.

Taking the best model from each site and averaging them yielded a spreading loss model of $16.1\log_{10}(R)$; therefore, detection range estimates for the Maryland sites were derived from the Passive Sonar Equation below, where *RL* is the received level, *SL* is the source level, and *R* represents the range (in meters) of the signal from the source to the receiver:

$$\mathrm{RL} = \mathrm{SL} - 16.1\log_{10}(\mathrm{R})$$

These calculations take into account source level and measured local ambient noise levels at each location. Since fin whale 20 Hz pulses occur in frequencies well below the playback sweeps that were modeled with the empirical data, and since fin whale vocalizations are likely to originate from off the

shelf as well as on the shelf, we included the spherical spreading loss model with the intermediate model, resulting in the following semi-empirical model for fin whales:

$$\mathrm{RL} = \mathrm{SL} - 20\log_{10}(\mathrm{R}) + 16.1\log_{10}(\mathrm{R})$$

Source levels for calls of each focal whale species were estimated using values documented in the peer-reviewed scientific literature (Table 3.3.1a). Ambient noise measurements for species-specific bandwidths (Table 3.3.1a) were calculated for Summer, Autumn, Winter, and Spring of the first full year of recording (5 November 2014 – 4 November 2015). Using the $16.1\log_{10}(\mathrm{R})$ model, we estimated and averaged the detection ranges per season for each of the four whale species across all site locations, during high (95th percentile), median (50th percentile), and low (5th percentile) noise conditions. For this process, we focused on a representative subset of survey sites that spanned the extent of the survey area to capture overall noise levels whilst being more computationally efficient: sites T-1M, A-1M, A-3M, A-4M, A-7M, and T-2M.

Table 3.3.1a Species-specific source levels and bandwidth used in the detection range calculations for four baleen whale species.

Species	Source Levels	Species-Specific Bandwidth	Center Frequency 1/3rd Octave Bandwidths
Fin Whale	189 dB (Weirathmueller et al. 2013)	15 – 25 Hz (Weirathmueller et al. 2013)	16 – 25 Hz
Humpback Whale	169 dB (Au et al. 2006)	29 – 2480 Hz (Dunlop et al. 2007)	28.2 – 562 Hz
Minke Whale	168 dB (Risch et al. 2014)	50 – 300 Hz (Risch et al. 2014)	50 – 315 Hz
North Atlantic Right Whale	172 dB (Hatch et al. 2012)	71 – 224 Hz (Urazghildiiev et al. 2009; Hatch et al. 2012)	71 – 224 Hz

3.3.2 Baleen Whale Acoustic Occurrence

A 25% stratified subsample of recording days (Table 3.3.2a) for every survey site were examined in Raven Pro 1.5 (Cornell Bioacoustics Research Program, Ithaca NY) to quantify the daily and hourly acoustic occurrence of four focal baleen whale species: fin whale, humpback whale, minke whale, and North Atlantic right whale. Due to occasional incidents of trawling and instrumentation failure, analysis effort varied between survey sites, ranging from 36 – 273 analysis days. Data were examined and reported in three broad spatial regions: inshore, offshore, and within the Maryland WEA.

Table 3.3.2a Number of analysis days per month per recording site. No data were collected or analyzed at sites A-6M, A-8M, T-3*M, and T-3M during select time periods.

	T-1M	A-1M	A-2M	A-3M	A-4M	A-5M	A-6M	A-7M	A-8M	T-2M	T-3*M	T-3M
Nov 2014	7	7	7	7	7	7		7		7		7
Dec 2014	4	7	7	7	7	7		7		7		7
Jan 2015	8	8	8	8	8	8		8		8		1
Feb 2015	7	7	7	7	7	7		7		7		
Mar 2015	8	8	8	8	8	8		8		8		
Apr 2015	7	7	7	7	7	7	3	7	3	7		
May 2015	8	8	8	8	8	8	8	8	8	8		
Jun 2015	8	8	8	8	8	8	8	8	8	8		
Jul 2015	7	7	5	7	7	7	7	7	7	7		
Aug 2015	8	8	6	8	8	8	8	8	8	8		
Sep 2015	8	8	4	8	8	8	8	8	7	8		4
Oct 2015	7	7	7	7	7	7	7	7	7	7		7
Nov 2015	8	8	8	8	8	8	8	8	8	8		8
Dec 2015	8	8	8	8	8	8	8	8	8	8	6	2
Jan 2016	7	7	7	5	7	7	7	7	7	7	7	
Feb 2016	8	8	8	1	8	8	7	8	8	8	7	
Mar 2016	7	7	7	7	7	7		7	7	7		
Apr 2016	8	8	8	8	8	8		8	8	8		
May 2016	8	8	8	8	8	8		8	8	8	4	
Jun 2016	7	7	7	7	7	7		7	7	7	7	
Jul 2016	8	8	8	8	8	8	1	8	7	8	8	
Aug 2016	8	8	8	8	8	8	8	8		8	8	
Sep 2016	7	7	7	7	7	7	7	7		7	7	
Oct 2016	8	8	8	8	8	8	8	8		8	8	
Nov 2016	7	7	7	7	7	7	7	7		7	5	
Dec 2016	7	8	8	8	8	8	8	8		2		
Jan 2017	5	8	8	8	8	8	3	8		8		
Feb 2017	7	7	7	7	7	7		7		7		
Mar 2017	8	8	8	8	8	8		8		8		
Apr 2017	7	7	7	7	7	7		7		7		
May 2017	8	8	8	8	8	8		8		8		
Jun 2017	7	7	7	7	7	7	4	7		7	7	
Jul 2017	8	8	8	8	8	8	8	8		8	8	
Aug 2017	8	8	8	8	8	8	8	8		8	8	
Sep 2017	7	7	7	7	7	7	7	7		7	7	
Oct 2017	8	8	8	8	8	8	8	8		8	8	
Total Analysis Days	**266**	**273**	**265**	**264**	**273**	**273**	**156**	**273**	**116**	**267**	**105**	**36**

3.3.2.1 Fin Whale

Fin whale acoustic presence was determined as the occurrence of three or more consecutive 20 Hz species-specific notes, a subunit of fin whale song produced predominately by males (Figure 3.3.2.1a) (Watkins et al. 1987; Thompson et al. 1992; McDonald et al. 1995; Clark and Gagnon 2002). Fin whale song notes were identified by visually inspecting time-aligned concatenated spectrograms (1024-pt fast Fourier transform (FFT), Hann window, 50% overlap, frequency resolution of 1.95 Hz, time resolution of 256 ms) in a 300 s duration window between 10 – 100 Hz. The acoustic presence of fin whales was annotated every hour for each survey site.

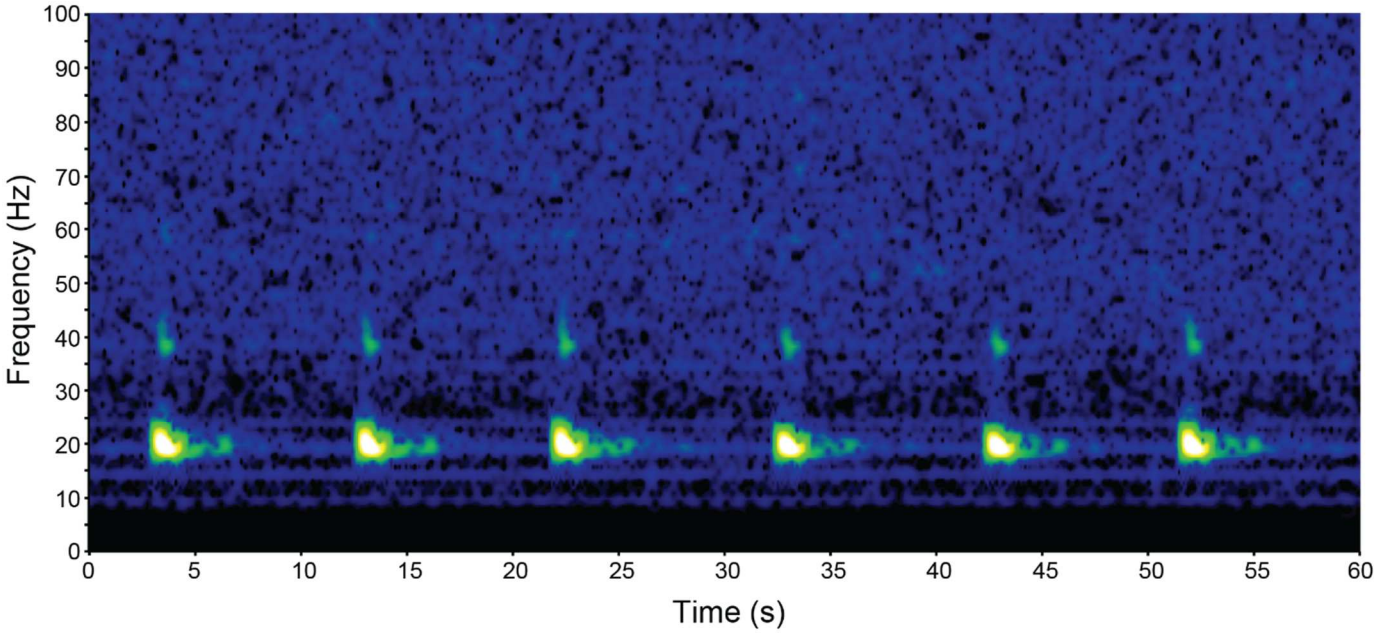

Figure 3.3.2.1a. Spectrogram of fin whale song
Fin whale song recorded October 26, 2016. Spectrogram parameters: 2048 point fast Fourier transform (FFT), Hann window, 90% overlap.

3.3.2.2 Humpback Whale

Humpback whales, which produce highly variable, frequency modulated signals in the form of structured song (produced predominantly by males) (Figure 3.3.2.2a) and call sequences (Payne and McVay 1971; Chabot 1988; Dunlop et al. 2007; Dunlop et al. 2008; Stimpert et al. 2011; Murray et al. 2014) were annotated every hour for each survey site. Acoustic data were examined manually using 150 s spectrograms spanning 10 – 800 Hz, with a 512-pt FFT, Hann window, 50% overlap, frequency resolution of 3.91 Hz, and time resolution of 128 ms.

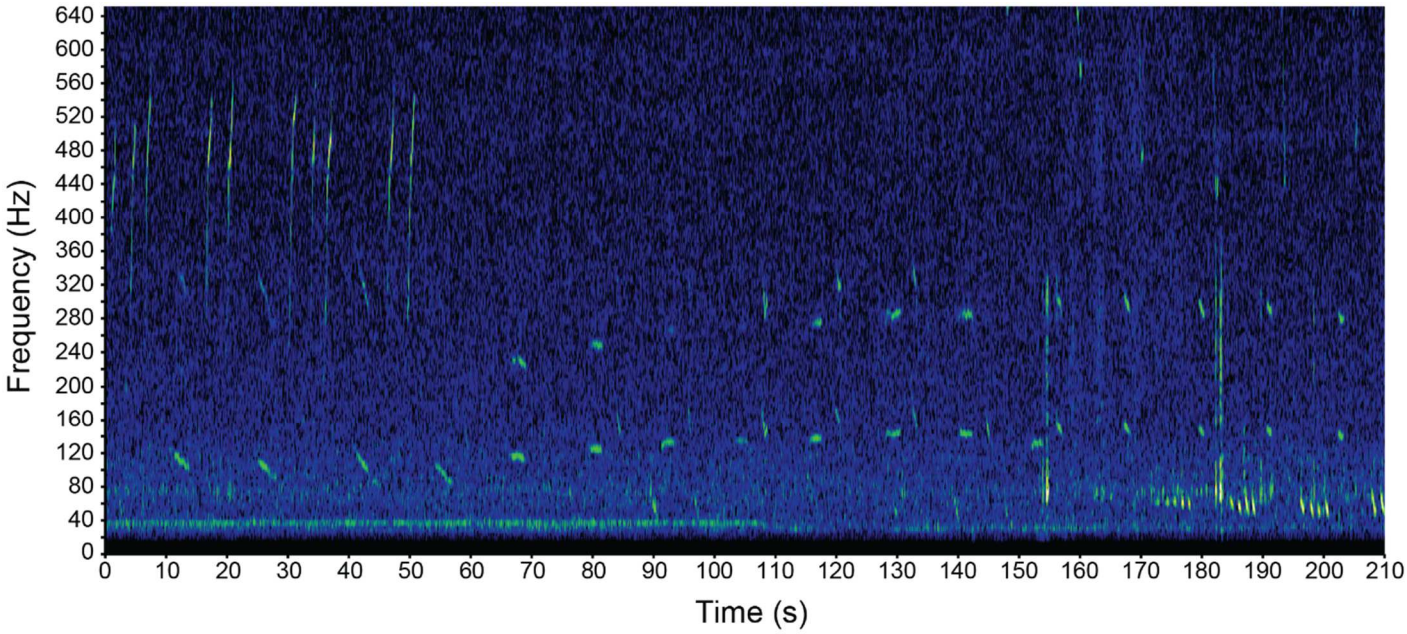

Figure 3.3.2.2a. Spectrogram of humpback whale song
Humpback whale song recorded May 5, 2015. Spectrogram parameters: 512 point fast Fourier transform (FFT), Hann window, 90% overlap.

3.3.2.3 Minke Whale

Minke whales, which produce a series of pulsed signals called a 'pulse train' (Figure 3.3.2.3a) (Risch et al. 2013; Risch et al. 2014), were used to indicate minke whale acoustic presence. Acoustic data were examined with a custom automated detection algorithm (Dugan et al. 2013; Popescu et al. 2013) designed to detect the presence of minke whale pulse trains. All automated detection events were reviewed in 10 – 500 Hz spectrograms, with 256-pt FFT, Hann window, 50% overlap, frequency resolution of 7.81 Hz, temporal resolution of 64 ms, and 120 s duration. Minke whale detections were annotated, and all false positive and questionable detections were removed from analysis.

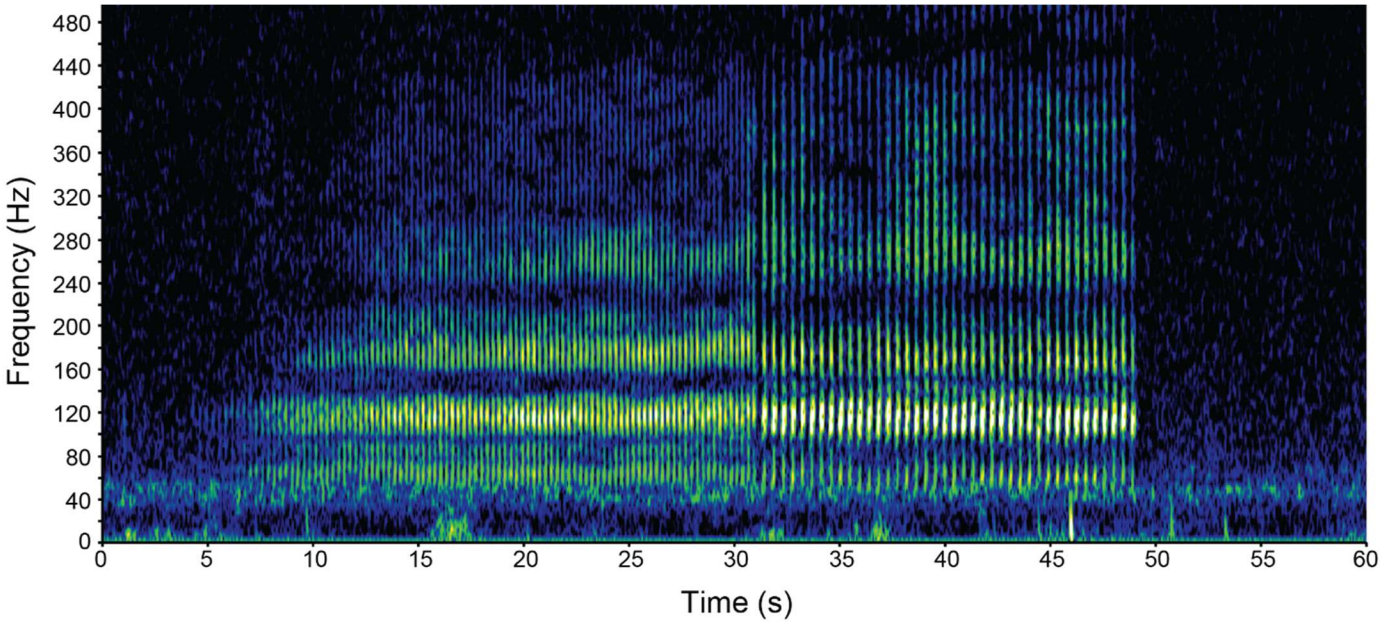

Figure 3.3.2.3a. Spectrogram of minke whale pulse train
Minke whale pulse train recorded on April 3, 2015. Spectrogram parameters: 512 point fast Fourier transform (FFT), Hann window, 90% overlap.

3.3.2.4 North Atlantic Right Whale

North Atlantic right whale acoustic occurrence was determined by the detection of 'up-calls' (contact calls; Figure 3.3.2.4a), produced by both male and female North Atlantic right whales (Parks and Tyack 2005; Clark et al. 2007; Mellinger et al. 2007; Parks and Clark 2007). Acoustic data were examined with a MATLAB-based automated detection algorithm (Dugan et al. 2013) designed to detect the presence of North Atlantic right whale up-calls. All automated detection events were reviewed in 3 s duration, 50 – 300 Hz bandwidth spectrograms using the Selection Review tool in Raven Pro 1.5. Following methods in Hodge et al. (2015), 60 s, 10 – 500 Hz spectrograms (256-pt FFT, Hann window, 50% overlap, frequency resolution of 7.81 Hz, time resolution of 64 ms) were reviewed 5 min before and after each putative North Atlantic right whale up-call in order to distinguish detections from other possible sources of sound, including humpback whales. All false positive and questionable detections were removed from analysis.

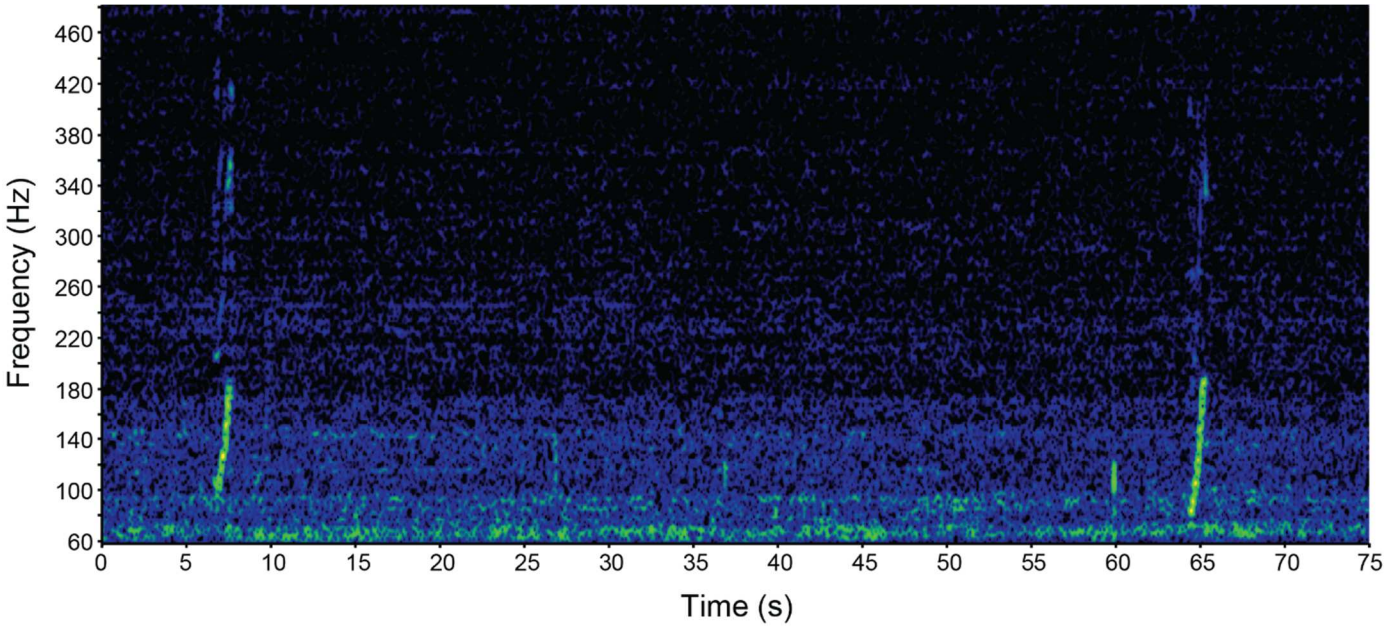

Figure 3.3.2.4a. Spectrogram of North Atlantic right whale up-calls
North Atlantic right whale up-calls recorded January 17, 2015. Spectrogram parameters: 1024 point fast Fourier transform (FFT), Hann window, 90% overlap.

3.3.2.5 Baleen Whale Acoustic Occurrence Analysis

Daily acoustic occurrence of each focal whale species for each survey site was considered with the presence of at least one species-specific call per day. Percent daily presence per month (percent monthly presence) for each site was normalized for recording effort by dividing the number of days containing species-specific calls by the number of recording days analyzed within the month:

$$\%\ \text{monthly presence} = \left(\frac{\#\ days\ per\ month\ with\ acoustic\ presence}{\#\ days\ analyzed\ per\ month}\right) \times 100$$

Since there were multiple survey sites occurring within the WEA (sites A-1M through A-8M), the percent monthly presence was averaged for each month, and reported as an average monthly WEA presence with standard error. The average monthly offshore presence with standard error was also calculated for the multiple survey sites occurring offshore of the WEA (sites T-2M, T-3*M, and T-3M). Percent monthly presence at site T-1M is reported as the monthly inshore presence of the WEA. To examine seasonal trends in baleen whale occurrence, seasons were defined as follows: Autumn (October – December), Winter (January – March), Spring (April – June), and Summer (July – September). An ANOVA and Tukey's HSD post-hoc test were performed in JMP Pro 12 (SAS) to examine inter-annual variability in baleen whale species presence inshore, offshore, and within the WEA.

In order to determine the relative spatial occurrence of each focal species inshore, offshore, and within the WEA, daily acoustic occurrence for each species per survey site was divided by the total number of recording days analyzed per survey site across the entire 3-year monitoring period. Given the proximity of survey areas and the estimated acoustic detection range for each species (see Sections 3.3.1 and 4.1 "Baleen Whale Acoustic Detection Range Estimates"), it is possible some species-specific signals were detected at multiple sites. However, similar to Risch et al. (2013), results of this analysis are

reported as relative spatial occurrence patterns inshore, offshore, and within the WEA, so adjustments for detection range overlap were not factored in to the spatial analysis.

3.3.2.6 North Atlantic Right Whale and Minke Whale Detector Performance Evaluation

In order to evaluate the performance of the North Atlantic right whale up-call detection algorithm and the minke whale pulse train detection algorithm, 24 randomly selected analysis days were reviewed for the occurrence of North Atlantic right whale up-calls and minke whale pulse trains. A human observer annotated and compiled every occurrence of a North Atlantic right whale up-call and minke whale pulse train to build a truth dataset that was compared to the results from each automated detection algorithm test dataset. True detections (TD) were identified as North Atlantic right whale up-calls and minke whale pulse trains found by both analysts and the automated detectors, while missed detections (MD) were identified as the North Atlantic right whale up-calls and minke whale pulse trains found by analysts but missed by the automated detectors. The missed detection rate was calculated to evaluate the performance of the North Atlantic right whale up-call detection algorithm and the minke whale pulse train detection algorithm:

$$\text{Missed Detection Rate} = \left(\frac{MD}{TD + MD}\right)$$

There is currently no agreed upon approach to evaluating the performance of automated detection algorithms for passive acoustic monitoring (e.g. Urazghildiiev and Clark 2006; Hodge et al. 2015; Mellinger et al. 2016). Precision and recall are commonly used by both the ecological and signal processing community (e.g. Digby et al. 2013); however, there is not agreement on the temporal scale of this analysis. Signal processing engineers typically characterize detector performance on the basis of the algorithm's ability to detect all calls. However, from a passive acoustic monitoring perspective, it is important to have the scale of detector evaluation be directly relevant to the data resolution for analysis. Since we do not exclusively analyze the occurrence data for all calls, evaluating the performance exclusively on all calls alone is not appropriate or useful in understanding uncertainty in acoustic presence. Thus, we evaluated detector performance at two additional analysis-relevant scales: 1) the detection of daily presence to understand uncertainty for baleen whale occurrence, and 2) the detection of hourly presence to understand uncertainty for baleen whale occurrence (for GARMA models).

To test if signal-to-noise ratio (SNR) influenced detector performance, SNR was measured in both truth and test datasets, and a Kruskal-Wallis test was performed in JMP Pro 12 (SAS) to determine if there was a significant difference in SNR between missed detections (MD) and true detections (TD).

3.3.2.7 Generalized Auto-regressive Moving Average (GARMA) Models

Temporal patterns of acoustic occurrence across the 3-year survey period were explored using Generalized Auto-regressive Moving Average (GARMA) models (Benjamin et al. 2003) for the following: North Atlantic right whale at survey sites T-1M, A-5M, and T-2M; humpback whale at survey sites T-1M, A-5M, and T-2M; and fin whale at survey site A-5M only (to avoid potential pseudo-replication due to large detection range estimates). GARMA models accommodate non-Gaussian distribution time-series data with potential time-dependent covariates, and are beneficial for continuous data as they control for autocorrelation (e.g. the acoustic occurrence in one hour or day is influenced by the acoustic occurrence in a previous hour or day). The formula for the GARMA model is as follows:

$$(\mu_t) = X_t'\beta + \sum_{j=1}^{p} \varphi_j \{g(Y_{t-j}) - X_{t-j}'\beta\} + \sum_{j=1}^{q} \theta_j \{g(Y_{t-j}) - g(\mu_{t-j})\}$$

Where $g(\cdot)$ is the link function, μ_t is a conditional mean of the dependent variable, β is the regression coefficients, φ_j and θ_j are the auto-regressive and moving average parameters, and p and q are the orders, respectively (Benjamin et al. 2003).

The response variable included in the models was the acoustic presence of species-specific calls in an hour, and the explanatory variables included in the models were the sine and cosine transformed Julian day and hour (UTC) of the day. The explanatory variables were transformed to model cyclical annual and daily patterns; we applied two pairs of sinusoidal functions: $\sin(2\pi t/d)$ and $\cos(2\pi t/d)$, where period d is one day or one year, and t is the hour of the day or Julian day, respectively (Wingfield et al. 2017).

Covariates were compared to the hourly acoustic detection of focal species using GARMA models with a binomial distribution in R (R Core Team 2017) (gamlss.util package; Stasinopoulos et al. 2016). The Akaike Information Criterion (AIC) was used for model selection, and residual autocorrelation and partial autocorrelation plots were used to assess if any serial dependence remained uncaptured by the models.

3.3.2.8 Generalized Additive Models (GAM)

In order to assess if and how environmental variables may affect baleen whale occurrence, we compared the acoustic presence of baleen whale species across the 3-year survey period to environmental variables by fitting Generalized Additive Models (GAMs) (Wood 2006). GAMs are tools to infer correlative relationships between predictor variables (e.g. environmental covariates) and response variables (e.g. daily acoustic occurrence), and are particularly useful for nonparametric datasets (Wood 2006; Zuur et al. 2009).

Sea surface temperature (SST (°C); GOES Imager) and surface chlorophyll-a concentration (Chl-a (mg m^{-3})); Moderate Resolution Imaging Spectroradiometer (MODIS) onboard the Aqua satellite) data were collected from the Environmental Research Division Data Access Program (ERDDAP) database using the NOAA Coastwatch Xtractomatic tool (http://coastwatch.pfeg.noaa.gov/xtracto/) in R (R Core Team 2017). Weekly median values of the environmental data were collected over the course of the 3-year study, and were averaged within a 10 km radius of survey sites T-1M, A-5M, and T-2M.

A 25% stratified subsample of recording days were examined for the daily acoustic occurrence of North Atlantic right whales and humpback whales at survey sites T-1M, A-5M, and T-2M (see Section 3.3.2.5 "Baleen Whale Acoustic Occurrence Analysis"). Due to the large estimated detection range for fin whales that may overlap multiple survey sites (see Section 4.1 "Baleen Whale Acoustic Detection Range Estimates"), we determined the daily acoustic occurrence of fin whales at site A-5M within the WEA. Since individual fin whale calls were simultaneously detectable across multiple MARUs, analyzing calls on all recorders would have caused pseudo-replication. Thus, we went with the most central location for reporting fin whale presence to analyze in the context of environmental covariates. Minke whales were excluded from environmental data analysis due to their rare acoustic occurrence during the 3-year survey period (see Section 4.2 "Baleen Whale Acoustic Occurrence").

Weekly median environmental variables (SST and natural log Chl-a concentration) were compared to the acoustic detection of North Atlantic Right Whales at survey sites T-1M, A-5M, and T-

2M using GAM models with a binomial distribution in R (mgcv package; Wood 2006). Weekly median environmental variables were compared to the acoustic detection of humpback whales at survey sites T-1M, A-5M, and T-2M using GAM models with a binomial distribution; a GAM model with a binomial distribution was fit for fin whale acoustic occurrence at site A-5M only. The AIC was used for model selection, and the function 'gam.check' (mgcv package) was used to assess the goodness of fit by looking at the model residuals (Wood 2006; Zuur et al. 2009). Residual autocorrelation and partial autocorrelation plots were used to assess if any serial dependence remained uncaptured by the models.

3.3.3 Acoustic Localization of North Atlantic Right Whales

The MARUs deployed at the survey sites within the WEA constitute a time-synchronized array that can be used to localize the source of species-specific signals. The position of the source of a sound that is recorded on three or more MARUs in the array can be estimated, given knowledge of the array geometry and the speed of sound (e.g. Urazghildiiev and Clark 2013). In practice, the accuracy and precision with which a given sound source (e.g. a vocalizing whale) can be localized depends primarily on the signal-to-noise ratio of the recorded sound on each MARU and on the source's actual location relative to the array; however, oceanographic and environmental conditions can also influence the ability to localize signals.

Location estimates for North Atlantic right whale up-calls were modeled using the correlation sum estimation (CSE) Locator Tool (see Appendix B) in Raven 2.0 (Bioacoustics Research Program 2018). In order to estimate the accuracy and precision of the CSE localization algorithm, we referred to empirical data from synthetic playback signals that were transmitted in the survey area during June 2017 (see Figure 3.3.1a). The 300 – 600 Hz synthetic sweep tones were played at 17 known locations along two perpendicular transect lines spanning west-east and south-north of the WEA. Synthetic signals that were recorded on three or more MARUs were processed through the CSE localization algorithm (see Appendix B), producing an estimated latitude and longitude for each locatable synthetic tone. Estimated geographic coordinates were compared to the known position of the sound source using a custom script that uses spherical geometry to compute the distance between the truth position and the position output by the CSE locator algorithm. As a measure of the precision of the result, the standard deviation was computed to be the greater of the latitude and longitude standard deviations, converted into meters.

Acoustic data were examined from the North Atlantic right whale detection algorithm mentioned above; automated detections were validated as either North Atlantic right whale detections or false positives during whale occurrence analysis (see Section 3.3.2 "Baleen Whale Acoustic Occurrence"). All false positive and questionable detections were removed from analysis.

True detections of North Atlantic right whale up-calls were reviewed in 60 s, 10 – 500 Hz time-aligned concatenated spectrograms (256-pt FFT, Hann window, 50% overlap, frequency resolution of 7.81 Hz, time resolution of 64 ms) for the occurrence of a minimum of three up-calls (arrivals) recorded on a minimum of three MARUs. The following criteria were used to determine if the arrivals were likely produced by the same source (North Atlantic right whale): 1) the arrival pattern of detections occurred on three or more sensors proximate to each other, 2) the frequency, duration, and slope of each arrival were similar, and 3) the signal-to-noise ratio was consistent between arrivals. True detections that violated the above criteria were removed from analysis.

True detections that met the above criteria (i.e. potentially locatable detections) were processed in the CSE Locator Tool in Raven 2.0 (Bioacoustics Research Program 2018). In addition to providing the estimated latitude and longitude of the source of the true detections, the CSE locator estimated times at which the up-call was expected to be recorded by each sensor in the acoustic array, given the estimated location of the calling whale. These predicted arrival times were displayed as boxes on the concatenated

spectrograms, and location estimates were considered reliable if the arrival boxes aligned properly with the actual arrivals of the whale call. Arrival boxes were visually reviewed for proper alignment in 60 s, 10 – 500 Hz time-aligned concatenated spectrograms (256-pt FFT, Hann window, 50% overlap, frequency resolution of 7.81 Hz, time resolution of 64 ms) in Raven Pro 1.5 (Bioacoustics Research Program 2015). A qualitative scoring scheme was developed to rate the alignment of the arrival boxes: 1) An arrival received a score of 1.0 if the signal was entirely within the arrival box, 2) an arrival received a score of 0.5 if the signal was ≥ 50% within the arrival box, 3) an arrival received a score of 0.25 if 25 – 50% of the signal was within the arrival box, and 4) an arrival received a score of -0.25 if < 25% of the signal was within the arrival box. The sum of scores for each arrival of a locatable call was divided by the number of visible arrivals for an overall qualitative score of the estimated location:

$$\text{Quality of Estimated Location} = \frac{Sum\ of\ arrival\ scores}{number\ of\ visible\ arrivals}$$

Arrivals with a qualitative score ≥ 0.4 were considered to have acceptable location estimates. This threshold was established after inspecting alignments with various qualitative scores. Failure of the arrival boxes to align properly with the actual arrivals of the whale call (qualitative score < 0.4) was indicative of an erroneous location estimate, and were removed from analysis.

Although a subset of true detections (n = 5496 detections; see Section 4.3 "North Atlantic Right Whale Location Estimates") did not obtain a reliable estimated location (given our methods described above), the first arrival (i.e. the survey site at which the first recording of the locatable call occurred) was annotated for all potentially locatable detections in order to determine the closest site to the sound source. The relative first arrival distribution across survey sites was compared in order to determine monthly and seasonal patterns of North Atlantic right whale movements inshore, offshore, and within the WEA.

Following methods in Rice et al. (2014), true detections with reliable location estimates were reviewed in ArcGIS (ESRI, Redlands, CA) to investigate spatial and temporal position and movement patterns of vocalizing North Atlantic right whales. Daily plots of location estimates were visually inspected to reveal patterns of sequential North Atlantic right whale up-calls that appeared to indicate the movement of a source animal. The timing of these sequential up-calls were measured to determine if they occurred within a plausible calling rate for North Atlantic right whales (Matthews et al. 2001). Detections included in putative up-call tracks were then visually inspect in Raven Pro 1.5 (Bioacoustics Research Program 2015) to compare amplitude and call characteristics; up-calls with similar amplitude, frequency bandwidth, and duration were considered likely produced by the same sound source (whale). Taking into account the curvature of the earth's surface, the distance traveled (km) between sequential up-call locations was calculated using the spherical law of cosines, where φ is latitude, λ is longitude, and R is the earth's radius (mean radius = 6,371 km):

$$\text{Distance (d)} = \text{acos}(sin\ \varphi 1\ \cdot\ sin\ \varphi 2\ +\ cos\ \varphi 1\ \cdot\ cos\ \varphi 2\ \cdot\ cos\ \Delta\lambda\ )\ \cdot\ R$$

The track speed (km/h) was calculated between sequential up-calls in each putative track to determine if they were consistent with documented swim speeds for North Atlantic right whales (Mate et al. 1997). The total distance traveled and the total time span for each putative up-call track was measured to calculate the overall up-call track speed, and the bearing (heading) of putative call tracks was calculated as follows:

$$\text{Bearing } \theta = atan2(\, sin\, \Delta\lambda \cdot cos\, \varphi 2\, , cos\, \varphi 1 \cdot sin\, \varphi 2 - sin\, \varphi 1 \cdot cos\, \varphi 2 \cdot cos\, \Delta\lambda\,)$$

where $\varphi 1, \lambda 1$ is the start point, $\varphi 2, \lambda 2$ is the end point, and $\Delta\lambda$ is the difference in longitude between the start point and the end point.

3.3.4 C-POD Validation

Despite their extensive use, studies estimating C-POD detection rates and the factors affecting the C-POD's detection accuracy are relatively scarce and have largely been conducted in shallow estuarine waters over short periods of time (Roberts and Read 2015) or at coastal sites close to shore (Nuuttila, Meier, et al. 2013). Due to their nearly global distribution, presence in nearshore habitats (Leatherwood and Reeves 1983), and frequent use of sound (Simard et al. 2010), bottlenose dolphins (*Tursiops truncatus*) have been the subject of many acoustic studies. They emit echolocation clicks with peak frequencies ranging above 100 kHz (Au et al. 1974; Wahlberg et al. 2011), but a lower frequency emphasis can occur when clicks are recorded off the beam axis (Au 1993; Au et al. 2012). Additionally, although it is known that particular click pattern characteristics, such as slow click-rates and irregular inter-click intervals (ICIs), can adversely affect C-POD detection rates (Chelonia, Ltd.), a measure of these effects and how changes in the background noise environment contribute to detection performance have not yet been investigated.

The objectives of this analysis were to evaluate C-POD bottlenose dolphin detection accuracy relative to recordings from SM3M acoustic recorders post-processed using PAMGUARD, and to determine factors affecting C-POD performance. Bottlenose dolphins are commonly sighted in the study area from May to September, with occasional occurrence during other times of the year (Barco et al. 1999; Toth et al. 2011; Roberts et al. 2016). The acoustic environment and dolphin click characteristics during PAMGUARD detections (true positive and false negative C-POD detections) were investigated to determine factors that may affect the performance of the C-POD. While we could not independently verify PAMGUARD detections, given the customization afforded by PAMGUARD and the manual verification by trained bio-acousticians, PAMGUARD results were considered a reliable indicator of dolphin occurrence at the hourly scale (Yack et al. 2009).

3.3.4.1 Acoustic Data Collection and Analysis

Data were collected at three sites: T-1C, A-5C, and W-3C (Figure 3.2d). C-POD recordings were analyzed by the C-POD.exe software provided by the manufacturer, Chelonia, Ltd. This software has click detection filter settings of "Low," "Moderate", or "High" corresponding to the probability of click trains being produced by a cetacean. PAMGUARD software (version 1.15.09 Beta; Gillespie et al. 2009) was used to visualize SM3M recordings at the corresponding time and location and to detect dolphin echolocation clicks. PAMGUARD detects clicks by first running the recording through a digital pre-filter, set as a high pass 4th order Butterworth infinite impulse response (IIR) filter at 6 kHz. The pre-filtered signal is then run through a high-pass 'trigger filter' (2nd order Butterworth IIR at 2 kHz). The trigger measures background noise and compares the signal level to the noise level. When the signal exceeds 12 dB re 1 µPa above the noise level, a click clip begins, and once the signal falls below this 12 dB threshold, the clip ends. Given the dynamic nature of the background noise, PAMGUARD generated sample noise measurements at 1 s intervals to minimize the number of false click detections caused by background noise.

Clicks detected by the PAMGUARD click detector were then analyzed by a more selective click classifier. This classifier uses the signal after it has been filtered by the trigger filter (high-pass at 2 kHz). Clicks are then classified if the energy of a test (18 – 24 kHz) frequency band exceeds that of a control (10 – 16 kHz) band by 6 dB re 1 µPa. This discriminative classifier was created to include the lower frequency of off-axis bottlenose dolphin echolocation clicks (Au 1993; Au et al. 2012). Classifier accuracy was tested on a sample of several hours of recordings that were validated by experienced bio-acousticians, who also conducted visual and aural verification of PAMGUARD detections. The presence of echolocation clicks was used as a proxy for dolphin presence. These detections were considered indicative of the occurrence of dolphins and were used to validate the C-POD detections (Roberts and Read 2015).

3.3.4.2 C-POD Detection Rate Calculations

The false positive rate (FPR), true positive rate (TPR), false negative rate (FNR), and true negative rate (TNR) of the C-PODs were calculated using definitions from Roberts and Read (2015):

	True	False
Positive	$TPR = \frac{TP}{P}$	$FPR = \frac{FP}{A}$
Negative	$TNR = \frac{TN}{A}$	$FNR = \frac{FN}{P}$

where TP was the number of true positive hours and FP was the number of false positive hours, defined as hours in which dolphin detections by the C-POD were validated or rejected (no corresponding dolphin click detection) by the PAMGUARD analysis, respectively. FN was the number of false negative hours and TN was the number of true negative hours, defined as the number of hours in which dolphins were not detected by the C-POD and the PAMGUARD analysis did or did not concurrently detect clicks, respectively. The term *P* was the total number of hours dolphins were present and *A* was the total number of hours dolphins were absent as determined by the PAMGUARD analysis. Hours in which at least one dolphin click or click train was detected were designated as detection-positive hours. If a C-POD detected dolphins when the SM3M was off during its duty cycle, that hour was removed from the analysis as the C-POD detection could not be directly validated by data from the SM3M recorder.

Positive and negative predictor values (PPV and NPV, respectively) were calculated to estimate the probability that minutes with or without detections reflected true presence or absence of echolocation clicks as determined by PAMGUARD (Roberts and Read 2015):

$$PPV = \frac{TP}{(TP+FP)}, NPV = \frac{TN}{(TN+FN)}$$

Pearson correlations between cumulative detection-positive hours by the C-POD and PAMGUARD were calculated for each deployment. Detection rate analysis was performed for C-POD results using results from the “High” and “Moderate” filters, and the “High”, “Moderate”, and “Low” filters. The number of hours between a PAMGUARD dolphin detection that was missed by the C-POD (a FN hour) to when it was detected by the C-POD (a TP hour) was calculated to determine the ability of C-PODs to detect dolphins on hourly and daily scales.

3.3.4.3 Factors Affecting C-POD Detection Performance

We examined the effects of sound characteristics, specifically of background noise and dolphin clicks, on the ability of C-PODs to detect dolphin click trains for T-1C April – June 2017, A-5C July – September 2016, and W-3C November 2016 – January 2017. During PAMGUARD dolphin detections, classified as C-POD TP or FN detections, the background noise and click sound characteristics were compared, allowing us to determine if the acoustic properties were different when the C-POD had accurately detected dolphins than when it had failed to detect them.

The TP and FN minutes were selected where clicks classified by PAMGUARD were followed or preceded by a 1 s period containing no detectable clicks when visualized in spectrograms (using Raven Pro 1.5 Bioacoustics Research Program 2015). The number of clicks per minute and ICIs from these recordings were estimated from the PAMGUARD click classifier, with ICIs greater than 2 seconds long being removed to discard gaps between click trains. The one second periods with no detectable clicks were treated as representative of the background noise at the time the dolphin clicks were produced. Each one second background noise sample was filtered (4^{th} order high-pass Butterworth at 20 kHz). The root mean square (RMS) of the sound pressure level (SPL) was calculated for both the original and filtered samples. This would indicate the SPL of the high frequency content of the background noise (corresponding to the lower frequency range of the C-POD). Peak-to-peak (P2P) SPLs of classified clicks within one second of the background noise samples were calculated using start and duration times estimated by PAMGUARD. Signal extraction and subsequent processing was performed using a custom script in MATLAB 2017a (MathWorks, Inc.).

The ICIs and click SPLs indicated the received sound level at the C-POD hydrophone, as well as click patterns that could prevent the C-POD from identifying click trains. A binomial logistic regression was used to investigate any significant differences between FN and TP detections in relation to background noise and click characteristics. The TP or FN status of the recording minute was assigned as the binomial response variable, 1 or 0 respectively. The explanatory variables were RMS SPLs of the original and high-pass filtered signals (20 – 24 kHz), mean and standard deviation of click P2P SPLs, number of clicks per minute, minimum ICI, inter-quartile range of ICIs, and location (a categorical variable for sites T-1C, T-2C, and W-3C, with A-5C as the reference level).

3.3.5 Odontocete Occurrence

3.3.5.1 Species Classification

The C-POD software is currently unable to distinguish between bottlenose and common dolphin click detections (Robbins et al. 2016). These two species are difficult to distinguish acoustically, even from their whistles (Oswald et al. 2007; Azzolin et al. 2014), so we used visual sightings to aid in assigning species to our acoustic detections. The visual sightings data were from fine-scale shipboard and aerial surveys (Barco et al. 2015; Williams et al. 2015) during 2012 – 2015 within our study area (sightings data between 38.12 and 38.50°N were included in the analysis). There were a total of 529 bottlenose dolphin and 35 common dolphin sightings from these surveys. There was only one sighting of spotted (*Stenella frontalis*) and white-sided dolphins (*Lagenorhynchus acutus*), and because of the rarity of these species they were not considered further in our analysis, although a caveat is that our acoustic detections may occasionally have included these species.

The distribution of sightings of bottlenose and common dolphins indicated temporal and spatial differences in occurrence (Barco et al. 2015; Williams et al. 2015). Each of the sightings was therefore assigned to a season (December to February, March to May, June to August, or September to November) and a distance from shore block (Figure 3.3.5.1a). Distance blocks were assigned by choosing the

midpoints between each C-POD site (Block A – within 22 km from shore; Block B – 22 – 41 km offshore; Block C – 41 – 57 km offshore; Block D – greater than 57 km offshore).

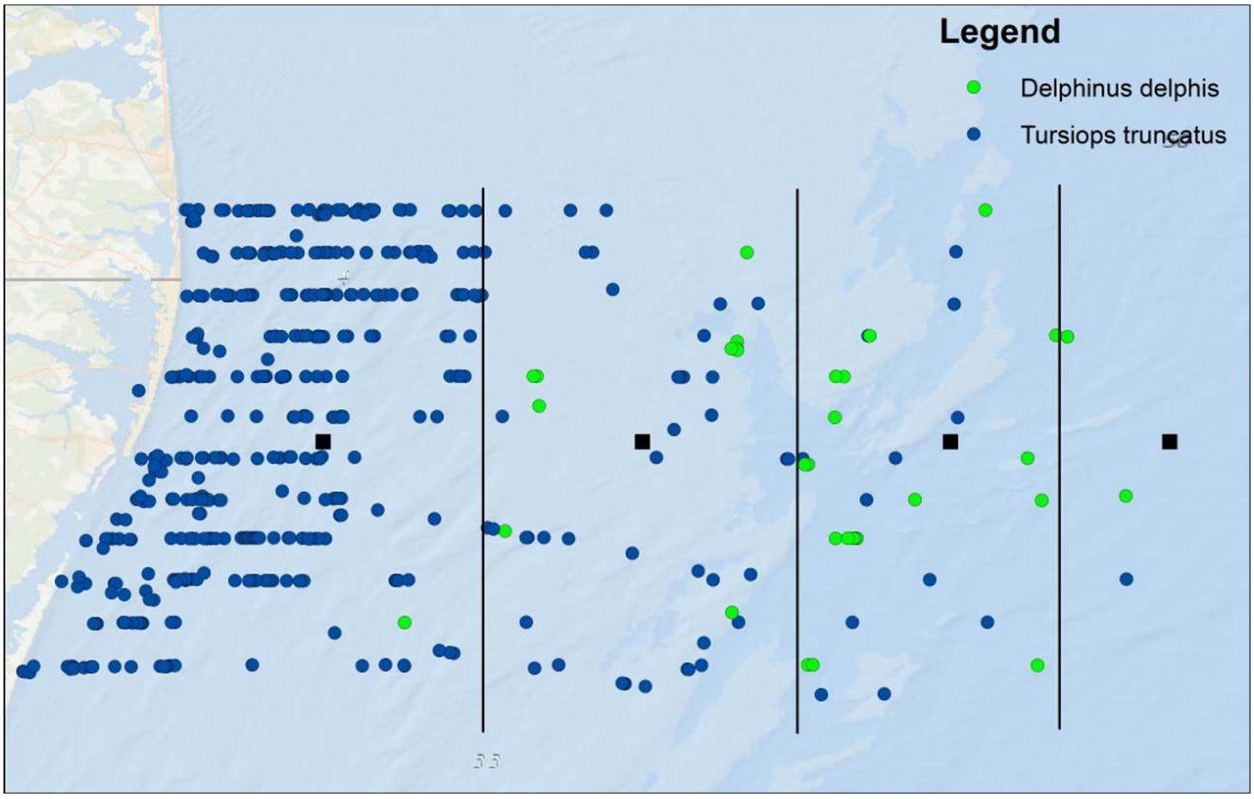

Figure 3.3.5.1a. Boat and aerial surveys of bottlenose and common dolphins
Map of bottlenose (*Tursiops truncatus*) and common (*Delphinus delphis*) dolphin sightings from boat-based and aerial surveys (Barco et al. 2015; Williams et al. 2015). The C-POD sites are shown as black squares and the vertical black lines indicate the boundaries of the four distance blocks centered at each C-POD site.

Random forest classifiers have been used to classify ambiguous detections to the species level (Oswald 2013; Roberts et al. 2016). A random forest model uses multiple decision trees to classify the response based on random subsets of the predictor variables, and outputs the mode of the classifications from each tree (Brieman 2001). Here, our response variable was the species sighted – bottlenose or common dolphin – and the predictors were season and distance block. We used a random subset of 70% of the sightings data to build the model, and the remaining 30% to test the model's performance. The default of 500 decision trees was used. Goodness of fit was assessed using receiver operating characteristic (ROC) curves (Boyce et al. 2002) and confusion matrices (Fielding and Bell 1997). The randomForest package (Liaw and Wiener 2002) and ROCR package (Sing et al. 2005) were used in R version 3.2.3 (R Core Team 2015).

3.3.5.2 Odontocete Occurrence Analysis

We used generalized auto-regressive moving average models (GARMAs) to investigate temporal trends in dolphin and porpoise detections (Benjamin et al. 2003). The response was the presence/absence of dolphins in each hour as our C-POD validation analysis indicated this was a robust measure of dolphin occurrence. Since harbor porpoises were present less frequently we used the number of minutes per hour that they were detected for our porpoise model. The explanatory variables were the same as the baleen whale occurrence analysis and in Wingfield et al. (2017) with the day of the year and time of day and also

year to investigate inter-annual variation. Julian day and hour of the day (EST) were both transformed using pairs of sine and cosine functions. The year was included as a categorical variable. We classified November 2014 – October 2015 as "Year 1", November 2015 – October 2016 as "Year 2", and November 2016 – October 2017 as "Year 3". We modelled data for each site and species separately, except at sites T-2C and T-3C, where we combined both dolphin species as there were fewer detections and greater uncertainty in the species classification.

We investigated the relationship between dolphin detections and environmental variables, using the same method and variables that we used to analyze the initial porpoise data in Wingfield et al. (2017). The response variable was the proportion of hours per week that dolphins or porpoises were detected, and the explanatory variables were weekly median sea surface temperature (°C) weekly median natural log of chlorophyll-a concentrations, and the weekly median of the fraction of the moon illuminated. We used generalized additive models (GAMs) with a Gaussian distribution to analyze the data. Week numbers were assigned using the ISO week date standard (ISO-8601). We modeled the data for each site and species separately. The occurrence of harbor porpoises during the first 18 months of the study was not significantly related to the fraction of the moon illuminated (Wingfield et al. 2017) and exploratory analysis suggested no association with the 3-year porpoise or dolphin occurrence. We therefore did not include this variable in our final models.

Roberts et al. (2016) developed habitat-based density models for several species of cetaceans, including harbor porpoises, off the US east coast using aerial and boat-based sightings data. A porpoise positive hour (PPH) is an hour during which the C-POD software identified at least one porpoise click train. Roberts et al.'s monthly density estimates (2016) were compared with the median number of PPHs per day, total PPHs per month, maximum PPHs per day, and proportion of days per month harbor porpoises were present in the study area offshore of Maryland based on our acoustic detection data using Spearman's rank correlation tests for T-1C, A-5C, T-2C, and T-3C (Brookes et al. 2013; Williamson et al. 2016).

3.3.6 Bottlenose Dolphin Abundance and Behavior

3.3.6.1 Individual Dolphin Identification from Signature Whistles

Bottlenose dolphins have the additional ability to encode individual identity information through the frequency modulation patterns of their whistles (Janik 2009). These frequency modulated whistles, known as signature whistles, are unique to each individual bottlenose dolphin. Signature whistles are developed early in the dolphin's life as a means of communicating identity and maintaining group cohesion (Deecke and Janik 2006). Once a calf develops its own signature whistle, the whistle remains stable for many years, if not the rest of the dolphin's life (Sayigh et al. 1990). In the wild, almost half of all whistles emitted by bottlenose dolphins can be classified as signature whistles (Buckstaff 2004). The frequency of occurrence of these whistles increases upon meeting other dolphins and during periods of separation from other individuals (Quick and Janik 2012).

Previous studies have used underwater recording and analysis methods to successfully identify signature whistles (Sayigh et al. 1990; Deecke and Janik 2006; Quick and Janik 2012; Gridley et al. 2014). By applying signature whistle identification methods described in these studies to passive acoustic data sets, it may be possible to monitor dolphins over long periods of time at sea. This acoustic analysis gives insights into the movement, population, and frequency of occurrence of individuals within the detection area and allows for changes to be tracked over time.

Using signature whistle identification methods as described by Janik (2006), the goals of individual dolphin identification were to:

- Determine the number of unique signature whistles collected via passive acoustic monitoring to estimate the number of dolphins in the detection area within the Maryland WEA at A-5C and inshore at T-1C.
- Determine how frequently individual dolphins visit A-5C and T-1C based on matching identical signature whistles during our acoustic recording time series to identify whether there is site fidelity.
- Determine whether the same dolphins are returning to the Maryland WEA (A-5C) every year and amongst seasons by comparing signature whistles from 2016 and 2017 during summer and winter.

3.3.6.1.1 Defining and Detecting Signature Whistles

In the summer of 2016 between 27 July and 24 September, an SM3M was deployed at A-5C, 28 meters deep and 30 kilometers off the coast of Ocean City, Maryland (Figure 3.2d). Two additional deployments at this site occurred during the winter of 2017 on 11 January through 5 April, and the summer of 2017 on 7 June to 2 October. Between 13 June and 12 September 2017, a second SM3M recorder was deployed at T-1C, a site 20 meters deep and 12 kilometers off Ocean City, Maryland (Figure 3.2d). Signature whistles were identified from recordings at these two locations. All acoustic recordings were reviewed for dolphin whistles at T-1C. However, this was highly time consuming. For the recordings from site A-5C, the PAMGUARD software (version 1.15.09 Beta, Gillespie et al. 2009) was first used to detect the occurrence of dolphin whistles and then the data were subsampled whereby 2 hours of recordings with the highest number of detected whistles were reviewed for each day. The selection of 2 hours was based on an analysis of the number of unique individual signature whistles identified from the T-1C recordings in relation to the number of hours per day reviewed. A mean of 22%, 63%, 71%, and 75% of individual signature whistles were identified for 1, 2, 3 and 4 reviewed hours per day. In order to balance the manual review time and the number of signature whistles identified, a subsampling regime of 2 hours per day was selected as the most effective trade-off.

We used the definitions by Janik et al. (2013), and Gridley et al. (2014) to identify signature whistles. Our identification process heavily relied on a bout analysis method of signature whistle identification known as SIGnature IDentification (SIGID), developed by Janik et al. (2013). SIGID is a conservative signature whistle identification method, but highly restricts the likelihood of false positives.

Whistles emitted by dolphins can be broken into smaller fragments called contours. These contours are narrow band tonal signals with the fundamental frequency above 3 kHz. Dolphins often form whistles by looping these contours multiple times continuously, or looping them with a separation gap of less than 250 ms. Sometimes contours are not looped at all and instead form a standalone whistle. This looping of contours is characteristic of both signature and non-signature whistles (Figure 3.3.6.1.1a). In our analysis, we included contours that were greater than 1 ms in duration and excluded any harmonics (Gridley et al. 2014).

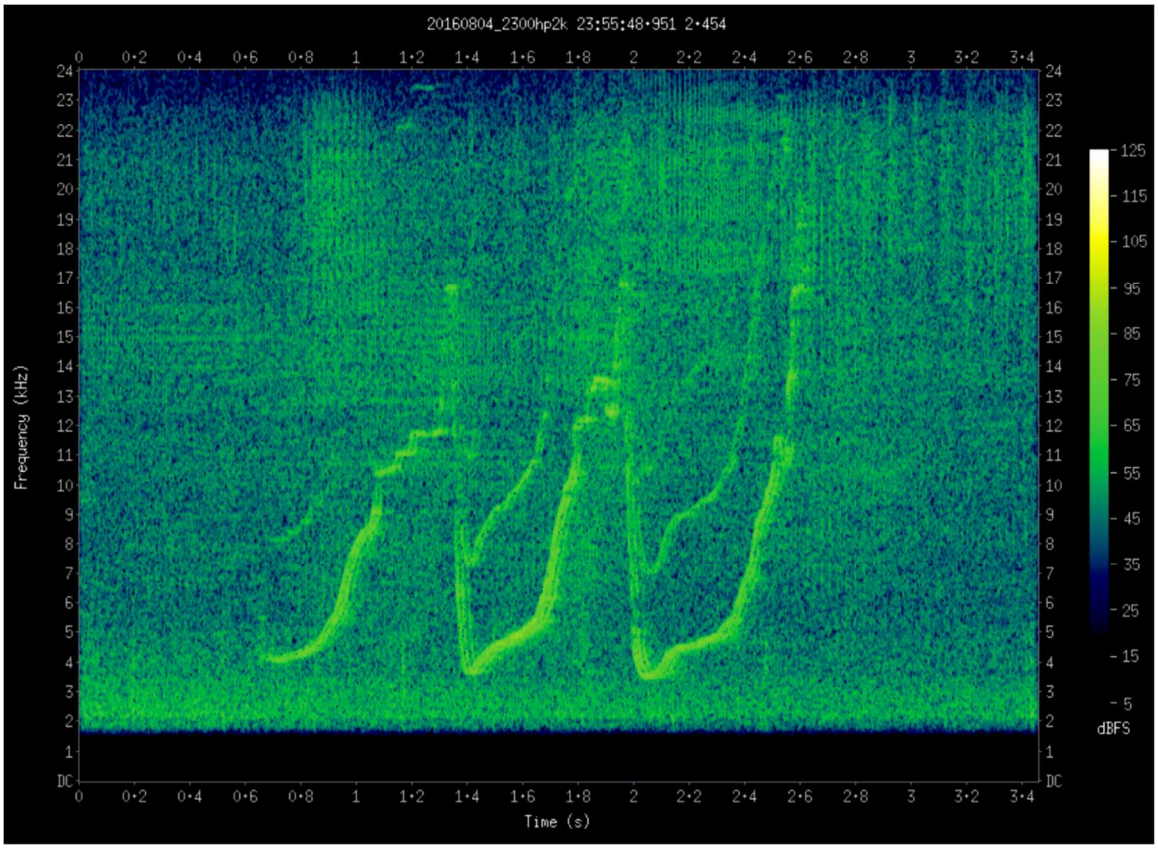

Figure 3.3.6.1.1a. Signature whistle spectrogram
Spectrogram of an identified signature whistle recorded on 4 August 2016 at 23:55:48 EST.

The whistle's context partly separates signature whistles from whistles of other types. Often, these signature whistles are delivered in bout patterns where the same whistle is repeated multiple times (Figure 3.3.6.1.1b). A bout pattern of signature whistles can be described as a group of consecutive signature whistles where the start of one whistle is between 1 and 10 s after the end of the immediately preceding whistle in the bout. This gap between whistles is known as the inter-whistle interval (IWI). We identified bouts of signature whistles when there were three or more consecutive signature whistles, with each whistle having an IWI of 1 – 10 s (Janik et al. 2013; Gridley et al. 2014). By identifying these bouts of whistles, we were able to identify individual signature whistles contained within bouts.

Following these signature whistle definitions and detection guidelines, signature whistles were detected manually in Raven Pro 1.4 (Bioacoustics Research Program 2011). With the duty cycle, the SM3M recorded audio for either two minutes or five minutes at a time depending on the deployment. Selections were only made on clearly defined whistles with high signal to noise ratios (Heiler et al. 2016). After selecting signature whistles, a custom-written computer script was used to cut smaller individual audio clips containing individually identified signature whistles.

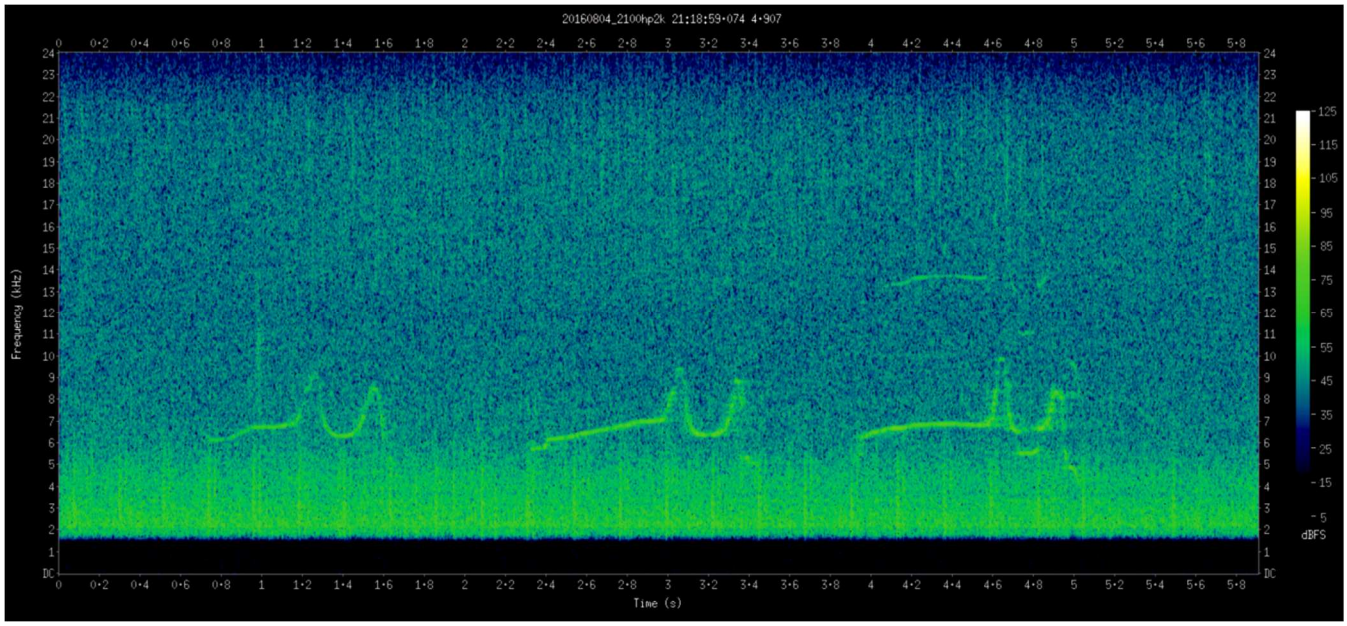

Figure 3.3.6.1.1b. Signature whistle bout spectrogram
A bout of three signature whistles recorded on 4 August 2016 at 21:18:59 EST.

3.3.6.1.2 Categorization of Signature Whistles

Signature whistles were compared and sorted into groups based on similarities in frequency modulation pattern. Since signature whistles are unique to individual bottlenose dolphins, each group represented the presence of a unique dolphin. There have been various approaches to signature whistle categorization, which can be classified broadly into two methods: manual sorting where one or more people sort whistles into groups visually and unsupervised automated sorting through the use of computer software or a neural network. Many studies report using a combination of the two methods (Quick and Janik 2012; Janik et al. 2013; Gridley et al. 2014). In our approach, we relied heavily on the use of automated sorting via a neural network. After automated sorting, we reviewed the results and verified categories manually.

Before conducting neural network categorization of the signature whistles, the contours of each signature whistle were extracted using the Beluga software. Beluga is a sound analysis program written in MATLAB by researchers at the University of St. Andrews, and is specifically designed to extract contours for neural network sorting. Each signature whistle audio clip collected in Raven was loaded into Beluga. Once clips were loaded, the software generated spectrograms with an FFT length of 2048, a frame length of 512, and an overlap of 87% between frames. From these spectrograms, signature whistles were extracted and saved as MATLAB readable files for neural network sorting.

After contour extraction in Beluga, signature whistles were sorted using ARTwarp (Deecke and Janik 2006), a MATLAB based neural network. ARTwarp uses two main variables to fine tune the sorting process. First, the time warping function allows each contour to be slightly sped up or slowed down. Frequency modulation patterns of signature whistles of the same type have little variation, but the duration of identical whistles may vary slightly (Janik et al. 1994). This warping function takes into account small changes in whistle duration by speeding up or slowing down contours to test them more accurately against signature whistles with the same modulation pattern. Second, the vigilance parameter dictates the degree of similarity between whistles required to be considered part of the same category (Deecke and Janik 2006). In our study, a warping function of three was used in combination with a

vigilance parameter of either 94% based on parameters used by Janik et al. (2013) and Gridley et al. (2014) for whistles from A-5C and 98% for T-1C. Based on trials using thresholds of 86% to 98%, this higher threshold for T-1C was selected to reduce the number of false positive signature whistle matches within the large data set. Upon running signature whistle contours through ARTwarp, categories of signature whistles were generated and manually verified.

3.3.6.1.3 Data Analysis

After signature whistle categorization via ARTwarp, we analyzed the number of unique categories of signature whistles. These unique categories each represented a group of identical signature whistles emitted by an individual bottlenose dolphin, and the number of unique categories gives information on the minimum number of bottlenose dolphins in our study area. By analyzing the date of occurrence of signature whistles within signature whistle categories, we examined whether bottlenose dolphins were returning to the study area and how frequently.

To determine the detection range of our acoustic recorder, we selected 20 high-quality, clearly defined signature whistles. Based on the loudness and clarity of these selected whistles, we assumed that the dolphins emitting these whistles were in close proximity to our acoustic recorder. Using Raven bioacoustics software, we then examined the acoustic recordings from the same type of device at sites located 3 km, 8 km, and 20 km from our recorder to determine if the same whistle was detected across different sites.

3.3.6.2 Dolphin Foraging Behavior

Population-level consequences of disturbance may be greater if animals are interrupted or displaced whilst performing critical functions, such as feeding, that lead to a reduction in growth or survival (King et al. 2015). We therefore investigated dolphin foraging behavior to determine when and where it occurred. Optimal foraging theory predicts that individuals will aim to maximize their fitness by maximizing their energetic food intake whilst minimizing the time and energy costs of searching and handling prey (Schoener 1971; Krebs et al. 1974). When predators feed on patchily distributed prey, they are expected to spend more time searching for food in the vicinity of recent prey captures and to leave the patch when the capture rate reaches the average level in the habitat, assuming that a predator's food intake rate will decline with time within the patch (Charnov 1976). This behavior, known as area-restricted search (ARS), results in predators remaining in localized areas to forage once prey have been encountered because of the higher probability of further prey occurring within that patch (Pyke 1984; Kareiva and Odell 1987). This behavior has been observed in many species and empirical studies have mainly involved small invertebrates and birds (e.g. Evans 1976; Zach and Falls 1977; Williamson 1981; Amano and Katayama 2009). However, there been relatively few studies examining the foraging predictions of area-restricted search theory in free-ranging large predators.

In order to determine whether ARS behavior is initiated by prey capture in large marine predators, odontocetes are a good case study because they use echolocation for hunting, which can be detected using passive acoustic monitoring. As they approach prey, odontocetes produce echolocation clicks more frequently, known as a feeding buzz, allowing the identification of feeding events at a high temporal resolution. In this analysis, we used an echolocation click detector to identify fine-scale feeding activity by bottlenose and common dolphins to determine if they were exhibiting ARS behavior and if it was related to feeding success. Specifically, we tested the hypotheses: 1) the occurrence of feeding increases the likelihood of further feeding indicating there is a higher probability of encountering other prey items nearby, 2) animals remain longer in a patch when feeding occurs at the start of an encounter, and 3) the foraging pattern is consistent across species.

Data from November 2014 to April 2017 were used from our four core C-POD sites at approximately 15 km intervals: T-1C, A-5C, T-2C, and T-3C (Figure 3.2d). On a subset of the deployments in 2016, data from an SM3M acoustic recorder on the same mooring sampling at 48 kHz were used to verify the dolphin feeding detections (Figure 3.2d).

3.3.6.2.1 Encounter Classification

In order to identify distinct encounters, we used a subset of the data on the minute scale for a full year from T-1C because it was the site with the most dolphin detections. Only clicks of CetHi and CetMod quality were used. We then filtered the data to only include minutes during which dolphins were detected and examined the distribution of time intervals between dolphin detections to establish a threshold for defining separate encounters.

3.3.6.2.2 Foraging Inter-Click Interval Threshold

Following the procedure in Pirotta et al. (2014), we used a Gaussian mixture model of the inter-click intervals (ICIs) to define a threshold for foraging behavior. We extracted ICI data for each minute during 2015 and 2016 from T-1C so that we included different seasons and any potential inter-annual and seasonal variability in ICIs. We ran the Gaussian mixture model with three components on the natural log of the ICIs using the package "mixtools" (Benaglia et al. 2009) in R (R Core Team 2015). We chose three component distributions, meant to represent feeding buzzes, regular ICIs, and long ICIs between click trains (Pirotta et al. 2014).

3.3.6.2.3 Validation of Foraging Activity

C-PODs are known to be conservative in their click train detections (Roberts and Read 2015), and consequently may miss feeding buzzes leading to an underestimation of the number of minutes with foraging activity. In order to determine minutes that were incorrectly classified as non-foraging when foraging activity (feeding buzzes) occurred, we analyzed the acoustic recordings from the SM3M hydrophone, which was deployed alongside the C-POD during deployments in February – April 2016 and May – July 2016 at T-1C and July – November 2016 at A-5C. The duty cycle of the SM3M recorder for the T-1C deployments were ten minutes on and two minutes off and at A-5C was two minutes on and four minutes off. When the ICI from the C-POD was at or below the foraging ICI threshold indicating foraging activity and audio and visual inspection of a spectrogram of the SM3M acoustic recording concurred that a feeding buzz was present during that minute, it was labeled a true positive minute. A false negative minute was when a feeding buzz was identified in the SM3M recording, but the ICI from the C-POD had not met the foraging threshold. A false positive minute was one in which the ICI from the C-POD indicated foraging activity but the SM3M recording did not contain a detectable feeding buzz and a true negative minute was when both devices agreed that no feeding buzzes and hence foraging activity had occurred.

In order to identify predictors of missing feeding buzzes and correct the underestimation of foraging activity from the C-POD data, we used a random forest model. The response was a logical variable (True/False) indicating for each minute whether a feeding buzz was missed or not. The possible predictors included were hour of the day, season (May – September and October – April), minutes since the previous occurrence, minutes to the next occurrence, ICI from the C-POD data at the current, previous and next occurrence, and behavioral state based on the ICI from the C-POD (foraging or not foraging) for the current, previous and next minute. We used a random subset of 70% of the sightings data to build the model, and the remaining 30% for testing the model's performance. We used training data to train different versions of the random forest with default options and with class weights adjusted to achieve approximately the correct proportion of missed feeding buzzes as identified from the SM3M recordings.

The adjustments were made using the training data only and performance of the models assessed using the testing data. We used the final random forest model to predict when there were missed feeding buzzes in the remainder of the C-POD dataset (when there were no corresponding SM3M acoustic recordings) and converted minutes with predicted occurrences of missed feeding buzzes from being classified as non-foraging to foraging.

3.3.6.2.4 Behavioral State Transition Probabilities

For each location and dolphin species, we created a time series of behavioral states recorded each minute within a dolphin encounter. The behavioral states were 'foraging', 'not foraging', and 'unknown'. The last state was assigned to the minutes within an encounter when dolphins were not specifically detected by the C-POD, but were considered present based on our encounter threshold (see Section 3.3.6.2.1 "Encounter Classification"). Only encounters with at least 5 minutes of C-POD detections and at least one minute with foraging were included in this and all further analysis. Encounters with more than 60% of minutes classified as 'unknown' were not included. We applied a statistical test based on the $\chi 2$ statistic to test the null hypothesis (H_0) of Markov property (Anderson and Goodman 1957; Kullback et al. 1962). If the test rejected H0, then we applied the $\chi 2$ test to second-order sequences. Such sequences were created by joining consecutive states in a sliding window of length two. The higher order brings more combinations, but the corresponding transition probability matrix has structural zeros because the windows for aggregating the first-order states are sliding (overlapping). Thus, a selection of only three states is possible at each transition. For example, after a state not foraging-foraging, the possible states are foraging-foraging, foraging-not foraging, and foraging-unknown (Zucchini et al. 2016).

3.3.6.2.5 Factors Affecting Encounter Duration

The C-PODs have a detection range of up to 1.8 km (Nuuttila, Thomas, et al. 2013). Detections during an encounter where therefore considered within a patch of this radius. Using the methodology of survival analysis, we modeled time to event, T, which is the encounter lengths in minutes (analogue of survival times) and the event was that dolphins left the area as indicated by the end of the encounter. This was examined using a hazard function, which assesses the instantaneous risk of dolphins leaving the area at time t, conditional that they were present until that time (Fox 2008). We used a Cox proportional hazards model to assess the influence of covariates on the encounter duration and the likelihood of dolphins leaving the area. These covariates were the proportion of minutes classified as foraging within the whole encounter, during the first and second halves of the encounter, during the first, second and third terciles of the encounter, difference and absolute difference in proportion of foraging between the two halves or three terciles of the encounter, whether foraging occurred in the first minute of the encounter, and the season. A hazard ratio of 1 indicates no effect of the covariate, a hazard ratio less than 1 reduces the hazard (more likely to stay and have longer encounter duration), and a ratio greater than 1 increases the hazard (more likely to leave and have shorter encounter duration). The analysis was performed separately for bottlenose and common dolphins.

3.3.6.3 Dolphin Response to Storm Events

Understanding the responses of cetaceans to natural events, such as storms, helps to provide insight into their effects and to distinguish these disturbances from those caused by anthropogenic activities. During storms, ambient noise levels are elevated, and increased turbulence and mixing can rapidly alter the physical structure of the water column. These changes can affect many marine species, including cetaceans, either through direct displacement, or indirectly through movement of their prey. Low-frequency whale calls are more easily masked by the increased sound levels created during storms, and we therefore selected dolphins, which have higher frequency calls, as our focal species for analyzing

their response to disturbance caused by storm events. This approach could also be applied to other marine species that may be impacted.

3.3.6.3.1 Storm and Environmental Data

Storms that occurred during the summer and autumn in the study area were estimated using data obtained from the National Oceanic and Atmospheric Administration's (NOAA's) National Center for Environmental Information (NCEI) database and storm tracks from the National Weather Service's National Digital Forecast Database. Summer and Autumn storms were chosen for analysis because dolphins are most common in this coastal region during those seasons (Barco et al. 1999; Toth et al. 2011; Roberts et al. 2016). To determine the effects of the storm, the data were divided into an equal number of days (n = 14) for each of the before, during, and after storm periods. In 2016, tropical storm Hermine passed through the study area on 3 – 8 September. Therefore, 17 – 30 August, 31 August – 13 September, and 14 – 27 September were considered the before, during, and after periods, respectively, for 2016 (Table 3.3.6.3.1a). In 2017, tropical storms Jose and Maria moved through the region on 19 – 23 and 28 – 30 September, respectively. Consequently, 3 – 16 September, 17 – 30 September, and 1 – 14 October were the respective before, during, and after periods (Table 3.3.6.3.1a). Data from 2015 were used as a control because there were no tropical storms in this region during the correlating storm periods.

Table 3.3.6.3.1a Dates for the fourteen days used for periods before, during, and after the storm for each year

Year	Before	During	After
2016	17 – 30 August	31 August – 13 September	14 – 27 September
2017	3 – 16 September	17 – 30 September	1 – 14 October

Sea surface temperature anomaly (°C, SSTa) data were extracted from NOAA's ERDDAP database. Data were obtained from the Group for High Resolution Sea Surface Temperature (GHRSST), and Level 4 sea surface temperatures were produced with four-day latency as a retrospective dataset and with one-day latency as a near-real-time dataset (v4.1; https://podaac.jpl.nasa.gov/dataset/MUR-JPL-L4-GLOB-v4.1).

3.3.6.3.2 Acoustic Data Analysis

Data were analyzed from the four core C-POD sites (T-1C, A-5C, T-2C, T-3C; Figure 3.2d). Only click trains classified as being of high and moderate qualities by the C-POD's KERNO classifier were included in the analysis. Underwater sound measurements were obtained from the MARUs. The acoustic data were processed using the Raven-X toolbox (Bioacoustics Research Program, Cornell University) in MATLAB (Mathworks, Inc.). The metric of equivalent continuous sound pressure level (L_{eq}) was used to calculate the root-mean-square (rms) pressure within one-hour time bins to represent the ambient sound levels. These one-hour time bins were then averaged to obtain the average daily ambient sound levels.

3.3.6.3.3 Dolphin Occurrence and Behavior Metrics

To determine the effect of storm activity on dolphin occurrence and behavior, click data from the C-PODs were analyzed. The daily dolphin encounter metrics calculated included the average dolphin

click train duration, average inter-click intervals (ICIs), number of encounters, encounter length, and proportion of minutes per encounter spent foraging for each day. Because C-PODs are known to be conservative indicators of dolphin presence (Garrod et al. 2018), encounter duration was defined as the time during which a C-POD detected dolphins with up to 37 minutes between detections (threshold based on the distribution of detections and consistent with Bailey et al. 2010). Foraging behavior was defined as the presence of a buzz with an ICI of less than 9.201 ms, known as a feeding buzz (Carlström 2005; Pirotta et al. 2014), and the percentage of time spent foraging in an encounter was calculated.

3.3.6.3.4 Statistical Analysis

Changes in dolphin detection metrics across years and periods to determine the effect of the storms were analyzed using GARMAs. This type of model is used for non-Gaussian time-series data with potentially time-dependent covariates. The response variable in each model was a single detection metric (dolphin click train duration, average ICIs, number of encounters, encounter length, and proportion of minutes per encounter spent foraging), using the storm period (before, during, after) and the year (control: 2015 and storm: 2016 and 2017) as the explanatory variables. Models included an interaction term for the year and period to control for inter-annual or seasonal variation and to identify when there were significant effects related to the storms. Separate models were fit for each storm year: 2016 and 2017. Models were fit in the statistical software R (R Core Team 2017) using the package gamlss.util (Stasinopoulos et al. 2016). Models were selected using Akaike Information Criterion (AIC).

3.3.7 Ambient Noise Analysis

3.3.7.1 Sound Level Analysis

Acoustic data were processed using the Raven-X toolbox (Cornell Bioacoustics Research Program, Ithaca, NY) in MATLAB using a Hann window with zero overlap, a fast Fourier transform (FFT) size where Δ *time* = 1 s and Δ *frequency* = 1 Hz. We used the metric of equivalent continuous sound pressure level or L_{eq} (dB re: 1 µPa [rms]) to represent the average unweighted sound level of a continuous time-varying signal of pressure (Morfey 2001) over specified time intervals. The resulting root-mean-square pressure is expressed by:

$$L_{eq} = 10log_{10}\frac{1}{T}\int_{0}^{T}\left(\frac{P_m^2(t)}{P_{ref}^2}\right)dt$$

where T is the time interval, P_m is the measured sound pressure, t refers to time, and P_{ref} is the reference pressure of 1 µPa. Percentiles of the resulting L_{eq} values were used to quantify spatial and temporal variation in ambient noise levels.

Long-term spectrograms were generated to visually represent ambient noise variation in the time and frequency domain, where L_{eq} values were averaged within discrete 1-hour time bins. While the MARUs recorded continuously, the AMARs were duty-cycled with differing sample rates and bit-depths between cycles, therefore the L_{eq} values that were averaged within each 1-hour time bin for the AMARs were based on the available data within that hour of time, which were then used to represent noise levels for the hour. Spectrograms were generated with linear and 1/3rd octave frequency scales.

Since 1/3rd octave bandwidths approximates the frequency sensitivity of the mammalian (and marine mammal) ear (Southall et al. 2007), frequency bandwidths based on 1/3rd octaves were selected to represent the frequency band in which each target species hearing is potentially most sensitive (Table

3.3.7.1a). The bandwidth of 1/3rd of an octave is the cube root of $2(2^{1/3})$ of the highest frequency multiplied by the cube root of the lowest frequency.

Table 3.3.7.1a Referenced signal type and frequency band of the four baleen whale target species

Species	Target Signal	Frequency Band	1/3rd Octave Band (lower – upper)
North Atlantic Right Wwhale	Up-call	71 – 224 Hz (Hatch et al. 2012)	70.8 – 224 Hz
Humpback Whale	Song	29 – 2480 Hz (Dunlop et al. 2007)	28.2 – 708 Hz
Fin Whale	20 Hz pulse	15 – 25 Hz (Weirathmueller et al. 2013)	17.8 – 28.2 Hz
Minke Whale	Pulse train	50 – 300 Hz (Risch et al. 2014)	44.7 – 355 Hz

Power spectral density (PSD) plots of L_{eq} values were used to statistically compare the dominant frequencies of the following survey sites representing spatial regions inshore, offshore, and within the WEA: T-1M, A-5M, A-7M, and T-2M. The PSD plot captures variation of sound pressure levels across the frequency domain of long-term ambient noise data (Wenz 1972) by representing the sound pressure level (dB re: $1\mu Pa^2/Hz$) as a function of frequency in the signal (Merchant et al. 2013). Here, data from the specified time duration and site location are represented using three percentiles (5^{th}, 50^{th}, and 95^{th}).

To illustrate the overall variation in ambient noise levels between sites, we calculated the cumulative percent distribution of L_{eq} values at each recording site and frequency band, which illustrates the percentage of time that sound pressure levels reached a particular L_{eq} value. The cumulative percent distribution allows for a direct comparison of the statistical noise characteristics of each site within a particular frequency band. Species-specific frequency bands (Table 3.3.7.1a) were used to represent the range in which each whale species' hearing is likely most sensitive, and the bandwidth in which each whale species' target vocalizations occur (Dunlop et al. 2007; Hatch et al. 2012; Weirathmueller et al. 2013; Risch et al. 2014). Additionally, we looked at the full frequency band (10 – 800 Hz 1/3rd octave center frequencies), which reflects the effective frequency band recorded by the MARU as a result of the high- and low-pass filters.

To validate the accuracy of noise measurements for the MARU, we conducted a statistical comparison of 1-hr L_{eq} values between the AMAR and the co-located MARU at site A-8M deployed during Deployment 02 (16 April 2015 – 21 September 2015). The AMAR hydrophone is more sensitive and a rigorous noise characterization process had previously been conducted that provided an opportunity for a similar analysis to be conducted for the MARUs. We used the full frequency band and subsampled every 6^{th} hour (i.e. 25% stratified subsample) for temporal independence. A paired t-test was performed in JMP Pro 12 (SAS) to determine if there was a significant difference in corresponding hourly L_{eq} values between the AMAR and co-located MARU.

To illustrate how often the sound levels surpassed the 120 dB take threshold, as used for U.S. regulatory evaluations of impact (see Southall et al. 2007 for a summary and critique of this threshold), we plotted the percentage of time that exceeded 120 dB per site. To illustrate acute incidences of sound levels that surpassed the 120 dB take threshold in the full frequency band, we plotted the percentage of 10

s time bins per hour that exceeded 120 dB per site. Additionally, to illustrate chronic exposure, we plotted the percentage of hours throughout the survey period that surpassed the 120 dB take threshold for each focal species frequency band and the full frequency band.

3.3.7.2 Dolphin Whistle Characteristics in Relation to Ambient Noise Levels

Odontocetes have complex social structures that are likely maintained through their diverse and individually specific vocalizations (Connor et al. 1998). Bottlenose dolphins produce whistles that serve a critical role in social communication, conveying individual identity and other information through contour shape (Janik et al. 2006). Vessel traffic and noise have been found to affect marine mammal foraging behavior (Pirotta et al. 2015; Blair et al. 2016; Wisniewska et al. 2018) and the sound frequency of their calls (Heiler et al. 2016; van Ginkel et al. 2017). However, little is known about how the complexity of their calls changes in response to real-time ambient noise levels experienced by the animals. We addressed this by investigating whether the acoustic characteristics of bottlenose dolphin whistles changed in response to concurrent ambient noise levels. Our study area experiences relatively high levels of vessel traffic that we hypothesized would result in regularly elevated noise conditions and could consequently impact dolphin call patterns. We were unable to conduct a similar analysis of baleen whale species compared to ambient noise because: 1) mysticete calls were lower in number than dolphins, so we were limited by a relatively low sample size, 2) daily presence is not a sufficient resolution to compare whale occurrence with noise levels, since ambient noise levels vary on shorter timescales, and 3) mysticete calls overlap with anthropogenic and environmental noise, so there is a risk of masking of whale calls during higher ambient noise levels.

3.3.7.2.1 Data Collection and Analysis

Acoustic recordings were collected using a bottom-mounted SM3M during July – September 2016, located within the Maryland WEA at A-5C (Figure 3.3.7.2.1a). Spectrograms were visually inspected for bottlenose dolphin whistles with high signal-to-noise ratios in Raven (version 1.5, Bioacoustics Research Program 2015) (Heiler et al. 2016). For each whistle selected, 11 characteristics were measured: duration; start and end frequencies; minimum, maximum, and delta frequency (maximum – minimum frequency); presence of harmonics, and number of extrema, inflection points, saddles and steps (Figures 3.3.7.2.1b and 3.3.7.2.1c).

Ambient noise levels were calculated for the 2 second period prior to selected whistles (Marley et al. 2017). PAMGUARD 's Noise Monitor Module was used to measure root-mean-square (rms) sound pressure levels in both the broadband signal (2 Hz – 24 kHz) and one-third octave band levels (TOLs) centered on frequencies from 12.5 Hz to 20 kHz. Ambient noise levels for each two-minute recording across the entire deployment period were also calculated to determine how frequently relatively high noise levels (>120 dB re 1 µPa rms, the U.S.A. marine mammal regulatory threshold for behavioral disruption from continuous noise) occurred.

Spectrum density levels (SDL) were calculated to compare between different TOLs and broadband noise using the formula below, in which the received sound level is in dB, Δf is the difference between the bandwidths' upper and lower limits, and the SDL units are dB re 1µPa^2/Hz.

$$SDL = ReceivedSoundLevel - 10Log_{10}\Delta f$$

To evaluate whistle characteristics from as many dolphins as possible within the population, whistles were selected from multiple days and encounters, where a new encounter occurred when there was > 37 minutes between detections (based on the distribution of detections across the deployment period).

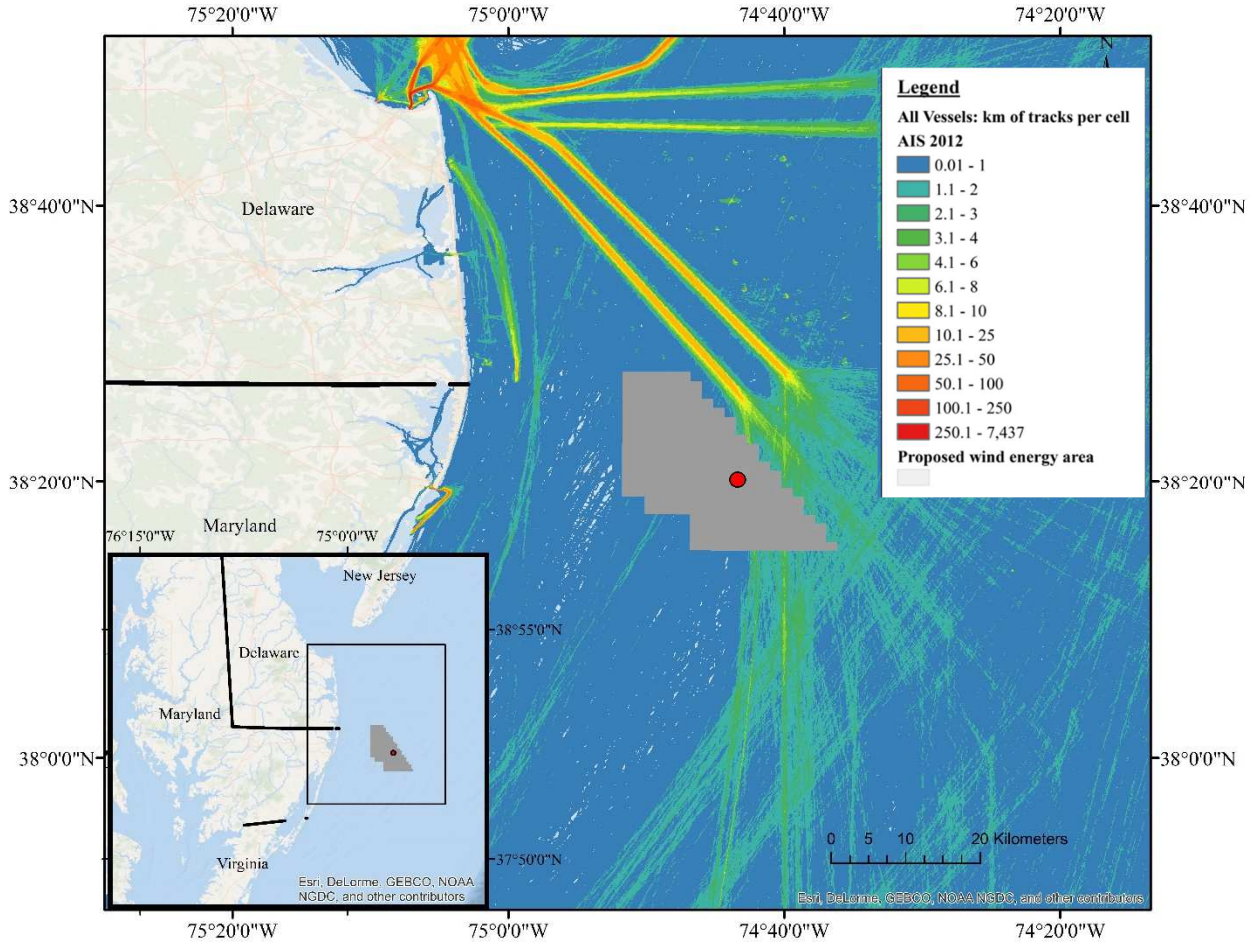

Figure 3.3.7.2.1a. Acoustic data collection site A-5C and 2012 commercial vessel traffic
Map of proposed wind energy area (shaded grey blocks), density of commercial vessel traffic (from automatic identification system (AIS) data for 2012 from marinecadastre.gov), and our hydrophone (red circle).

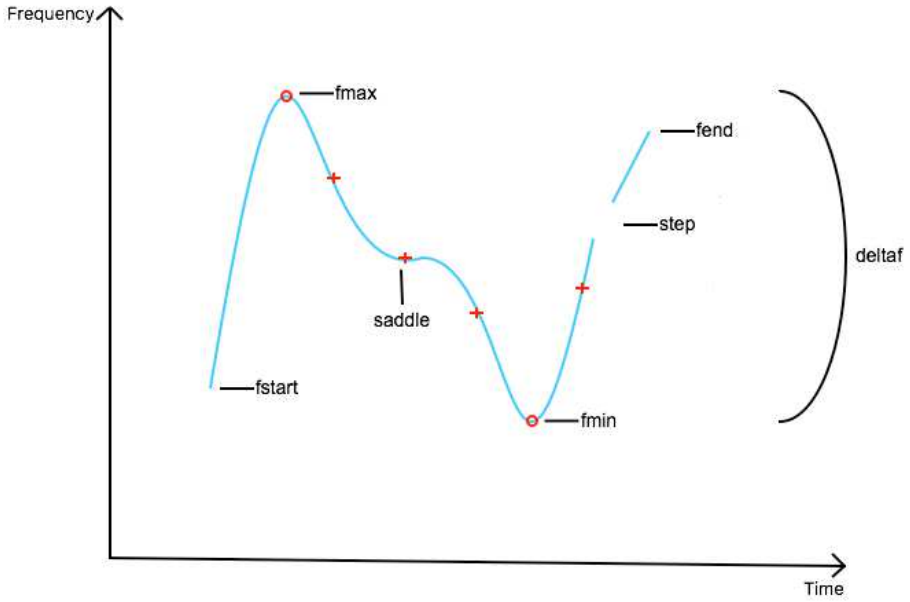

Figure 3.3.7.2.1b. Measured whistle characteristics
Whistle characteristics measured were fstart = start frequency, fend = end frequency, fmax = maximum frequency, fmin = minimum frequency, deltaf = delta frequency (fmax-fmin), inflection points = +, and local extrema = O.

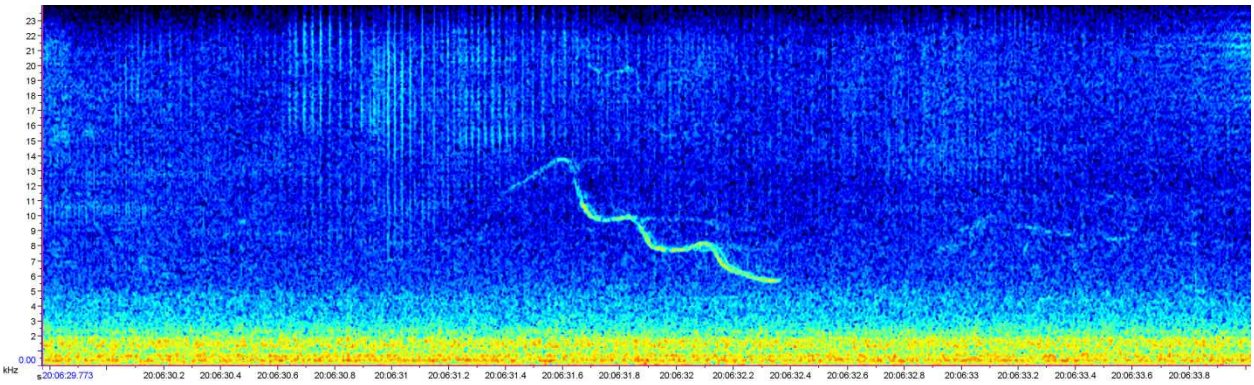

Figure 3.3.7.2.1c. Example spectrogram of a dolphin whistle

3.3.7.2.2 Statistical Analysis

The effect of ambient noise levels at each frequency band was tested on the suite of whistle characteristics using a Multivariate Analysis of Variance (MANOVA). Generalized Estimating Equations (GEEs) were then fitted with each whistle characteristic as the response variable and the suite of ambient noise levels that were statistically significant in the MANOVAs as the explanatory variables. The encounter identification number (where an encounter consisted of continuous detections) was treated as the cluster grouping with an exchangeable working correlation structure. A Holm-Bonferroni sequential correction for multiple tests was applied (Holm 1979). All statistical analyses were conducted in the software R (R Core Team 2018), and the GEEs were fit using the geepack package in R (Halekoh et al. 2006).

4 Results

4.1 Baleen Whale Acoustic Detection Range Estimates

Fin whale detection range estimates crossed the entire width of the continental shelf and included areas beyond the shelf edge under both median (210 km) and 5th percentile (440 km) noise conditions (Table 4.1a). Spring had the lowest median noise conditions in the fin whale bandwidth, yielding an average estimated detection range of 235 km, with a maximum distance of 414 km at site T-1M (Table 4.1b; Figure 4.1a). Autumn had the highest noise levels within the fin whale bandwidth, resulting in an average estimated range of 182 km (Figure 4.1a).

Table 4.1a Detection range estimates (km) for the four baleen whale species during 5th, 50th, and 95th percentile noise conditions between 5 November 2015 and 4 November 2016.

Noise Percentile	North Atlantic Right Whale	Humpback Whale	Fin Whale	Minke Whale
5th	80.7	72.0	440.0	38.6
50th	22.2	20.0	210.2	10.3
95th	2.9	3.8	44.2	2.0

Table 4.1b Fin whale 20 Hz pulse detection range (km) estimates based on median noise levels between 5 November 2015 and 4 November 2016.

Site	Autumn	Winter	Spring	Summer	Average
T-1M	374.7	400.7	414.1	268.6	364.5
A-1M	179.9	209.0	258.5	214.7	215.5
A-3M	203.2	259.0	310.3	345.3	279.4
A-4M	115.4	124.0	147.0	226.3	153.2
A-7M	104.7	99.5	154.6	188.2	136.7
T-2M	111.9	85.3	123.0	127.8	112.0
Average	181.6	196.3	234.6	228.5	210.2

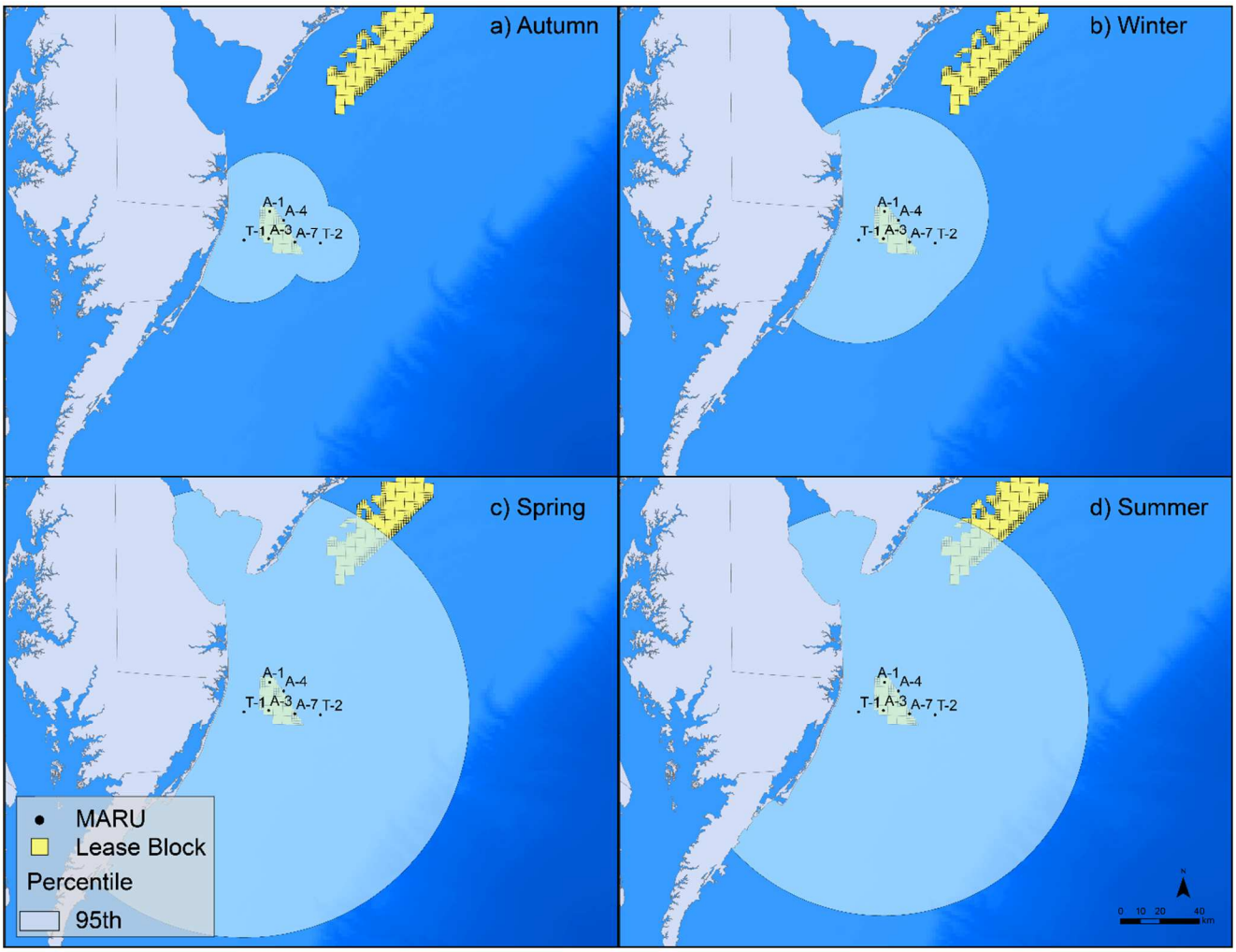

Figure 4.1a. Seasonal detection range estimates for fin whale
The 95th percentile seasonal detection range estimates for a) Autumn, b) Winter, c) Spring, and d) Summer.

Humpback whale estimated detection ranges averaged approximately 20 km, with distances up to 72 km during quieter noise conditions, and less than 4 km during noisy conditions (Table 4.1a). Average seasonal detection range across all survey sites varied, with the lowest average median detection range occurring during Autumn (9 km), and the highest average median detection range occurring during the spring (29 km) (Table 4.1c; Figure 4.1b).

Table 4.1c Humpback whale song detection range (km) estimates based on median noise levels between 5 November 2015 and 4 November 2016.

Site	Autumn	Winter	Spring	Summer	Average
T-1M	22.0	31.2	30.5	7.4	22.8
A-1M	8.3	19.9	29.5	18.0	18.9
A-3M	9.7	23.5	35.0	14.2	20.6
A-4M	4.2	16.2	26.1	18.9	16.3
A-7M	4.8	17.1	25.8	26.9	18.7
T-2M	4.9	17.7	29.5	38.0	22.5
Average	9.0	20.9	29.4	20.6	20.0

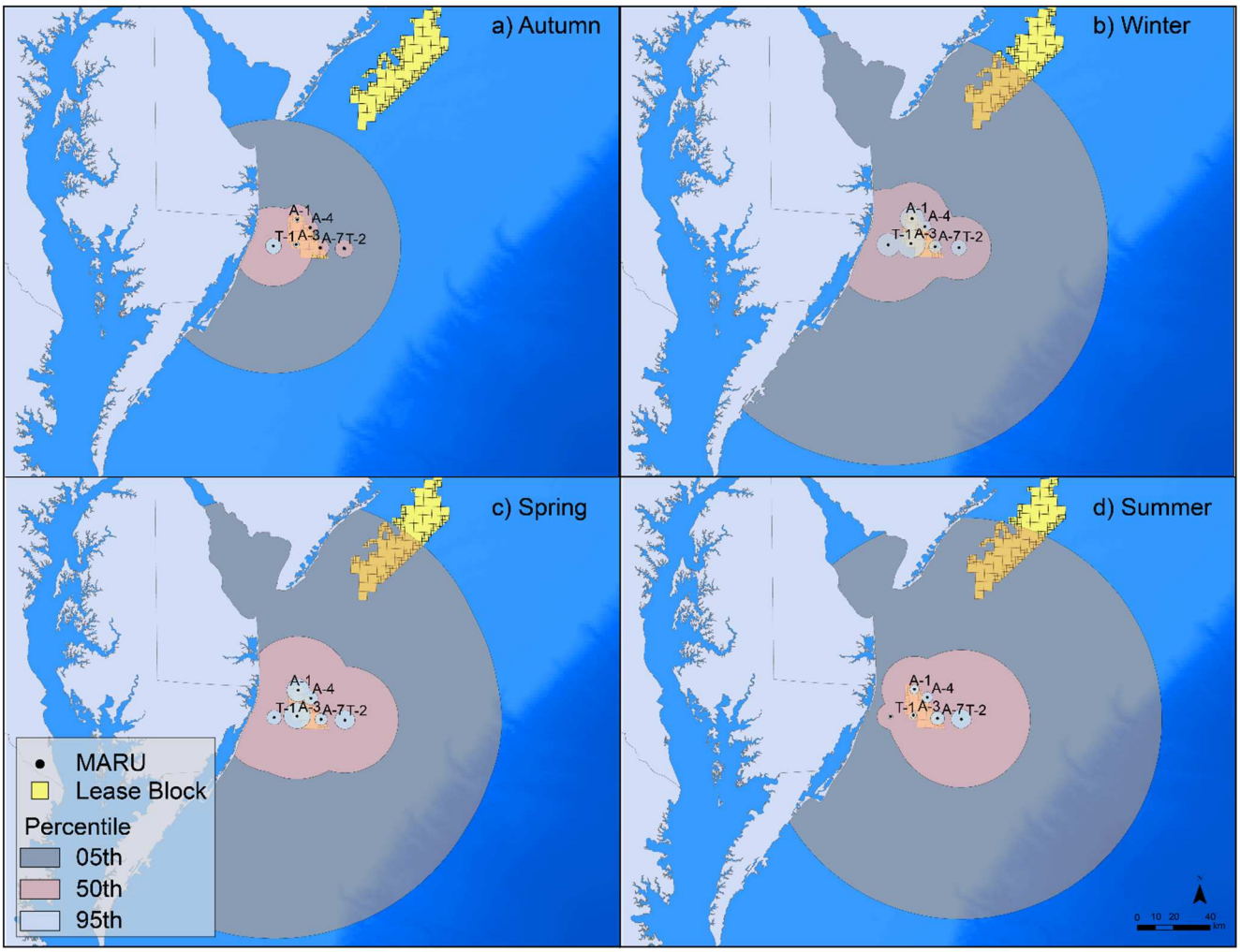

Figure 4.1b. Seasonal detection range estimates for humpback whale
The 5th, 50th, and 95th percentile seasonal detection range estimates for a) Autumn, b) Winter, c) Spring, and d) Summer.

Average minke whale detection range estimates during median noise levels was 10 km (Table 4.1a), with notable seasonal variation, with Autumn having more than twice the range (19.44 km) than all other seasons (Table 4.1d; Figure 4.1c).

Table 4.1d Minke whale pulse train detection range (km) estimates based on median noise levels between 5 November 2015 and 4 November 2016.

Site	Autumn	Winter	Spring	Summer	Average
T-1M	28.1	19.2	10.4	5.9	15.9
A-1M	19.8	6.6	7.1	7.5	10.2
A-3M	21.3	7.4	11.2	8.4	12.1
A-4M	15.5	4.0	4.8	6.0	7.6
A-7M	15.9	4.0	5.3	6.4	7.9
T-2M	16.1	4.4	5.2	6.2	8.0
Average	19.4	7.6	7.3	6.7	10.3

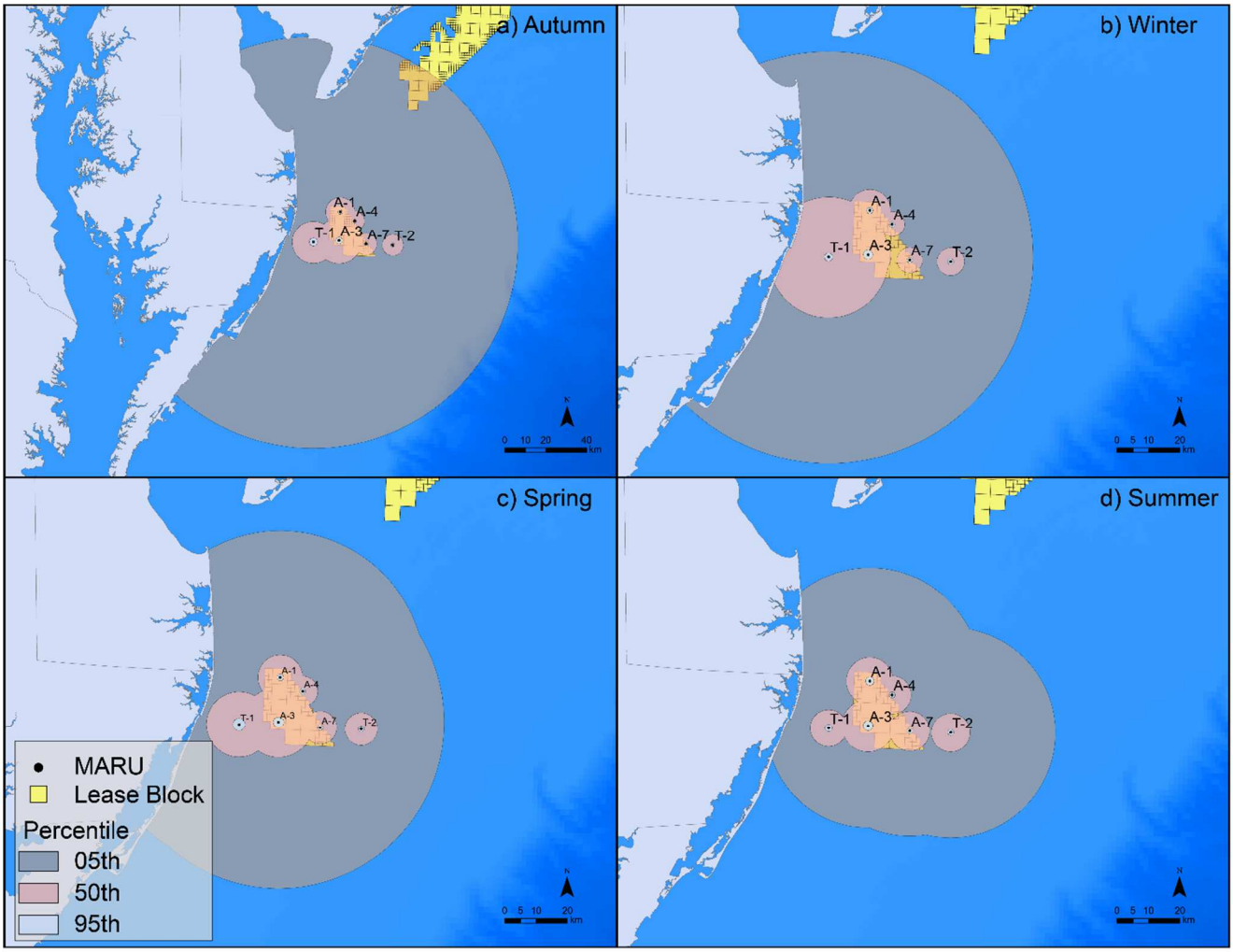

Figure 4.1c. Seasonal detection range estimates for minke whale
The 5th, 50th, and 95th percentile seasonal detection range estimates for a) Autumn, b) Winter, c) Spring, and d) Summer. Note the different spatial scale for panel (a).

Median detection range estimates for North Atlantic right whales averaged approximately 22 km, with ranges reaching 80 km in low ambient noise conditions and less than 3 km in high ambient noise conditions (Table 4.1a). Autumn ambient noise conditions (Table 4.1e; Figure 4.1d) allowed for the longest detection range (25 km), while summer had the shortest (21 km).

Table 4.1e North Atlantic right whale up-call detection range (km) estimates based on median noise levels between 5 November 2015 and 4 November 2016.

Site	Autumn	Winter	Spring	Summer	Average
T-1M	49.9	48.2	31.1	15.5	36.2
A-1M	26.5	18.7	20.0	24.7	22.5
A-3M	29.0	22.2	30.7	27.4	27.3
A-4M	14.3	13.6	14.2	19.8	15.5
A-7M	15.9	13.3	15.2	18.3	15.7
T-2M	15.9	14.3	15.9	18.8	16.2
Average	25.2	21.7	21.2	20.7	22.2

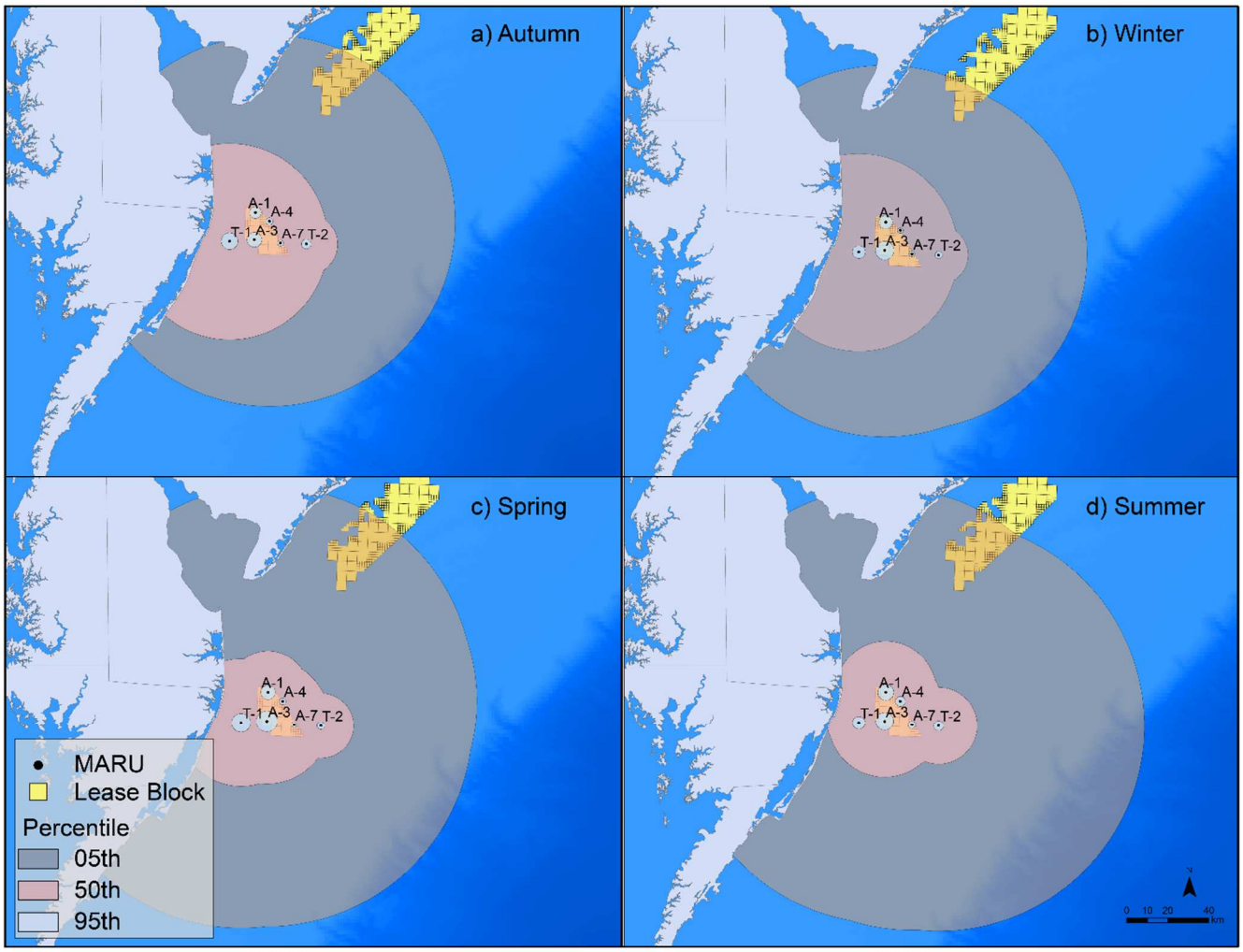

Figure 4.1d. Seasonal detection range estimates for North Atlantic right whale
The 5th, 50th, and 95th percentile seasonal detection range estimates for a) Autumn, b) Winter, c) Spring, and d) Summer.

4.2 Baleen Whale Acoustic Occurrence

All four baleen whale species were acoustically detected inshore, offshore, and within the Maryland Wind Energy Area (WEA) throughout the approximately 3-year recording period.

4.2.1 Fin Whale

In the 25% stratified sample of days analyzed, a total of 14,457 hourly detections were confirmed as fin whale 20 Hz pulses. Fin whale pulses were detected at each survey site within and surrounding the Maryland WEA (Figure 4.2.1a). Fin whale mostly occurred offshore of the WEA, with the greatest percent daily acoustic presence occurring at site T-2M (73.7%) and site T-3M (97.2%; Figure 4.2.1a). The exception is site T-3*M, where fin whales were acoustically detected 59% of the days analyzed; however, this low percentage is likely an artifact of the few days sampled at this site. The high percentage of acoustic occurrence at site T-3M is also likely an artifact of the few days sampled at this survey site.

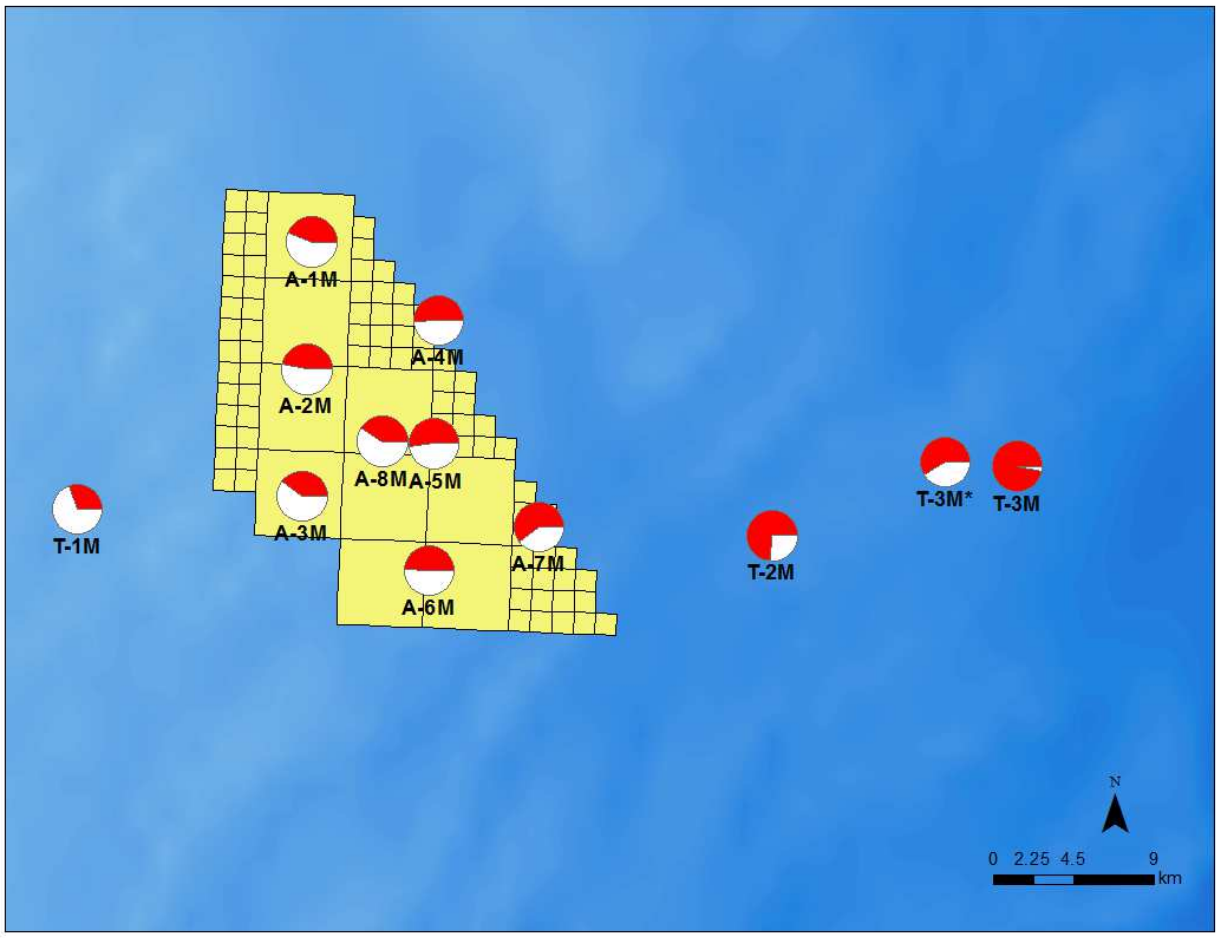

Figure 4.2.1a. Fin whale relative spatial occurrence
Percent daily acoustic presence of fin whales within and surrounding the Maryland Wind Energy Area (WEA). Red indicates percent presence over the 3-year survey period.

Fin whale acoustic presence was detected at sites within the WEA (Figure 4.2.1a), ranging 40 – 60% of days analyzed; pulses were also acoustically detected inshore (site T-1M) of the WEA during 30.2% of the days analyzed. While fin whale acoustic detection range estimates exceeded width of the shelf edge under median (50th percentile) and low (5th percentile) noise conditions (see Section 4.1 "Baleen Whale Acoustic Detection Range Estimation"), we did observe fin whale pulses at site T-1M during noisy (95th percentile) conditions (n = 97 hours). Since fin whale acoustic detection range is estimated to be approximately 44 km during 95th percentile noise conditions, and since site T-1M is approximately 40 km inshore of site T-2M (i.e. an offshore survey site), it is plausible that fin whales do occur within the WEA and are not only located offshore.

Fin whale pulses were detected acoustically in 20 of the 36 months surveyed inshore of the WEA, 34 of the 36 months surveyed offshore of the WEA, and 32 of the 36 months surveyed within the WEA. Fin whale seasonal presence peaked during the autumn (October – December) and winter (January – March) months across all three spatial regions (Figure 4.2.2b). Fin whales were not detected during the following: select spring (April 2015, June 2015, April – June 2016, and April – June 2017) and summer (July – September 2015, July – August 2016, and July – August 2017) months inshore of the WEA; select spring (June 2015, June 2016, April 2017, and June 2017) months within the WEA; and select spring

(June 2017) and summer (July 2016) months offshore of the WEA (Figure 4.2.1b). An ANOVA showed no significant difference in acoustic presence between years for each surveyed spatial region (inshore: DF = 2, p = 0.94; WEA: DF = 2, p = 0.56; offshore: DF = 2, p = 0.41).

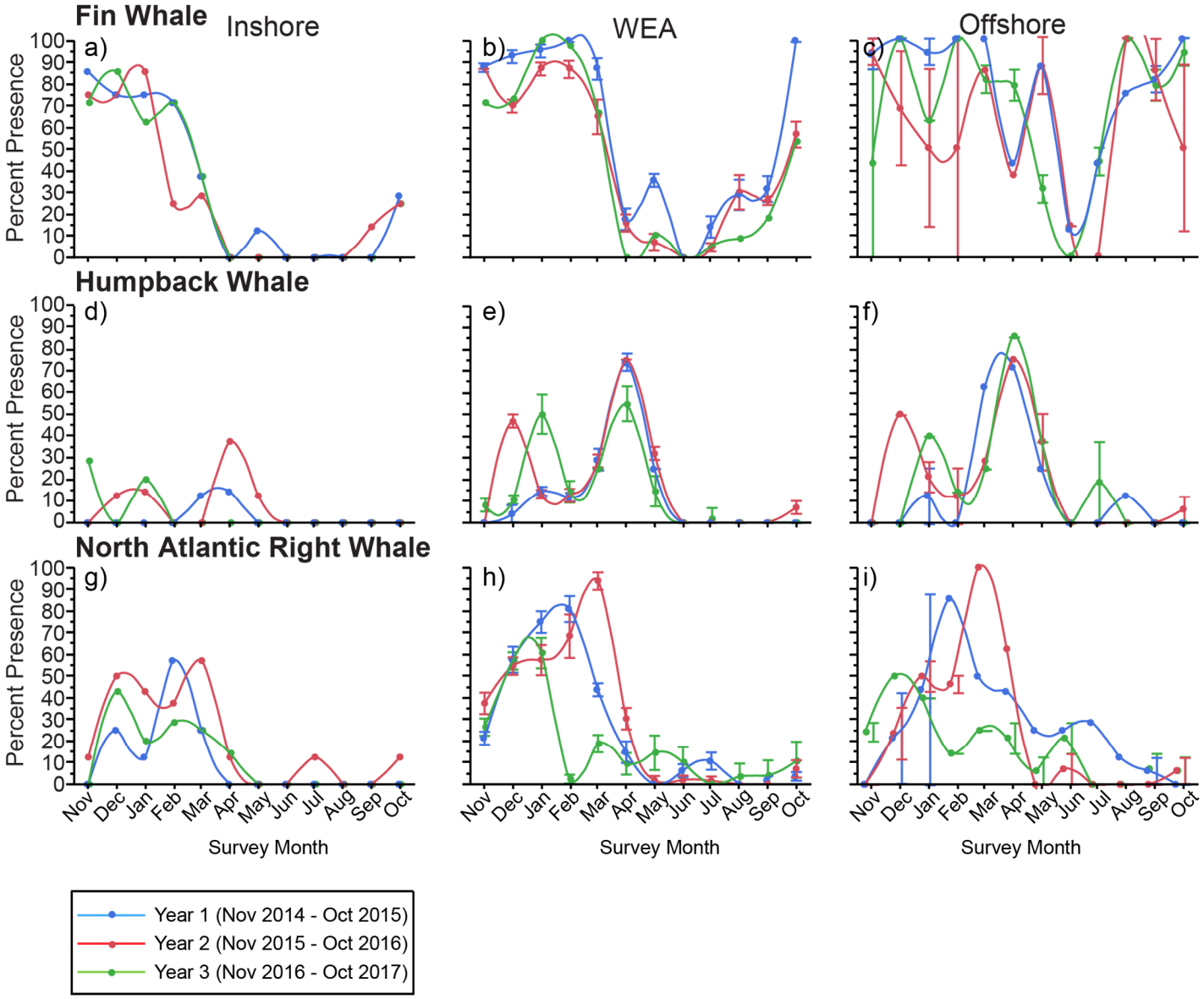

Figure 4.2.1b. Temporal acoustic occurrence of fin, humpback, and North Atlantic right whales in nearshore, WEA, and offshore regions of the survey area

Percent monthly acoustic presence (mean ± standard error) for focal baleen whale species over the 3-year project period. Fin whales: inshore, panel (a); WEA, panel (b); offshore, panel (c). Humpback whales: inshore, panel (d); WEA, panel (e); offshore, panel (f). North Atlantic right whales: inshore, panel (g); WEA, panel (h); offshore, panel (i).

While fin whale pulses were detected at low levels (0 – 35.9% monthly presence) during the spring (April – June) and summer (July – September) months inshore and within the WEA, they were detected offshore of the WEA at comparatively higher levels (12.5 – 100% monthly presence) during the spring and summer, with the exception of July 2016 (Figure 4.2.1b). Since fin whale presence was not

constant across seasons, the changing presence is suggestive of seasonal movements occurring inshore/offshore of the survey area.

4.2.2 Humpback Whale

During the 3-year survey period, a total of 2301 hourly detections were confirmed as humpback whale song and call sequences. Humpback whale song and call sequences were detected at each of the surveyed sites within and surrounding the WEA (Figure 4.2.2a). Humpback whales were acoustically detected in 8 of the 36 months sampled inshore of the WEA, 17 of the 36 months sampled offshore of the WEA, and 20 of the 36 months sampled within the WEA. Although humpback whales were detected at all of the survey sites, they were most frequently detected offshore of the WEA at site T-2M (18.9% daily acoustic presence). Humpback whales also frequently occurred within the WEA, ranging from 9.9 – 18.6% daily acoustic presence.

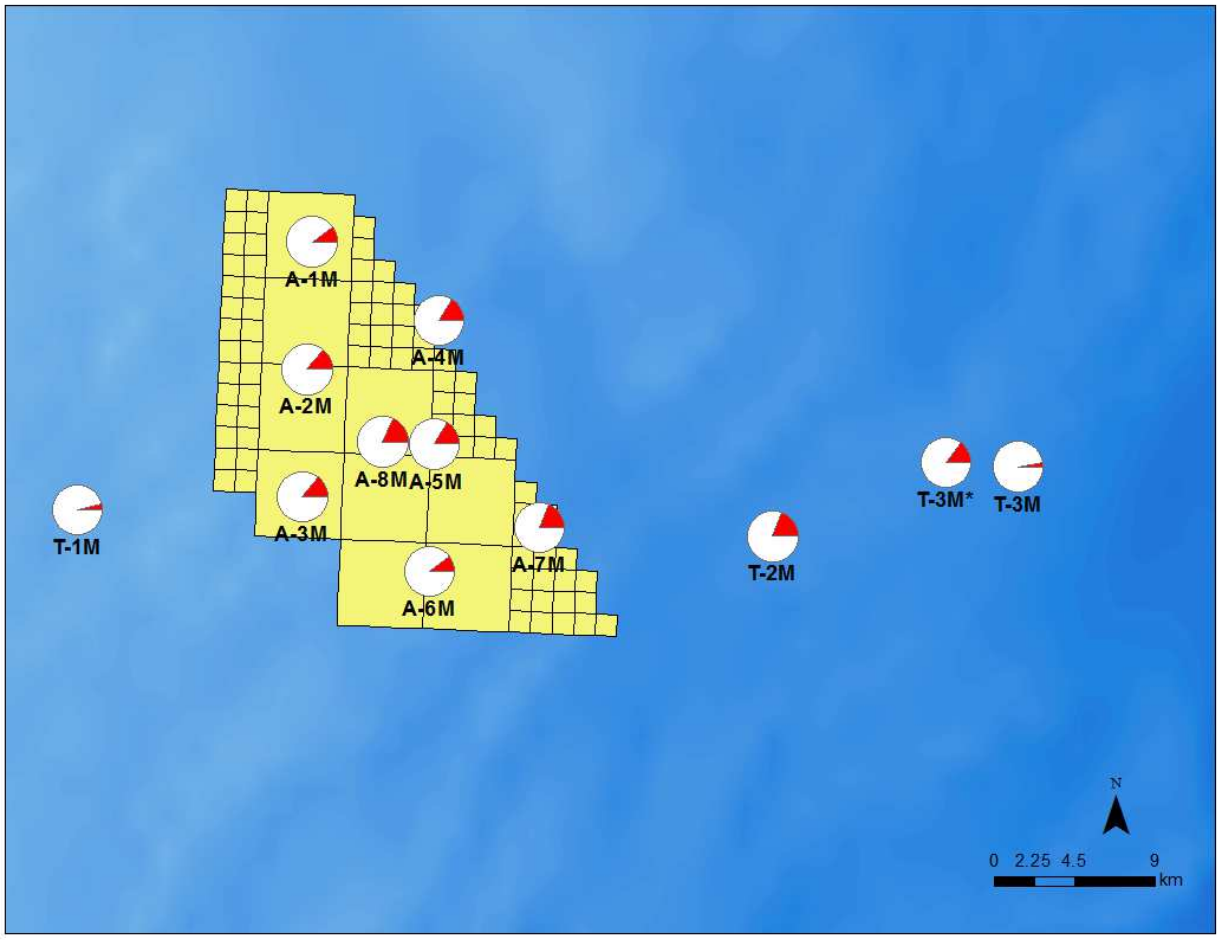

Figure 4.2.2a. Humpback whale relative spatial occurrence
Percent daily acoustic presence of humpback whales within and surrounding the Maryland Wind Energy Area (WEA). Red indicates percent presence over the 3-year survey period.

During the winter (January – March) months within and offshore of the WEA, there was an increase in presence that peaked in spring (April – June), with the highest monthly percent presence occurring in April (> 54% monthly presence) across all three years of the survey period (Figure 4.2.1b). Acoustic occurrence also peaked during April 2016 inshore of the WEA, at 37.5% monthly presence.

Humpback whales had low levels of monthly presence during the summer (July – September) and autumn (October – December) (Figure 4.2.1b), suggesting a seasonal acoustic presence in the survey area. An ANOVA showed no significant difference in humpback whale percent monthly presence across the 3-year survey period inshore, offshore, and within the WEA (inshore: DF = 2, p = 0.54; WEA: DF = 2, p = 0.86; offshore: DF = 2, p = 0.92).

4.2.3 Minke Whale

The minke whale pulse train detection algorithm identified 186,044 candidate minke whale pulse train events; upon review, 53 of these detector events were validated as true minke whale pulse trains (for an evaluation of minke whale detector performance, see Section 4.2.5 "North Atlantic Right Whale and Minke Whale Detector Performance Evaluation"). Pulse trains occurred during a total of 11 analysis days across the 3-year survey period (Table 4.2.3a).

Table 4.2.3a Dates, sites, and number of minke whale pulse trains detected inshore, offshore, and within the Maryland Wind Energy Area (WEA).

Date	Site	Region	Number of Pulse Trains
11/14/2014	T-2M	Offshore	1
11/14/2014	A-3M	WEA	1
11/14/2014	A-5M	WEA	1
1/1/2015	T-1M	Inshore	1
4/3/2015	T-2M	Offshore	4
4/3/2015	A-2M	WEA	1
4/3/2015	A-4M	WEA	1
4/3/2015	A-5M	WEA	2
3/12/2016	T-2M	Offshore	2
4/13/2016	T-2M	Offshore	1
4/25/2016	T-2M	Offshore	10
4/25/2016	A-4M	WEA	2
4/25/2016	A-5M	WEA	2
4/25/2016	A-8M	WEA	1
2/19/2017	A-4M	WEA	1
2/23/2017	A-1M	WEA	1
3/15/2017	A-1M	WEA	1
4/24/2017	T-3*M	Offshore	4
5/10/2017	T-2M	Offshore	4
5/10/2017	T-3*M	Offshore	9
5/10/2017	A-5M	WEA	2
5/10/2017	A-7M	WEA	1

While minke whale pulse trains were rarely detected, they occurred inshore, offshore and within the WEA (Figure 4.2.3a). Minke whales were acoustically detected in 1 of the 36 months sampled inshore (site T-1M) of the WEA, 6 of the 36 months sampled offshore of the WEA, and 6 of the 36 months sampled within the WEA. An ANOVA showed no significant inter-annual variability in minke whale acoustic occurrence (inshore: DF = 2, p = 0.38; WEA: DF = 2, p = 0.55; offshore: DF = 2, p = 0.74).

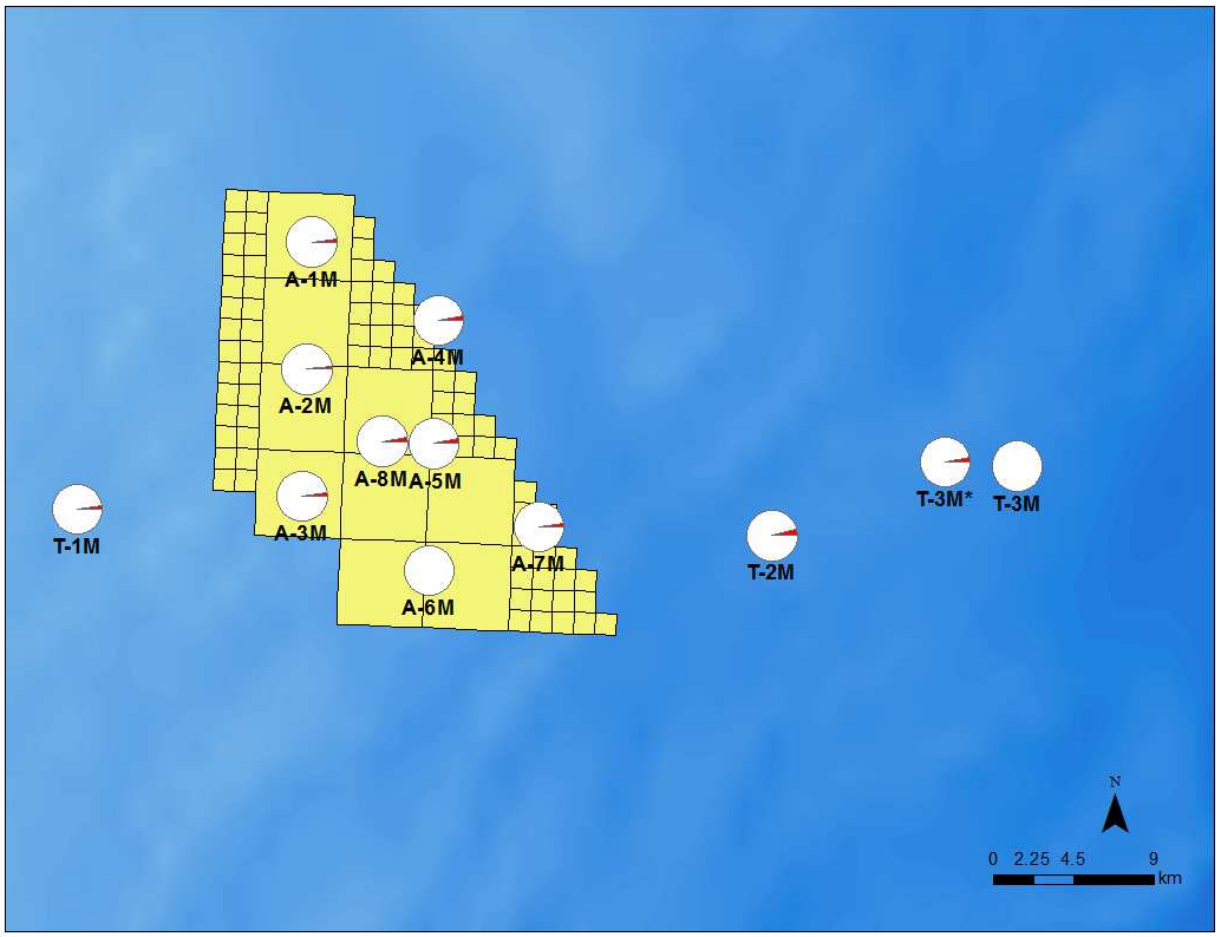

Figure 4.2.3a. Minke whale relative spatial occurrence
Percent daily acoustic presence of minke whales within and surrounding the Maryland Wind Energy Area (WEA). Red indicates percent presence over the 3-year survey period.

4.2.4 North Atlantic Right Whale

35,510 of the 431,348 North Atlantic right whale up-call detection events reviewed were validated as true North Atlantic right whale up-calls (for an evaluation of North Atlantic right whale detector performance, see Section 4.2.5 "North Atlantic Right Whale and Minke Whale Detector Performance Evaluation"). North Atlantic right whales were detected at each of the surveyed sites within the WEA, as well as sites T-1M, T-2M, and T-3*M (Figure 4.2.4a). No detections were found at site T-3M, likely an artifact of the few days sampled at this site. North Atlantic right whales were detected 17 of the 36 months sampled inshore of the WEA, 27 of the 36 months sampled offshore of the WEA, and 31 of the 36 months sampled within the WEA.

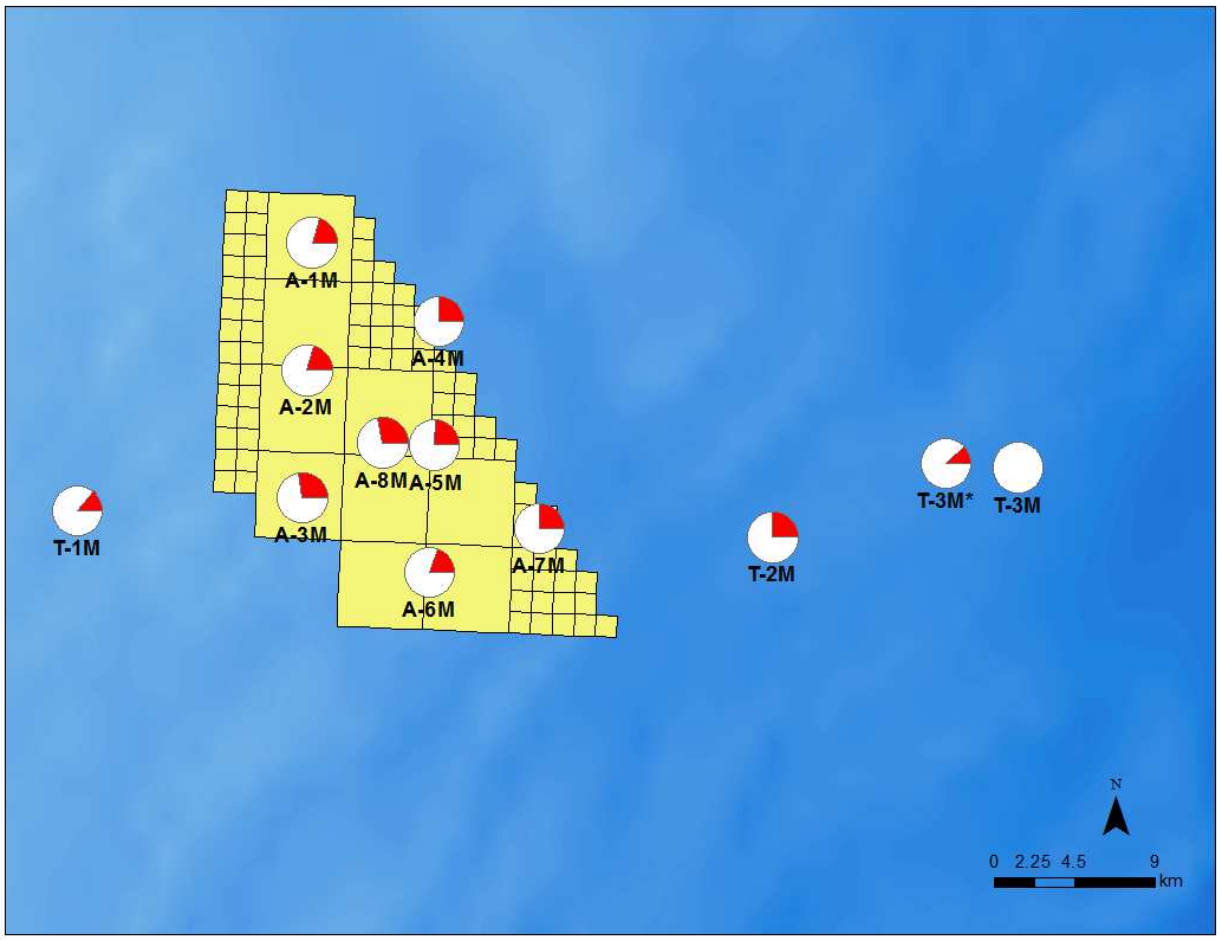

Figure 4.2.4a. North Atlantic right whale relative spatial occurrence
Percent daily acoustic presence of North Atlantic right whales within and surrounding the Maryland Wind Energy Area (WEA). Red indicates percent presence over the 3-year survey period.

North Atlantic right whales were detected during every season within the WEA, including low levels of presence (1.6 – 10.7% monthly presence) during the summer months (July – September) across the 3-year survey period (Figure 4.2.1b). North Atlantic right whales also showed a distinct seasonal pattern of acoustic presence during the first two years of the study within the WEA: up-calls were detected at moderate levels (21.4 – 57.7% monthly presence) during late autumn (November – December), and peaked during the winter months (January – March) between 43.8 – 93.9% monthly presence (Figure 4.2.1b). While an ANOVA showed no significant difference in percent monthly presence between years within the WEA (DF = 2, p = 0.60), peak presence occurred slightly earlier during the third year of the survey period (December 2016 – January 2017, with 57.1% and 60.7% peak monthly presence, respectively) when compared to the previous two years. Despite this slight shift in peak presence, the overall seasonal pattern of North Atlantic right whale acoustic occurrence was similar between all three years of the survey period.

The same North Atlantic right whale seasonal presence patterns that occurred within the WEA also occurred inshore and offshore of the WEA (Figure 4.2.1b). Inshore of the WEA, peak seasonal presence occurred during winter months, ranging between 12.5 – 57.1% monthly presence; peak seasonal presence also occurring during the winter in offshore of the WEA, at levels comparable to those found

within the WEA (25 – 100% monthly presence). North Atlantic right whales were detected during every season inshore and offshore of the WEA, with comparably low levels of presence during the summer months (6.3 – 28.6% monthly presence) as was found within the WEA (Figure 4.2.1b). An ANOVA and Tukey's HSD post-hoc test showed no inter-annual variability between years surveyed inshore and offshore the WEA (inshore: DF = 2, p = 0.35; offshore: DF = 2, p = 0.60).

4.2.5 North Atlantic Right Whale and Minke Whale Detector Performance Evaluation

In the 24 randomly selected analysis days reviewed for detector performance evaluation, the North Atlantic right whale up-call detection algorithm and the minke whale pulse train detection algorithm determined a total number of 4485 up-call detections and 59 pulse train detections (Table 4.2.5a). A fraction of these detector events were North Atlantic right whale up-call (n = 2536) and minke whale pulse train (n = 26) true detections (TD), yielding a true detection rate of 56.5% and 44.1%, respectively (Table 4.2.5a). The North Atlantic right whale up-call detection algorithm missed 43.5% of the total number of true up-calls, and the minke whale pulse train detection algorithm missed 55.9% of the total number of true pulse trains. While the North Atlantic right whale up-call detector missed a fraction of individual up-calls, the detector found 98.5% of hours and 100% of days in which North Atlantic right whale up-calls were present (Table 4.2.5b). Consequently, the up-call detector had a low probability of missing the hourly and daily occurrence of North Atlantic right whale up-calls. The minke whale pulse train detection algorithm also had a low probability of missing the hourly and daily occurrence of pulse trains, finding 91.7% of hours and 100% of days in which minke whale pulse trains were present (Table 4.2.5c).

Table 4.2.5a Performance of the automated detection algorithms used to detect North Atlantic right whale up-calls and minke whale pulse trains. Total detections = true detections (TD) found by the automated detection algorithms + missed detections (MD) found by the human analyst. Performance measures include the TD and MD rate.

	North Atlantic Right Whale Up-Calls	Minke Whale Pulse Trains
Total Detections	4485	59
True Detections	2536	26
True Detection Rate (TD/(TD+MD))	56.5%	44.1%
Missed Detections	1949	33
Missed Detection Rate (MD/(TD+MD))	43.5%	55.9%

Table 4.2.5b Hourly and daily performance of the North Atlantic right whale up-call detection algorithm.

North Atlantic Right Whale Up-call Detector		
Hourly Performance		
	True Hours Acoustic Occurrence	65
	Missed Hours Acoustic Occurrence	1
	True Hour Detection Rate	98.5%
Daily Performance		
	True Days Acoustic Occurrence	11
	Missed Days Acoustic Occurrence	0
	True Day Detection Rate	100%

Table 4.2.5c Hourly and daily performance of the minke whale pulse train detection algorithm.

Minke Whale Pulse Train Detector		
Hourly Performance		
	True Hours Acoustic Occurrence	12
	Missed Hours Acoustic Occurrence	1
	True Hour Detection Rate	91.7%
Daily Performance		
	True Days Acoustic Occurrence	4
	Missed Days Acoustic Occurrence	0
	True Day Detection Rate	100%

There was a significant difference in signal-to-noise ratio (SNR) between missed detections (MD; mean = 13.84) and true positive (TP; mean = 14.90) North Atlantic right whale up-calls (Kruskal-Wallis, $S = 3894205$, $Z = 12.19$, $p (> |Z|) < 0.0001$), suggesting that the up-call detector performance was likely influenced by ambient noise levels (Figure 4.2.5a). There was no significant difference in SNR between MD (mean = 15.46) and TP (mean = 15.52) minke whale pulse trains (Kruskal-Wallis, $S = 1099$, $Z = -0.077$, $p (> |Z|) = 0.93$), suggesting ambient noise levels unlikely explain the performance of the minke whale pulse train detector.

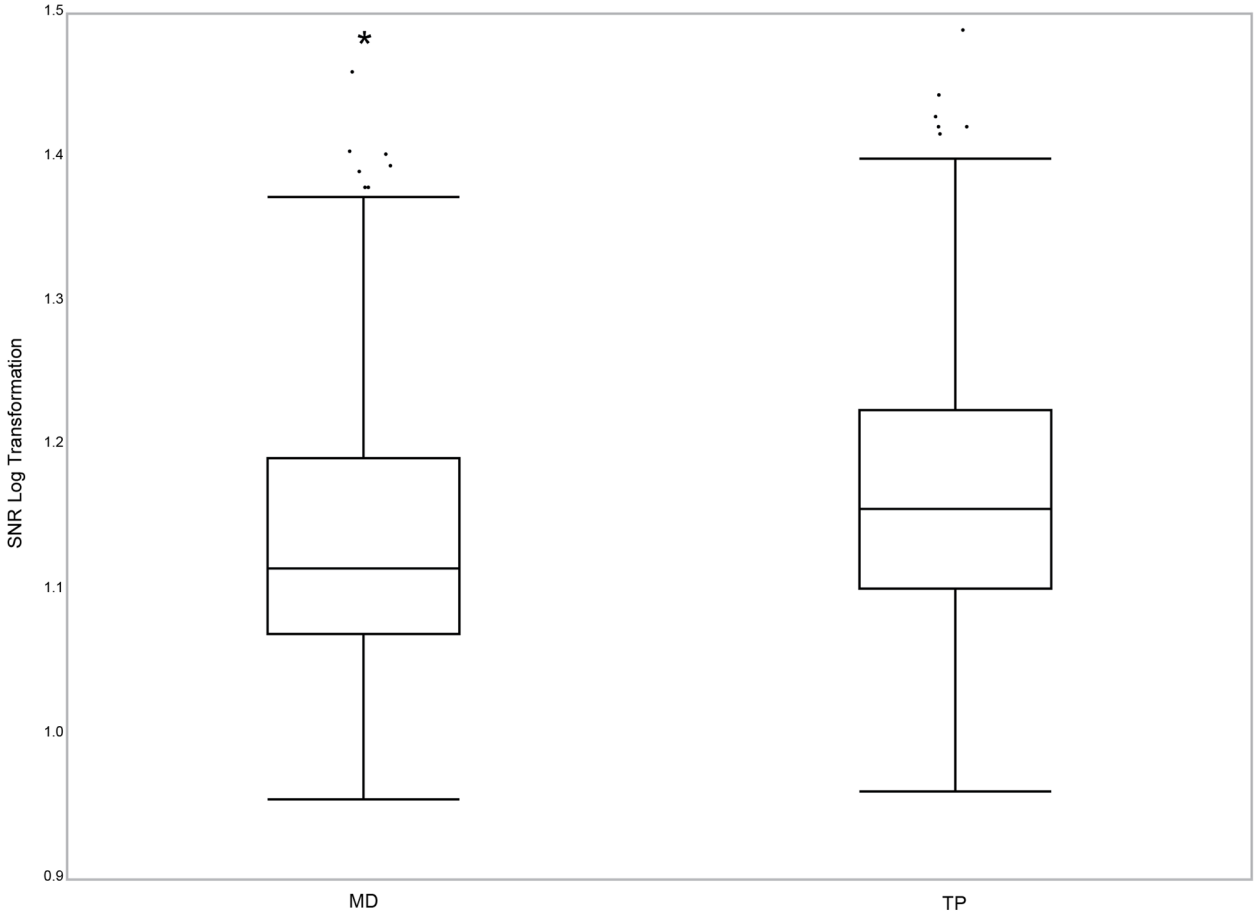

Figure 4.2.5a. North Atlantic right whale log transformed signal to noise ratio (SNR) values for missed detections (MD) and true positives (TP)
The box and whisker plots show the minimum, first quartile, median, third quartile, and maximum log transformed SNR values for missed North Atlantic right whale detections (MD) and true positive North Atlantic right whale detections (TP); the asterisk indicates a significant difference in SNR values between MD and TP.

4.2.6 Generalized Auto-regressive Moving Average (GARMA) Models

A binomial distribution had the best fit (lowest AIC scores) for GARMAs modeling the temporal patterns for the following: North Atlantic right whale occurrence at site T-1M (n = 6432 hours, or 268 analysis days), A-5M (n = 6552 hours, or 273 analysis days), and T-2M (n = 6288 hours, or 262 analysis days); humpback whale occurrence at site T-1M, A-5M, and T-2M; and fin whale occurrence at site A-5M. Given the rare occurrence of minke whale pulse trains, minke whale temporal occurrence patterns were not modeled in a GARMA.

At survey site A-5M, Julian day was included in all final models for North Atlantic right whale, humpback whale, and fin whale as a significant predictor for the number of hours whales were detected in a day (Table 4.2.6a). These results suggest baleen whale acoustic presence at survey site A-5M had a significant seasonal pattern, corroborating our findings from baleen whale occurrence analysis (see results above for North Atlantic right whale, humpback whale, and fin whale). North Atlantic right whale detections were present significantly more often during late autumn (December, n = 77 hours) and winter months (January, n = 80 hours; February, n = 121 hours; March, n = 76 hours), while humpback whale detections were present significantly more often during early spring months (April, n = 124 hours)

(Figure 4.2.6a). Fin whale detections were present significantly more often during the winter (January, n = 372 hours; February, n = 261 hours; March, n = 175 hours) and autumn (October, n = 218 hours; November, n = 303 hours; December, n = 258 hours) (Figure 4.2.6a).

Table 4.2.6a Estimated parameters (standard errors in parentheses) from the generalized auto-regressive moving average (GARMA) models for North Atlantic right whale, humpback whale, and fin whale data at site A-5M. BI = binomial, β values are the regression coefficients, φ_1 and φ_2 are the auto-regressive and moving average parameters.

Species	Distribution	$\beta_{Intercept}$	β_{sinday}	β_{cosday}	$\beta_{coshour}$	φ_1	φ_2
North Atlantic Right Whale	BI	-13.64*** (1.82)	5.35*** (0.94)	9.26*** (1.39)	0.83** (0.31)	0.77*** (0.03)	—
Humpback Whale	BI	-37.69*** (7.92)	22.09*** (4.77)	7.07*** (2.07)	—	0.69*** (0.04)	0.25*** (0.04)
Fin Whale	BI	-10.64*** (1.98)	—	14.69*** (2.67)	—	0.67*** (0.02)	0.24*** (0.02)

At survey site A-5M, the hour of the day was retained as a significant factor for the North Atlantic right whale GARMA model, but not for the humpback whale or fin whale GARMA models (Table 4.2.6a). These results suggest North Atlantic right whale acoustic presence had a significant diel pattern at survey site A-5M, while no significant diel pattern was found for humpback whale or fin whale (Figure 4.2.6b). Peaks in North Atlantic right whale detections occurred during 00:00 UTC (n = 27 days) and 23:00 UTC (n = 27 days), while the lowest occurrence occurred during 08:00 UTC (n = 10 days) 09:00 UTC (n = 9 days) (Figure 4.2.6b).

At survey site T-1M, Julian day was included in all final models for North Atlantic right whale and humpback whale as a significant predictor for the number of hours whales were detected in a day (Table 4.2.6b). These results suggest baleen whale acoustic presence at survey site T-1M had a significant seasonal pattern, corroborating our findings from baleen whale occurrence analysis (see results above for North Atlantic right whale and humpback whale). North Atlantic right whale detections were present significantly more often during late autumn (December, n = 25 hours) and winter (January, n = 15 hours; February, n = 22 hours; March, n = 34 hours) (Figure 4.2.6a). Humpback whale detections were present significantly more often during late winter (March, n = 3 hours) and early spring (April, n = 4 hours; May, n = 3 hours) (Figure 4.2.6a).

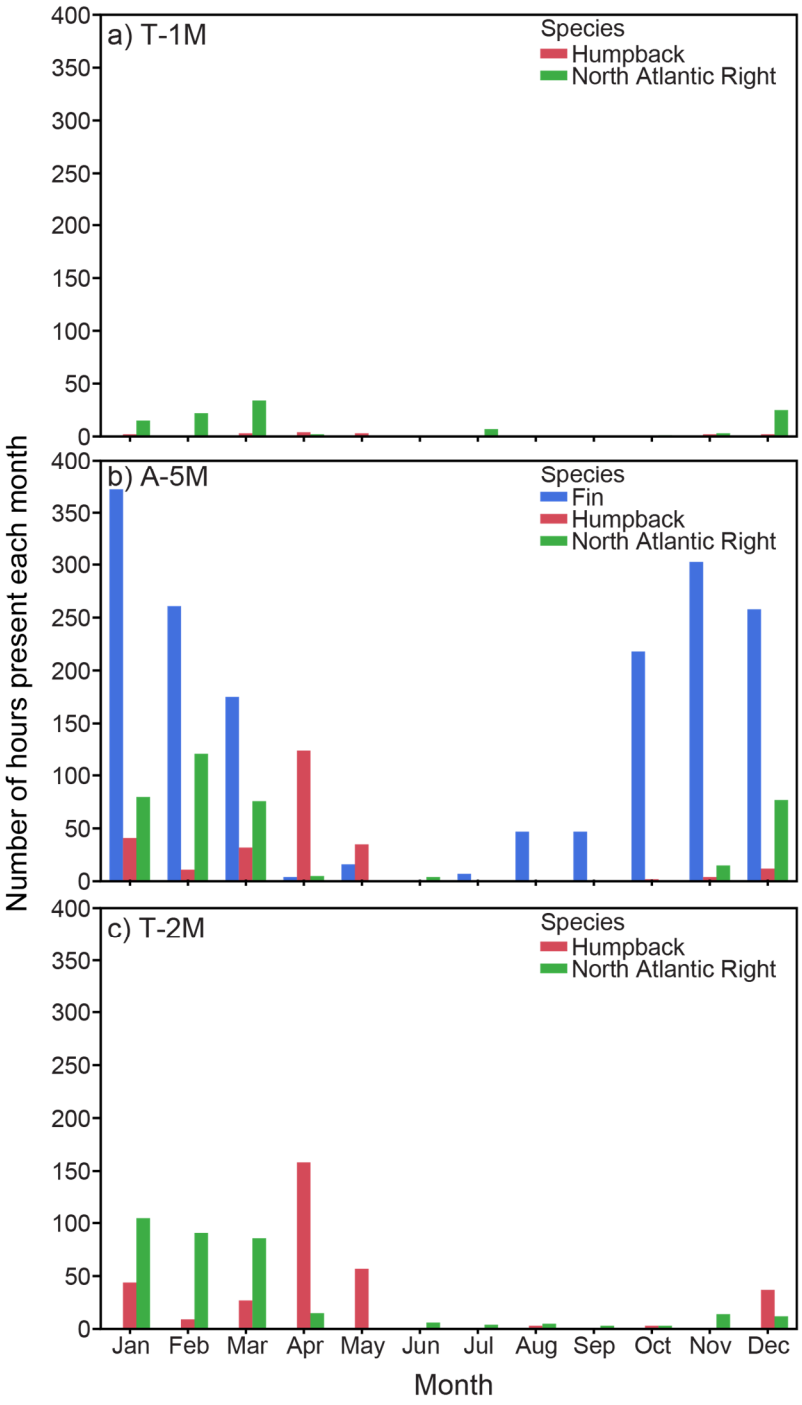

Figure 4.2.6a. Total number of hours that calls of baleen whale species were detected for survey sites T-1M, A-5M, and T-2M

In the above figure, hours of baleen whale presence for each Julian day is aggregated into calendar months for survey sites T-1M (a), A-5M (b), and T-2M (c). The Julian day was a significant factor in the generalized auto-regressive moving average (GARMA) models for North Atlantic right whale and humpback whale at survey site T-1M (a); GARMA models for North Atlantic right whale, humpback whale, and fin whale at survey site A-5M (b); GARMA models for North Atlantic right whale and humpback whale at survey site T-2M (c). Due to the large estimated detection range for fin whale pulses that may overlap multiple survey sites, temporal patterns of fin whale were determined at survey site A-5M only to avoid pseudo-replication.

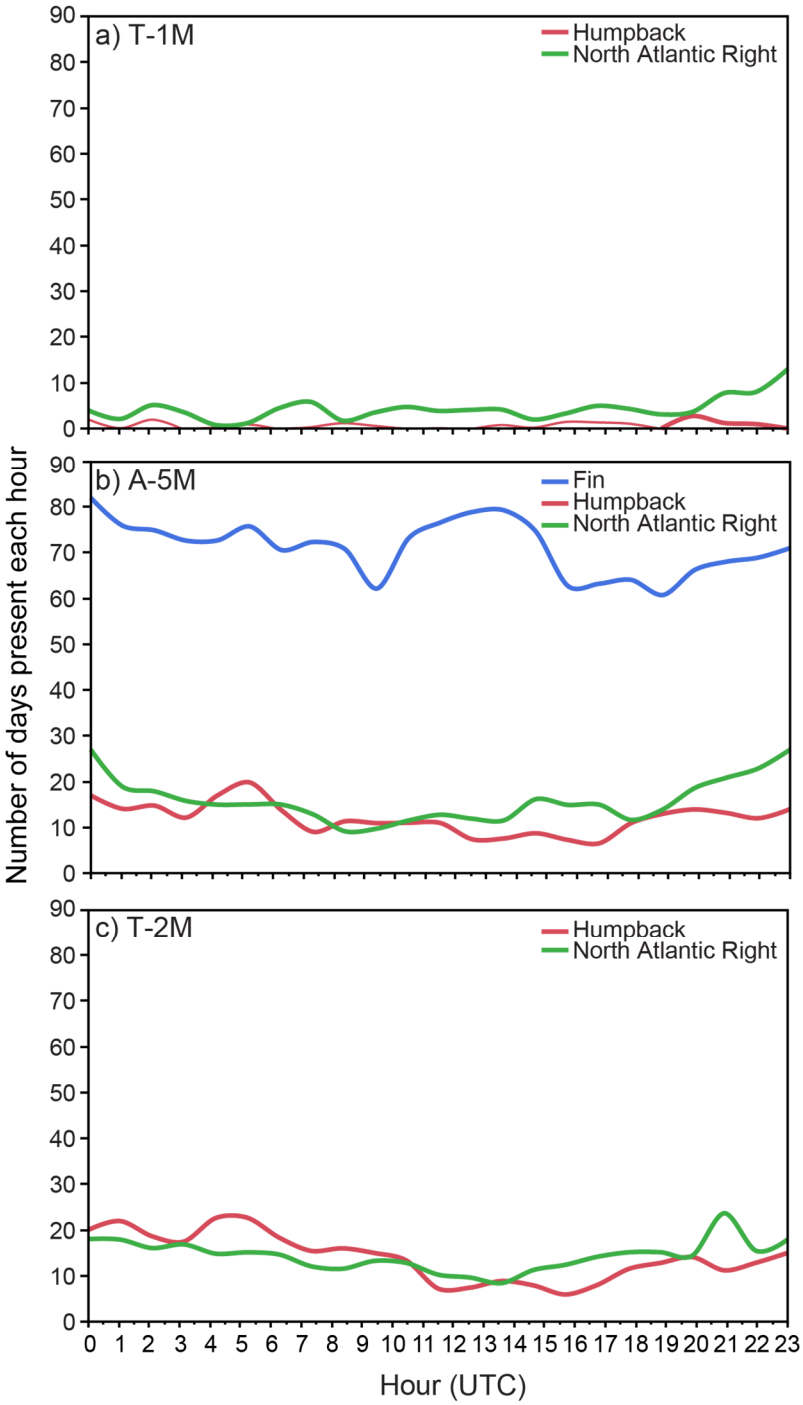

Figure 4.2.6b. Total number of days that calls of baleen whale species were detected for each hour (in UTC) at survey sites T-1M, A-5M, and T-2M

The hour of the day was a significant factor in the generalized auto-regressive moving average (GARMA) model of hourly North Atlantic right whale presence at site A-5M (b), and the GARMA model of hourly humpback whale presence at site T-2M (c). The hour of the day was not a significant factor for GARMA models of hourly North Atlantic right whale and humpback whale presence at site T-1M (a), and the GARMA model of hourly fin whale presence at site A-5M (b). Due to the large estimated detection range for fin whale pulses that may overlap multiple survey sites, temporal patterns of fin whale were determined at survey site A-5M only to avoid pseudo-replication.

Table 4.2.6b Estimated parameters (standard errors in parentheses) from the generalized auto-regressive moving average (GARMA) models for North Atlantic right whale and humpback whale at site T-1M. BI = binomial.

Species	Distribution	Intercept	sinday	cosday	sinhour	coshour
North Atlantic Right Whale	BI	-5.35*** (0.26)	1.34*** (0.23)	2.21*** (0.28)	—	—
Humpback Whale	BI	-6.49*** (0.38)	1.23** (0.45)	0.60 (0.40)	-0.56 (0.37)	0.47 (0.36)

The hour of the day was not a significant factor for either the North Atlantic right whale GARMA model or the humpback whale GARMA model (Table 4.2.6b). These results suggest no significant diel pattern was found for North Atlantic right whale or humpback whale at site T-1M (Figure 4.2.6b).

At survey site T-2M, Julian day was included in all final models for North Atlantic right whale and humpback whale as a significant predictor for the number of hours whales were detected in a day (Table 4.2.6c). These results suggest baleen whale acoustic presence at survey site T-2M had a significant seasonal pattern, corroborating our findings from baleen whale occurrence analysis (see results above for North Atlantic right whale and humpback whale). North Atlantic right whale detections were present significantly more often during winter (January, n = 105 hours; February, n = 91 hours; March, n = 86 hours) (Figure 4.2.6a). Humpback whale detections were present significantly more often during December (n = 37 hours), January (n = 44 hours), April (n = 158 hours), and May (n = 57 hours) (Figure 4.2.6a).

Table 4.2.6c Estimated parameters (standard errors in parentheses) from the generalized auto-regressive moving average (GARMA) models for North Atlantic right whale and humpback whale at site T-2M. BI = binomial, β values are the regression coefficients, φ_1 and φ_2 are the auto-regressive and moving average parameters.

Species	Distribution	$\beta_{Intercept}$	$\beta_{sinhour}$	B_{sinday}	β_{cosday}	φ_1	φ_2
North Atlantic Right Whale	BI	-10.87*** (1.41)	—	4.50*** (0.77)	5.66*** (0.87)	0.76*** (0.03)	—
Humpback Whale	BI	-31.81*** (6.54)	1.06** (0.33)	18.48*** (3.87)	—	0.71*** (0.04)	0.22*** (0.04)

The hour of the day was retained as a significant factor for the humpback whale GARMA model, but not for the North Atlantic right whale GARMA model (Table 4.2.6c). These results suggest humpback whale acoustic presence had a significant diel at survey site T-2, while no significant diel

pattern was found for North Atlantic right whale. Peaks in humpback whale detections occurred during 00:00 – 01:00 UTC and 04:00 – 06:00 UTC ($n \geq 20$ days), while the lowest occurrence occurred during 12:00 UTC (n = 7 days), 15:00 UTC (n = 7 days), and 16:00 UTC (n = 6 days) (Figure 4.2.6b).

4.2.7 Generalized Additive Models (GAM)

A binomial distribution had the best fit (lowest AIC scores) for GAM models of the environmental variables for the following: North Atlantic right whale occurrence at site T-1M (n = 268 analysis days), A-5M (n = 273 analysis days), and T-2M (n = 262 analysis days); humpback whale occurrence at site T-1M, A-5M, and T-2M; fin whale occurrence at site A-5M. Given the rare occurrence of minke whale pulse trains, minke whale occurrence patterns were not modeled in a GAM.

The results of the GAM model at survey site A-5M suggest the environmental covariates SST and log-transformed Chl-a concentration were significantly (SST: $p < 0.001$; Chl-a: $p = 0.029$) related to the acoustic occurrence of North Atlantic right whales during the 3-year survey period (Table 4.2.7a). The GAM model explained 32.7% of the deviance in North Atlantic right whale acoustic occurrence at site A-5M.

Table 4.2.7a Generalized additive model (GAM) results used to relate the weekly acoustic occurrence of North Atlantic right whales to sea surface temperature (SST) and the natural logarithm of chlorophyll-a (ln Chl-a) concentration at site A-5M.

Site A-5M, North Atlantic Right Whale				
Parametric Coefficients				
	Estimate	Standard Error	z	P (>|z|)
Intercept	-2.20	0.32	-6.78	<0.001***
Smooth Terms				
	Estimated Degrees of Freedom	Reference Degrees of Freedom	χ^2	P
SST	1.71	2.076	39.63	<0.001***
ln (Chl-a)	2.38	2.75	8.70	0.023*
$R^2 = 0.30$	Deviance explained = 32.7%	UBRE = -0.24	Scale est. = 1	n = 260

North Atlantic right whale acoustic occurrence and SST were also significantly related in the GAM models for site T-1M ($p < 0.001$; Table 4.2.7b) and site T-2M ($p < 0.001$; Table 4.2.7c); Chl-a concentration was not significantly related to North Atlantic right whale acoustic occurrence for GAM models at either survey site (Table 4.2.7b; Table 4.2.7c). The GAM models explained 23.1% and 22.4% of the deviance in North Atlantic right whale acoustic occurrence at site T-1M and site T-2M, respectively.

Table 4.2.7b Generalized additive model (GAM) results used to relate the weekly acoustic occurrence of North Atlantic right whales to sea surface temperature (SST) and the natural logarithm of chlorophyll-a (ln Chl-a) concentration at site T-1M.

Site T-1M, North Atlantic Right Whale				
Parametric Coefficients				
	Estimate	Standard Error	z	P (>|z|)
Intercept	-2.79	0.37	-7.48	<0.001***
Smooth Terms				
	Estimated Degrees of Freedom	Reference Degrees of Freedom	χ^2	P
SST	1.000	1.000	22.086	<0.001***
ln (Chl-a)	1.90	2.27	3.29	0.24
R^2 = 0.16	Deviance explained = 23.1%	UBRE = -0.37	Scale est. = 1	n = 257

Table 4.2.7c Generalized additive model (GAM) results used to relate the weekly acoustic occurrence of North Atlantic right whales to sea surface temperature (SST) and the natural logarithm of chlorophyll-a (ln Chl-a) concentration at site T-2M.

Site T-2M, North Atlantic Right Whale				
Parametric Coefficients				
	Estimate	Standard Error	z	P (>|z|)
Intercept	-1.39	0.20	-7.00	<0.001***
Smooth Terms				
	Estimated Degrees of Freedom	Reference Degrees of Freedom	χ^2	P
SST	1.78	2.16	39.27	<0.001***
ln (Chl-a)	1.47	1.79	1.46	0.33
R^2 = 0.25	Deviance explained = 22.4%	UBRE = -0.072	Scale est. = 1	n = 251

The statistically significant GAM models at site A-5M, T-1M, and T-2M were represented visually with smoothing curves to determine how the environmental covariates related to acoustic occurrence of North Atlantic right whales (Figure 4.2.7a). The smoothing curves suggest a negative relationship between SST and North Atlantic right whale acoustic occurrence at site A-5M, site T-1M, and site T-2M (Figure 4.2.7a); as SST increased, acoustic presence of North Atlantic right whales decreased. Consequently, North Atlantic right whales occurred more frequently when SST was low at each of the three survey sites, with a peak occurrence at or below 5°C (Figure 4.2.7a). The smoothing curve suggests a non-linear relationship between Chl-a concentration and North Atlantic right whale acoustic occurrence at site A-5M; North Atlantic right whale acoustic occurrence decreased as Chl-a concentration levels increased, until it reached a plateau (Figure 4.2.7a). After the plateau, North Atlantic right whale acoustic presence increased slightly as Chl-a concentration increased.

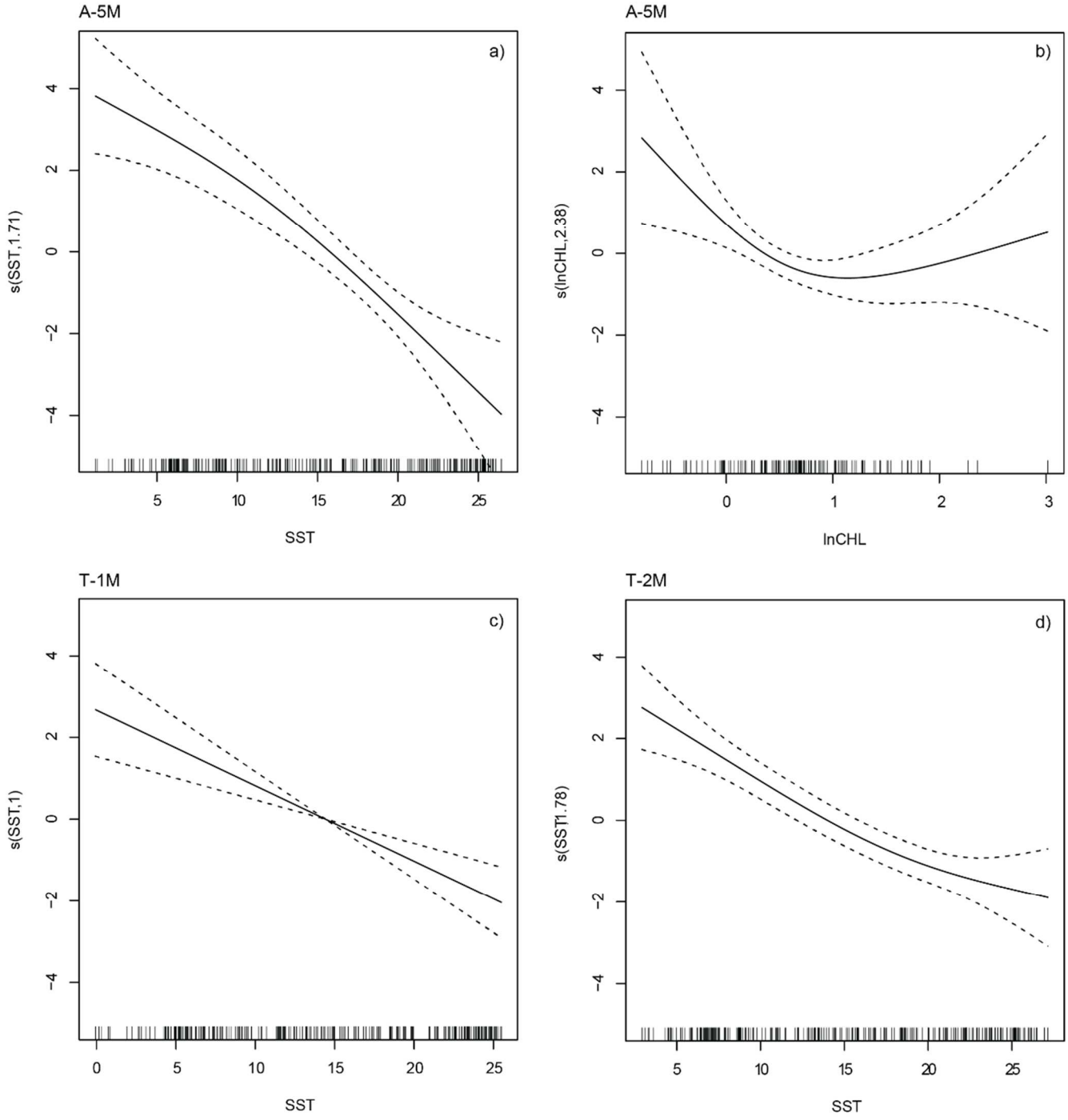

Figure 4.2.7a. North Atlantic right whale generalized additive model (GAM) smoothing curves for sites A-5M, T-1M, and T-2M

Smoothing curves for (a) North Atlantic right whale occurrence in relation to SST (°C) at site A-5M, (b) North Atlantic right whale occurrence in relation to Chl-a concentration (mg m^{-3}) at site A-5M, (c) North Atlantic right whale occurrence in relation to SST (°C) at site T-1M, and (d) North Atlantic right whale occurrence in relation to SST (°C) at site T-2M. The predictor is on each x-axis, the fitted smooth function on the y-axis, and the dashed lines are error bands. Tick marks on the x-axes (rug plots) show the distribution of the underlying data.

The results of the GAM model at survey site A-5M suggest SST was significantly related to the acoustic occurrence of humpback whales during the 3-year survey period ($p < 0.001$), while Chl-a concentration was not significant (Table 4.2.7d). The GAM model explained 31.6% of the deviance in humpback whale acoustic occurrence at site A-5M.

Table 4.2.7d Generalized additive model (GAM) results used to relate the weekly acoustic occurrence of humpback whales to sea surface temperature (SST) and the natural logarithm of chlorophyll-a (ln Chl-a) concentration at site A-5M.

Site A-5M, Humpback Whale				
Parametric Coefficients				
	Estimate	Standard Error	z	P (>|z|)
Intercept	-3.27	0.84	-3.90	<0.001***
Smooth Terms				
	Estimated Degrees of Freedom	Reference Degrees of Freedom	χ^2	P
SST	2.48	2.81	16.32	<0.001***
ln (Chl-a)	2.46	2.79	7.92	0.10
$R^2 = 0.27$	Deviance explained = 31.6%	UBRE = -0.35	Scale est. = 1	n = 260

The results of the GAM model at survey site T-2M suggest the environmental covariates SST and log-transformed Chl-a concentration were significantly (SST: $p < 0.001$; Chl-a: $p = 0.037$) related to the acoustic occurrence of humpback whales during the 3-year survey period (Table 4.2.7e). The GAM model explained 36.1% of the deviance in humpback whale acoustic occurrence at site T-2M.

We did not observe statistically significant relationships between humpback whale acoustic occurrence and environmental covariates at survey site T-1M.

Table 4.2.7e Generalized additive model (GAM) results used to relate the weekly acoustic occurrence of humpback whales to sea surface temperature (SST) and the natural logarithm of chlorophyll-a (ln Chl-a) concentration at site T-2M.

Site T-2M, Humpback Whale				
Parametric Coefficients				
	Estimate	Standard Error	z	P (>|z|)
Intercept	-2.52	0.40	-6.28	<0.001***
Smooth Terms				
	Estimated Degrees of Freedom	Reference Degrees of Freedom	χ^2	P
SST	5.23	6.27	36.176	<0.001***
ln (Chl-a)	2.06	2.61	8.47	0.037*
$R^2 = 0.33$	Deviance explained = 36.1%	UBRE = -0.32	Scale est. = 1	n = 251

The statistically significant GAM models at site A-5M and T-2M were represented visually with smoothing curves to determine how the environmental covariates related to acoustic occurrence of humpback whales (Figure 4.2.7b). The smoothing curves suggest a non-linear relationship between SST and humpback whale acoustic occurrence at survey sites A-5M and T-2M; humpback whale presence increased as SST increased, until acoustic occurrence peaked at approximately 10°C (Figure 4.2.7b). Humpback whale acoustic occurrence then decreased as SST increased. The smoothing curve suggests a positive relationship between Chl-a concentration and humpback whale acoustic occurrence at site T-2M (Figure 4.2.7b).

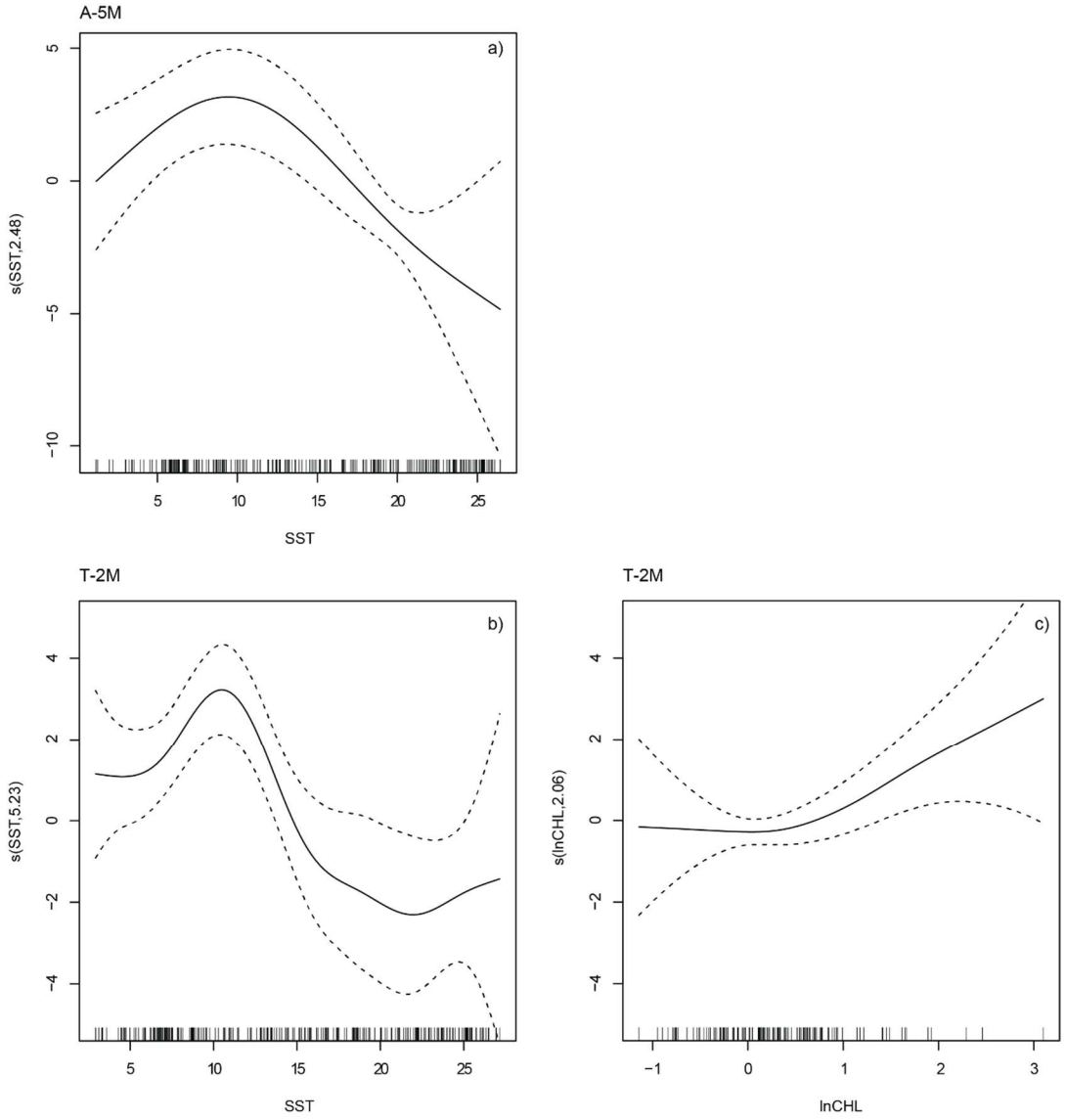

Figure 4.2.7b. Humpback whale generalized additive model (GAM) smoothing curves for sites A-5M and T-2M

Smoothing curves for (a) humpback whale occurrence in relation to SST (°C) at site A-5M, (b) humpback whale occurrence in relation to SST (°C) at site T-2M, and (c) humpback whale occurrence in relation to Chl-a concentration (mg m^{-3}) at site T-2M. The predictor is on each x-axis, the fitted smooth function on the y-axis, and the dashed lines are error bands. Tick marks on the x-axes (rug plots) show the distribution of the underlying data.

The results of the GAM model at survey site A-5M suggest SST was significantly related to the acoustic occurrence of fin whales during the 3-year survey period ($p < 0.001$), while Chl-a concentration was not significant (Table 4.2.7f). The GAM model explained 23.5% of the deviance in fin whale acoustic occurrence at site A-5M.

Table 4.2.7f Generalized additive model (GAM) results used to relate the weekly acoustic occurrence of fin whales to sea surface temperature (SST) and the natural logarithm of chlorophyll-a (ln Chl-a) concentration at site A-5M.

Site A-5M, Fin Whale				
Parametric Coefficients				
	Estimate	Standard Error	z	P (>|z|)
Intercept	0.25	0.19	1.33	0.18
Smooth Terms				
	Estimated Degrees of Freedom	Reference Degrees of Freedom	χ^2	P
SST	5.64	6.68	35.99	<0.001***
ln (Chl-a)	7.52	8.45	15.79	0.071
$R^2 = 0.24$	Deviance explained = 23.5%	UBRE = 0.17	Scale est. = 1	n = 260

The statistically significant GAM model at site A-5M was represented visually with a smoothing curve to determine how the environmental covariate SST related to the acoustic occurrence of fin whales (Figure 4.2.7c). The smoothing curve suggests a negative, non-linear relationship between SST and fin whale acoustic occurrence at site A-5M (Figure 4.2.7c); as SST increased, acoustic presence of fin whales decreased. Consequently, fin whales occurred more frequently when SST was at or below 5°C (Figure 4.2.7c). Fin whale acoustic occurrence stabilized at a plateau between 10 – 20°C, before decreasing again with increased SST.

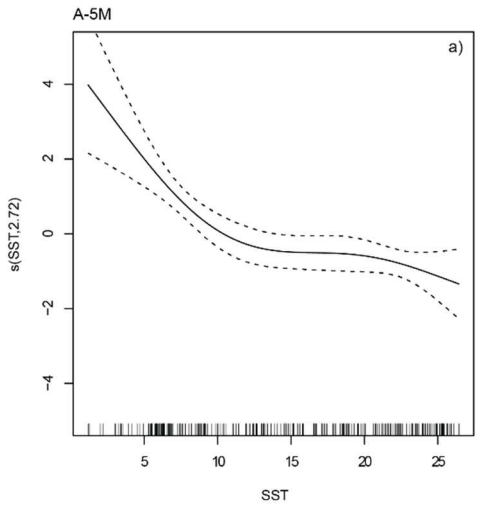

Figure 4.2.7c. Fin whale generalized additive model smoothing curve for site A-5M
Smoothing curve for fin whale occurrence in relation to SST (°C) at site A-5M. The predictor is on the x-axis, the fitted smooth function on the y-axis, and the dashed lines are error bands. Tick marks on the x-axis (rug plot) show the distribution of the underlying data.

4.3 North Atlantic Right Whale Location Estimates

We located the 17 known locations of playback tones along the two perpendicular transect lines (spanning west-east, and south-north) of the WEA, and compared the estimated locations of the playback tones to the known positions of the sound source. We also noted the locator tool score for each estimated location; the score was calculated as a weighted average of the number of channels with a normalized correlation with the first arrival above a threshold of 0.1, the average of the cross-correlation peaks for the channels above thresholds, and the distance between the theoretical time differences of arrival (TDOAs) and the peaks of the cross-correlation functions. The minimum score was 0 and the maximum score was 10.

Along the west-east transect, not pruned by locator score, the median error was 609 meters (n = 71) with a corresponding standard deviation of 195 meters (Figure 4.3a). When pruned at a locator score of 5.0, the median error was 320 meters (n = 48) with a standard deviation of 126 meters (Figure 4.3b).

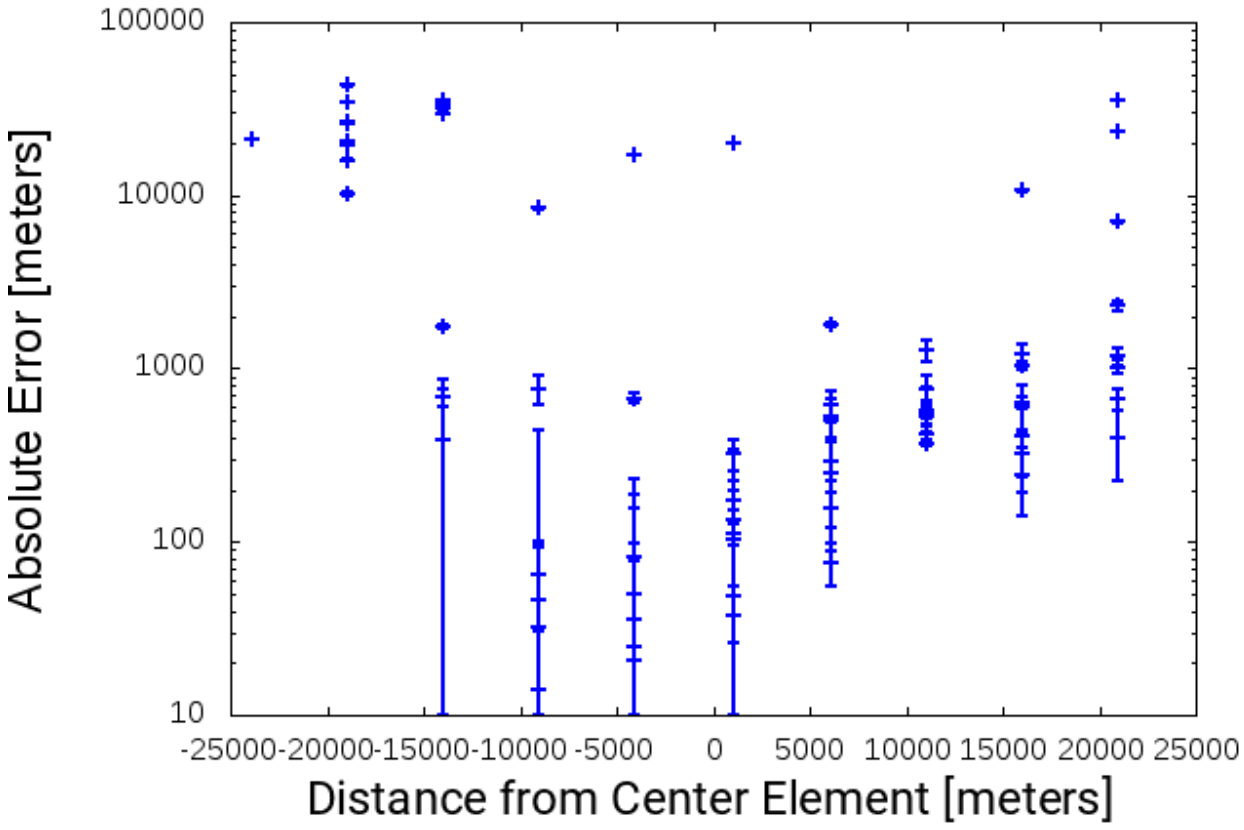

Figure 4.3a. Absolute error of playback tone locations along the west-east transect
The absolute error was computed as the distance between the locator output and the GPS location of the source vessel. The GPS locations were compensated for a constant velocity drift of the source vessel. Error bars were computed from the 95% confidence regions of the locator output.

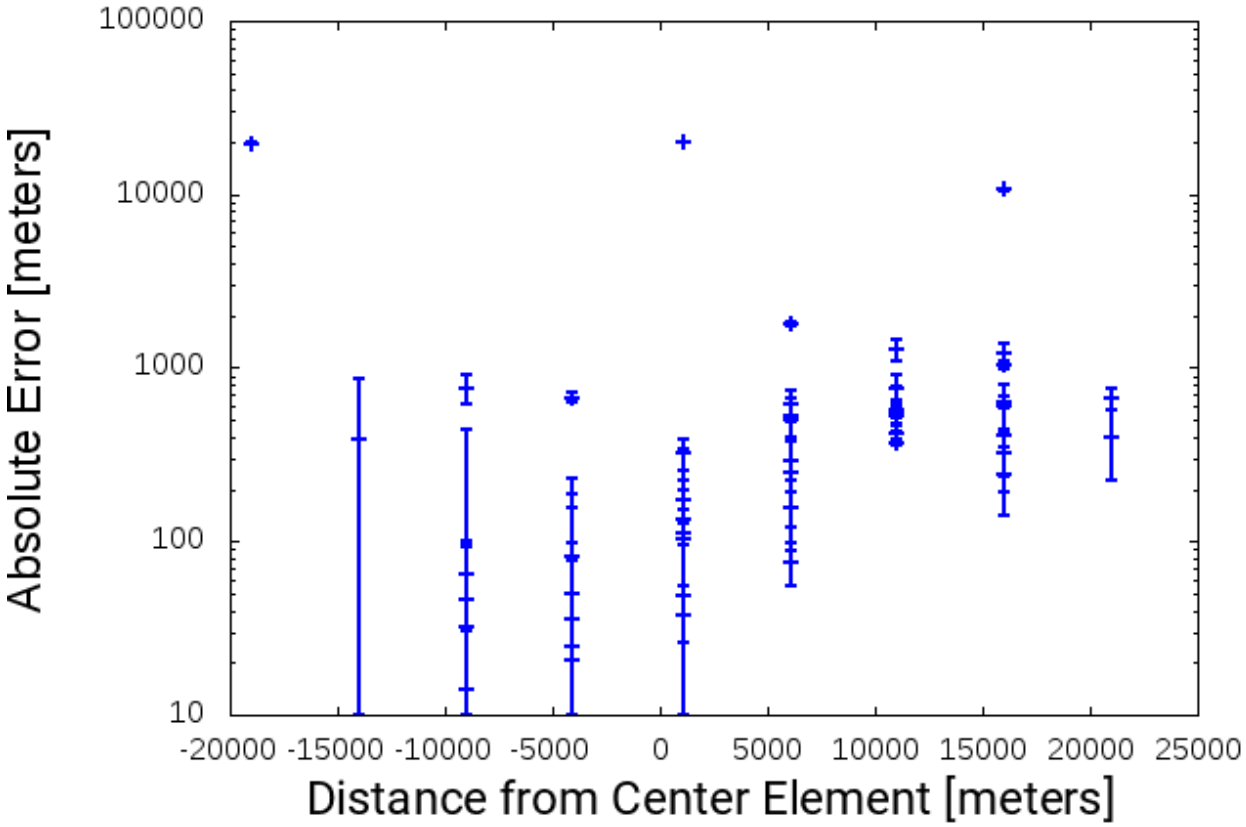

Figure 4.3b. Absolute error of playback tone locations with a locator score ≥ 5.0 along the west-east transect

The absolute error was computed as the distance between the locator output and the GPS location of the source vessel. The GPS locations were compensated for a constant velocity drift of the source vessel. Error bars were computed from the 95% confidence regions of the locator output.

Along the south-north transect, the median error was 3036 meters (n = 32) with a standard deviation of 65.32 meters (Figure 4.3c). When pruned at a locator score of 5.0, the median error was 277 meters (n = 9) with a standard deviation of 68.5 meters (Figure 4.3d).

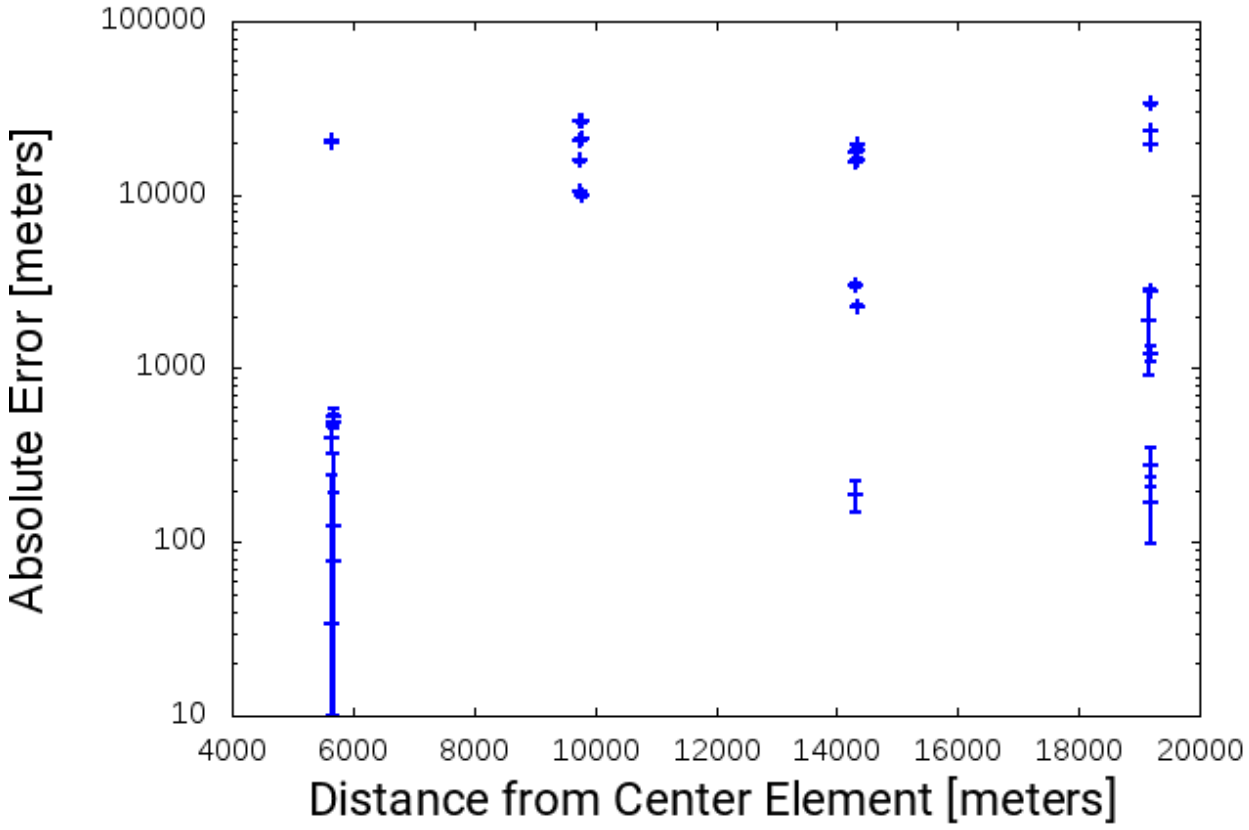

Figure 4.3c. Absolute error of playback tone locations along the south-north transect
The absolute error was computed as the distance between the locator output and the GPS location of the source vessel. The GPS locations were compensated for a constant velocity drift of the source vessel. Error bars were computed from the 95% confidence regions of the locator output.

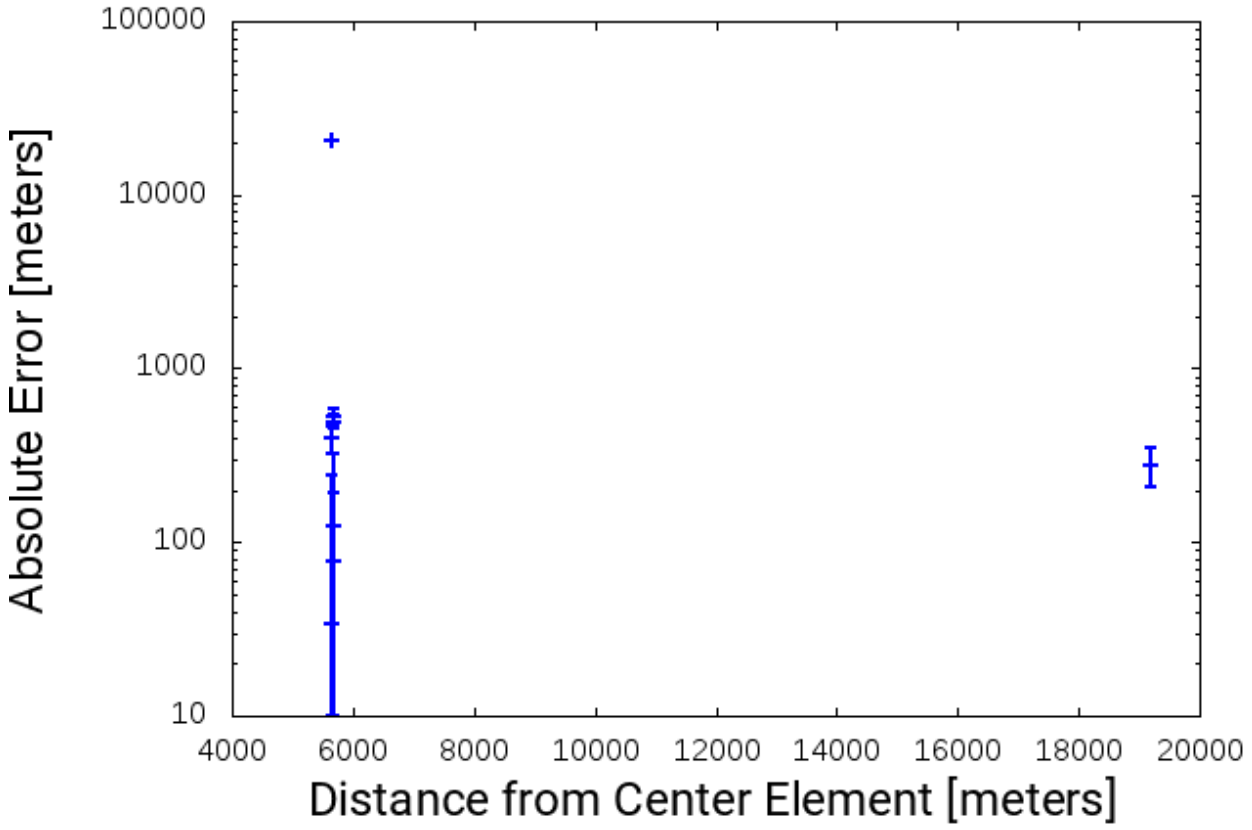

Figure 4.3d. Absolute error of playback tone locations with a locator score ≥ 5.0 along the south-north transect

The absolute error was computed as the distance between the locator output and the GPS location of the source vessel. The GPS locations were compensated for a constant velocity drift of the source vessel. Error bars were computed from the 95% confidence regions of the locator output.

Table 4.3a summarizes the locator error across both transects. Our conclusions derived the table's contents hinge on how closely the locator scoring system parallels human judgement. We believe that trained analysts are more capable of discerning valid locator output than the scoring system employed. The median and standard deviation of the locator output with score greater than 5 represents a worst-case scenario; human operators could have undoubtedly achieved a lower median error. The standard deviations are strictly a function of the sharpness of the energy peaks, and are believed to be more consistent with results obtainable by human operators. The north-south transect entry in Table 4.3a clearly shows considerable bias, the source of which is unclear. Given the results of Table 4.3a, we estimate that the accuracy in the human-browsed location data was approximately 300 meters, with a precision on the order of 100 meters.

Table 4.3a Median error along the entirety of the west-east and south-north transect and the associated locator standard deviation.

Transect	Median Error (meters)	Standard Deviation (meters)
West-East	609	195
West-East, score > 5.0	320	126
South-North	3036	65.3
South-North, score > 5.0	277	68.5

Of the 35,510 true North Atlantic right whale up-call detections validated during whale occurrence analysis, a total of 7475 were deemed potentially locatable (recorded on a minimum of three or more MARUs) and were processed in the CSE Locator Tool in Raven 2.0 (Table 4.3b). After visually inspecting the alignment of the arrival boxes, it was determined that a fraction of these potentially locatable up-calls (n = 1979) had a qualitative score ≥ 0.4, and were thus considered to have acceptable location estimates (Table 4.3b; Table 4.3c). The performance of the CSE localization algorithm was likely due to low SNR of North Atlantic right whale up-calls, high ambient noise levels, low density of sensors, or a combination thereof.

Table 4.3b Number of analysis days, number of North Atlantic right whale detector events, number of true positive up-call detections, number of potentially locatable up-call detections, and number of locatable up-call detections.

Number Analysis Days	Number North Atlantic Right Whale Detector Events	Number True Positive North Atlantic Right Whale Up-calls	Number Potentially locatable North Atlantic Right Whale Up-calls (≥ 3 arrivals)	Number of Locatable North Atlantic Right Whale Up-calls
273	431,348	35,510	7475	1979

Reliable location estimates of up-calls across the 3-year survey period spanned inshore, offshore, and within the WEA (Figure 4.3e). Kernel density analysis showed higher densities of located up-calls occurring along the eastern edge of the WEA; high densities of located up-calls also occurred offshore of the WEA and within the northern region of the WEA (Figure 4.3e).

North Atlantic right whale up-call location estimates varied between months (Figure 4.3f), suggesting a seasonal pattern of movement in the survey area. Aggregates of up-calls were located throughout the WEA during the month of January across the 3-year survey period; up-call aggregates also occurred offshore of the southeastern edge of the WEA (Figure 4.3f). During the month of February, up-calls were distributed within the southern portion of the WEA and outside the northeast part of the WEA. Up-calls located during the month of March were widely distributed inshore, offshore, and within the WEA, with aggregates occurring mostly offshore and along the eastern edge of the WEA (Figure 4.3f). Only two reliable up-call locations occurred during April, both of which were located offshore of the WEA. A few reliable locations occurred during the month of November along the southern edge and the northern tip of the WEA. Location aggregates during December predominately occurred along the central-western WEA as well as offshore of the northeastern and eastern part of the WEA (Figure 4.3f). No reliable location estimates occurred during the May to October timeframe.

Table 4.3c Number of location estimates by location quality score. Calls with location quality scores that are < 0.4 are excluded from locations analysis.

Quality Score Range (min : max)	Number of North Atlantic Right Whale Up-calls
0.90 : 1.00	490
0.80 : 0.89	306
0.70 : 0.79	307
0.60 : 0.69	346
0.50 : 0.59	364
0.40 : 0.49	166
0.00 : 0.39	5496

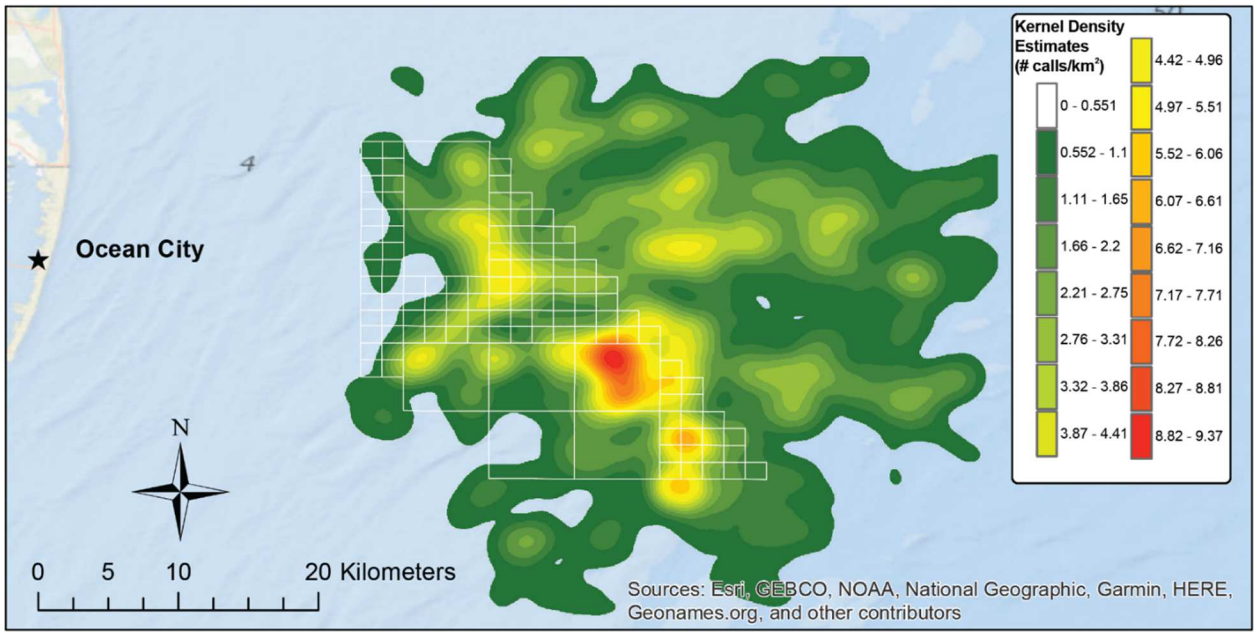

Figure 4.3e. Kernel density of North Atlantic right whale up-call location estimates
Kernel density estimation of the number of locatable North Atlantic right whale up-calls per square kilometer across the 3-year survey period.

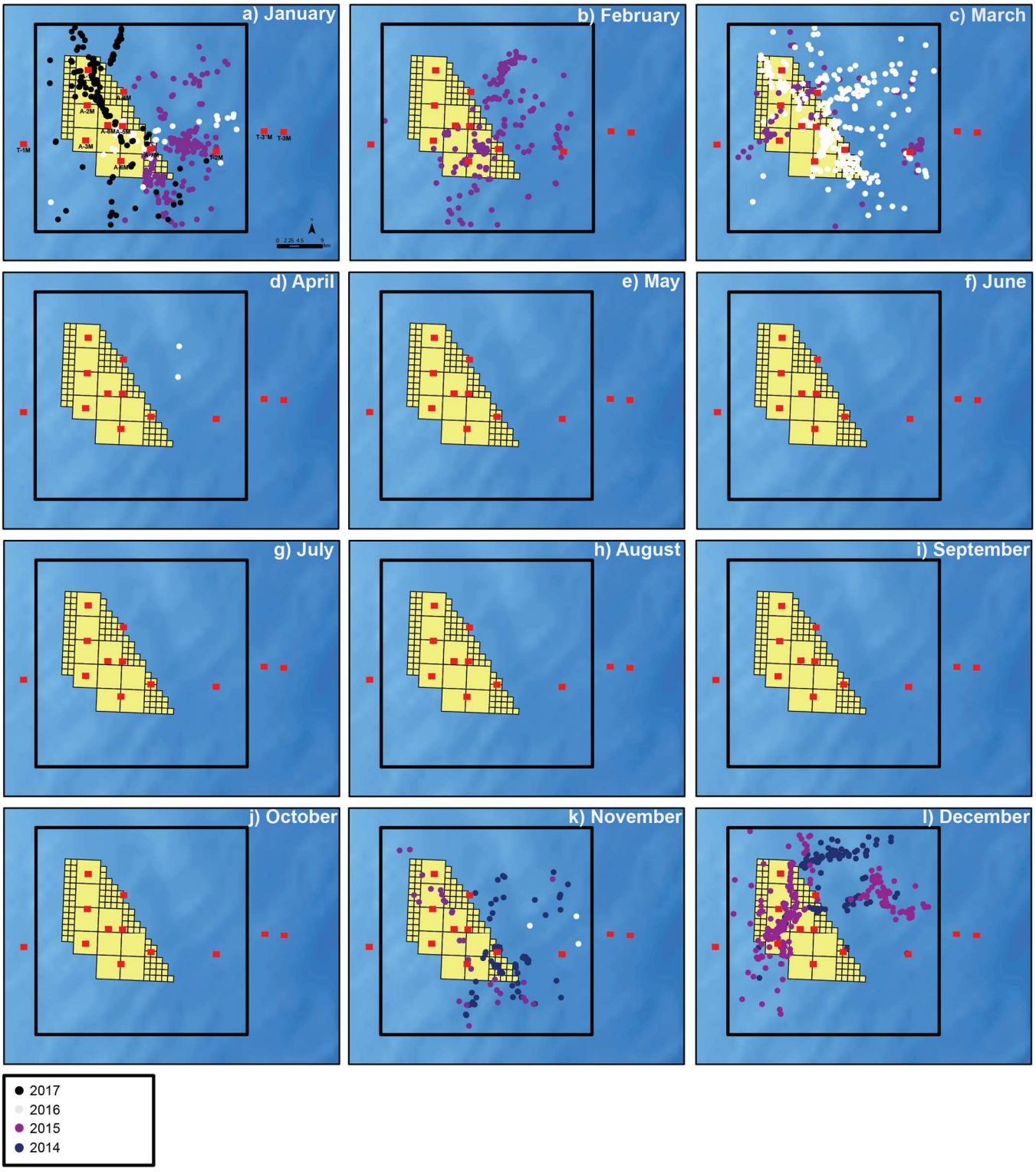

Figure 4.3f. Monthly location estimates of North Atlantic right whale up-calls
North Atlantic right whale location estimates during (a) January, (b) February, (c) March, (d) April, (e) May, (f) June, (g) July, (h) August, (i) September, (j) October, (k) November, and (l) December. Red squares indicate survey sites, and colored dots indicate year in which location estimate occurred.

A total of 7475 first arrival up-calls (i.e. the survey site at which the first recording of the locatable call occurred) showed a relative distribution of North Atlantic right whale up-calls occurring across all survey sites (except T-3M) during the 3-year survey period (Figure 4.3g). The distribution of first arrival up-calls varied between sites, with the greatest percentage of up-calls occurring at site A-7M (21.9%), A-5M (18.2%), and A-4M (17.5%) along the eastern edge of the WEA (Figure 4.3g, Table 4.3d).

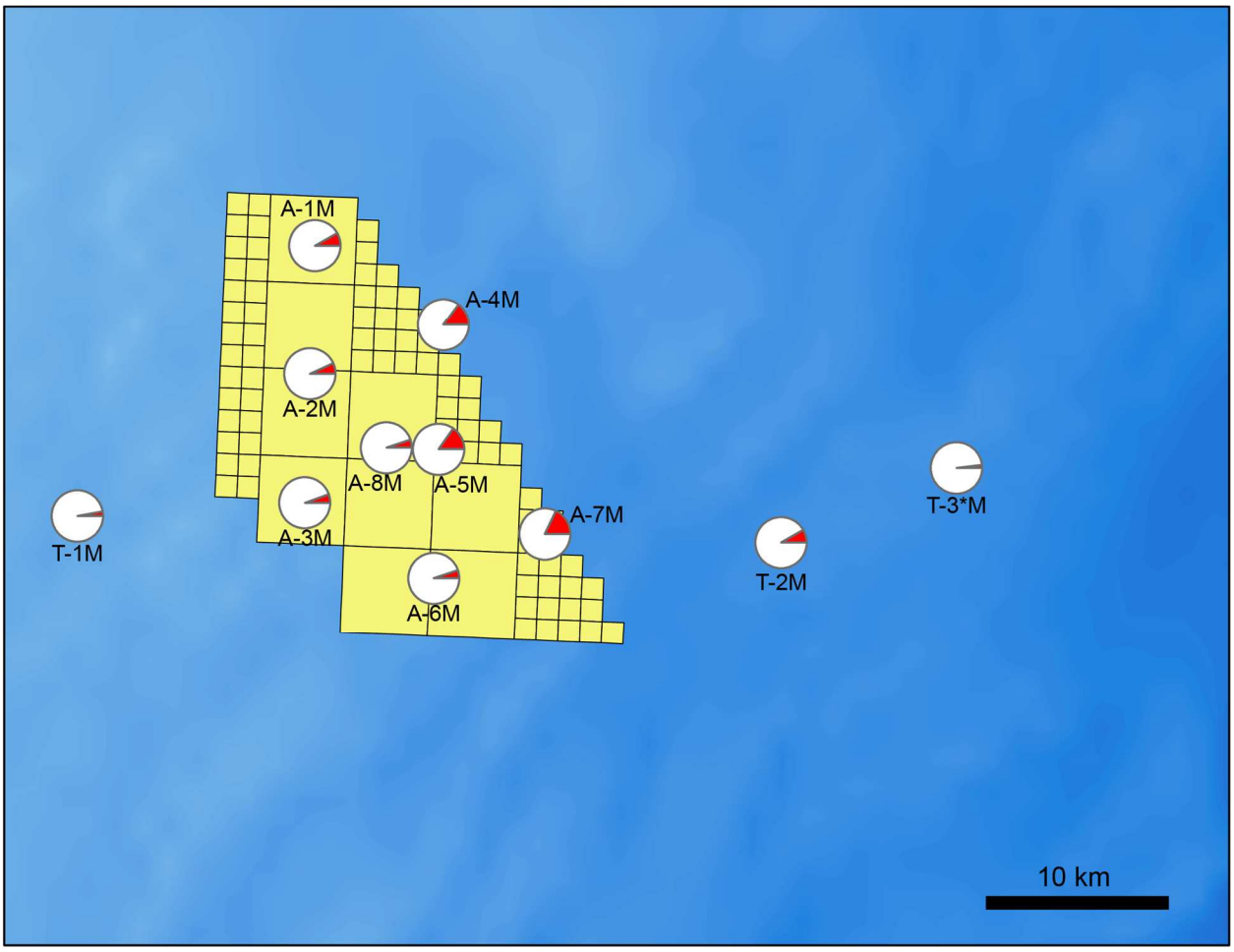

Figure 4.3g. Relative distribution of first arrival North Atlantic right whale up-calls
Relative distribution of first arrival North Atlantic right whale up-calls inshore, offshore, and within the Maryland WEA during the 3-year survey period. Red indicates the relative proportion of first arrivals.

Table 4.3d Total number and percentage of North Atlantic right whale up-call first arrivals detected during the 3-year survey period at each survey site.

Site	Number of First Arrivals	Percent
T-1M	20	0.3%
A-1M	671	9.0%
A-2M	537	7.2%
A-3M	432	5.8%
A-4M	1305	17.5%
A-5M	1361	18.2%
A-6M	421	5.6%
A-7M	1636	21.9%
A-8M	402	5.4%
T-2M	673	9.0%
T-3*M	17	0.2%

A seasonal pattern of relative distribution of first arrival up-calls was observed across the 3-year survey period. Most first arrival up-calls occurred during winter (January – March), with the greatest overall proportion of calls occurring at sites A-7M (19.9%), A-5M (16.5%), and A-4M (13.4%) along the eastern edge of the WEA (Figure 4.3h, Table 4.3e). This coincides with the peak acoustic presence of North Atlantic right whales occurring during winter months (see Section 4.2 “Baleen Whale Acoustic Occurrence”). A relatively small proportion of first arrival up-calls occurred during autumn (October – December), with the greatest overall proportion of calls occurring at site A-4M (4%) (Figure 4.3h; Table 4.3e). Spring (April – June) had a low number of first arrival up-calls (n = 48; Table 4.3e), with the largest overall proportion (0.3%) occurring at site A-7M (Figure 4.3i). Only 8 first arrival up-calls were found during the summer months (July – September), with the greatest overall proportion (0.1%) occurring offshore of the WEA at site T-2M (Figure 4.3h, Table 4.3e).

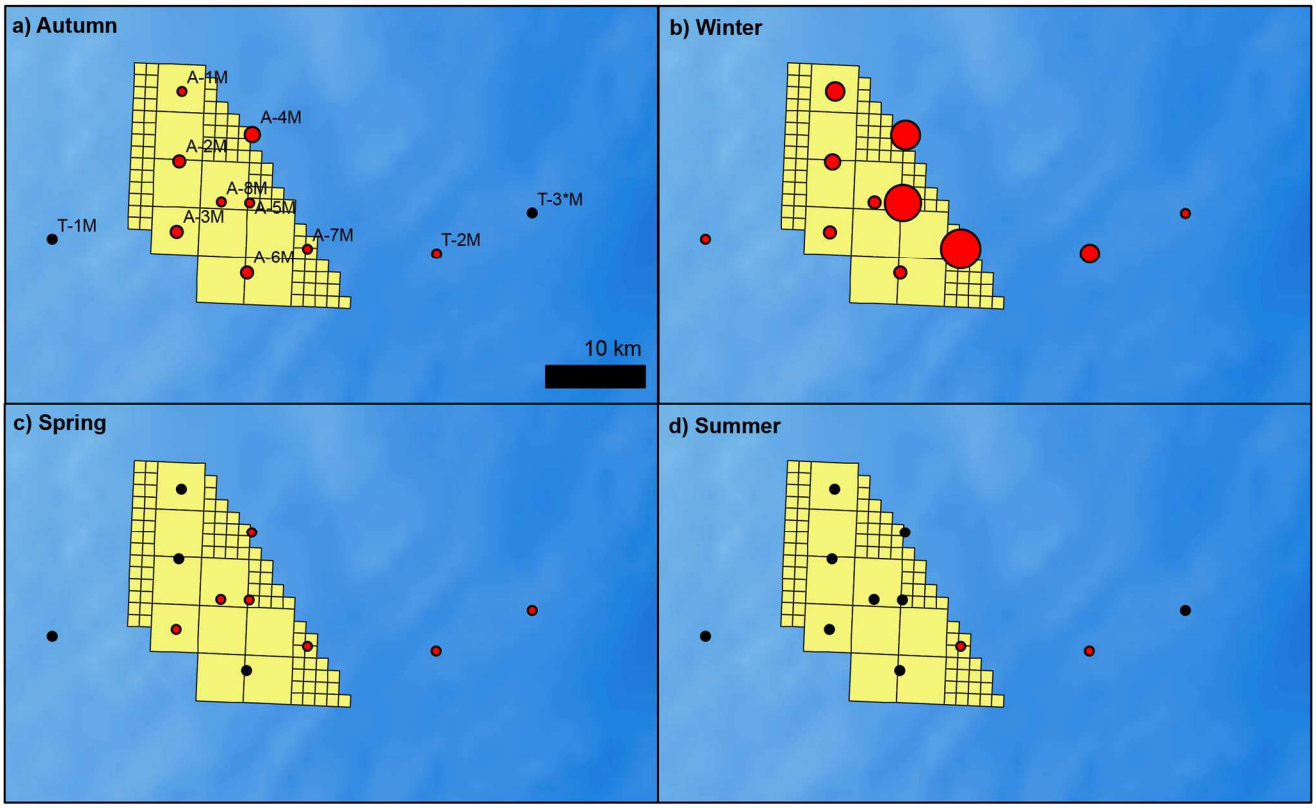

Figure 4.3h. Relative seasonal distribution of first arrival North Atlantic right whale up-calls
The relative distribution of first arrival North Atlantic right whale up-calls during (a) Autumn (October – December), (b) Winter (January – March), (c) Spring (April – June), and (d) Summer (July – September) months at each survey site indicated by red circles. The size of the red circle indicates the relative proportion of first arrivals across the entire 3-year survey period. Black circles indicate no first arrival North Atlantic right whale up-calls occurred at that site.

Table 4.3e Total number and proportion (%) of first arrival North Atlantic right whale up-calls detected during autumn (October – December), winter (January – March), spring (April – June), and summer (July – September) months at each survey site.

Site	Number of First Arrivals: Autumn	Proportion (%) Autumn	Number of First Arrivals: Winter	Proportion (%) Winter	Number of First Arrivals: Spring	Proportion (%) Spring	Number of First Arrivals: Summer	Proportion (%) Summer
T-1M	0	0%	20	0.3%	0	0%	0	0%
A-1M	105	1.4%	566	7.6%	0	0%	0	0%
A-2M	176	2.4%	361	4.8%	0	0%	0	0%
A-3M	206	2.8%	225	3.0%	1	0.01%	0	0%
A-4M	300	4.0%	1000	13.4%	5	0.07%	0	0%
A-5M	115	1.5%	1231	16.5%	14	0.2%	0	0%
A-6M	203	2.7%	218	2.9%	0	0%	0	0%
A-7M	125	1.7%	1491	19.9%	20	0.3%	1	0.01%
A-8M	113	1.5%	284	3.8%	5	0.1%	0	0%
T-2M	90	1.2%	574	7.7%	2	0.03%	7	0.1%
T-3*M	0	0%	16	0.2%	1	0.01%	0	0%

When examining the locations of detected North Atlantic right whale calls in aggregate, there appeared to be a number of calls that formed lines, suggesting possible tracks of calling individual animals. We examined the spatial and temporal properties of over 100 putative tracks from across the project, and detailed time series analysis revealed that the overwhelming majority of these calls did not actually form tracks; the calls did not occur in a linear sequence in space and time. Many times, when analyzing the sequence of calls, the next spatially occurring call occurred several hours after the first call making it less likely that it was produced by the same whale, or the next call occurring in time was located in a spatial location that appeared unrealistic for the movement of these whales and was thus unlikely to be part of an individual whale's track. In being conservative in our approach, we are showing data for all of the tracks that we had confidence could potentially be tracks of individual animals. For calls that were separated by times greater than 20 minutes or distances greater than 1 km, we did not feel confident that these calls were part of a track produced by a single animal. Consequently, North Atlantic right whale up-call track analysis yielded a total of 5 putative call tracks; 3 of the putative call tracks occurred on 31 December 2015, while the remaining two tracks occurred on 7 December 2015 and 25 December 2016 (Figure 4.3i).

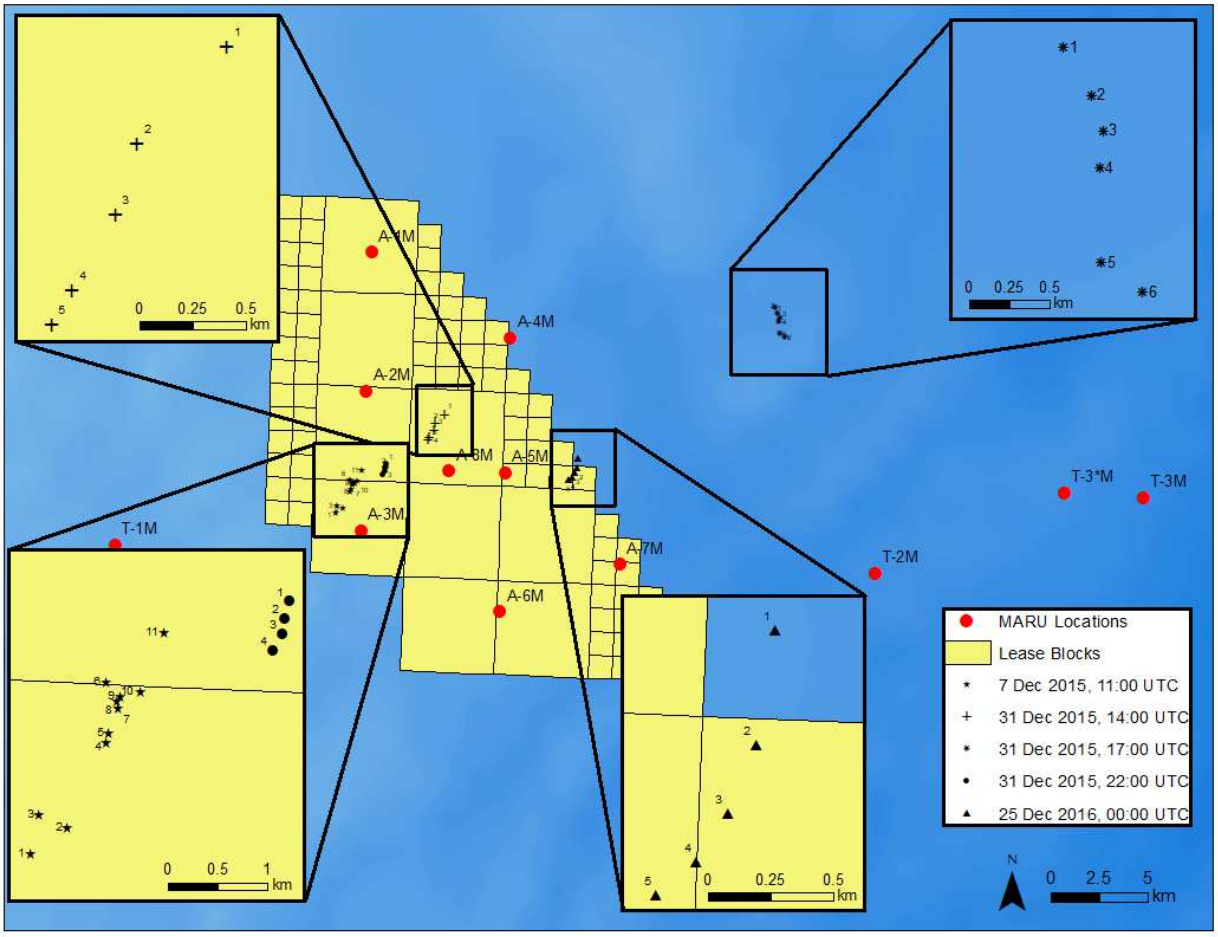

Figure 4.3i. Putative North Atlantic right whale up-call tracks
Putative North Atlantic right whale up-call tracks occurring during 7 December 2015, 31 December 2015, and 25 December 2016. Numbers indicate overall direction of movement between the start and end time of each track.

The putative call track occurring during 7 December 2015 (n = 11 locations) traveled an overall distance of 2.58 km in a northeast direction (bearing 028°) through the WEA, at an average velocity of 6.38 km/h (Figure 4.3i). The putative call track occurring during the 31 December 2015 at the 14:00 UTC hour (n = 5 locations) traveled an overall distance of 1.55 km in a southwest direction (bearing 210°) through the WEA, at an average speed of 9 km/h (Figure 4.3i). While the track occurring at the 17:00 UTC hour during 31 December 2015 moved in an overall northeast direction (bearing 196°) through the WEA, the sequence of locations (n = 4) showed more circuitous movements, covering an overall distance of 0.5 km at a speed of 5.59 km/h (Figure 4.3j). The putative call track occurring during the 22:00 UTC hour on 31 December 2015 (n = 6 locations) moved in an overall southwest direction (bearing 160°) offshore of the WEA; the distance covered during this putative call track was 1.6 km at an average velocity of 3.51 km/h (Figure 4.3j). Lastly, the track occurring during 25 December 2016 (n = 5 locations) moved in an overall southwest direction (bearing 202°) from offshore the WEA into the WEA (Figure 4.3j). This track traveled an overall distance of 1.16 km at an average speed of 2 km/h.

4.4 C-POD Validation

4.4.1 C-POD Detection Rate

In all deployments, the total C-POD detection-positive hours using the "High" and "Moderate" filters were lower than those found using PAMGUARD with manual verification (Table 4.4.1a). The proportion of hours for which the C-POD correctly indicated dolphin presence (PPV) was extremely high (mean 99.6%; all deployments ≥ 99%), indicating that the accuracy of C-POD dolphin detections was very high. As such, there were very few false positive detections, with a maximum false positive rate (FPR) of only 0.01%. The true negative rate (TNR) was very high (all deployments ≥ 99%). However, there were a large number of detection-positive hours from PAMGUARD with no corresponding detection by the C-POD. This false negative rate (FNR) was highly variable (range 47 – 76%) indicating the C-POD missed a relatively high number of detection-positive hours, but the rate at which detections were missed was not consistent across deployments. Therefore, C-PODs only correctly predicted hourly absence of dolphins (NPV) a mean of 67% of the time (range 46 – 93%).

Using the "High", "Moderate", and "Low" C-POD filters increased the number of detection-positive hours compared to the "High" and "Moderate" filters, but the PAMGUARD analysis indicated that some of these click train detections were not from dolphins. The TPR increased, however so did the FPR, meaning the C-POD accurately predicted dolphin presence less often when using the “Low” filter (mean PPV 79%) relative to when only the “High” and “Moderate” filters were used (mean PPV 99.6%). In the majority of deployments, the proportion of hours that the C-POD correctly predicted dolphin absence increased marginally with the inclusion of the “Low” filter (NPV higher by 2 – 8%), but at T-1C during May – June 2016, the “Low” filter classified every hour as detection-positive, resulting in a 0% NPV.

Table 4.4.1a Results of PAMGUARD dolphin detection and corresponding true positive (TP), false positive (FP), true negative (TN), and false negative (FN) detection hours and rates, and positive predictive (PP) and negative predictive (NP) values for C-PODs using the "High" and "Moderate" filter (bold text) and "High", "Medium", and "Low" filters (shaded).

	PAMGUARD results			C-POD results					
Location and deployment	**Recording effort (hours)**	**Dolphin presence (hours)**	**Dolphin absence (hours)**	**TP (hours, TPR)**	**FP (hours, FPR)**	**TN (hours, TNR)**	**FN (hours, FNR)**	**PP**	**NP**
T-1C February – May 2016	1364	689	675	172, 25%	0, 0%	675, 100%	517, 75%	100%	57%
				239, 35%	23, 3%	652, 97%	450, 65%	91%	59%
T-1C May – June 2016	882	629	253	332, 53%	2, <1%	251, 99%	297, 47%	99%	46%
				629, 100%	253, 100%	0, 0%	0, 0%	71%	0%
T-1C April – June 2017	1657	1013	644	375, 37%	2, <1%	639, 100%	641, 63%	99%	50%
				578, 57%	26, 4%	615, 96%	438, 43%	96%	58%
A-5C July – September 2016	1435	253	1182	111, 44%	0, 0%	1182, 100%	142, 56%	100%	89%
				147, 58%	43, 3.6%	1139, 96%	106, 42%	77%	91%
W-3C November 2016 – January 2017	1514	128	1386	31, 24%	0, 0%	1386, 100%	97, 76%	100%	93%
				59, 46%	38, 3%	1349, 97%	68, 54%	61%	95%
Average	1370	542	828	38%	<1%	99%	63%	99.6%	67%
				59%	23%	77%	41%	79%	61%

4.4.2 Detection Trends

Dolphins were present for a greater proportion of hours at T-1C than at A-5C or W-3C, peaking at T-1C during the April – June 2017 deployment. Using the "High" and "Moderate" filter results, C-POD detection accuracy at T-1C was similar across all deployments (Table 4.4.1a). The deployment with the least frequent dolphin presence (W-3C November 2016 – January 2017) had the lowest ability to correctly indicate presence (PPV) and the highest ability to indicate dolphin absence (NPV).

The cumulative detection-positive hours from the C-POD were significantly correlated with PAMGUARD detections relative to time of day for all deployments (T-1C February – April 2016: $r = 0.55$, $DF = 22$, $p = 0.005$; T-1C April – June 2016: $r = 0.48$, $DF = 22$, $p = 0.017$; A-5C July – September 2016: $r = 0.95$, $DF = 22$, $p < 0.001$; W-3C November – January: $r = 0.53$, $DF = 22$, $p = 0.008$), except at

T-1C during May to June 2016 where there was a weak diel pattern (r = 0.15, DF = 22, p = 0.48). While PAMGUARD consistently produced more detection-positive hours than the C-POD, the magnitude of these differences varied between deployments and sites. Despite this variability, the same diel pattern was generally observed using both detection methods. The diel pattern was most pronounced at A-5C during July – September 2016, with the highest levels of echolocation activity during the evening to early morning (Figure 4.4.2a).

At all sites, the majority of FN hours occurred within 24 hours of a TP hour (T-1C February – April 2016: 88%; T-1C May – June 2016: 100%; T-1C April – June 2017: 100%; A-5C July – September 2016: 95%; W-3C November 2016 – January 2017: 68%), and 50% of FN hours occurred within six hours or less of a TP hour (Figure 4.4.2b).

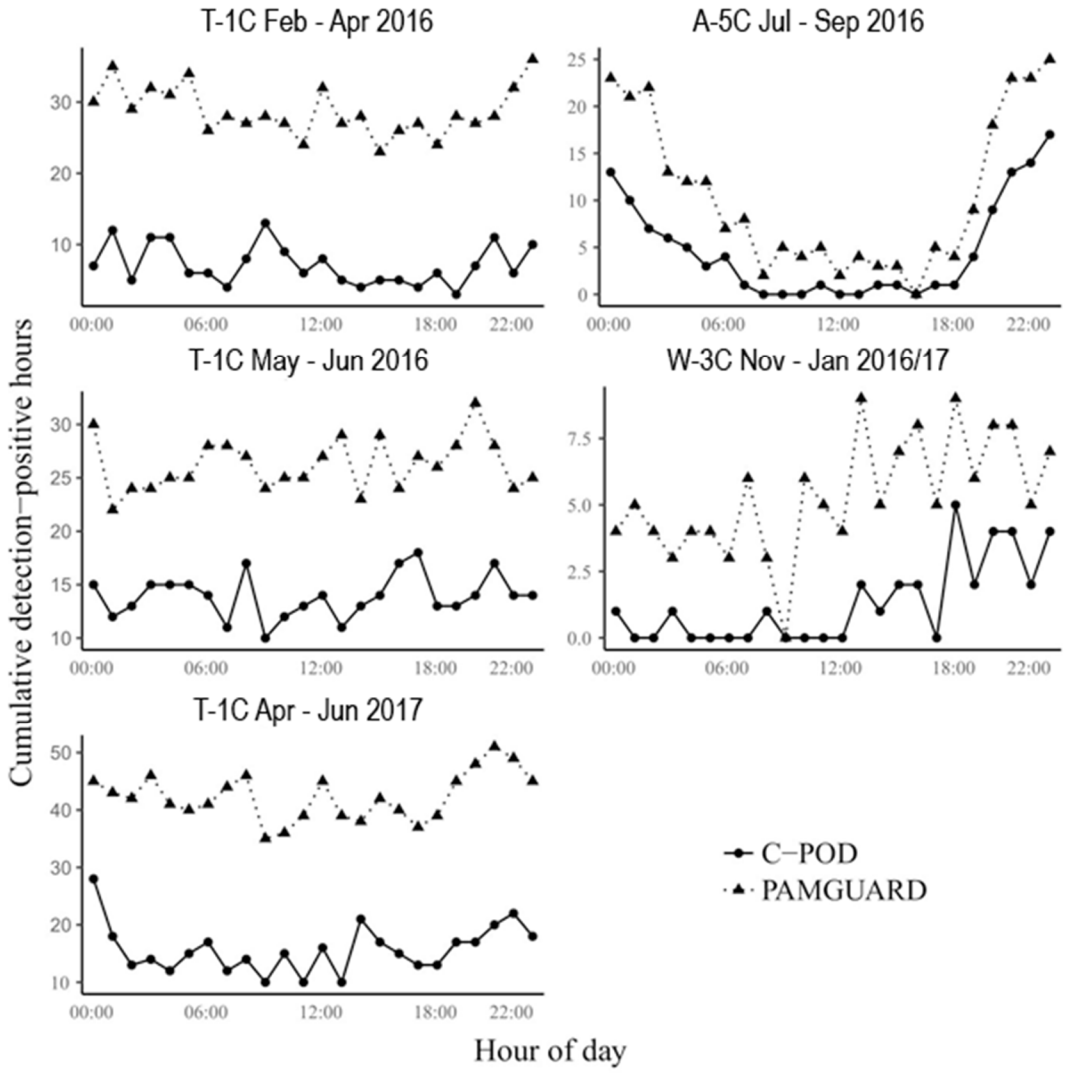

Figure 4.4.2a. Cumulative detection-positive hours
Cumulative detection-positive hours for both PAMGUARD and the C-POD for each hour of the day across all deployments.

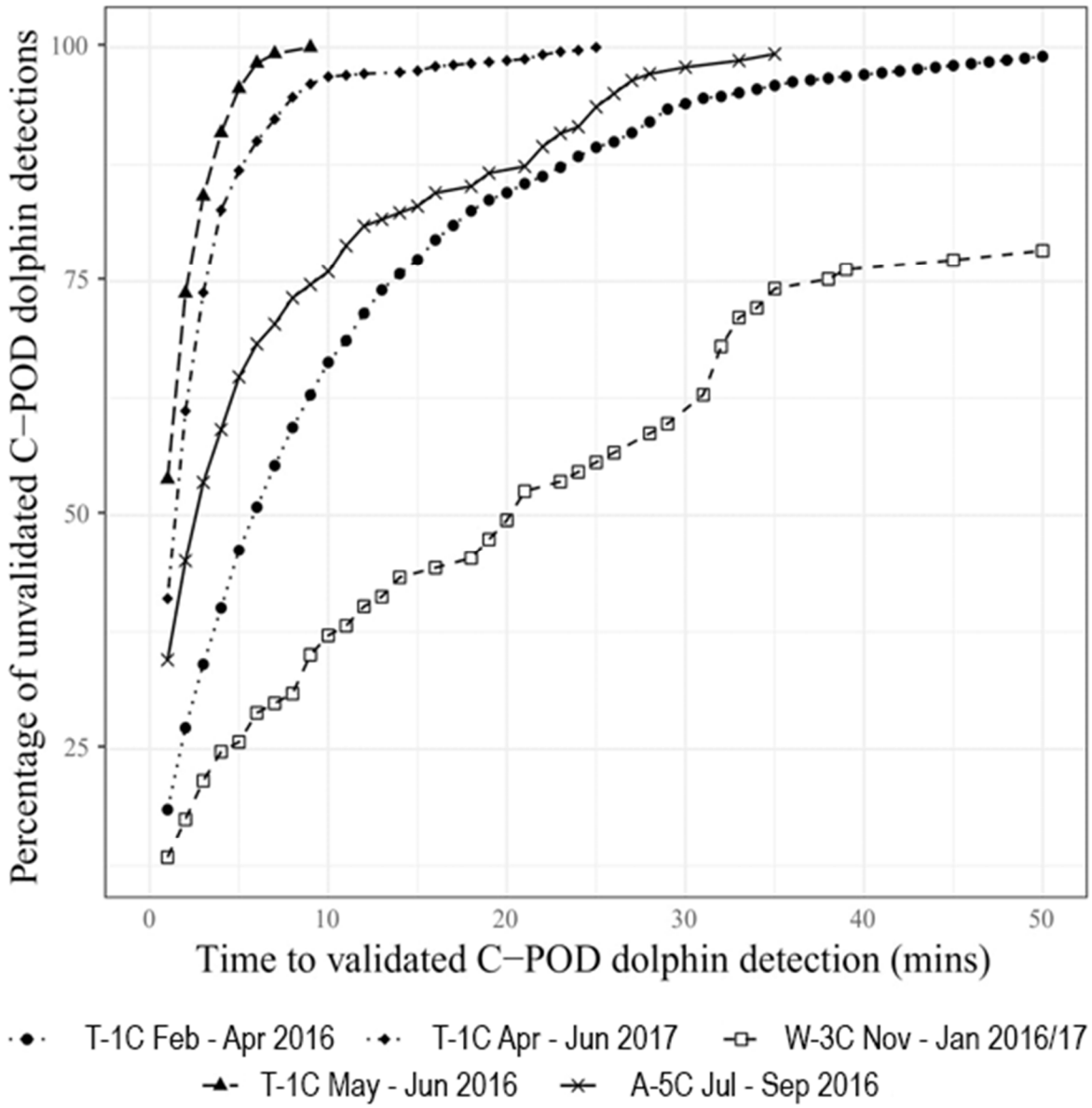

Figure 4.4.2b. Detection hour comparison between devices
Time difference between C-POD false negative detection hours (clicks detected by PAMGUARD but not by the C-POD) and true positive detection hours (clicks detected by both PAMGUARD and the C-POD) for each deployment.

4.4.3 Factors Affecting C-POD Detection Performance

High frequency background noise levels (20 – 24 kHz) and the number of dolphin clicks (from the PAMGUARD click classifier) significantly affected C-POD performance (Table 4.4.3a; Figure 4.4.3a). C-PODs were more likely to detect dolphin click trains during greater background noise above 20 kHz and when there were more dolphin clicks. The broadband background noise level, click P2P SPL and variation, minimum and inter-quartile range of ICIs, and location were not significantly related to the C-POD detecting (TP) or failing to detect dolphins (FN) (Table 4.4.3a).

Table 4.4.3a Results of the logistic regression for C-POD detection accuracy (defined as true positive (TP) or false negative (FN) detections) when dolphin clicks were detected by PAMGUARD in relation to click and soundscape variables from the SM3M recordings. The site location was included as a categorical variable where A-5C was the reference level. An asterisk denotes where p < 0.05.

	Regression results			
	Estimate	**Standard Error**	**Z value**	**P value**
Background broadband root mean square	0.014	0.093	0.15	0.88
Background high frequency (20 – 24 kHz) root mean square	0.26	0.072	3.56	<0.001*
Clicks per minute	0.025	0.005	4.79	<0.001*
Inter-click interval inter-quartile range	-0.87	1.13	-0.77	0.44
Minimum inter-click interval	-6.92	6.09	-1.14	0.26
Click peak-to-peak standard deviation	-0.17	0.17	-0.61	0.33
Mean click peak-to-peak	-0.03	0.047	-0.61	0.054
Site T-1C	0.57	1.63	0.35	0.73
Site W-3C	0.19	1.47	0.13	0.90

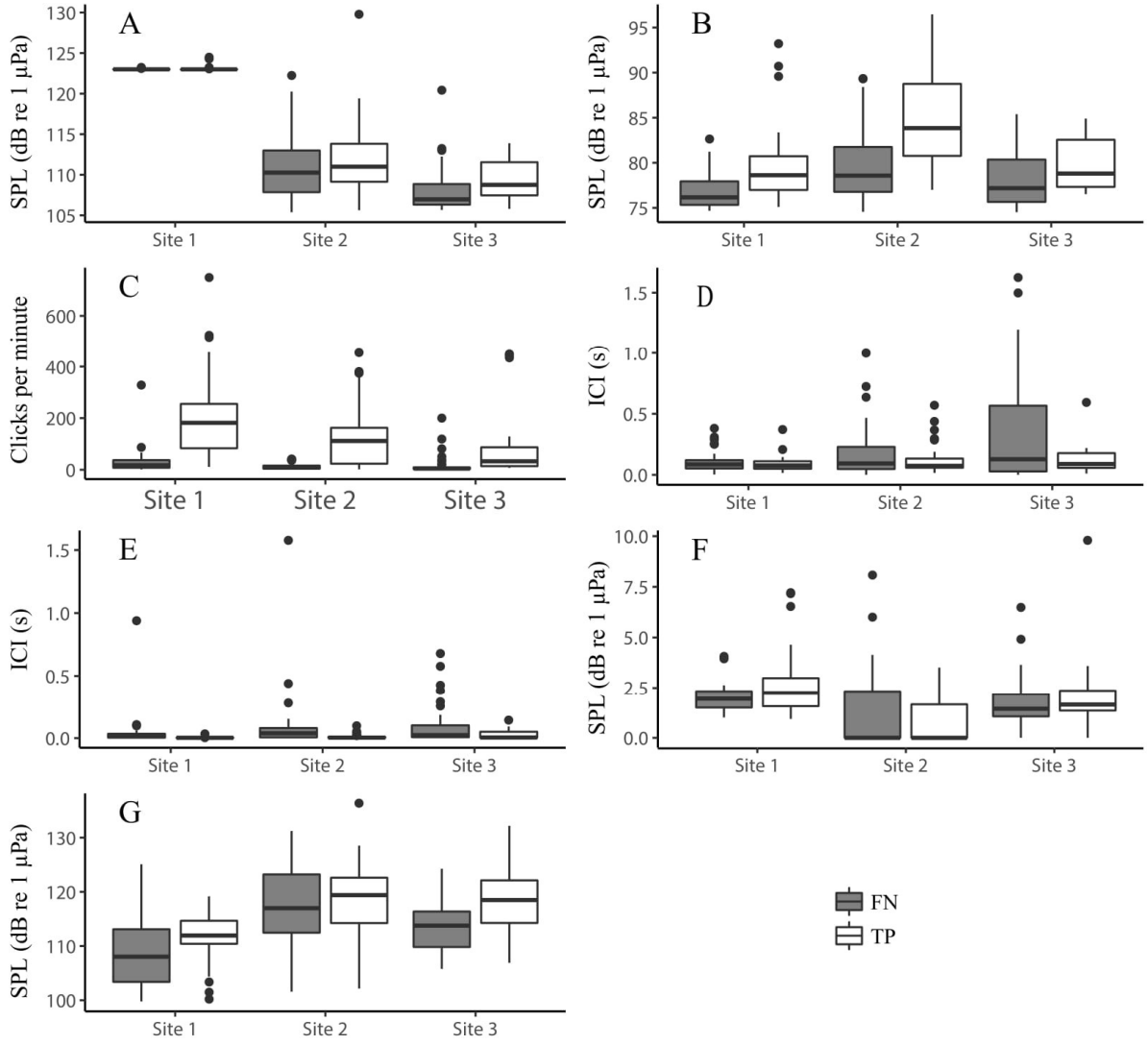

Figure 4.4.3a. True positive and false positive boxplots of background noise and click characteristics

Background noise and click characteristics for true positive (TP) and false negative (FN) C-POD dolphin detections: A. Background root mean square (RMS), B. High-frequency background RMS (20 – 24 kHz), C. Number of clicks per minute, D. Inter-click interval (ICI) inter-quartile range, E. Minimum ICI, F. Mean click peak-to-peak (P2P) mean, G. Click P2P RMS standard deviation.

4.5 Odontocete Occurrence

4.5.1 Species Classification

The random forest model performed well on the training dataset, correctly classifying 75% of the common dolphin sightings and 97% of the bottlenose dolphin sightings. We therefore proceeded to use this model to assign a species to our acoustic detections. The random forest classification model deemed all acoustic detections occurring at T-1C and A-5C (distance blocks A and B; < 22 km offshore and 22 – 41 km offshore) as bottlenose dolphins during all seasons. Detections at T-2C and T-3C (distance blocks

C and D; 41 – 57 km offshore and > 57 km offshore) were deemed bottlenose dolphins in summer and fall (June – November) and as common dolphins in winter and spring (December – May).

4.5.2 Bottlenose Dolphin Temporal Occurrence

For dolphin presence at site T-1C, the GARMA model with a Zero-Inflated Beta Binomial (ZIBB) distribution produced the best fit (lowest AIC score). For dolphin presence at site A-5C, a binomial (BI) distribution produced the best fit model. Sites T-2C and T-3C showed no significance of day, hour, or study year, so no model is shown for these sites.

Julian day was found to be a significant predictor of dolphin presence at both T-1C and A-5C, so it was included in both final models (Table 4.5.2a). This suggests a strong seasonal pattern in dolphin occurrence at these sites, with dolphins being detected more frequently in the spring and summer months than the autumn and winter months (Figures 4.5.2a – d). Hour of day was also found to be a significant predictor for both sites T-1C and A-5C (Figure 4.5.2e). Bottlenose dolphins were detected most often in the evening to early morning hours at T-1C and A-5C, suggesting a diel pattern in bottlenose dolphin acoustic occurrence at these sites (Figure 4.5.2e). There was significant inter-annual variability in the frequency of detections at sites T-1C and A-5C, with bottlenose dolphin presence significantly lower in Year 1 (November 2014 – October 2015) than other years (Figure 4.5.2f).

Table 4.5.2a Estimated parameters (standard errors in parentheses) from the generalized auto-regressive moving average (GARMA) models for dolphins at sites T-1C and A-5C. ZIBB = Zero-Inflated Beta Binomial, BI = Binomial, β values are the regression coefficients, φ_1 and φ_2 are the auto-regressive and moving average parameters.

Site	Distribution	$\beta_{Intercept}$	$\beta_{sinhour}$	$\beta_{coshour}$	β_{sinday}	β_{cosday}	β_{year}	φ_1	φ_2	φ_3
T-1C	ZIBB	-1.71 (0.29)	0.34 (0.07)	0.47 (0.07)	-1.71 (0.39)	-6.28 (1.26)	NA	1	0.03 (0.01)	0.03 (0.01)
A-5C	BI	-9.79 (1.95)	0.68 (0.09)	1.44 (0.12)	0.45 (0.23)	-2.35 (0.55)	0.77 (0.23)	1 (0.12)	-0.19 (0.06)	0.12 (0.03)

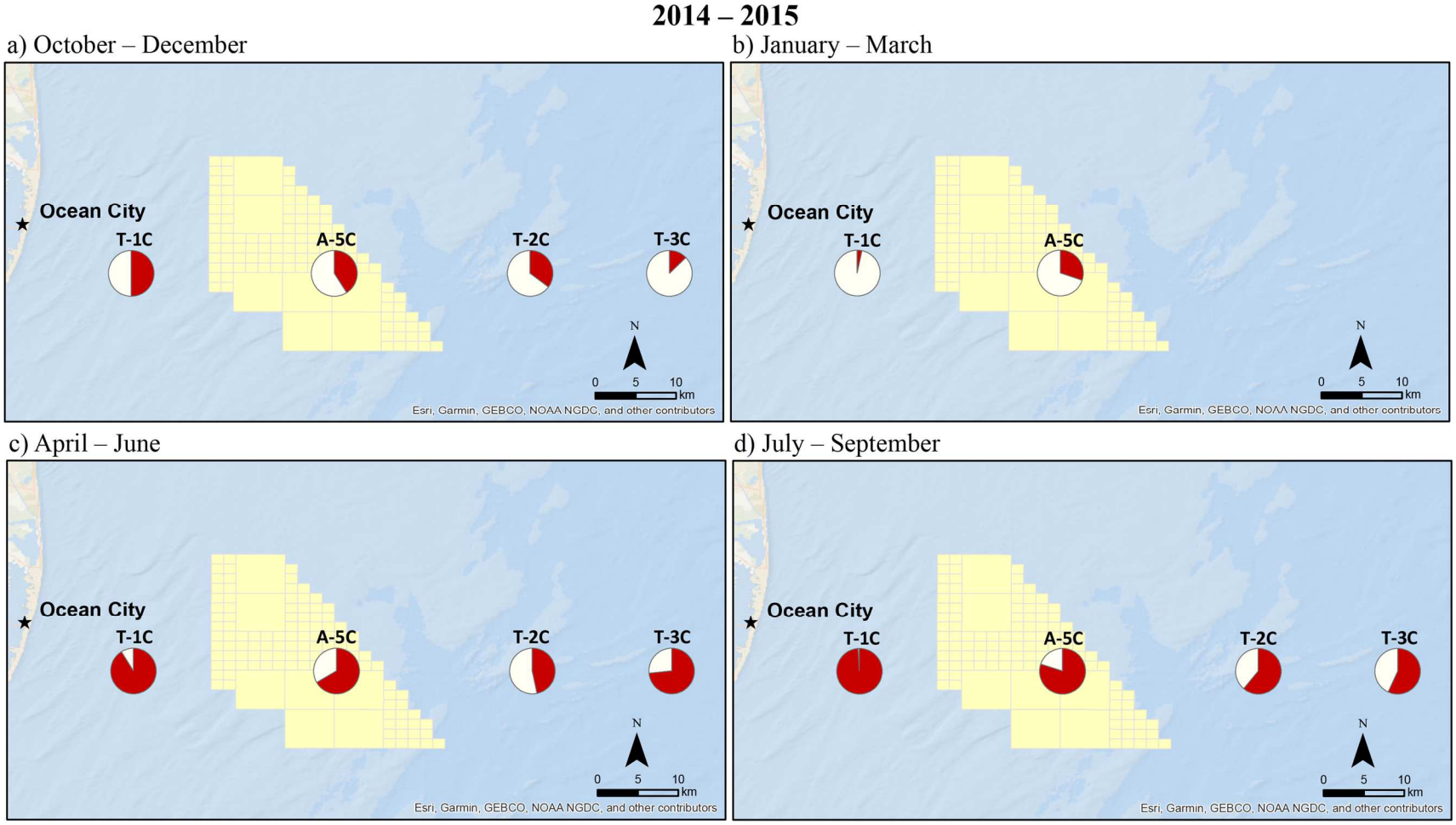

Figure 4.5.2a. Bottlenose dolphin seasonal proportion presence 2014 – 2015
Proportion of recording days present (red; number of days with at least one detection positive hour) for bottlenose dolphins from a) Fall (October – December), b) Winter (January – March), c) Spring (April – June), and d) Summer (July – September) of the November 2014 – October 2015 deployment year. Bottlenose dolphins were assumed not to be present at T-2C and T-3C December – May (see Section 4.5.1 "Species Classification"). Site T-3C began recording April 2015 (Figure 3.2f).

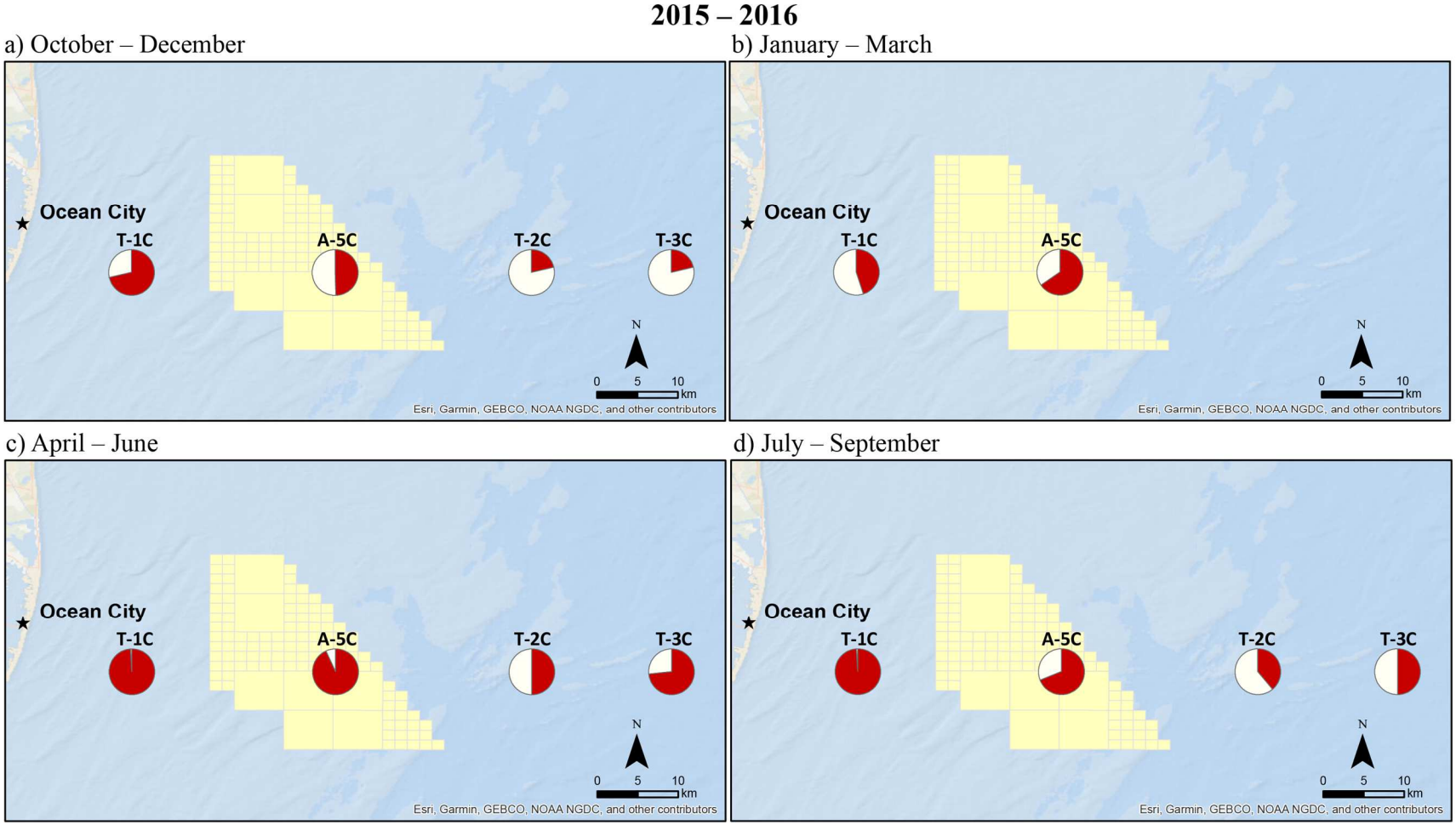

Figure 4.5.2b. Bottlenose dolphin seasonal proportion presence 2015 – 2016
Proportion of recording days present (red; number of days with at least one detection positive hour) for bottlenose dolphins a) Fall (October – December), b) Winter (January – March), c) Spring (April – June), and d) Summer (July – September) of the November 2015 – October 2016 deployment year. Bottlenose dolphins were assumed not to be present at T-2C and T-3C December – May (see Section 4.5.1 "Species Classification").

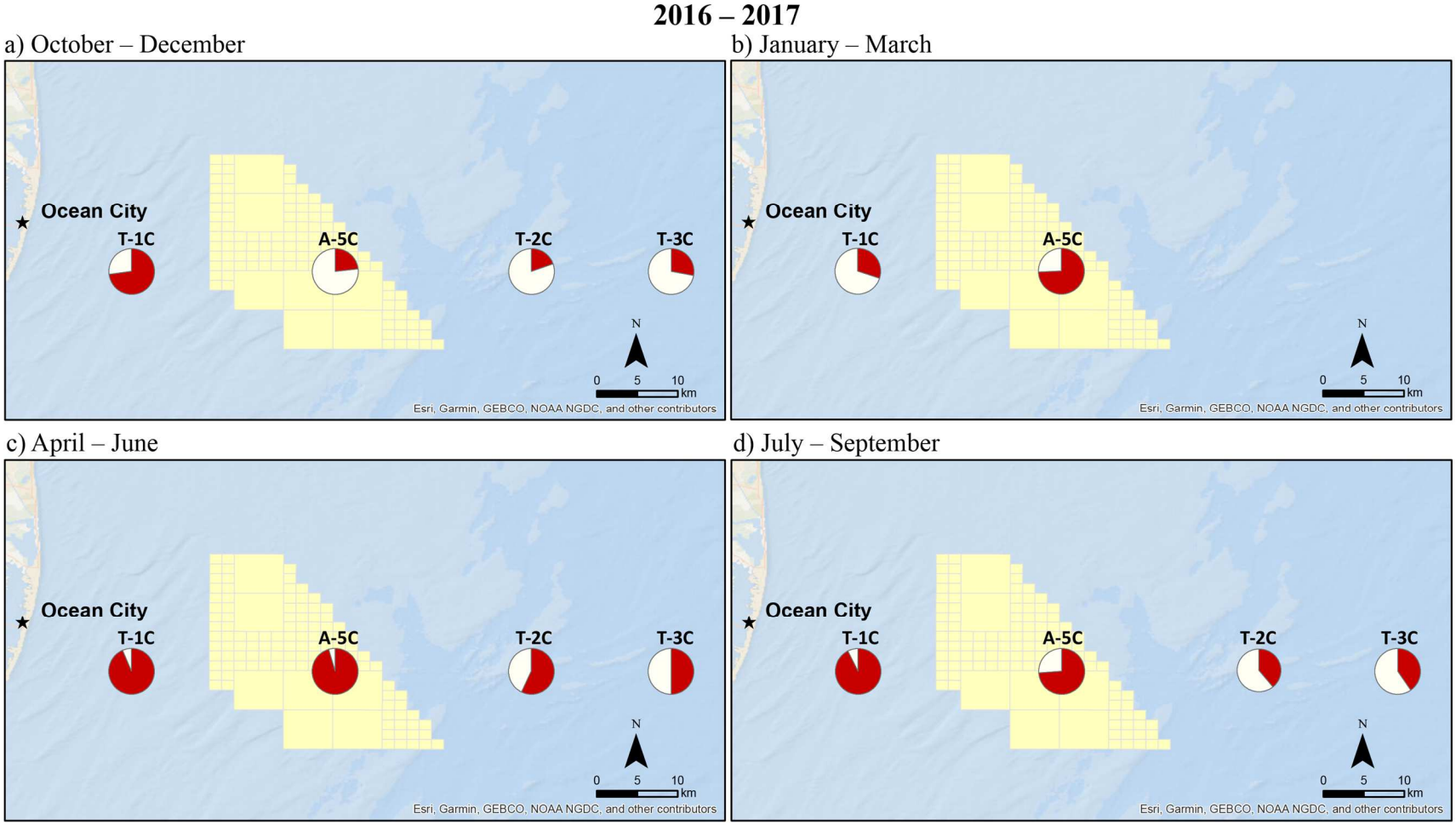

Figure 4.5.2c. Bottlenose dolphin seasonal proportion presence 2016 – 2017
Proportion of recording days present (red; number of days with at least one detection positive hour) for bottlenose dolphins from a) Fall (October – December), b) Winter (January – March), c) Spring (April – June), and d) Summer (July – September) of the November 2016 – October 2017 deployment year. Bottlenose dolphins were assumed not to be present at T-2C and T-3C December – May (see Section 4.5.1 "Species Classification").

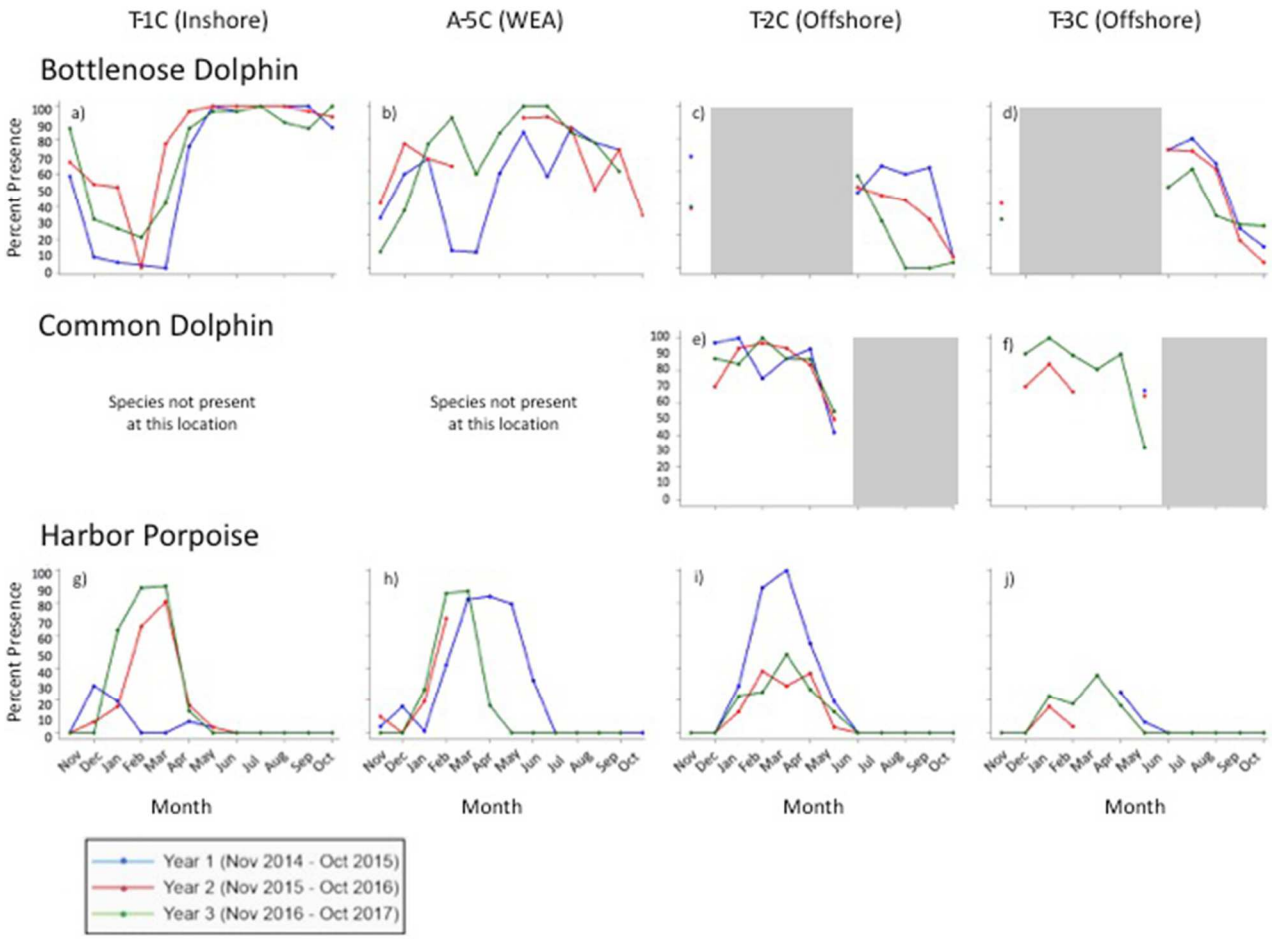

Figure 4.5.2d. Temporal occurrence of bottlenose dolphins, common dolphins, and harbor porpoises in nearshore, WEA, and offshore regions of the study area

Percent monthly acoustic presence for focal odontocete species over the 3-year project period. Bottlenose dolphin: a) inshore, b) WEA, c,d) offshore. Common dolphin: e,f) offshore. Harbor porpoise: g) inshore, h) WEA, I,j) offshore. Bottlenose dolphins were assumed not to be present at T-2C and T-3C December – May, and common dolphins were assumed only to be present at T-2C and T-3C December – May (gray boxes indicate assumed absence; see Section 4.5.1 "Species Classification").

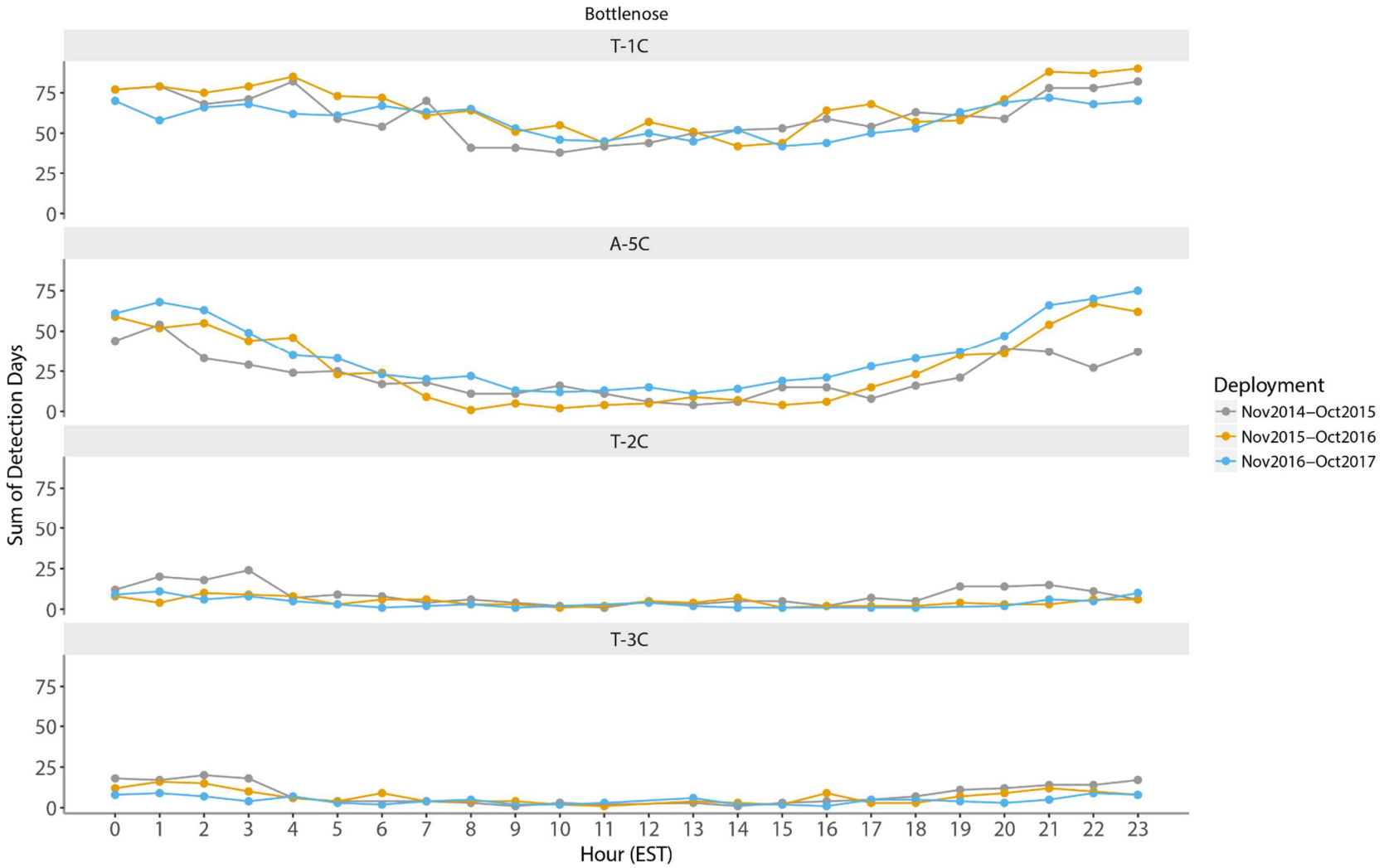

Figure 4.5.2e. Hourly bottlenose dolphin presence
Total number of days bottlenose dolphins were present at all sites by hour during each deployment year: November 2014 – October 2015 (gray), November 2015 – October 2016 (yellow), November 2016 – October 2017 (blue). Bottlenose dolphins were assumed not to be present at T-2C and T-3C December – May (see Section 4.5.1 “Species Classification”).

a) November 2014 – October 2015

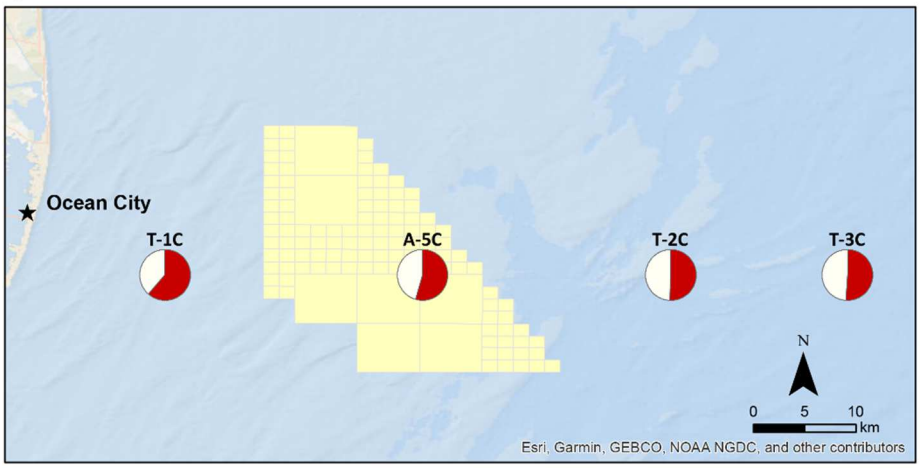

b) November 2015 – October 2016

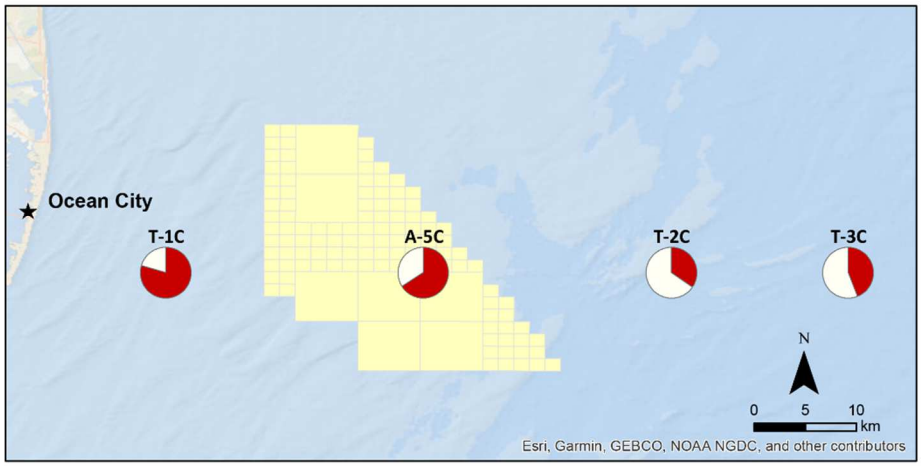

c) November 2016 – October 2017

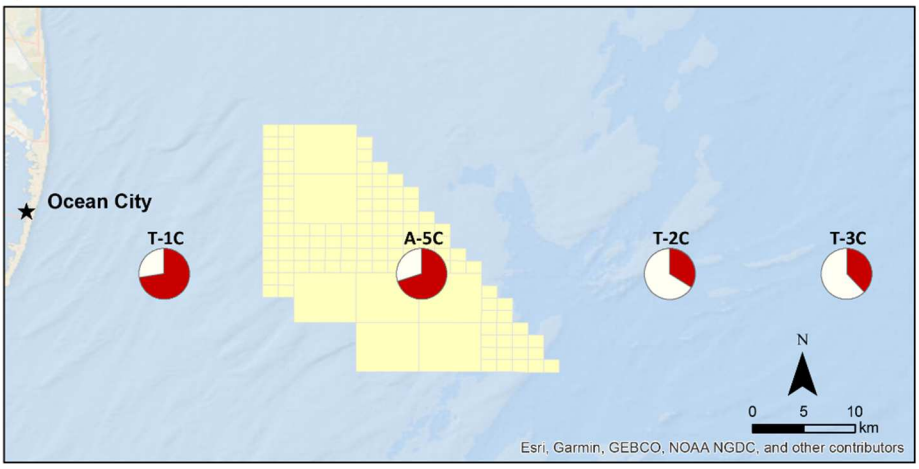

Figure 4.5.2f. Bottlenose dolphin yearly proportion presence
Proportion of recording days present (red; number of days with at least one detection positive hour per deployment year) for bottlenose dolphins from a) November 2014 – October 2015, b) November 2015 – October 2016, and c) November 2016 – October 2017. Bottlenose dolphins were assumed not to be present at T-2C and T-3C December – May (see Section 4.5.1 “Species Classification”).

A general additive model (GAM) with a Gaussian distribution was used to model the relationship between weekly bottlenose dolphin occurrence and the environmental parameters of sea surface temperature (SST) and Chlorophyll-a concentration (Chl-a) at sites T-1C and A-5C, located inshore and within the Maryland Wind Energy Area. At these sites, there was no significant relationship with Chl-a, and this term was removed from the final models. There was no significant effect of SST or Chl-a at sites T-2C and T-3C.

The GAM models were represented with smoother curves to determine the relationship between dolphin presence and average SST. Sea surface temperature was found to be a significant predictor of dolphin occurrence at both T-1C and A-5C, which suggests a seasonal pattern, as supported by the results of the GARMA models (Tables 4.5.2a – c; Figure 4.5.2g – h). Dolphin presence at the two sites peaked at an SST of approximately 19 – 21°C, with minimum occurrence at approximately 4 – 6°C.

Table 4.5.2b Generalized additive model (GAM) results used to relate the weekly hourly occurrence of bottlenose dolphins to sea surface temperature (SST) at site T-1C.

T-1C Bottlenose Dolphin				
Parametric Coefficients				
	Estimate	**Standard Error**	**t-value**	**p (>|t|)**
Intercept	0.17	0.010	17.59	<0.0001
Smoother Terms				
	Estimated Degrees of Freedom	**Reference Degrees of Freedom**	**F**	**p-value**
SST	1.95	2	41.75	<0.0001
R^2	**Deviance explained**	**GVC**	**scale estimate**	n = 138
0.038	38.8%	0.013	0.013	

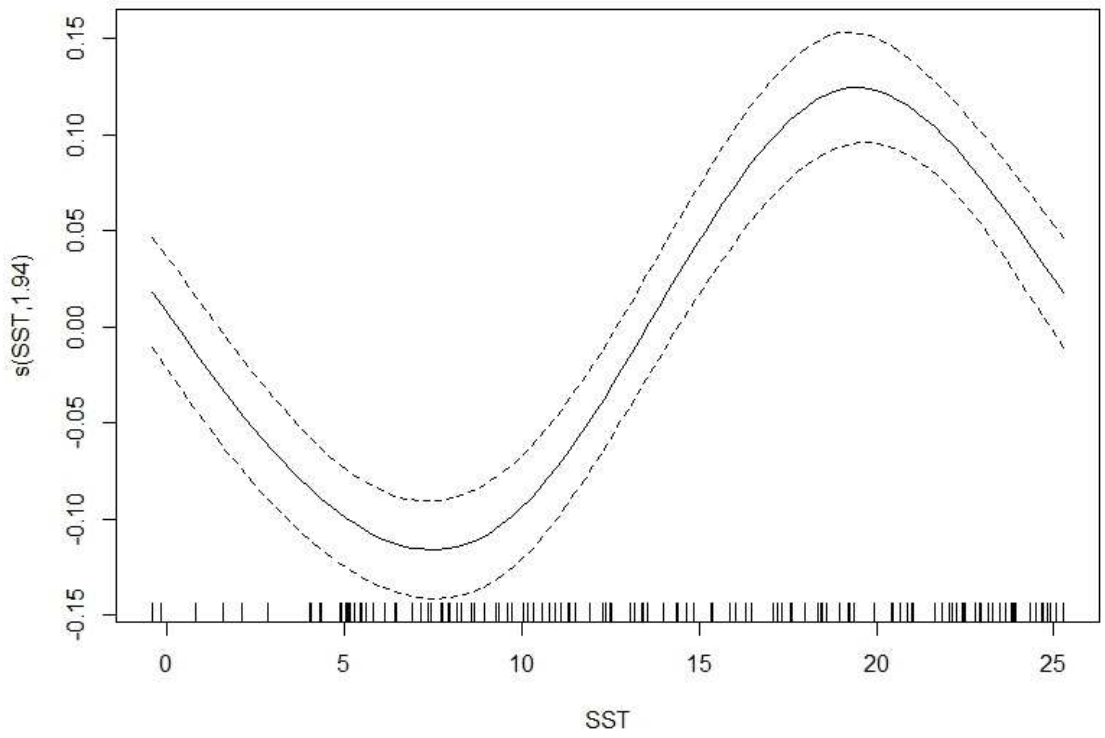

Figure 4.5.2g. Bottlenose dolphin generalized additive model (GAM) smoothing curves for sites T-1C

Smoothing curves for bottlenose dolphin occurrence in relation to SST (°C) at site T-1C. The predictor is on the x-axis, the fitted smooth function on the y-axis, and the dashed lines are error bands. Tick marks on the x-axis (rug plot) show the distribution of the underlying data.

Table 4.5.2c Generalized additive model (GAM) results used to relate the weekly hourly occurrence of bottlenose dolphins to sea surface temperature (SST) at site A-5C.

A-5C Bottlenose Dolphin				
Parametric Coefficients				
	Estimate	**Standard Error**	**t-value**	**p (>|t|)**
Intercept	0.081	0.006	12.58	<0.0001
Smoother Terms				
	Estimated Degrees of Freedom	**Reference Degrees of Freedom**	**F**	**p-value**
SST	1.474	2	2.56	0.034
R^2	**Deviance explained**	**GVC**	**scale estimate**	n = 129
0.038	4.9%	0.0054	0.0053	

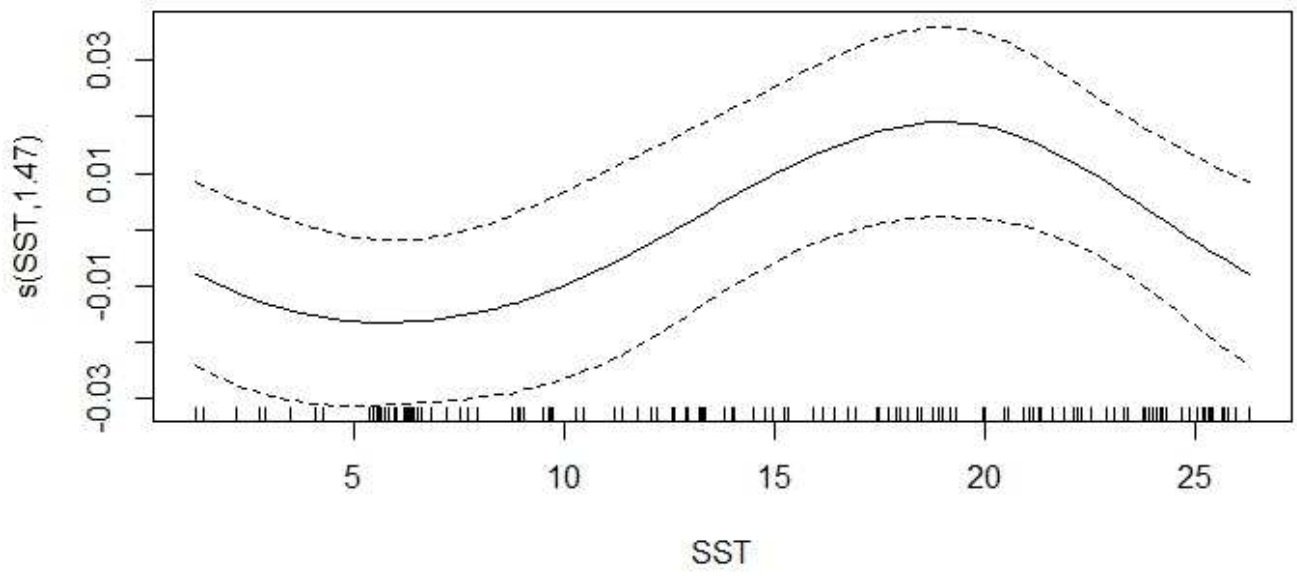

Figure 4.5.2h. Bottlenose dolphin generalized additive model (GAM) smoothing curves for sites A-5C

Smoothing curves for bottlenose dolphin occurrence in relation to SST (°C) at site A-5C. The predictor is on the x-axis, the fitted smooth function on the y-axis, and the dashed lines are error bands. Tick marks on the x-axis (rug plot) show the distribution of the underlying data.

4.5.3 Common Dolphin Temporal Occurrence

The GARMA model runs were combined for both dolphin species at the two sites offshore of the WEA because of higher uncertainty regarding the species classification. The inter-annual variation in the number of dolphin detections at sites T-2C and T-3C was not statistically significant (Figure 4.5.3a). There was no significant seasonal or diel pattern in dolphin occurrence (Figures 4.5.2d and 4.5.3b – e).

a) November 2014 – October 2015

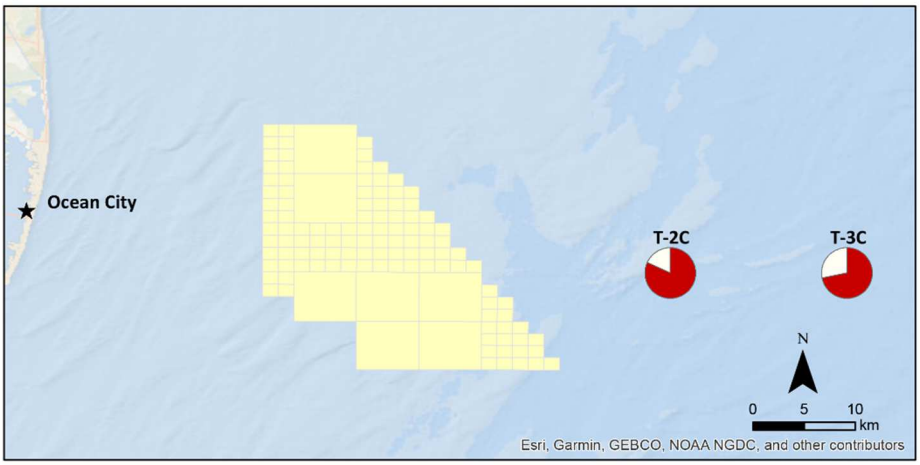

b) November 2015 – October 2016

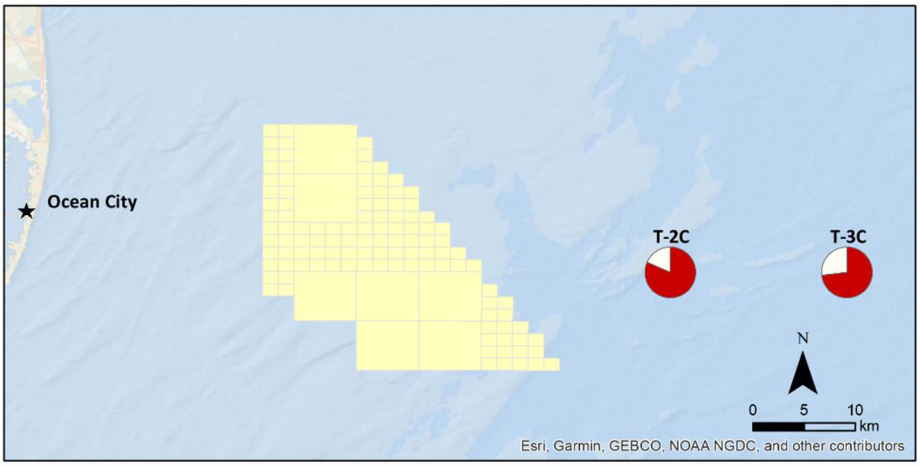

c) November 2016 – October 2017

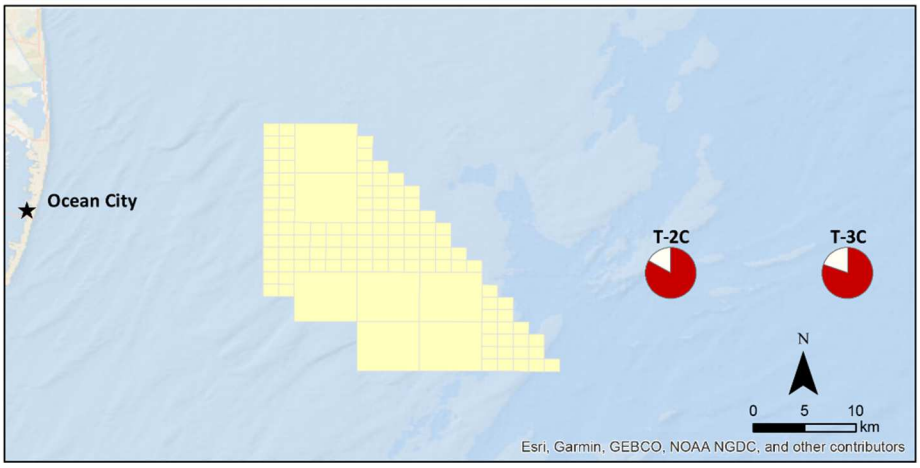

Figure 4.5.3a. Common dolphin yearly proportion presence
Proportion of recording days present (red; number of days with at least one detection positive hour per deployment year) for common dolphins from a) November 2014 – October 2015, b) November 2015 – October 2016, and c) November 2016 – October 2017. Common dolphins were assumed only to be present at T-2C and T-3C December – May (see Section 4.5.1 “Species Classification”).

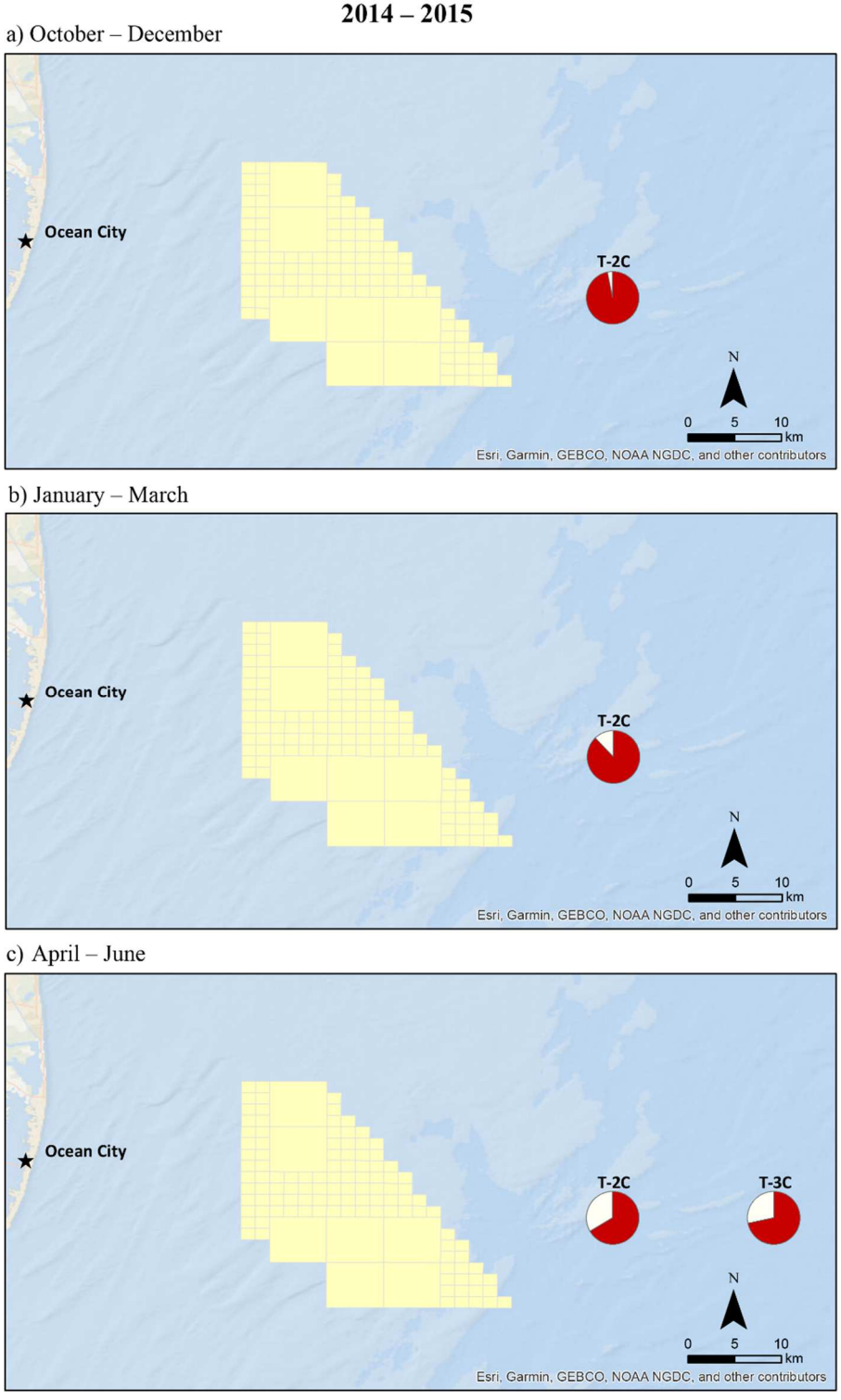

Figure 4.5.3b. Common dolphin seasonal proportion presence 2014 – 2015
Proportion of recording days present (red; number of days with at least one detection positive hour) for common dolphins from a) Fall (October – December), b) Winter (January – March), and c) Spring (April – June) of the November 2014 – October 2015 deployment year. Common dolphins were assumed only to be present at T-2C and T-3C December – May (see Section 4.5.1 "Species Classification"). Site T-3C began recording April 2015 for this year (Figure 3.2f).

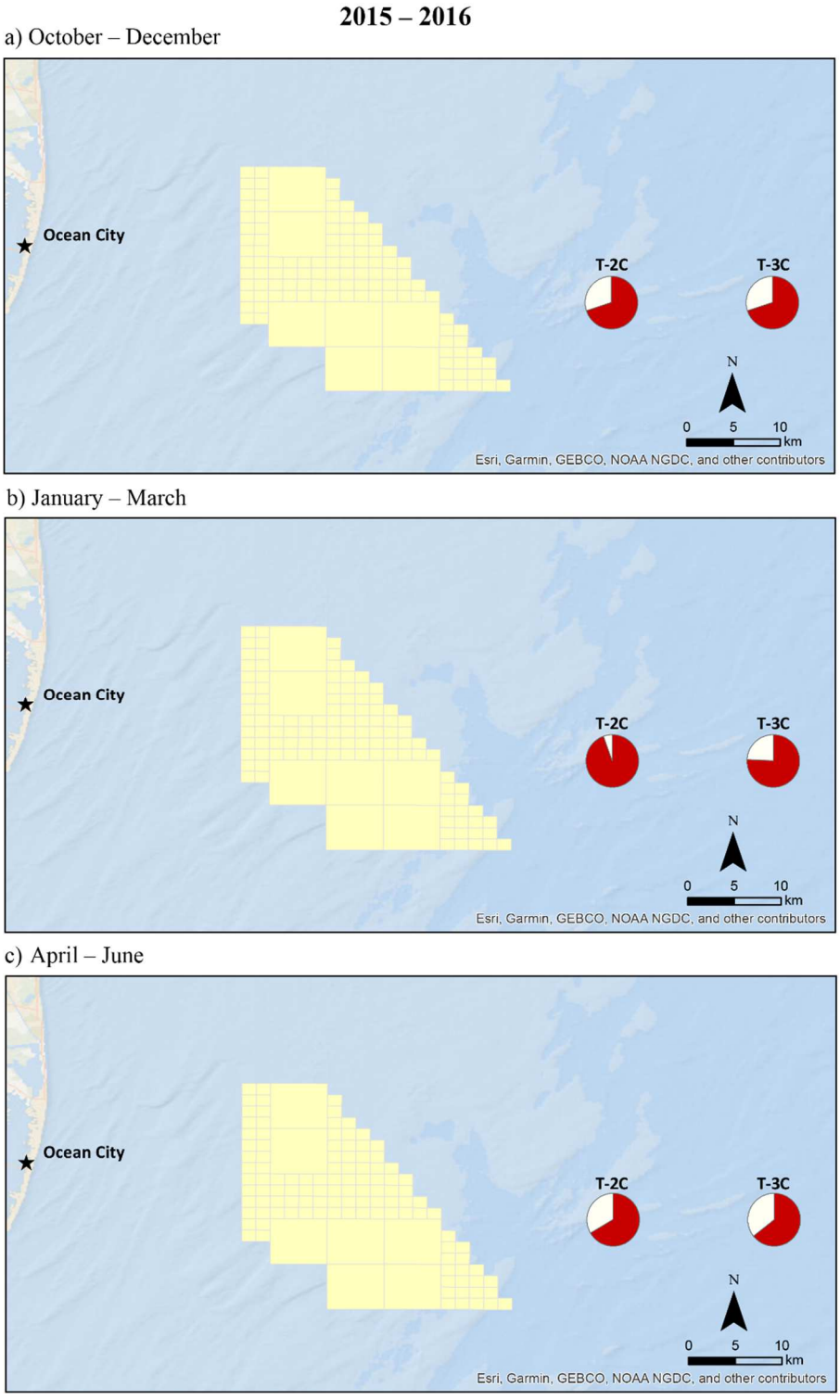

Figure 4.5.3c. Common dolphin seasonal proportion presence 2015 – 2016
Proportion of recording days present (red; number of days with at least one detection positive hour) for common dolphins from a) Fall (October – December), b) Winter (January – March), and c) Spring (April – June) of the November 2015 – October 2016 deployment year. Common dolphins were assumed only to be present at T-2C and T-3C December – May (see Section 4.5.1 “Species Classification”).

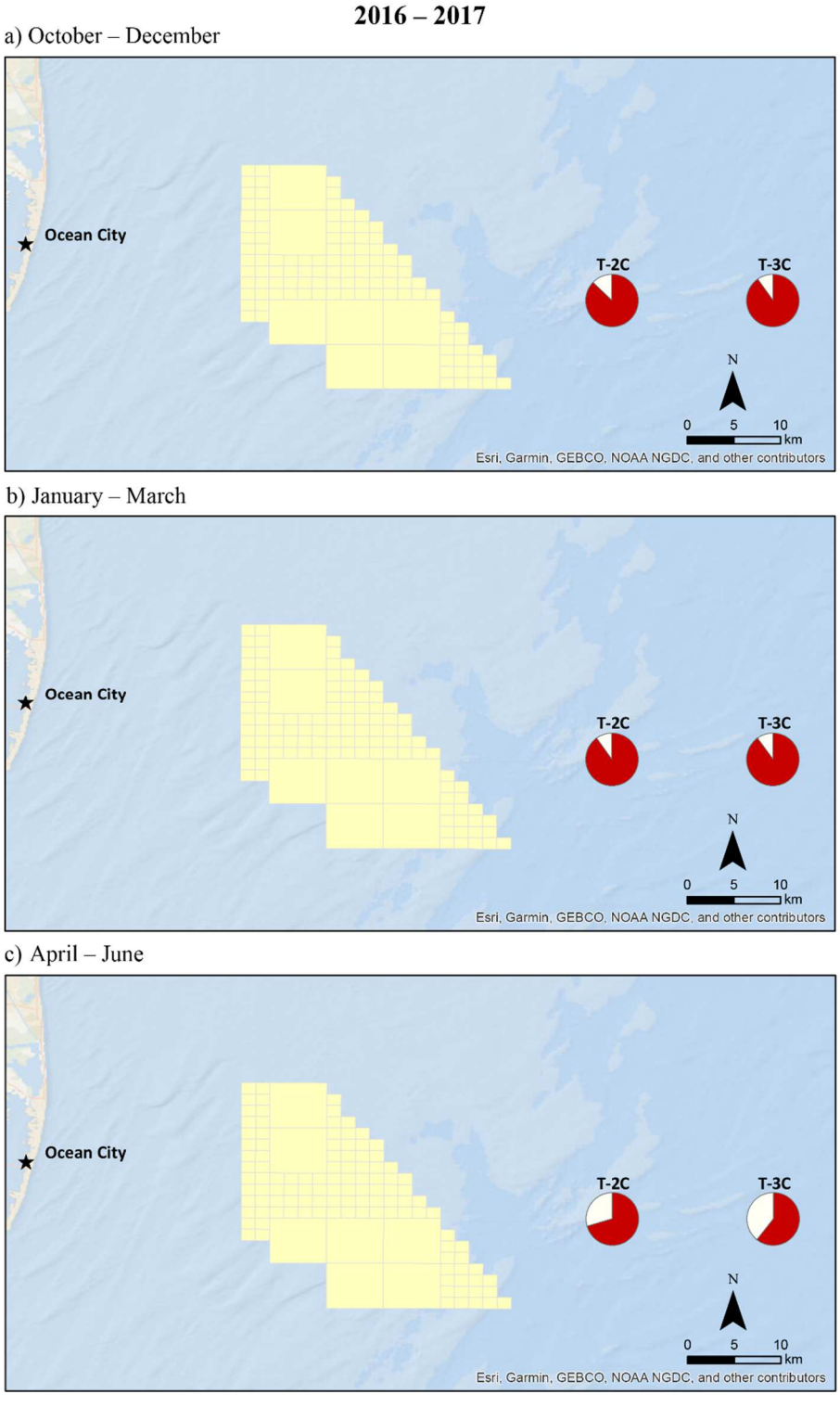

Figure 4.5.3d. Common dolphin seasonal proportion presence 2016 – 2017
Proportion of recording days present (red; number of days with at least one detection positive hour) for common dolphins from a) Fall (October – December), b) Winter (January – March), and c) Spring (April – June) of the November 2016 – October 2017 deployment year. Common dolphins were assumed only to be present at T-2C and T-3C December – May (see Section 4.5.1 “Species Classification”).

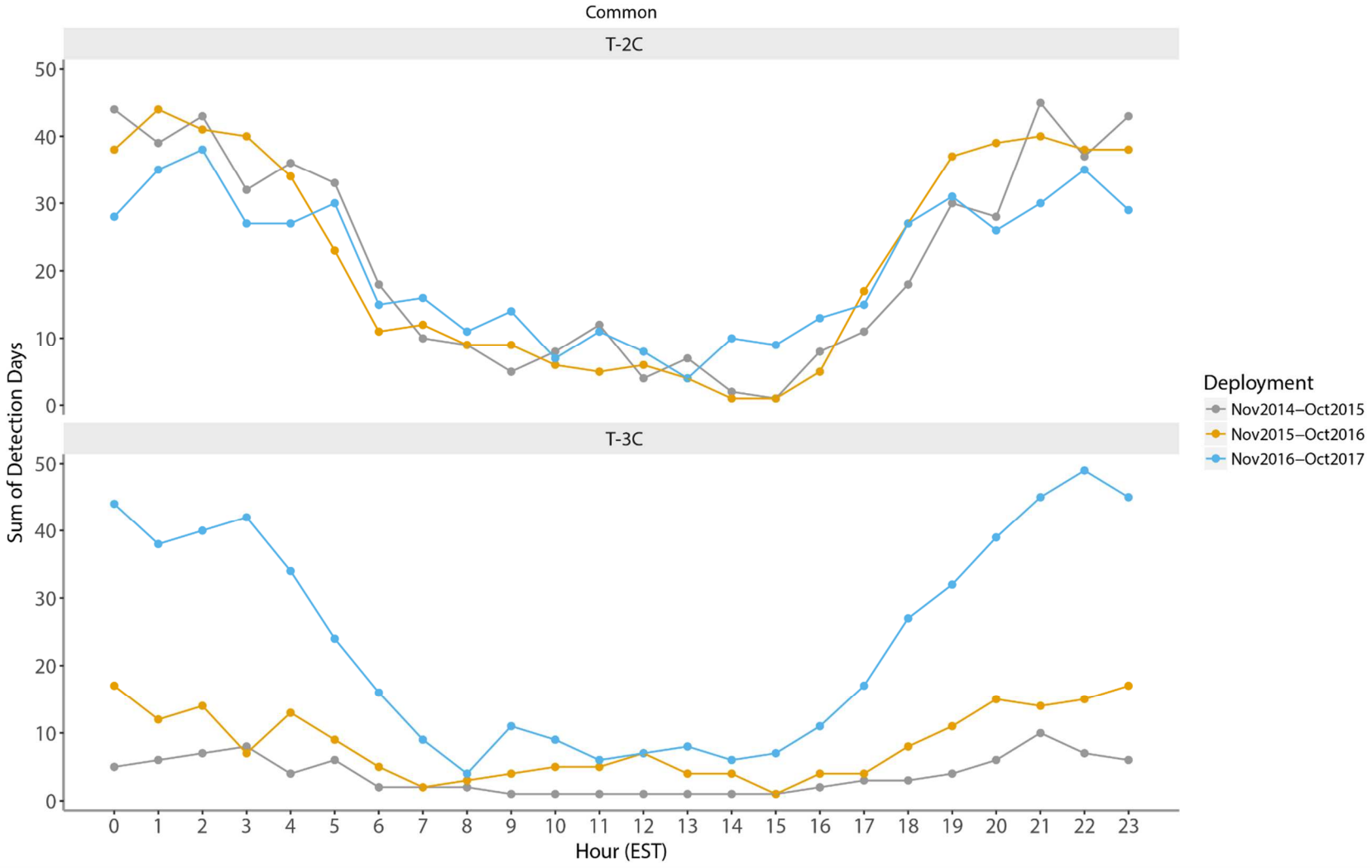

Figure 4.5.3e. Hourly common dolphin presence
Total number of days common dolphins were present at all sites by hour during each deployment year: November 2014 – October 2015 (gray), November 2015 – October 2016 (yellow), November 2016 – October 2017 (blue). Common dolphins were assumed only to be present at T-2C and T-3C December – May (see Section 4.5.1 “Species Classification”).

4.5.4 Harbor Porpoise Temporal Occurrence

A Poisson-inverse Gaussian (PIG) distribution had the best fit (lowest AIC scores) for GARMAs modeling the temporal patterns of porpoise occurrence at all sites. After adjusting for autocorrelation, the model for T-3C showed no significance of day, hour, or study year, so no model is shown here for that site.

Julian day was found to be a significant predictor of porpoise occurrence at all remaining sites and was included in all final models (Table 4.5.4a). This suggests a strong seasonal pattern in porpoise distribution at all sites in the study area (Figures 4.5.2d and 4.5.4a – c). Porpoises were detected significantly more often in the winter (January, n = 755 min; February, n = 1785 min; March, n = 3328 min) and spring months (April, n = 587 min; May = 341 min; June = 0 min) than summer (July, n = 0 min; August, n = 0 min; September, n = 0 min) or autumn (October, n = 0 min; November, n = 8 min, December, n = 73) at T-1C, A-5C, and T-2C (Figures 4.5.4a – c). At sites T-1C and A-5C, hour of the day was found to be a significant predictor of porpoise presence, suggesting a diel pattern in acoustic activity (Figure 4.5.4d). At sites T-1C and T-2C, year was found to be a significant predictor of porpoise detection, suggesting annual shifts in distribution. At site T-2C, porpoise occurrence was significantly higher November 2014 – October 2015 (Year 1) than November 2015 – October 2016 or November 2016 – October 2017 (Years 2 or 3) (Year 1, n = 3063 min; Year 2, n = 327 min; Year 3, n = 349 min), while at site T-1C this pattern was reversed, with porpoise occurrence being significantly higher in Year 3 (Year 1, n = 116 min; Year 2, n = 373 min; Year 3, n = 1068 min) (Figure 4.5.4e).

Table 4.5.4a Estimated parameters (standard errors in parentheses) from the generalized auto-regressive moving average (GARMA) models for harbor porpoises at sites T-1C, A-5C, and T-2C. PIG = Poisson-inverse Gaussian, β values are the regression coefficients, φ_1 and φ_2 are the auto-regressive and moving average parameters.

Site	Distribution	$\beta_{Intercept}$	$\beta_{sinhour}$	$\beta_{coshour}$	β_{sinday}	β_{cosday}	β_{year}	φ_1	φ_2
T-1C	PIG	-11.00 (0.33)	-0.23 (0.13)	0.65 (0.12)	6.55 (0.37)	4.87 (0.34)	1.51 (0.15)	NA	NA
A-5C	PIG	-26.26 (9.26)	0.59 (0.34)	1.26 (0.30)	30.07 (11.58)	13.87 (5.29)	NA	0.60 (0.05)	0.25 (0.06)
T-2C	PIG	-10.53 (5.01)	-	-	65.66 (16.20)	30.58 (7.49)	-19.38 (4.81)	0.68 (0.04)	0.21 (0.04)

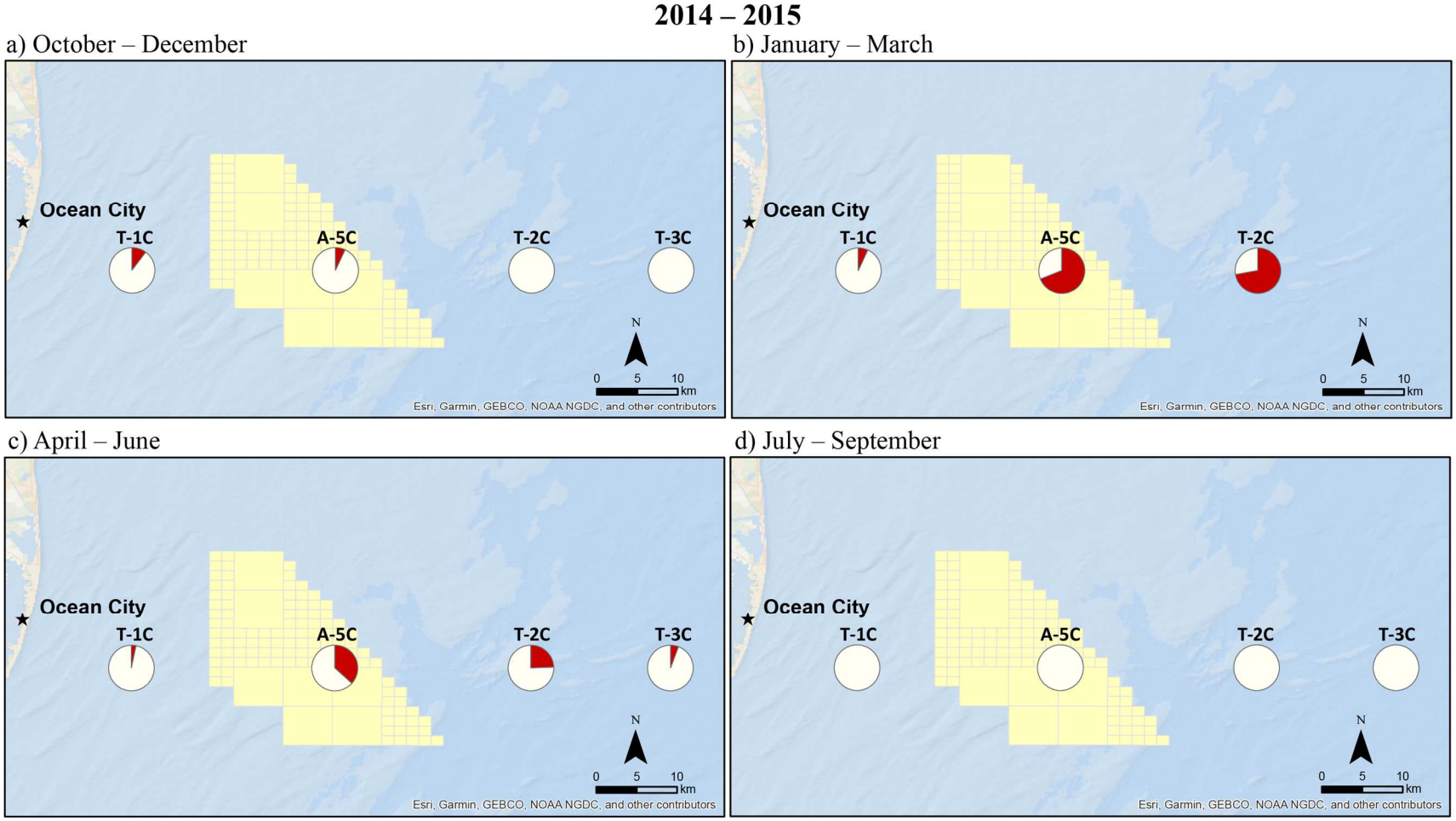

Figure 4.5.4a. Harbor porpoise seasonal proportion presence 2014 – 2015
Proportion of recording days present (red; number of days with at least one detection positive hour) for harbor porpoises from a) Fall (October – December), b) Winter (January – March), c) Spring (April – June), and d) Summer (July – September) of the November 2014 – October 2015 deployment year. Site T-3C began recording April 2015 (Figure 3.2f).

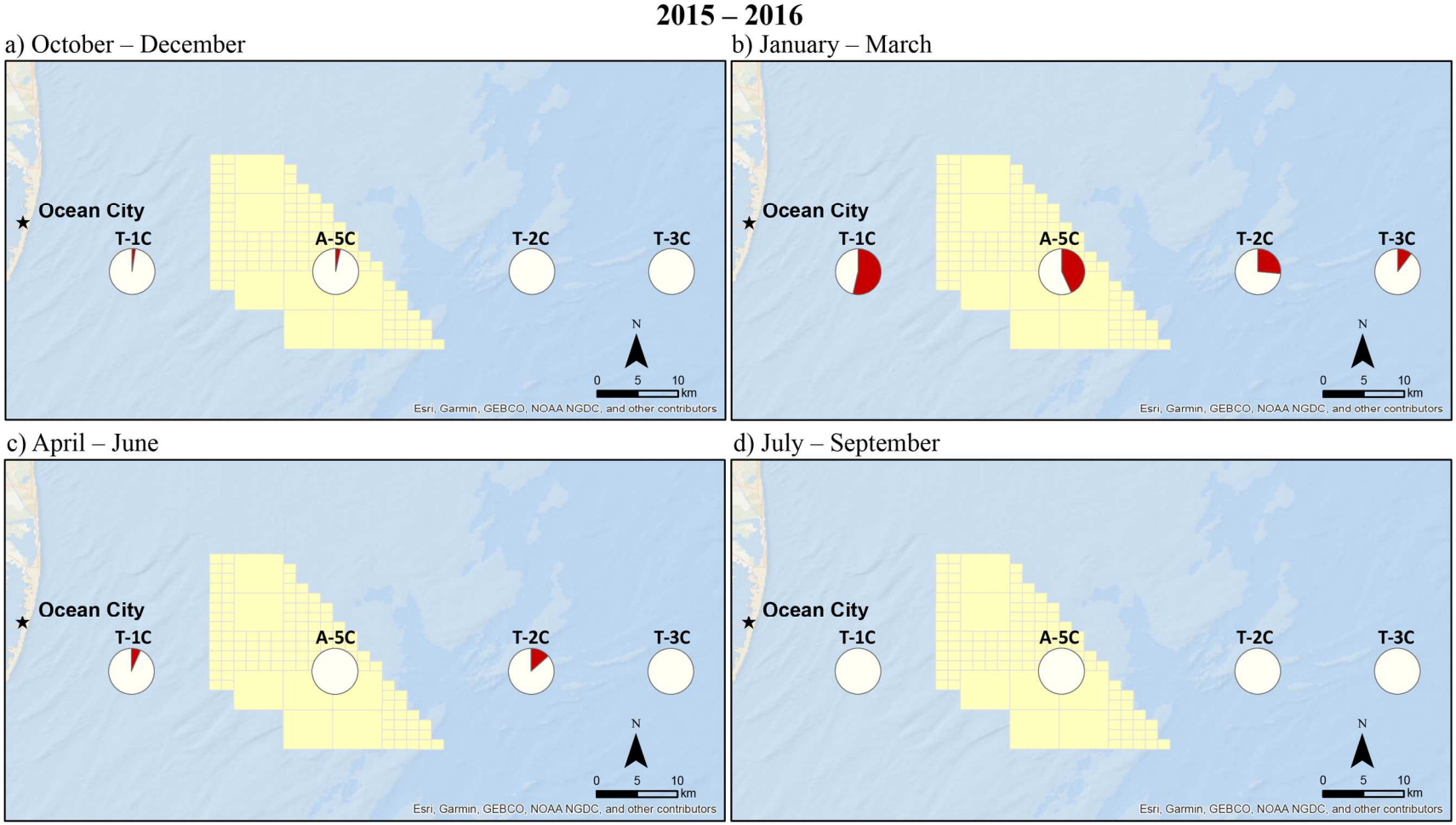

Figure 4.5.4b. Harbor porpoise seasonal proportion presence 2015 – 2016
Proportion of recording days present (red; number of days with at least one detection positive hour) for harbor porpoises a) Fall (October – December), b) Winter (January – March), c) Spring (April – June), and d) Summer (July – September) of the November 2015 – October 2016 deployment year.

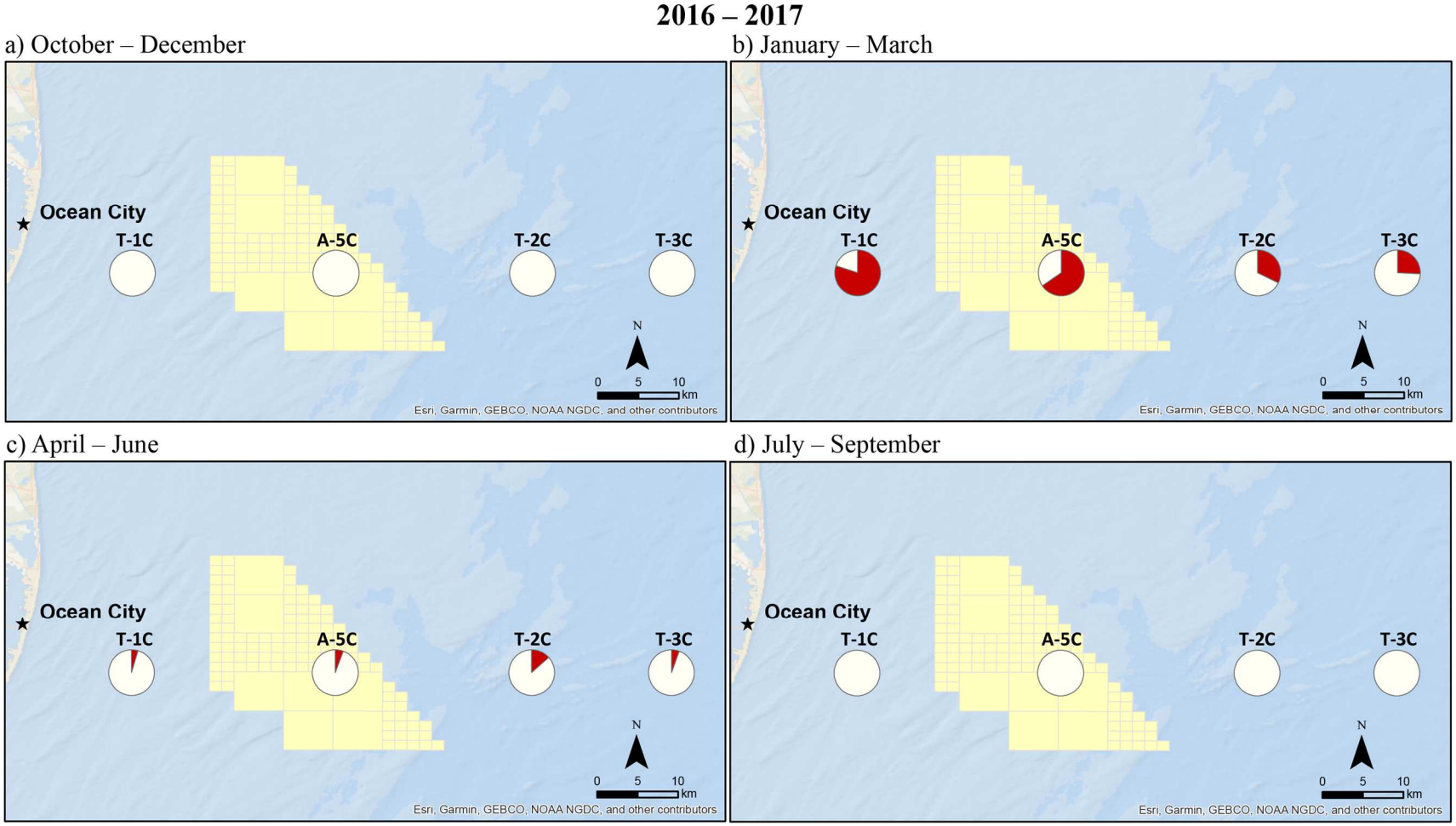

Figure 4.5.4c. Harbor porpoise seasonal proportion presence 2016 – 2017
Proportion of recording days present (red; number of days with at least one detection positive hour) for harbor porpoises from a) Fall (October – December), b) Winter (January – March), c) Spring (April – June), and d) Summer (July – September) of the November 2016 – October 2017 deployment year.

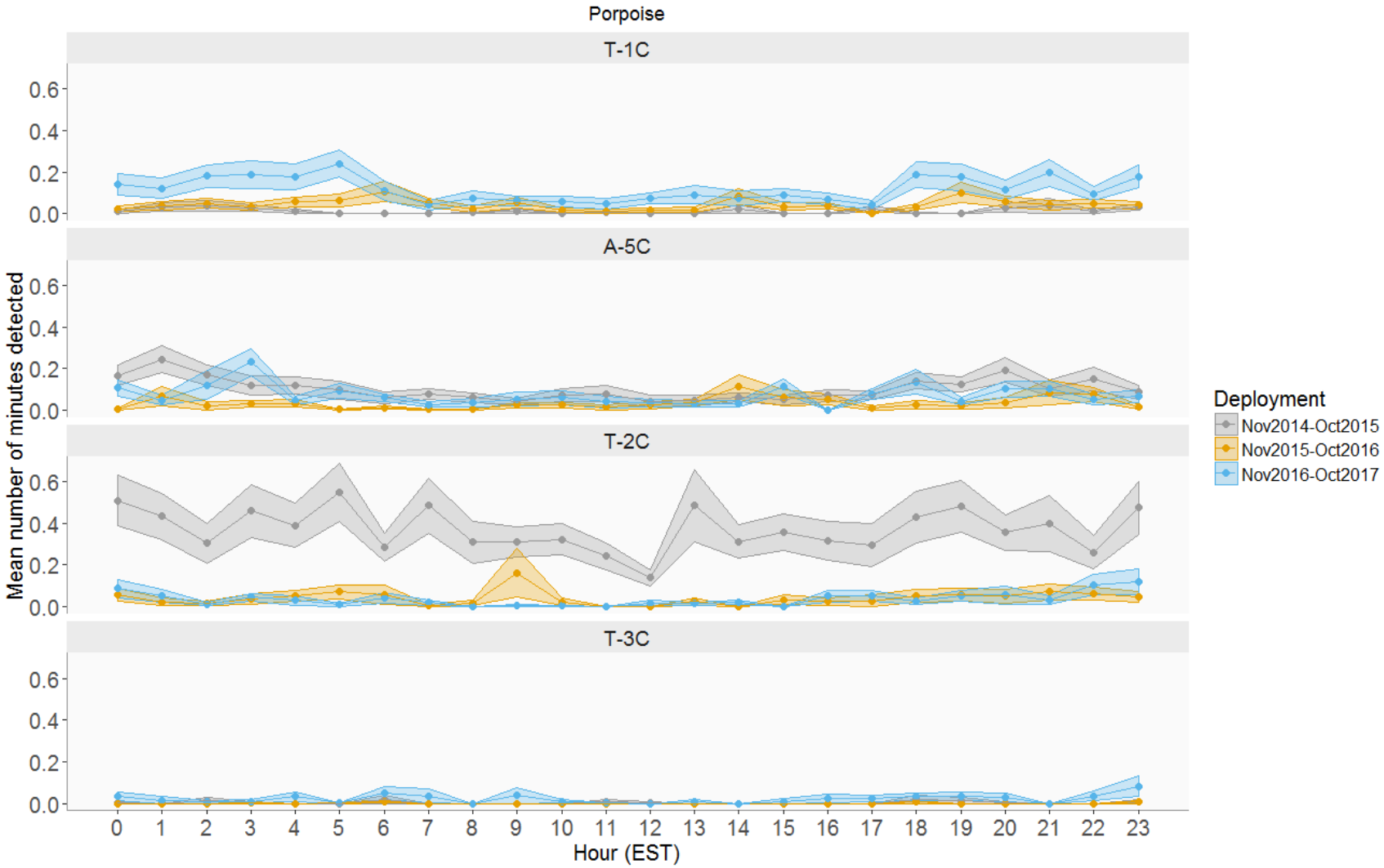

Figure 4.5.4d. Hourly harbor porpoise presence
Mean number of minutes harbor porpoises were present at all sites per hour during each deployment year: November 2014 – October 2015 (gray), November 2015 – October 2016 (yellow), November 2016 – October 2017 (blue). Shaded areas represent standard error.

a) November 2014 – October 2015

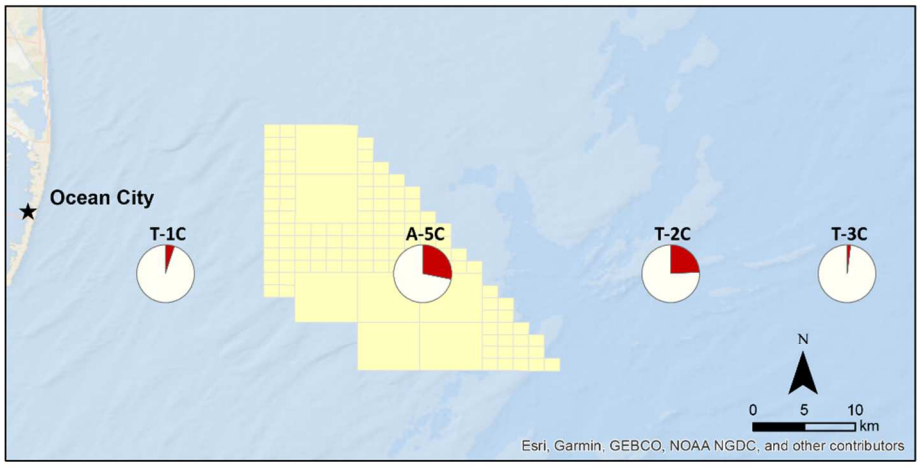

b) November 2015 – October 2016

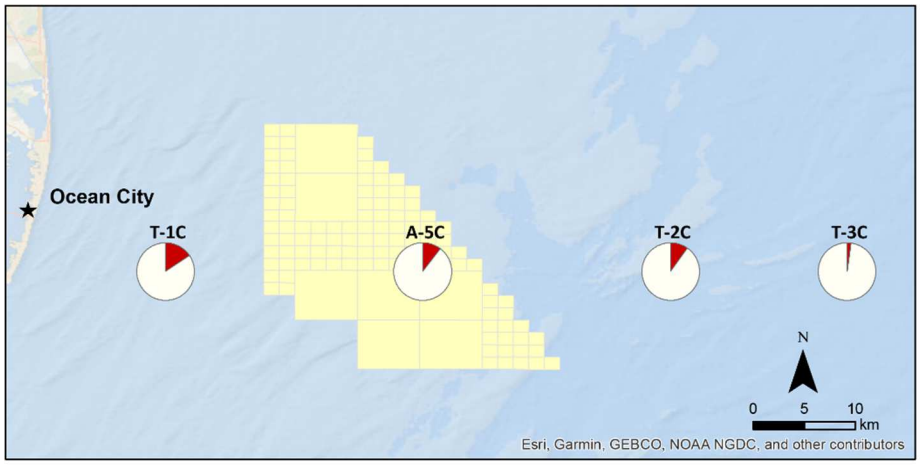

c) November 2016 – October 2017

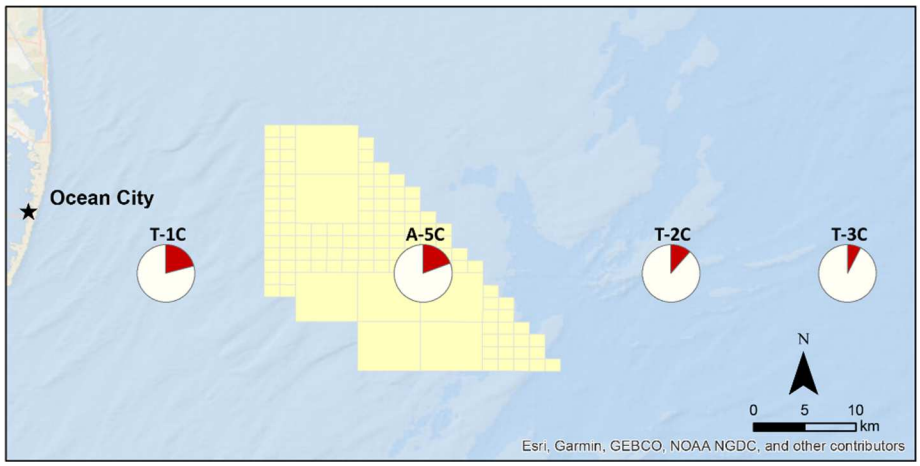

Figure 4.5.4e. Harbor porpoise yearly proportion presence
Proportion of recording days present (red; number of days with at least one detection positive hour per deployment year) for harbor porpoises from a) November 2014 – October 2015, b) November 2015 – October 2016, and c) November 2016 – October 2017.

A general additive model (GAM) with a Gaussian distribution was used to model the relationship between weekly porpoise occurrence the environmental parameters of sea surface temperature (SST) and Chlorophyll-a concentration (Chl-a) at sites T-1C, A-5C, and T-2C, located inshore, within, and offshore of the Maryland WEA. At these sites, there was no significant effect of Chl-a, and this term was removed from the final models. The final models explained 24.7%, 33.9%, and 14.8% of the deviance. There were no significant effects of SST or Chl-a at site T-3C.

Average SST was found to be a significant predictor of porpoise occurrence at T-1C, A-5C, and T-2C, which suggests a seasonal pattern, as supported by the results of the GARMA models above (Tables 4.5.4a – d; Figures 4.5.4f – h). Porpoise presence was found to be inversely related to SST. Porpoise presence at the three sites peaked at an SST of approximately 4 – 6°C, with minimum occurrence at approximately 18 – 19°C.

Table 4.5.4b Generalized additive model (GAM) results used to relate the weekly hourly occurrence of harbor porpoises to sea surface temperature (SST) at site T-1C.

T-1C Harbor Porpoise				
Parametric Coefficients				
	Estimate	**Standard Error**	**t-value**	**p (>|t|)**
Intercept	0.016	0.0030	5.21	<0.0001
Smoother Terms				
	Estimated Degrees of Freedom	**Reference Degrees of Freedom**	**F**	**p-value**
SST	1.92	2	21.2	<0.0001
R^2	**Deviance explained**	**GVC**	**scale estimate**	n = 138
0.24	24.7%	0.0013	0.0013	

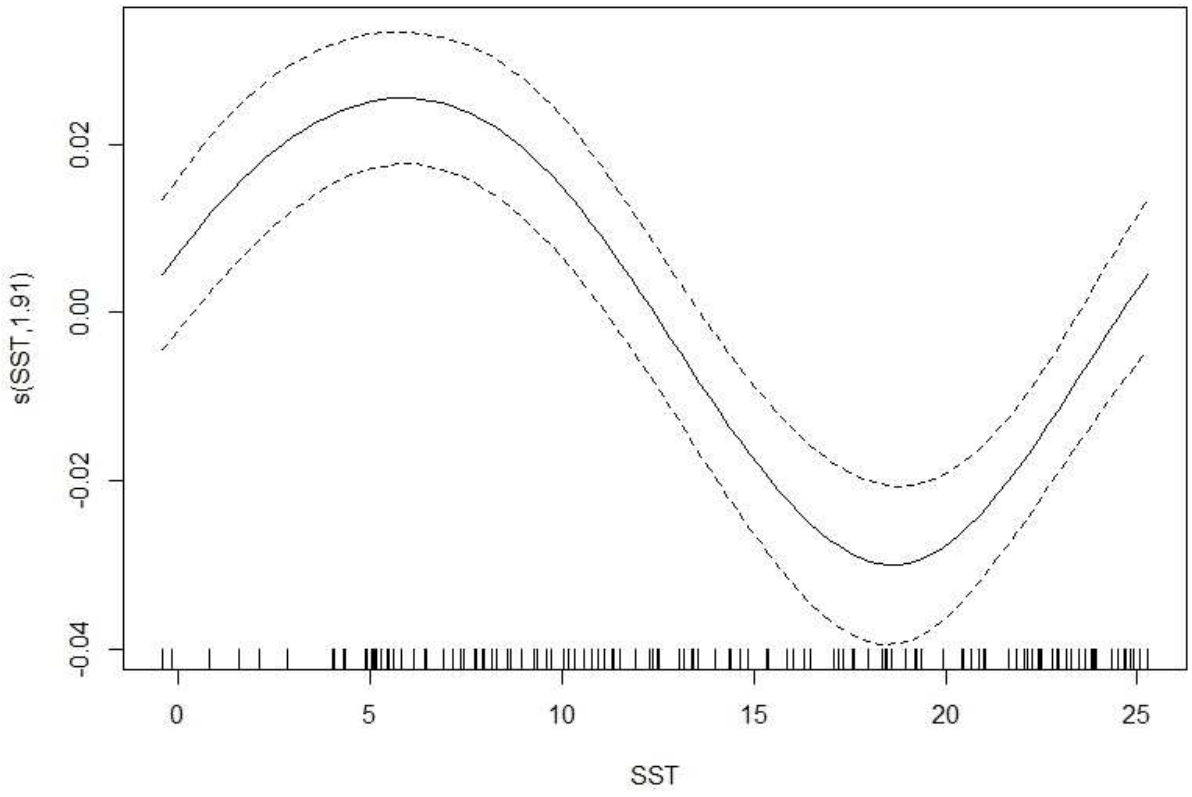

Figure 4.5.4f. Harbor porpoise generalized additive model (GAM) smoothing curves for sites T-1C
Smoothing curves for harbor porpoise occurrence in relation to SST (°C) at site T-1C. The predictor is on the x-axis, the fitted smooth function on the y-axis, and the dashed lines are error bands. Tick marks on the x-axis (rug plot) show the distribution of the underlying data.

Table 4.5.4c Generalized additive model (GAM) results used to relate the weekly hourly occurrence of harbor porpoises to sea surface temperature (SST) at site A-5C.

A-5C Harbor Porpoise				
Parametric Coefficients				
	Estimate	**Standard Error**	**t-value**	**p (>|t|)**
Intercept	0.022	0.003	6.93	<0.0001
Smoother Terms				
	Estimated Degrees of Freedom	**Reference Degrees of Freedom**	**F**	**p-value**
SST	1.95	2	31.34	<0.0001
R^2	**Deviance explained**	**GVC**	**scale estimate**	n = 129
0.33	33.9%	0.0013	0.0013	

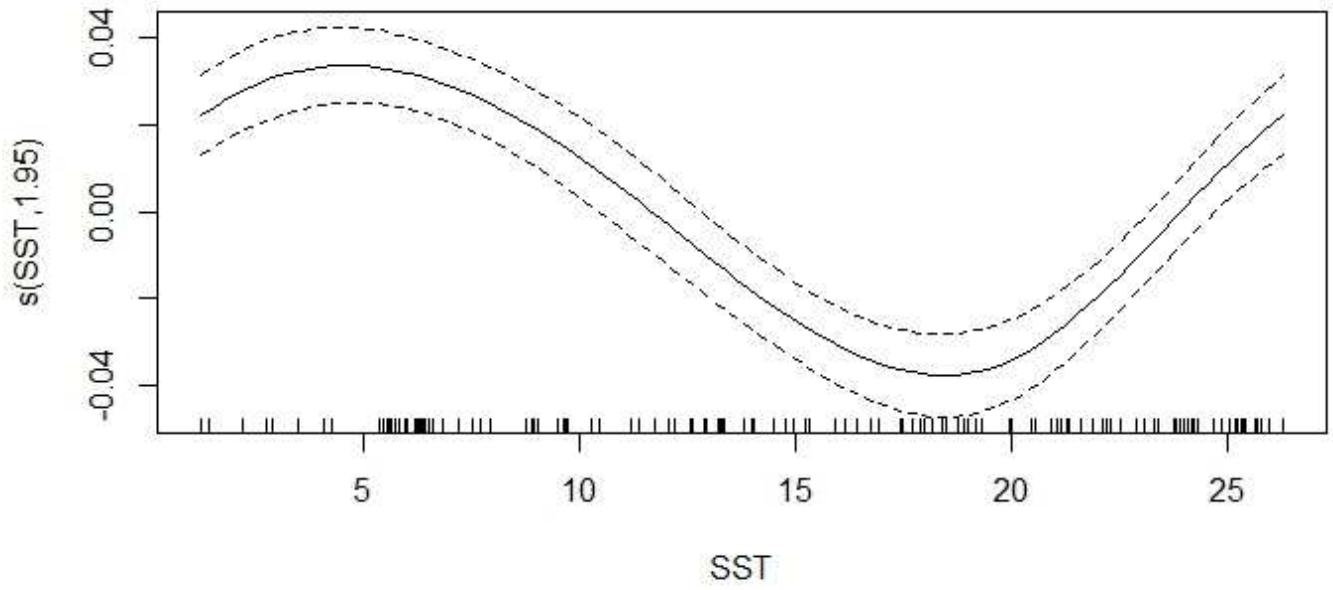

Figure 4.5.4g. Harbor porpoise generalized additive model (GAM) smoothing curves for sites A-5C
Smoothing curves for harbor porpoise occurrence in relation to SST (°C) at site A-5C. The predictor is on the x-axis, the fitted smooth function on the y-axis, and the dashed lines are error bands. Tick marks on the x-axis (rug plot) show the distribution of the underlying data.

Table 4.5.4d Generalized additive model (GAM) results used to relate the weekly hourly occurrence of harbor porpoises to sea surface temperature (SST) at site T-2C.

T-2C Harbor Porpoise				
Parametric Coefficients				
	Estimate	**Standard Error**	**t-value**	**p (>|t|)**
Intercept	0.028	0.0066	4.18	<0.0001
Smoother Terms				
	Estimated Degrees of Freedom	**Reference Degrees of Freedom**	**F**	**p-value**
SST	1.84	2	10.86	<0.0001
R^2	**Deviance explained**	**GVC**	**scale estimate**	n = 138
0.14	14.8%	0.0061	0.0060	

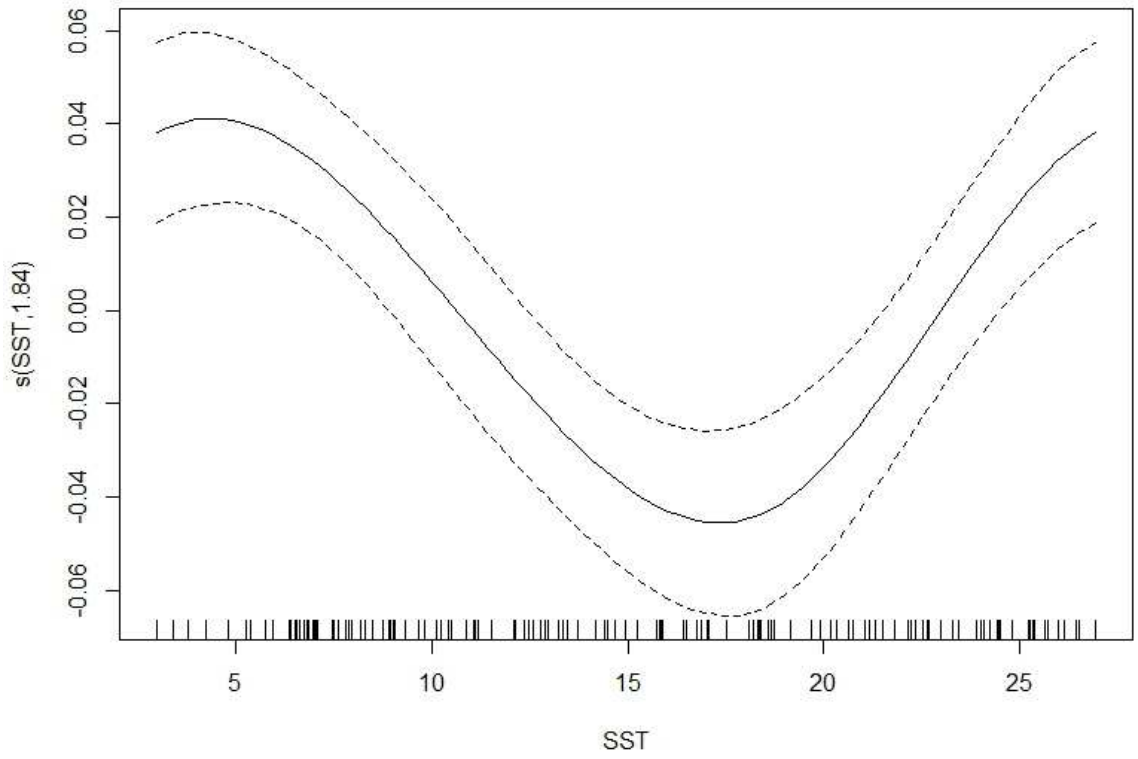

Figure 4.5.4h. Harbor porpoise generalized additive model (GAM) smoothing curves for sites T-2C
Smoothing curves for harbor porpoise occurrence in relation to SST (°C) at site T-2C. The predictor is on the x-axis, the fitted smooth function on the y-axis, and the dashed lines are error bands. Tick marks on the x-axis (rug plot) show the distribution of the underlying data.

Acoustic detections of harbor porpoises (median porpoise positive hours (PPHs) per day, total PPHs, maximum number of PPHs per day, and proportion of days per month detected) were significantly correlated with monthly habitat-based density estimates (Roberts et al. 2016) at sites A-5C, T-2C, and T-3C (Table 4.5.4e). The median number of PPHs per day at site 4 was 0 in all months, and therefore there is no correlation value for this metric. The strongest correlations were between predicted densities and the total number of PPHs at site A-5C (Figure 4.5.4i), and the median number of PPHs per day at site T-2C (Table 4.5.4e). None of the acoustic detection metrics from site T-1C were significantly correlated with the density estimates (Table 4.5.4e). The highest predicted density of harbor porpoises at this site occurred in October (Roberts et al. 2016), a month during which there were very few acoustic detections (Figure 4.5.4i).

Table 4.5.4e Spearman's rank correlation coefficients (p-values are in parentheses) for the median porpoise positive hours (PPHs) per day, total PPHs per month, maximum number of PPHs per day and proportion of days harbor porpoises were detected acoustically in each month compared to Roberts et al.'s (2016) monthly predictions of porpoise density at each site.

Acoustic Metric	T-1C	A-5C	T-2C	T-3C
Median PPHs	0.26 (0.41)	0.59 (0.04)	0.80 (0.00)	NA
Total PPHs	0.20 (0.54)	0.80 (0.00)	0.79 (0.00)	0.73 (0.01)
Maximum PPHs	0.23 (0.48)	0.78 (0.00)	0.76 (0.00)	0.74 (0.01)
Proportions	0.20 (0.52)	0.78 (0.00)	0.77 (0.00)	0.74 (0.01)

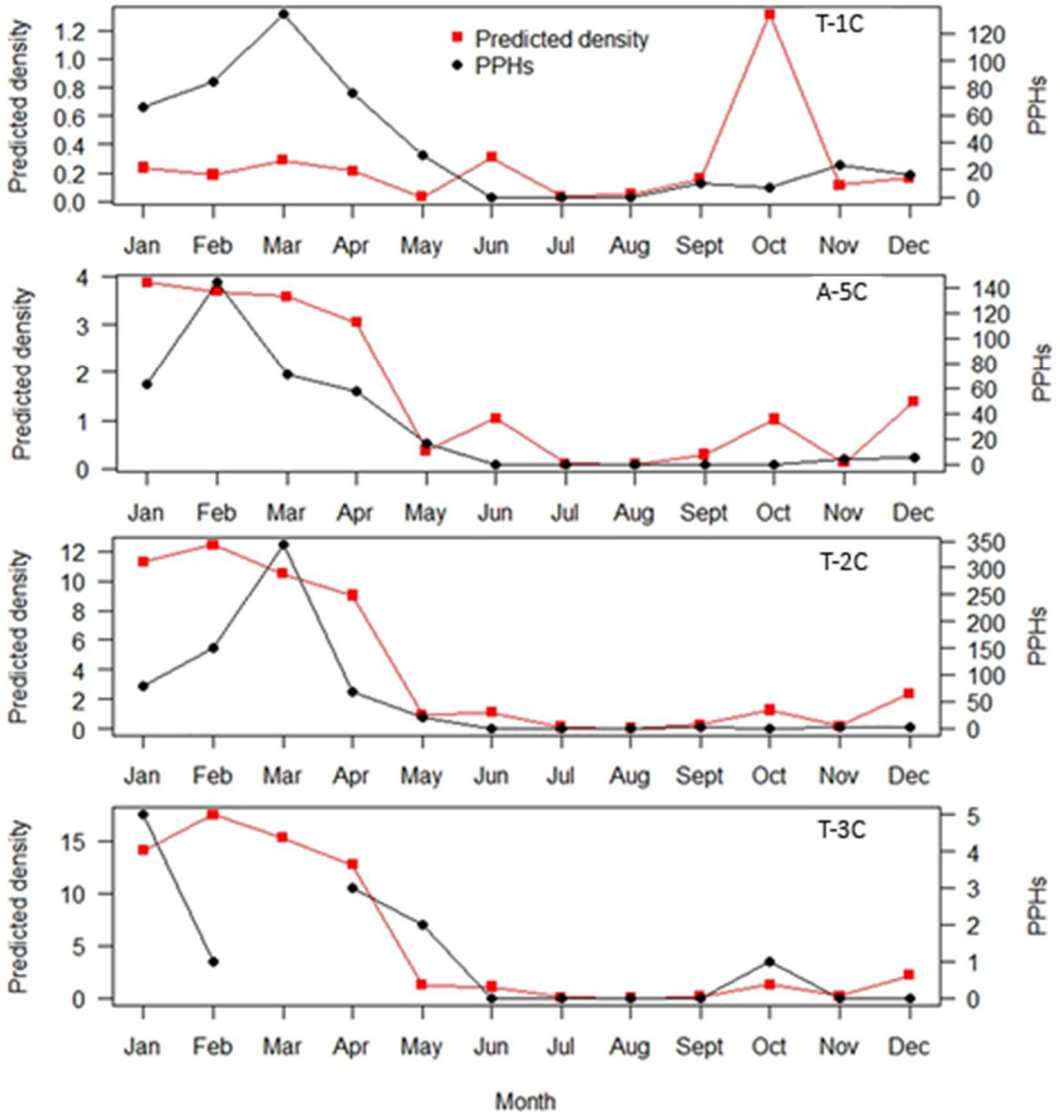

Figure 4.5.4i. Predicted and acoustically detected harbor porpoises
The predicted densities of harbor porpoises per month (red) and the total number of acoustically detected harbor porpoise positive hours (PPHs) per month offshore of Maryland (black). Predictions (in individuals per 100 km^2) are from Roberts et al.'s (2016) model and acoustic data were collected from November 2014 to May 2016. There were no acoustic data for March at T-3C.

4.6 Bottlenose Dolphin Abundance and Behavior

4.6.1 Individual Dolphin Identification from Signature Whistles

For site T-1C, signature whistle identification from 2,832 hours of acoustic data during summer 2017 resulted in 874 high-quality signature whistles (Table 4.6.1a). Neural network sorting in ARTwarp categorized these 874 whistles into 526 unique individual whistle categories. The majority of the whistle matches (237 of 348 total matches) were signature whistles produced within the same hour, which were classified as the same encounter and not included as reoccurrences. The remaining 111 whistles matches were either found on separate days, or in separate hours within the same day, and were thus labeled as reoccurrences of an individual. Of these 111 reoccurrences, 75 of them (68%) were found on separate days. Most reoccurrences were within the same week, with 51 days being the longest period between detected individual signature whistle reoccurrences.

For the subsample at site A-5C, signature whistle identification from 309 hours of acoustic data resulted in 398 signature whistles across all deployments (Table 4.6.1a). Neural network sorting in ARTwarp categorized these 398 signature whistles into 141 unique categories. By manually verifying and correcting ARTwarp's sorting, we re-sorted 57 signature whistles from the existing ARTwarp categories into an additional 33 categories. The final sorting resulted in a total of 174 unique signature whistle types (Figure 4.6.1a). Of the 174 dolphin signature whistles types, 77 of these dolphins were detected during the summer 2016, 55 during the winter 2017, and 42 in the summer 2017. Of these 174 signature whistle categories, 160 signature whistle categories (92%) exclusively contained signature whistles in which all whistle occurrences within that category were on the same day (Figure 4.6.1b). Signature whistles in these 160 categories were not identified again on any other days across all three deployments. The remaining 14 categories included whistles that were identified on at least one other day. All 14 of these signature whistle recurrences were within their deployment of initial detection and occurred up to 79 days apart. More than half (57%) of the recurrences appeared between 1 and 20 days after the first identification of the signature whistle, and the majority (71%) of all recurrences were during the winter 2017 deployment (Table 4.6.1b). Ten signature whistles recurred twice, and four signature whistles recurred three times. The mean time interval between recurrences was 25 days (SD = 21 days). The 2-hour subsampling regime is likely to have resulted in our detecting approximately 63% of individual whistles (based on an analysis of the T-1C recordings where all hours were reviewed), which means the number of individual dolphins at A-5C could have been underestimated and may have been on the order of 276. There were 10 individual signature whistles that occurred at both T-1C and A-5C in summer 2017.

Table 4.6.1a The number of bottlenose dolphin signature whistles and unique signature whistle categories in comparison with deployment, length of deployment, and hours of acoustic data analyzed.

Deployment	A-5C July – September 2016	A-5C January – April 2017	A-5C June – September 2017	T-1C June – September 2017	Total
Deployment Length (Days)	66	85	118	118	387
Hours Analyzed	88	86	135	2832	3141
Number of Signature Whistles Identified	168	150	80	874	1272
Number of Signature Whistles Categories	77	55	42	526	700

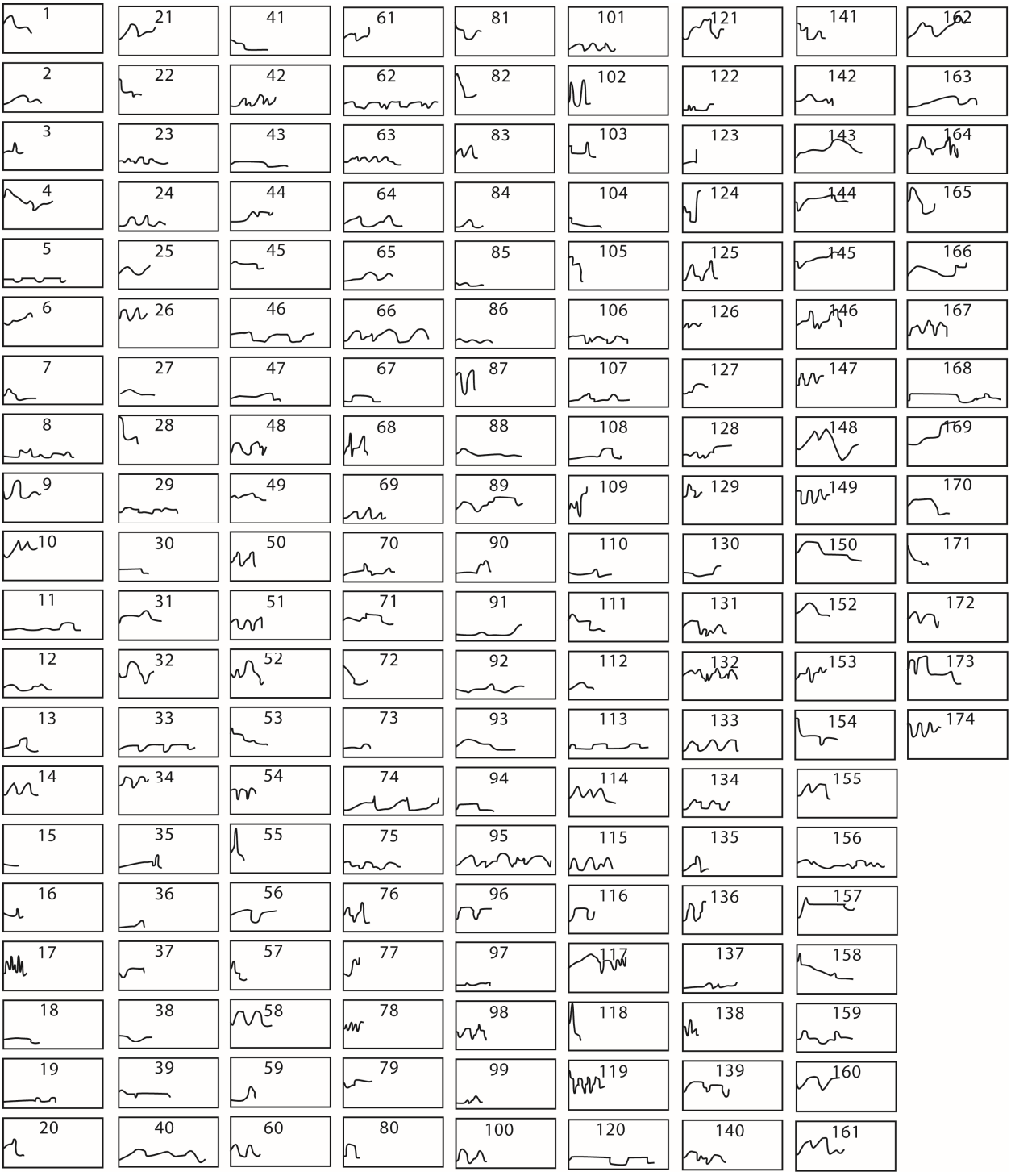

Figure 4.6.1a. ARTwarp signature whistle classifications at A-5C

Each numbered category depicts the contour of signature whistles that are contained within that category for site A-5C. Through categorization in ARTwarp and manual verification, 174 unique signature whistle categories were found. This diagram is based on images from in ARTwarp software.

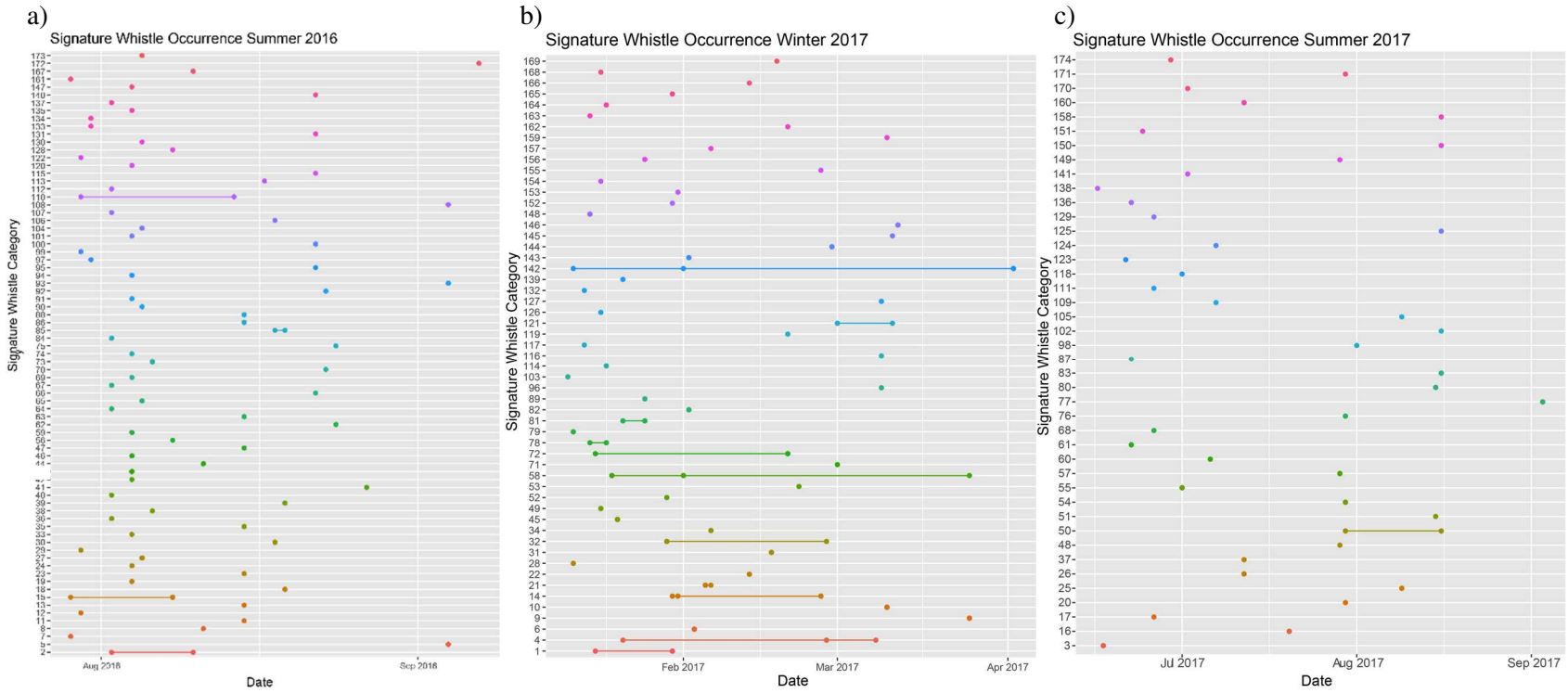

Figure 4.6.1b. Individual dolphin presence categorized by signature whistles at A-5C
Signature whistle occurrences within categories by deployment at A-5C: a) July – September 2016, b) January – April 2017, and c) June – September 2017. Each figure shows the occurrence of individual dolphins defined by their signature whistles within each deployment. Lines connecting dots indicate a dolphin revisiting the study site, A-5C.

Our analysis of the detection range of our acoustic recorder revealed that the same whistles could be detected 100% of the time at a recorder 3km away, 37% of the time at our site 8 km away, and undetected (0%) at the site 20 km away (Figure 4.6.1c). Based on this analysis, we estimate a 50% detection rate at 7km away from our recorder (Figure 4.6.1c).

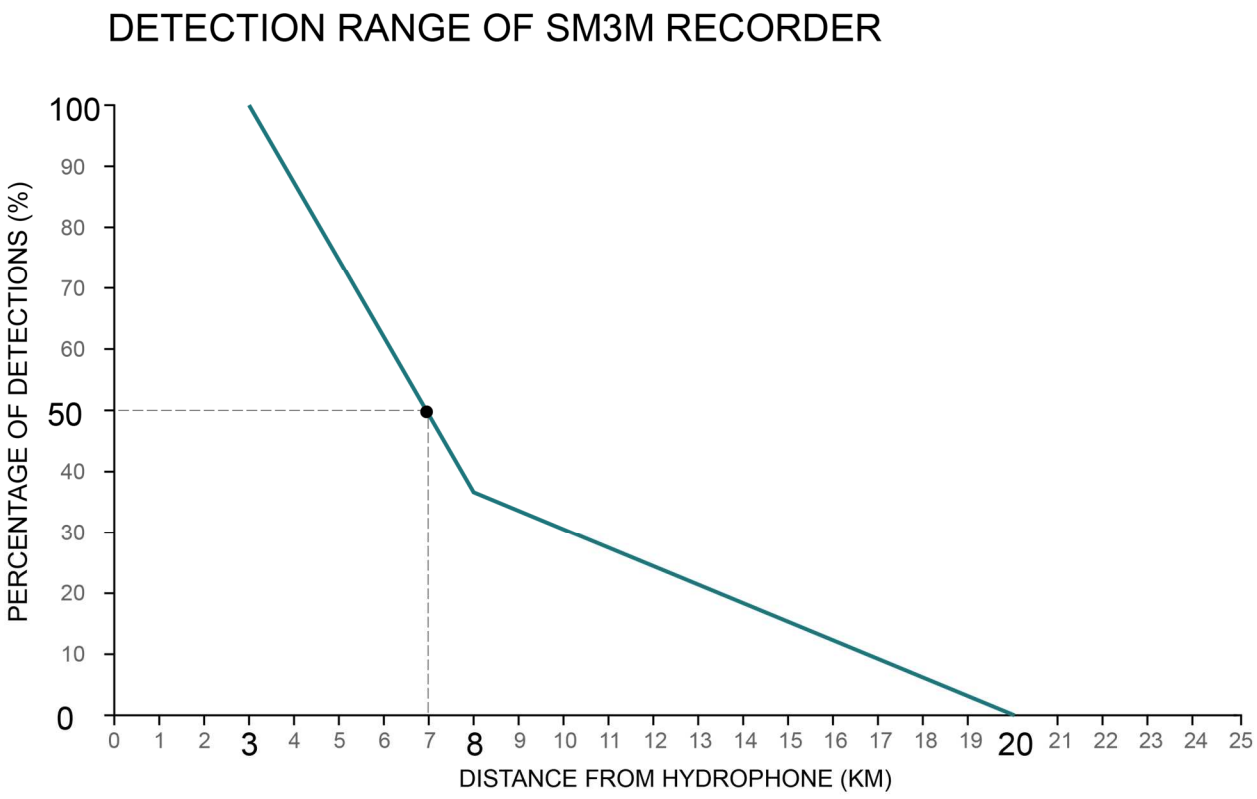

Figure 4.6.1c. Estimated SM3M detection range
Percentage of whistles detected at additional sites 3km (100%), 8km (37%), and 20km (0%) from the acoustic recorder used in this study. A detection rate of 50% is estimated at a distance of approximately 7 km.

4.6.2 Dolphin Foraging Behavior

4.6.2.1.1 Encounter Classification

The number of minutes between successive dolphin detections was 1 – 51,553 minutes (35.8 days) with the upper quartile of these time intervals being 37 minutes or less. We therefore deemed detection positive minutes occurring more than 37 minutes apart as different encounters, which was consistent with a previous study that visually confirmed dolphins spending >30 min in the area were detected by the T-POD, a predecessor to the C-POD (Bailey et al. 2010). Encounter numbers were then assigned to all of our dolphin detections, with bottlenose and common dolphin encounters numbered separately.

4.6.2.1.2 Foraging Inter-Click Interval Threshold

The Gaussian mixture model identified three distinct distributions, of which the peak at the shortest ICI occurred at ln(8.33) (Figure 4.6.2a). We defined the foraging ICI threshold as the peak plus two standard deviations giving ln(9.20), which is equivalent to 9.9 ms. A minute with at least one ICI at

or below this threshold was considered to be indicative of foraging activity. This was applied to the data for all sites from November 2014 to April 2017.

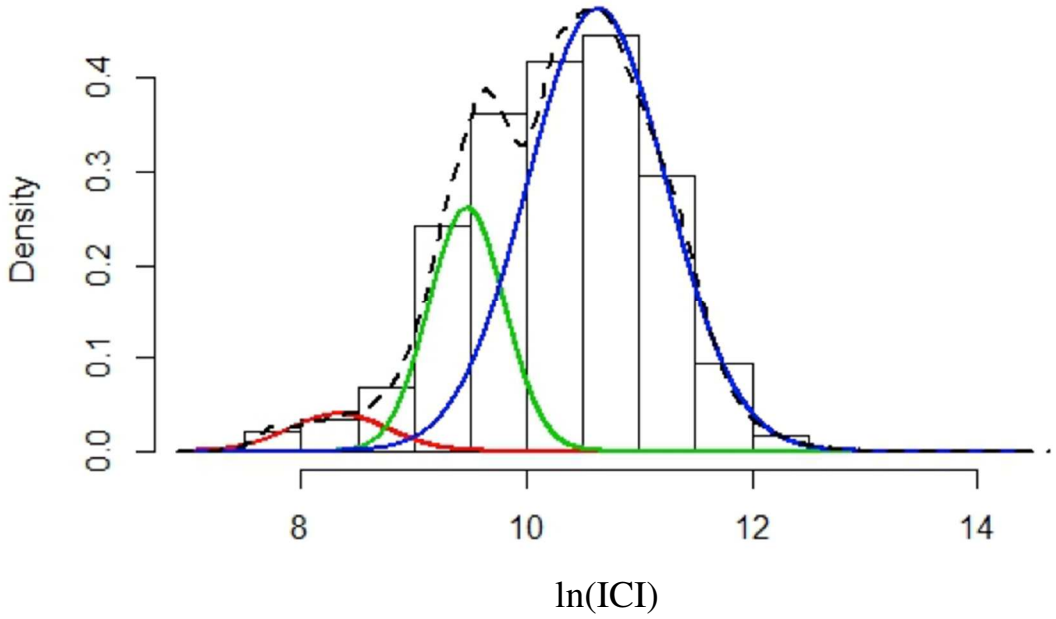

Figure 4.6.2a. Foraging inter-click interval Gaussian mixture model results
The results of the Gaussian mixture model for T-1C dolphin detection data during 2015 and 2016. The values on the x-axis are the natural logarithm of the ICIs in microseconds.

4.6.2.1.3 Validation of Foraging Activity

From the 995 minutes that were classified as foraging based on the ICIs from the C-POD data and that had corresponding SM3M recordings, 97.8% were confirmed to contain feeding buzzes (Table 4.6.2a). However, the false negative rate was relatively high (83.5%) indicating the C-POD detections were underestimating foraging activity at the minute scale. The random forest models to help account for this had an overall misclassification error on the testing data of 8.3% with default weights and 8.1% with tuned class weights. The error of the second random forest model was slightly smaller and the difference between the observed and predicted total number of minutes with missed feeding buzzes in the test data was also smaller for the second model (4.6%) than for the first model with default weights (17.3%). Thus, we proceeded with using the random forest model with tuned class weights because it delivered more accurate classification results, including the prediction of missed foraging activity. The variables of greatest importance in the model were the ICI, current and next behavioral state, and the ICI within the previous and next minute (Figure 4.6.2b). Using the random forest with tuned weights, we predicted minutes where there were missed feeding buzzes in the rest of the dataset, when no corresponding SM3M recordings were available, and labeled these minutes as foraging activity. These data were used in the rest of the analyses.

Table 4.6.2a Number of true positive (TP), false positive (FP), true negative (TN), false negative (FN) detections and minutes not within the duty cycle of the SM3M recordings (NA).

C-POD Feeding Buzz		SM3M Feeding Buzz	
T-1C February – April			
TP	197	FN	185
FP	9	TN	41
NA	38	NA	55
Total	244	Total	281
T-1C May – July			
TP	688	FN	702
FP	12	TN	151
NA	150	NA	177
Total	850	Total	1030
A-5C July – November			
TP	88	FN	118
FP	1	TN	6
NA	190	NA	200
Total	279	Total	324

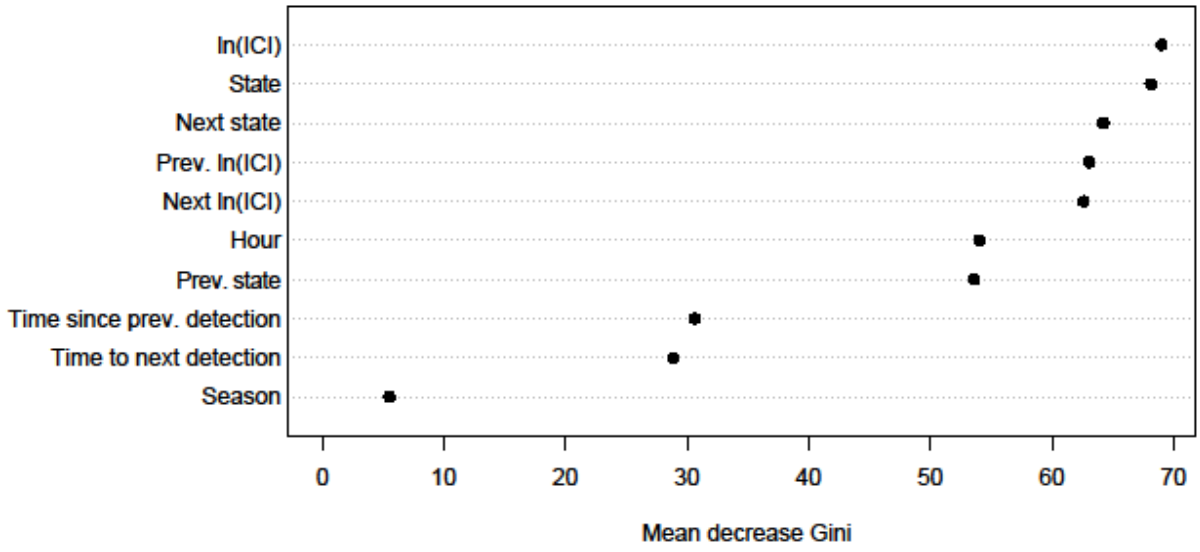

Figure 4.6.2b. Random forest variable plot
Variable importance plot from the random forest with tuned class weights, showing which variables primarily contribute to identifying missed foraging activity as measured by the Gini index.

4.6.2.1.4 Behavioral State Transition Probabilities

The hypotheses of Markovianity in a first-order Markov chain was rejected. However, at the 5% significance level, we could not reject the null hypothesis that the observed second-order chains of dolphin foraging activity had Markov property. This was found for all locations and both dolphin species. Overall, these results matched the earlier results of the random forest model showing the high importance

of the previous and next behavioral states (a triplet) in determining the behavioral state within the current minute (Figure 4.6.2c). For bottlenose dolphins at T-C, A-5C and T-2C, and for common dolphins at all sites, if the previous two behavioral states had been foraging then the most likely next state was foraging. Similarly, for all sites for bottlenose dolphins and for common dolphins at T-2C, if the previous two behavioral states had been not foraging then the most likely next state was also not foraging. If the previous two behavioral states were mixed with foraging and not foraging (or vice versa), then bottlenose dolphins had a higher likelihood of the previous state persisting into the current minute whereas this effect was not as strong for common dolphins where switching states in the majority of cases was as likely as state persistence.

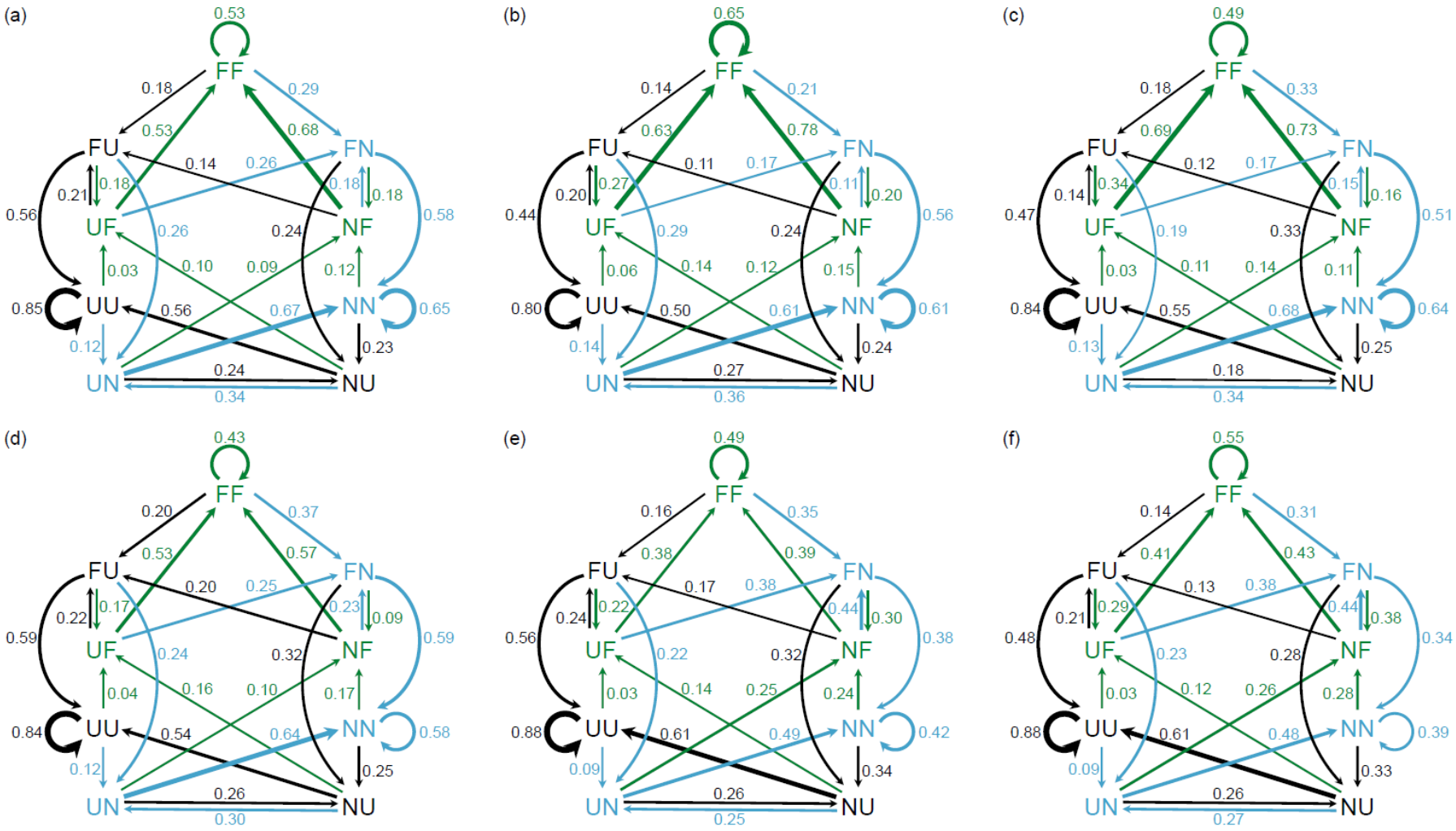

Figure 4.6.2c. Markov chain transition probabilities
Diagrams of the observed Markov chain for transition probabilities between second-order behavioral states (foraging, not foraging or unknown) for bottlenose dolphins at a) T-1C, b) A-5C, c) T-2C, d) and T-3C and for common dolphins at e) T-2C f) and T-3C.

4.6.2.1.5 Factors Affecting Encounter Duration

The mean encounter length for bottlenose dolphins was 25 minutes (range = 1 – 633 minutes, Figure 4.6.2d(a)). The mean proportion of time spent foraging during these encounters was 28% (Figure 4.6.2e). The Cox proportional hazards model showed that the proportion of minutes with foraging activity in the first third of an encounter significantly reduced the likelihood of dolphins leaving the area (Table 4.6.2h; Figure 4.6.2d(b)). Factors that significantly increased the likelihood of dolphins leaving the area (ending the encounter) were a high proportion of foraging activity in the second half of the encounter, a high difference in the proportion of foraging activity between the first and second half of the encounter and if the first behavioral state in the encounter was foraging. Season was a statistically significant factor in the model with shorter encounters during the winter and spring (October – April).

The mean encounter length for common dolphins was 17 minutes (range = 1 – 387 minutes, Figure 4.6.2f(a)). The mean proportion of time spent foraging was 35% (Figure 4.6.2g). Similar to bottlenose dolphins, the Cox proportional hazards model showed that the proportion of minutes with foraging activity in the first third of an encounter significantly reduced the likelihood of dolphins leaving the area (longer encounter durations), whereas a high proportion of foraging activity in the second half of the encounter and a high difference in the proportion of foraging activity between the first and second half of the encounter increased the likelihood of dolphins leaving the area (Figure 4.6.2f(b)).

Table 4.6.2h Results from the Cox proportional hazards regression models for encounters of bottlenose and common dolphins, where 'coef' is the coefficient estimate and the exponential of the coefficient, 'Exp(coef)', is the hazard ratio.

Variable	coef	Exp(coef)	se(coef)	95% CI	p-value
Bottlenose Dolphin					
Proportion of foraging in the first third of encounter	-0.36	0.70	0.11	0.57 – 0.86	0.001
Proportion of foraging in the second half of the encounter	0.24	1.28	0.10	1.05 – 1.55	0.014
Foraging state in the first minute of encounter	0.35	1.42	0.08	1.21 – 1.66	<0.001
Season: October – April	0.45	1.56	0.06	1.39 – 1.76	<0.001
Absolute difference in proportion of foraging between first and second half of encounter	1.58	4.87	0.13	3.80 – 6.25	<0.001
Common Dolphin					
Proportion of foraging in the first third of encounter	-0.36	0.70	0.13	0.54 – 0.90	0.006
Proportion of foraging in the second half of the encounter	0.55	1.73	0.16	1.28 – 2.34	<0.001
Absolute difference in proportion of foraging between first and second half of encounter	0.95	2.58	0.19	1.77 – 3.75	<0.001

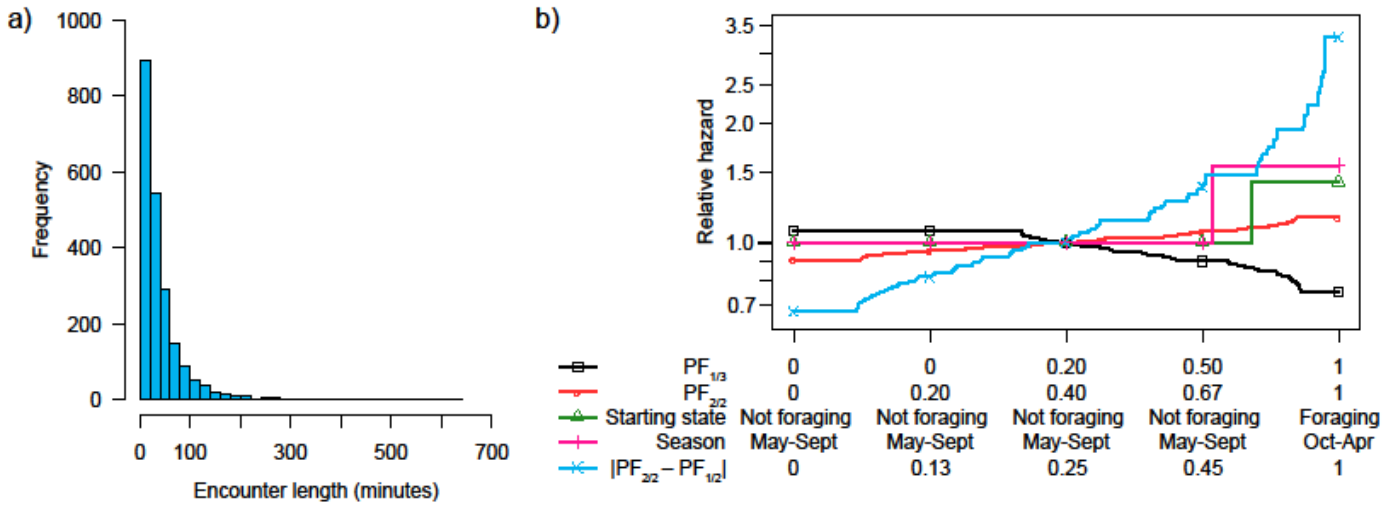

Figure 4.6.2d. Bottlenose dolphin encounter lengths and rank-hazards
Bottlenose dolphin a) encounter lengths with at least five C-POD detection positive minutes per encounter and b) rank-hazard plot where the x-axes shows levels of categorical variables and 0, 25, 50, 75 and 100th percentiles of continuous variables.

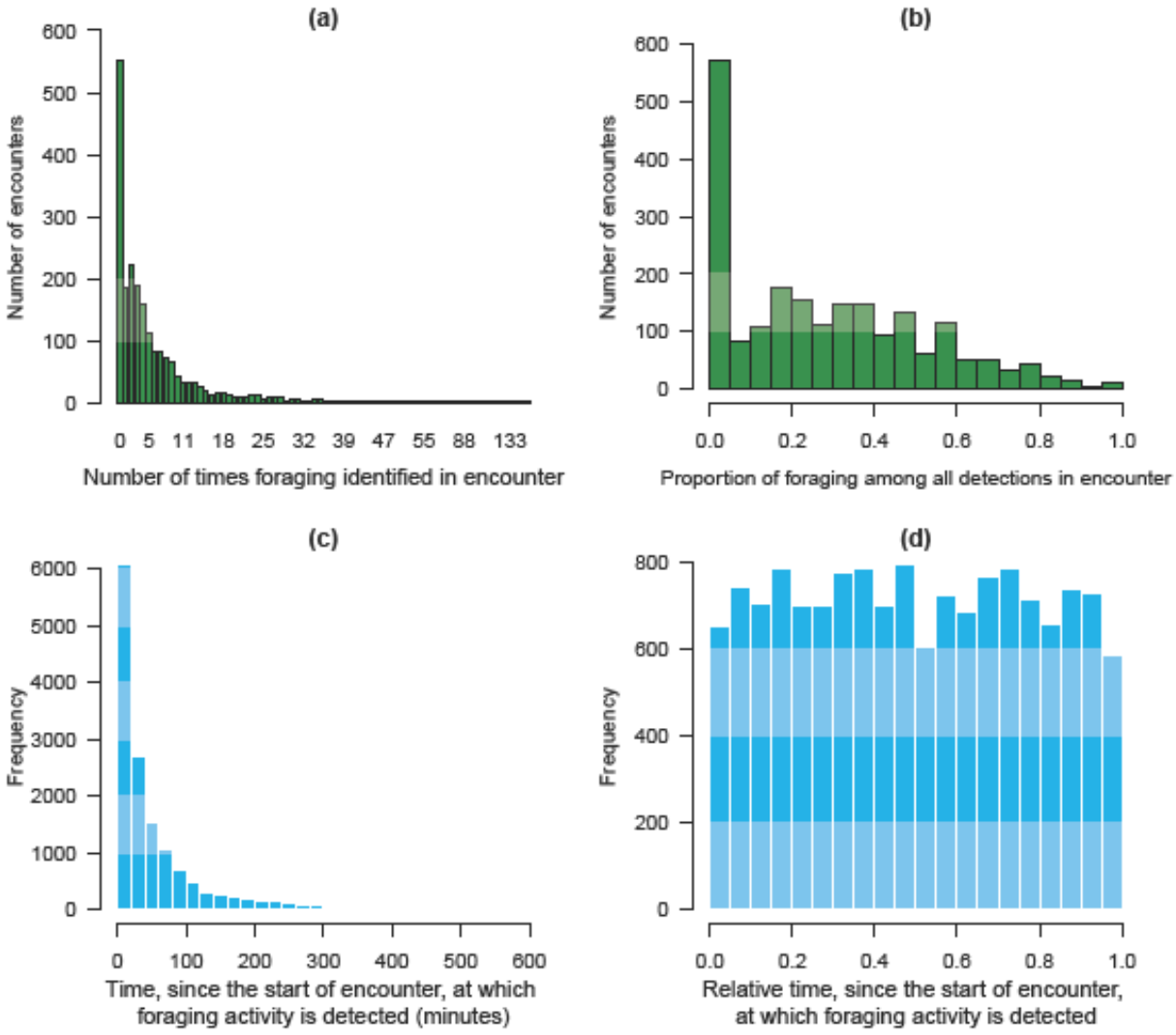

Figure 4.6.2e. Number and proportion of bottlenose dolphin encounters
a) Number and b) proportion of foraging minutes during bottlenose dolphin encounters with at least 5 C-POD detection positive minutes, and c) time and d) relative time of foraging since the start of the encounter.

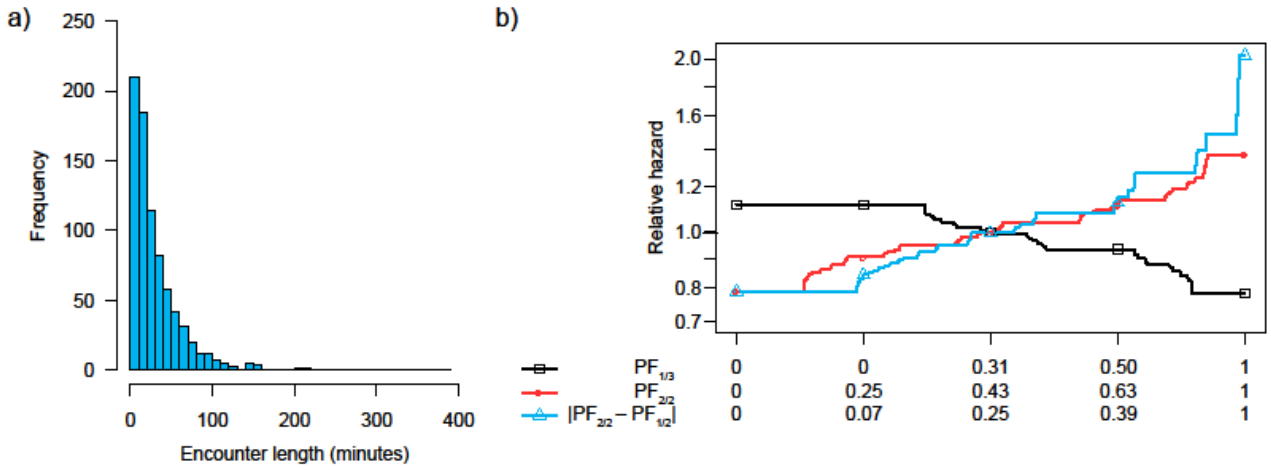

Figure 4.6.2f. Common dolphin encounter lengths and rank-hazards
Common dolphin a) encounter lengths with at least five C-POD detection positive minutes per encounter and b) rank-hazard plot where the x-axes shows levels of categorical variables and 0, 25, 50, 75 and 100th percentiles of continuous variables.

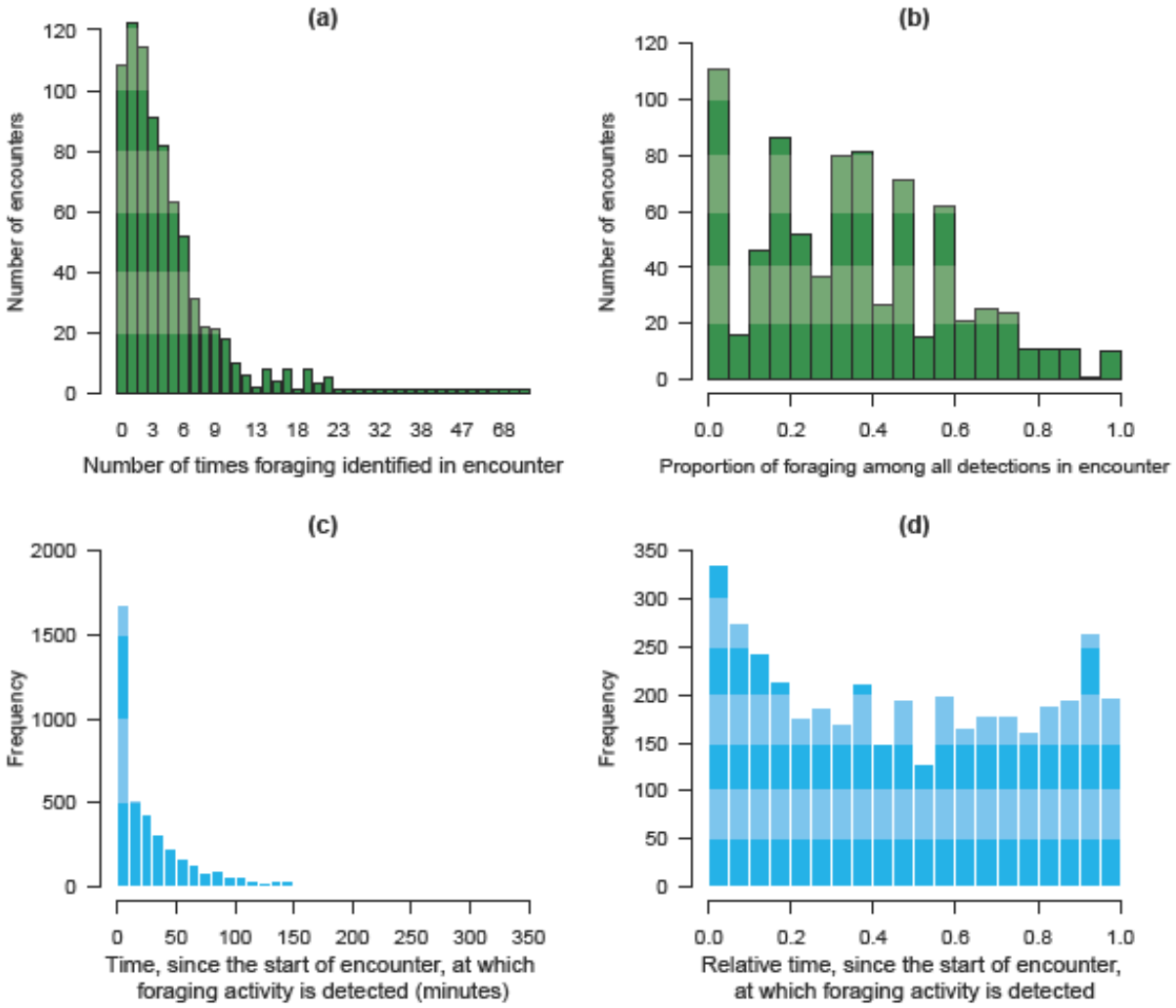

Figure 4.6.2g. Number and proportion of common dolphin encounters
a) Number and b) proportion of foraging minutes during common dolphin encounters with at least 5 C-POD detection positive minutes, and c) time and d) relative time of foraging since the start of the encounter.

4.6.3 Dolphin Response to Storm Events

There was a peak in SSTa during the storm events in 2016 and 2017 based on the daily data (Figure 4.6.3a), and there were significantly higher SSTa values across the 14-day storm period in 2017 than during the corresponding period in 2015 (Table 4.6.3a). Ambient sound levels were significantly lower after the storm event period in 2017 than during the corresponding period in 2015 (Table 4.6.3a). This was due to an ambient sound level peak in early October 2015 caused by high winds in the region. The highest ambient sound levels occurred during the storm periods in 2016, 2017, and the high winds in October 2015 (Figure 4.6.3a(b)).

Table 4.6.3a Results (p < 0.05) from the final generalized auto-regressive moving average models used to determine the differences in dolphin encounter and behavior metrics between periods and years, and whether these were affected by the storms.

Response Relative to 2015 Control	Estimate	Standard Error	P-value
Number of Encounters: 2016			
Year	-0.31	0.15	0.04
Train Duration: 2016			
Year	17.34	6.42	< 0.01
Percent Foraging: 2016			
Year	2.05	0.27	< 0.01
SSTa: 2017			
During: Year	1.03	0.24	< 0.01
Ambient Sound Level: 2017			
After: Year	-3.58	1.18	< 0.01
Number of Encounters: 2017			
During: Year	-0.31	0.15	0.03

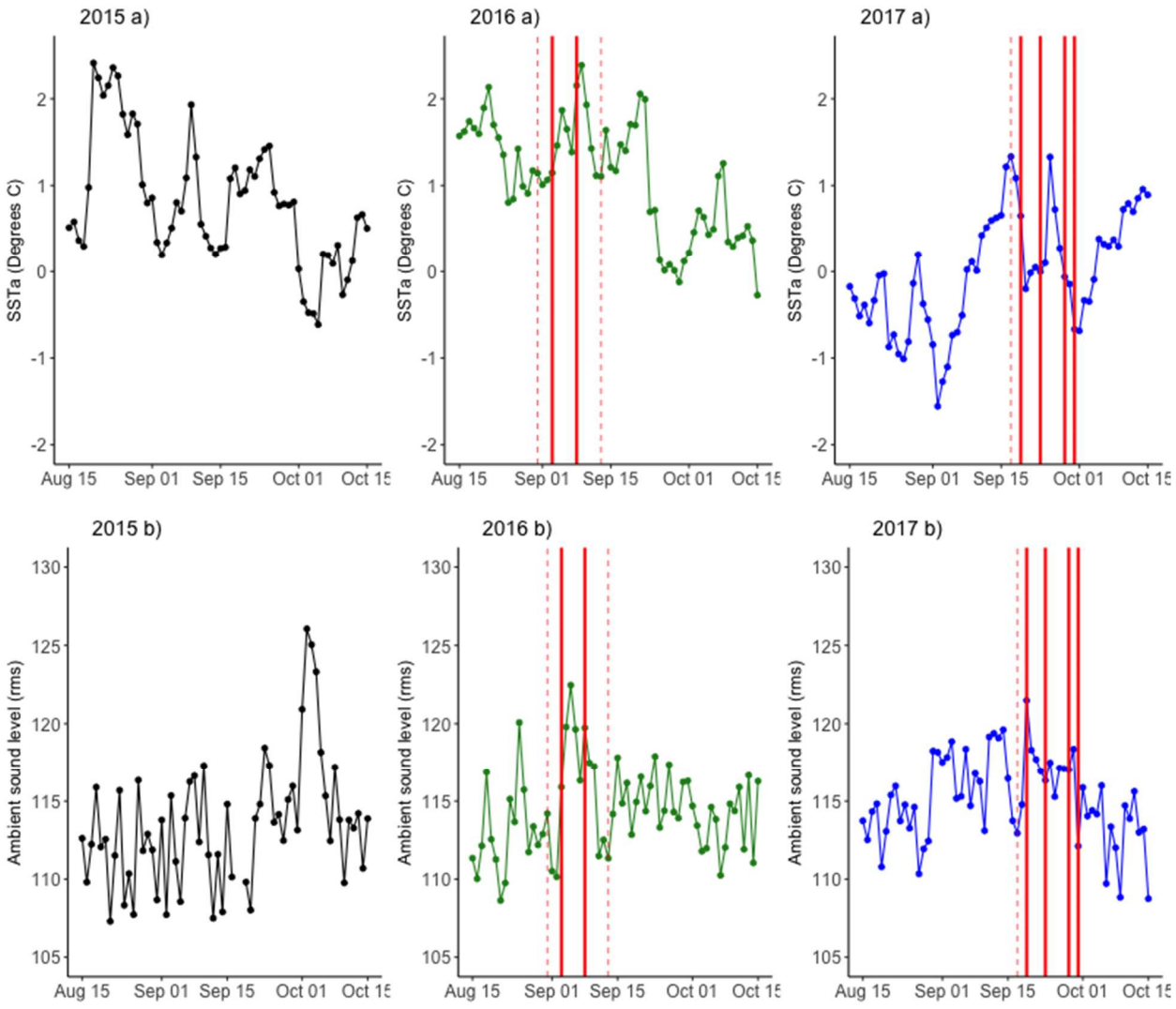

Figure 4.6.3a. SST anomaly and sound levels during the study period
a) Daily (16 August – 15 October) sea surface temperature anomaly (SSTa) for 2015 to 2017, and b) daily root mean square (rms) ambient sound levels for each year with solid red lines indicating the period when the storm was in the study area, and dashed red lines indicating the 14-day designated "during" period of the storms..

There were fewer daily average dolphin encounters per in 2016 compared to 2015 (Figure 4.6.3b(a)), and the three days with the fewest number of encounters in 2016 were during the storm period. While there were no significant differences in the duration of dolphin encounters across the 14-day periods between years or periods, the shortest dolphin encounter and the one day without any encounters occurred during the storm. The day with the lowest percentage of foraging per encounter in 2016 occurred during the storm, and the day with the highest percentage of foraging occurred following the storm period. Dolphin occurrence and behavior metrics (average dolphin click train duration, average ICI, number of encounters, encounter length, proportion of minutes per encounter spent foraging) in 2016 were not significantly different during the storm period than in the corresponding periods in 2015.

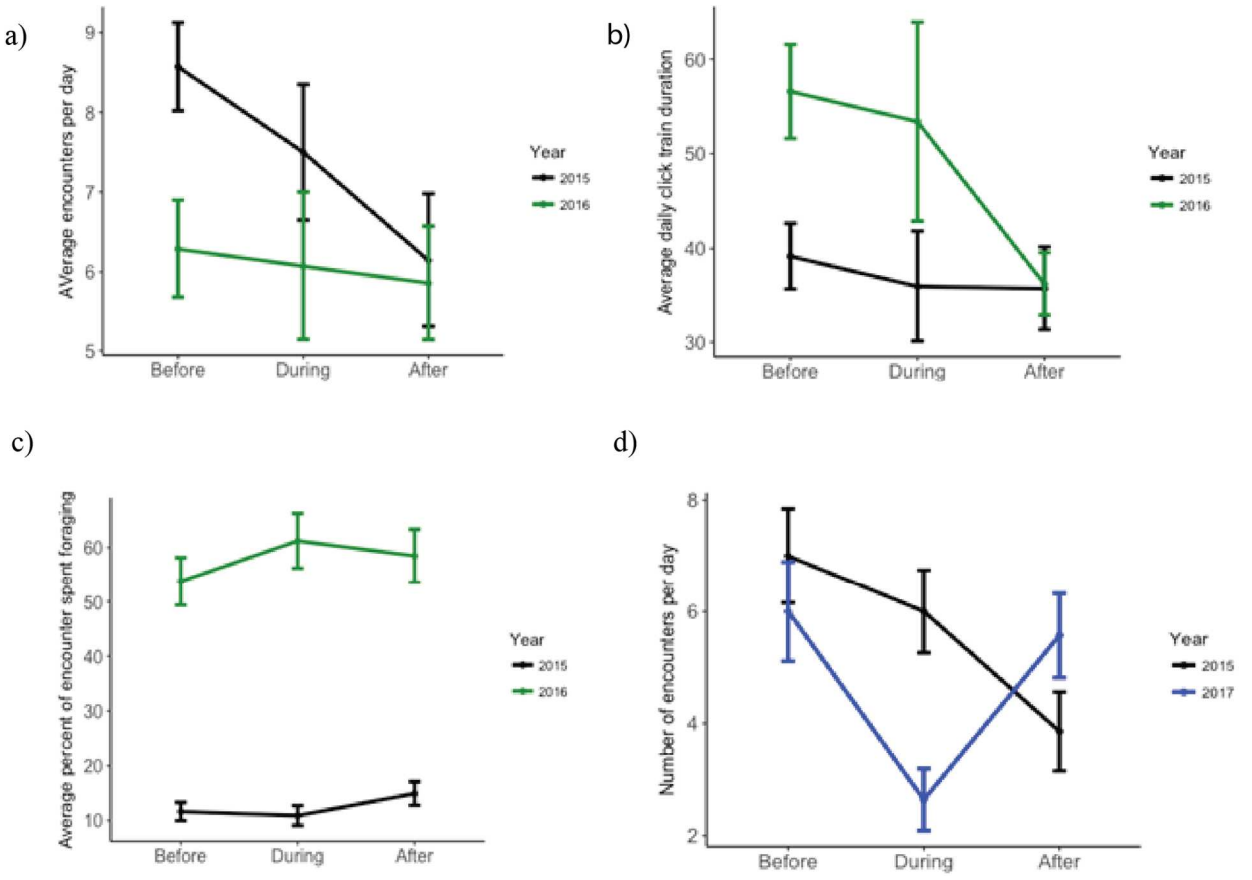

Figure 4.6.3b. Dolphin responses in relation to storm events
Graphs of the average values and standard error for the before, during, and after storm periods for a) encounters per day in 2015 and 2016, b) daily click train duration in 2015 and 2016, c) daily average of percent of encounter spent foraging in 2015 and 2016, and d) encounters per day in 2015 and 2017.

During the 2017 Atlantic hurricane season, the average number of dolphin encounters per day in the study area was significantly lower during the storm period compared to the corresponding period in 2015 (Table 4.6.3a; Figure 4.6.3b(d)). During the storm period in 2017, dolphins were not detected at all on two days in the study area. On days when dolphins were detected, no foraging behavior was detected for four consecutive days following the first storm. Further, foraging did not occur on 33.33% of these post-storm days (n = 4 of 12 days). The days with the two highest percentages of foraging per encounter occurred after the 2017 storm period. Other than the average number of encounters per day, no significant difference between periods or years for any of the dolphin occurrence or behavior metrics was observed.

4.7 Ambient Noise Analysis

4.7.1 Sound Level Analysis

To validate the accuracy of noise measurements for the Marine Autonomous Recording Unit (MARU) data, we compared a 25% stratified subsample of 1-hour Leq values (at 10 – 800 Hz 1/3rd octave center frequency band) between the AMAR and the co-located MARU deployed at site A-8M during 16 April 2015 – 21 September 2015. Statistical analysis showed no significant difference between corresponding hourly Leq noise values for the AMAR and co-located MARU (paired t-test; DF = 504, t =

1.64, p = 0.1). We can therefore assume our reported findings at all MARU survey sites are reliable estimates of ambient noise values within and surrounding the Maryland WEA.

The full linear frequency and 1/3-octave frequency band long-term spectrograms for subsampled sites T-1M, A-5M, A-7M, and T-2M show a qualitative overview of baseline ambient noise within and surrounding the Maryland WEA and allow for quick visual comparisons of noise levels between sites (Figures 4.7.1a – d; see Appendix C for 3-year long-term spectrograms for all survey sites). Warmer colors indicate an increase in noise levels, while cooler colors represent quieter noise conditions. The 1/3-octave band spectrograms illustrate persistent shipping noise at sites A-5M, A-7M, and T-2M; site T-1M appears to have comparatively less shipping noise (Figures 4.7.1a – d). Noise levels at site T-1M appear to increase during the summer months (July – September) each year during the 3-year survey period (Figure 4.7.1a), while noise levels at site A-5M, site A-7M, and site T-2M appear to increase during autumn months (October – December) each year during the 3-year survey period (Figures 4.7.1b – d). Fin whale 20 Hz pulses are visible in the 1/3rd octave spectrogram at sites T-1M, A-5M, A-7M, and T-2M. Abrupt loud noise levels in the lower frequencies (below 500 Hz) likely represent anthropogenic noise (e.g. shipping, mechanical, dredging). A notable noise event occurred in September 2015, where noise levels between 300 and 800 Hz were elevated across sites, likely due to a storm event. Between December 2015 and March 2016 at site T-3M*, an unidentified mechanical sound source caused noise levels to exceed 120 dB nearly 100% of the time.

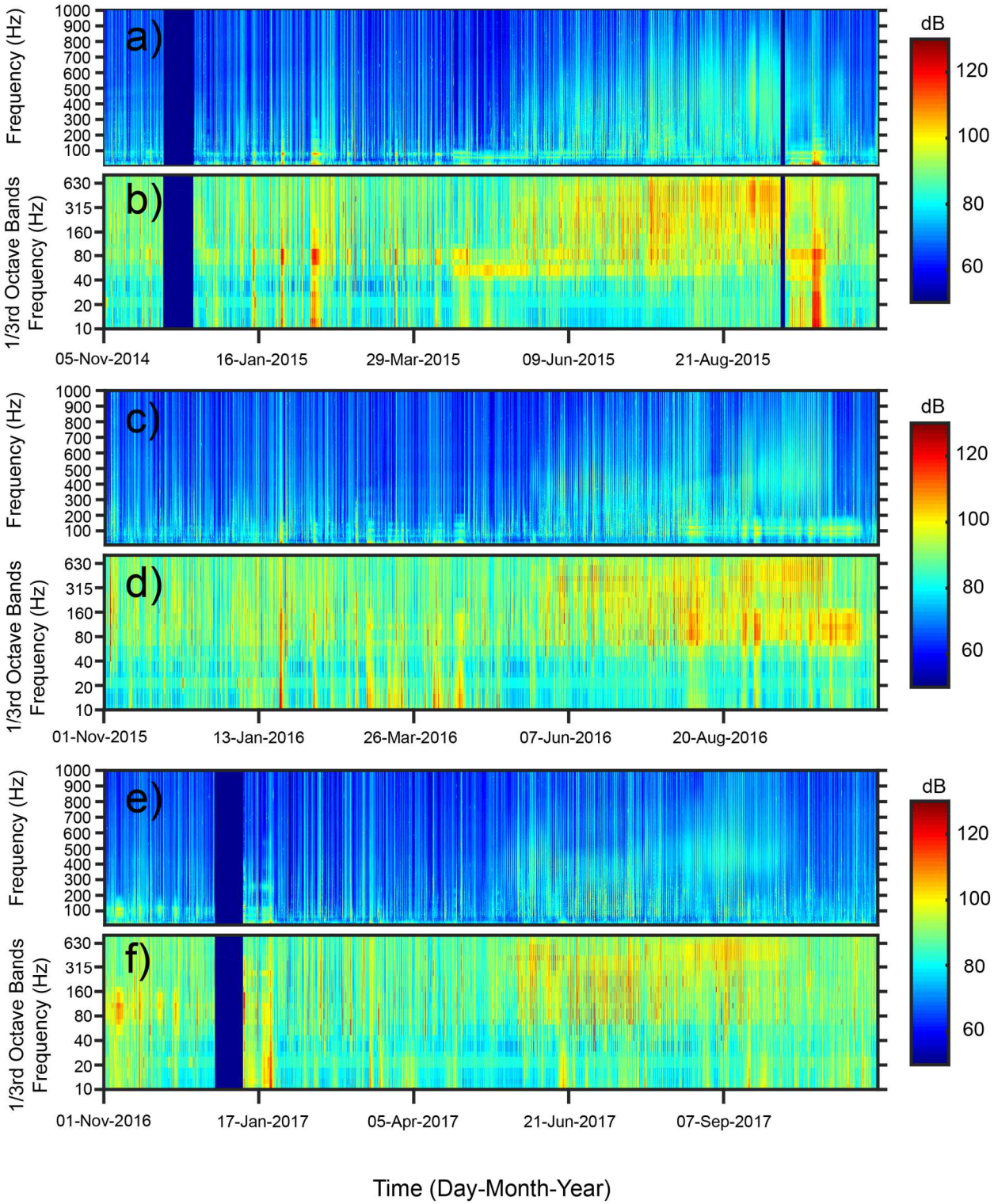

Figure 4.7.1a. Long-term spectrograms for site T-1M
Long-term spectrograms for a and b) year 1, c and d) year 2, and e and f) year 3 of the survey period. Panels a, c, and e represent noise on a linear scale (Δ *time* = 1 h, Δ *frequency* = 1 Hz) along the Y-axis, while panels b, d, and f represent noise on a 1/3rd octave scale (Δ *time* = 1 h). Dark blue sections indicate time periods with no sound data.

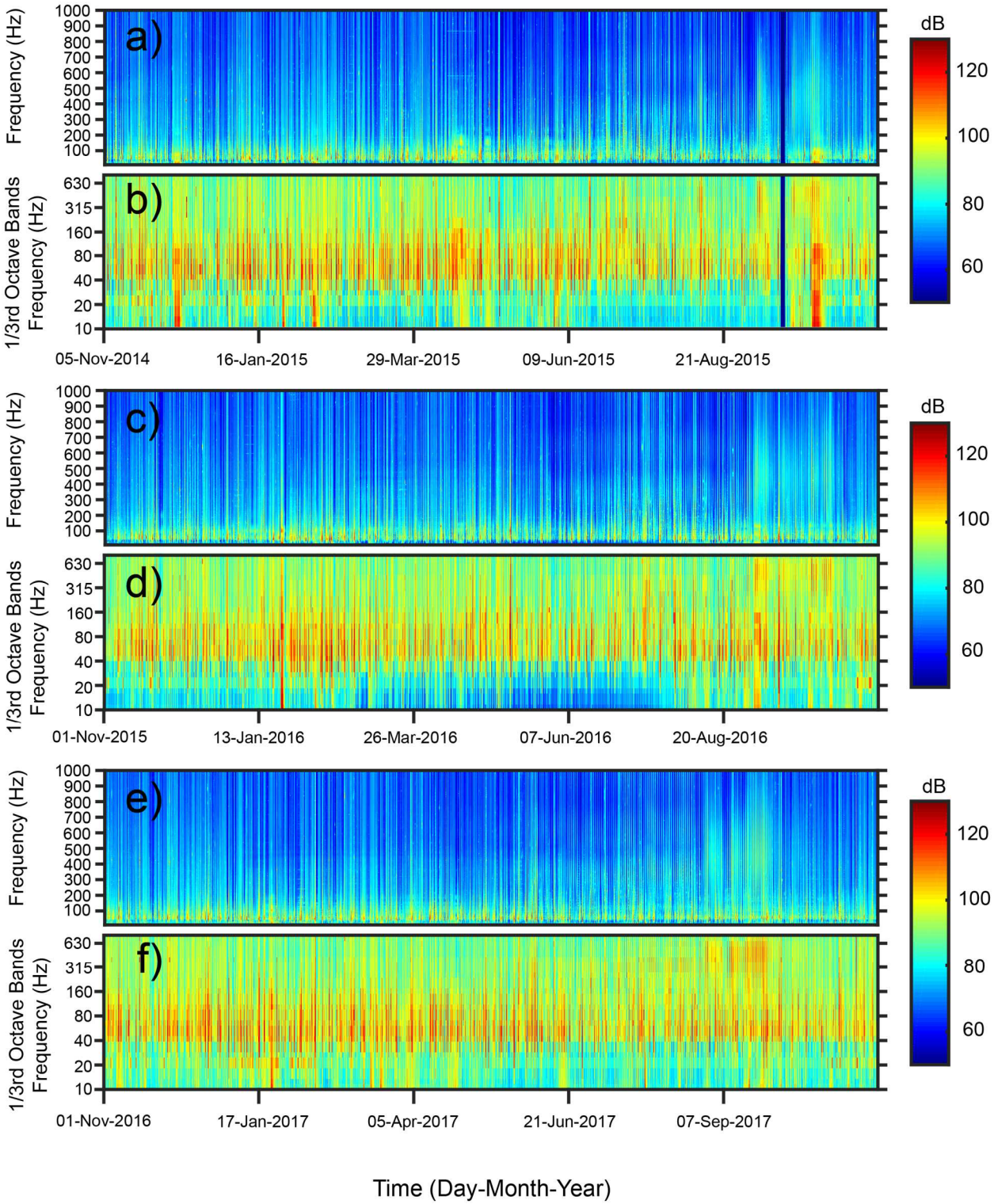

Figure 4.7.1b. Long-term spectrograms for site A-5M
Long-term spectrograms for a and b) year 1, c and d) year 2, and e and f) year 3 of the survey period. Panels a, c, and e represent noise on a linear scale (Δ *time* = 1 h, Δ *frequency* = 1 Hz) along the Y-axis, while panels b, d, and f represent noise on a 1/3rd octave scale (Δ *time* = 1 h). Dark blue sections indicate time periods with no sound data.

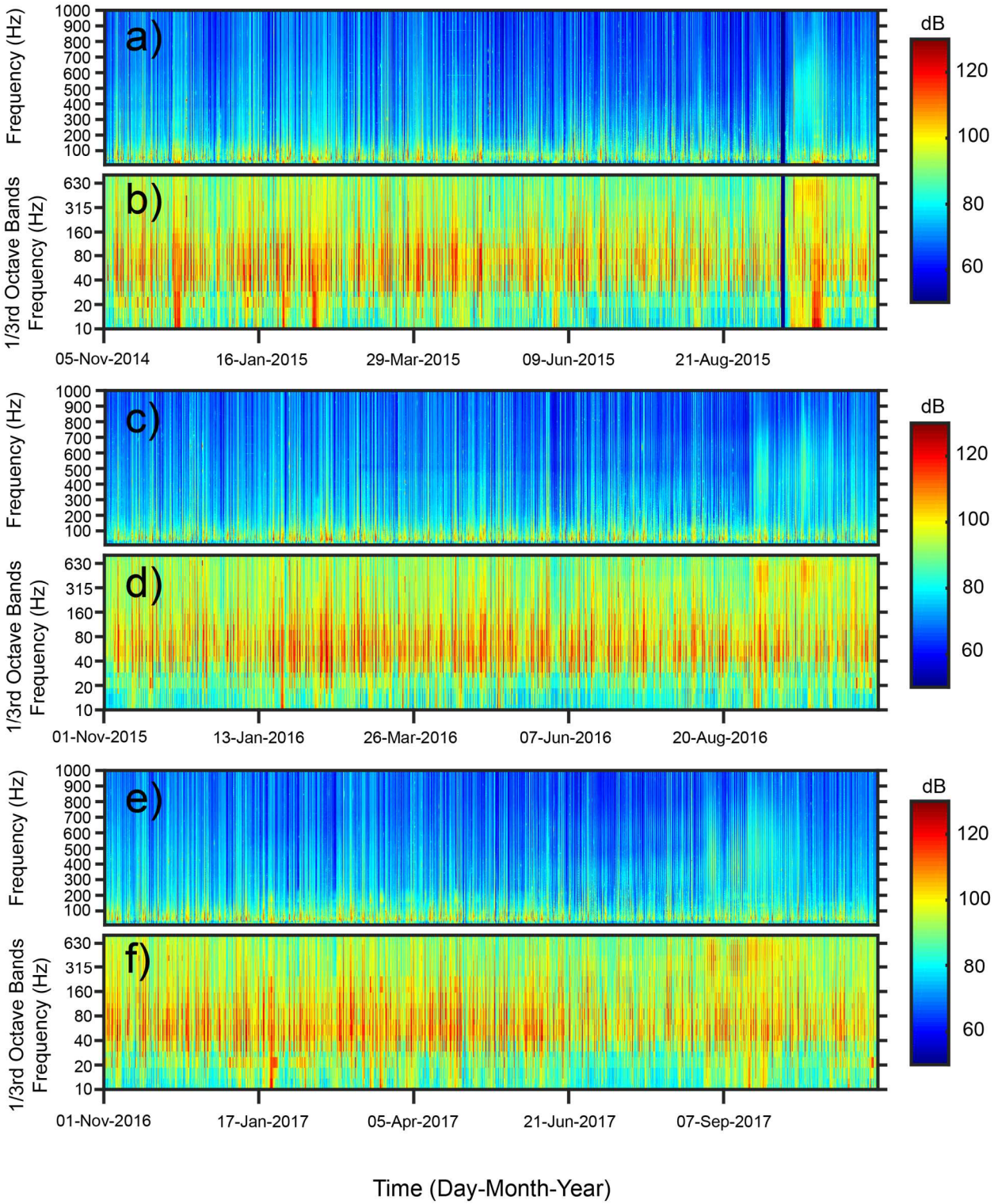

Figure 4.7.1c. Long-term spectrograms for site A-7M
Long-term spectrograms for a and b) year 1, c and d) year 2, and e and f) year 3 of the survey period. Panels a, c, and e represent noise on a linear scale (Δ *time* = 1 h, Δ *frequency* = 1 Hz) along the Y-axis, while panels b, d, and f represent noise on a 1/3rd octave scale (Δ *time* = 1 h). Dark blue sections indicate time periods with no sound data.

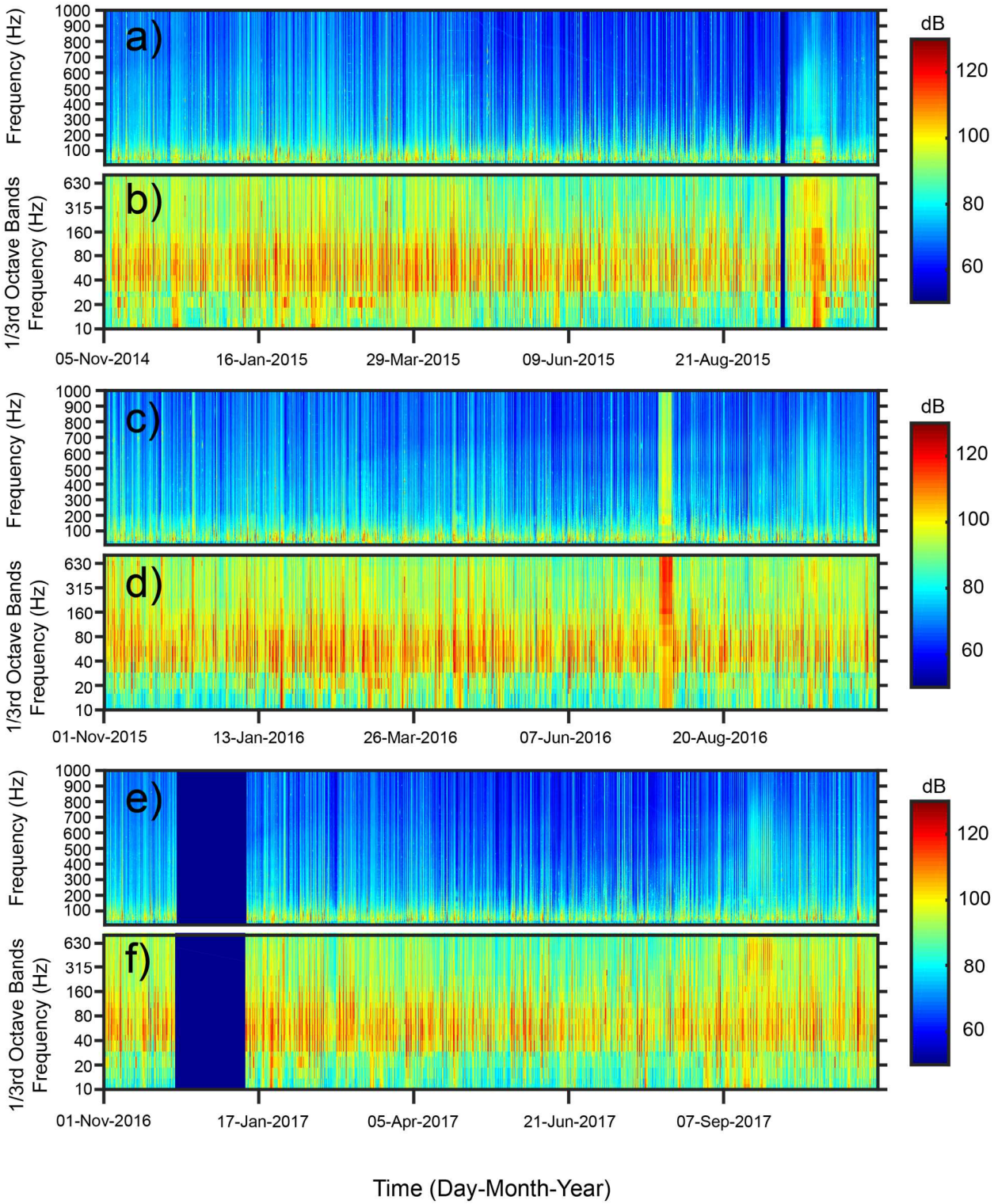

Figure 4.7.1d. Long-term spectrograms for site T-2M
Long-term spectrograms for a and b) year 1, c and d) year 2, and e and f) year 3 of the survey period. Panels a, c, and e represent noise on a linear scale (Δ *time* = 1 h, Δ *frequency* = 1 Hz) along the Y-axis, while panels b, d, and f represent noise on a 1/3rd octave scale (Δ *time* = 1 h). Dark blue sections indicate time periods with no sound data.

An ANOVA revealed a seasonal difference in noise values, and a Tukey's HSD post-hoc analysis confirmed differences at survey sites T-1M, A-5M, A-7M, and T-2M. Noise values were significantly higher during summer (July – September) months at site T-1M (DF = 3, F ratio = 179.09, $p < 0.0001$), while noise values were significantly higher during winter (October – December) months at sites A-5M (DF = 3, F ratio = 14.34, $p < 0.0001$), A-7M (DF = 3, F ratio = 25.78, $p < 0.0001$), and T-2M (DF = 3, F ratio = 23.05, $p < 0.0001$) (Figure 4.7.1e).

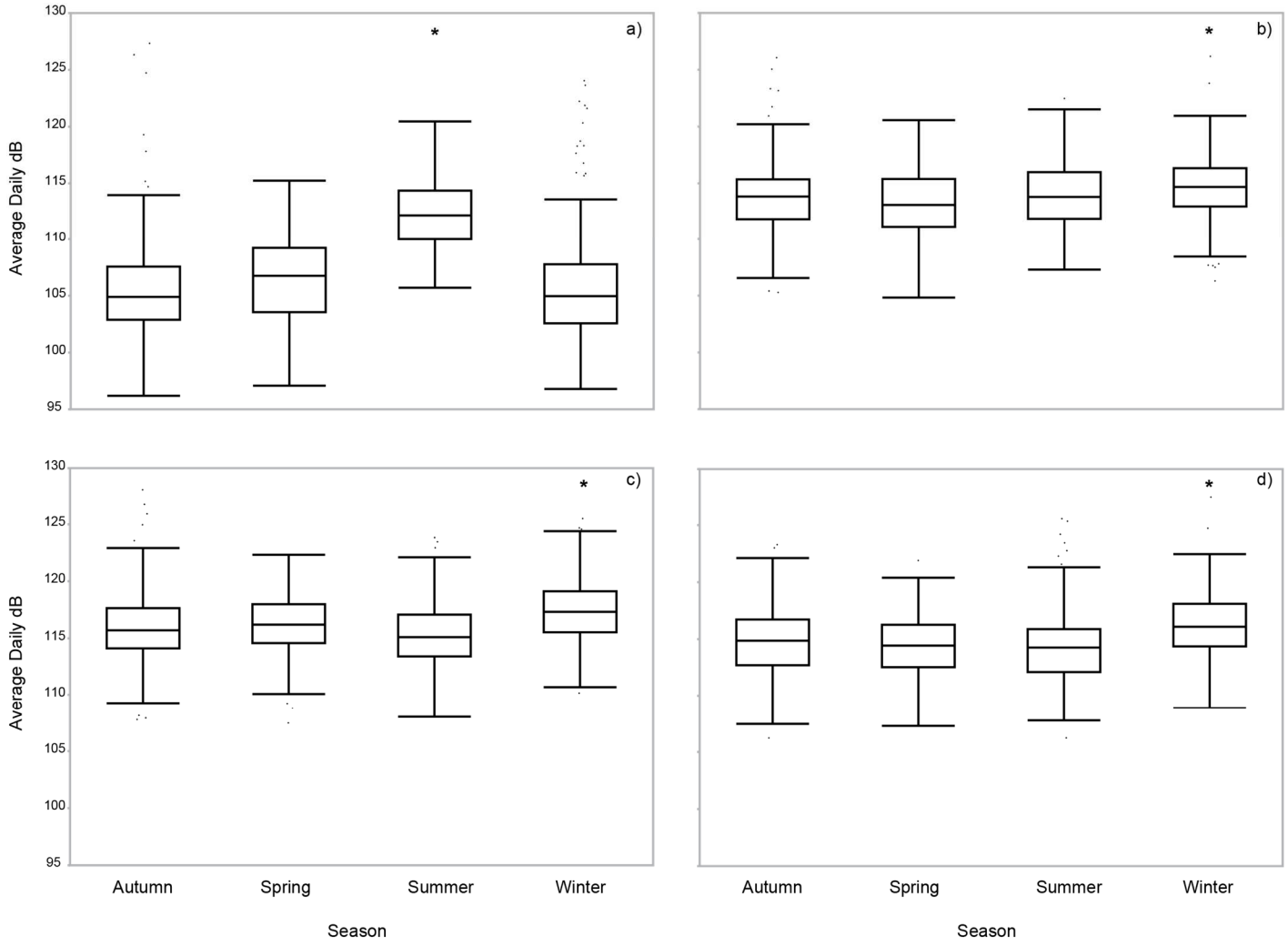

Figure 4.7.1e. Box and whisker plots of average daily noise values (dB) for sites T-1M, A-5M, A-7M, and T-2M

The box and whisker plots show the minimum, first quartile, median, third quartile, and maximum average daily dB values for (a) site T-1M, (b) site A-5M, (c) site A-7M, and (d) site T-2M.

The power spectral density plots were generated to show percentiles (99^{th}, 75^{th}, 50^{th}, 25^{th}, and 1^{st}) of sound power levels (dB) plotted as a function of frequency (Hz). The median (50^{th}) percentile curves reveal that while power spectrum levels above 200 Hz did not differ greatly between survey sites T-1M, A-5M, A-7M, and T-2M, there was a difference in power spectrum levels below 100 Hz (Figures 4.7.1f – i). Specifically, site A-7M and site T-2M had the highest sound levels compared to sites T-1M and A-5M (Figures 4.7.1f – i). The slight increase in power spectrum levels around 20 Hz at each subsampled site is likely due to the persistent occurrence of 20 Hz fin whale pulses throughout the 3-year survey.

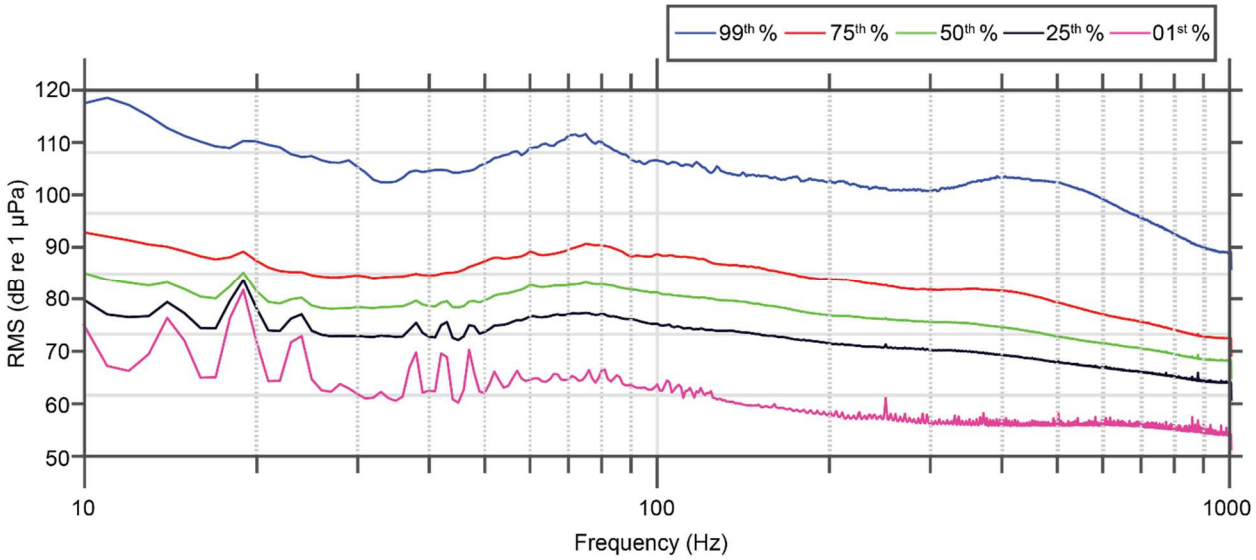

Figure 4.7.1f. Power spectral density for site T-1M
Frequency is represented on a log scale along the x-axis and sound level is represented along the y-axis on a linear scale. Each colored line represents the noise percentile for the site.

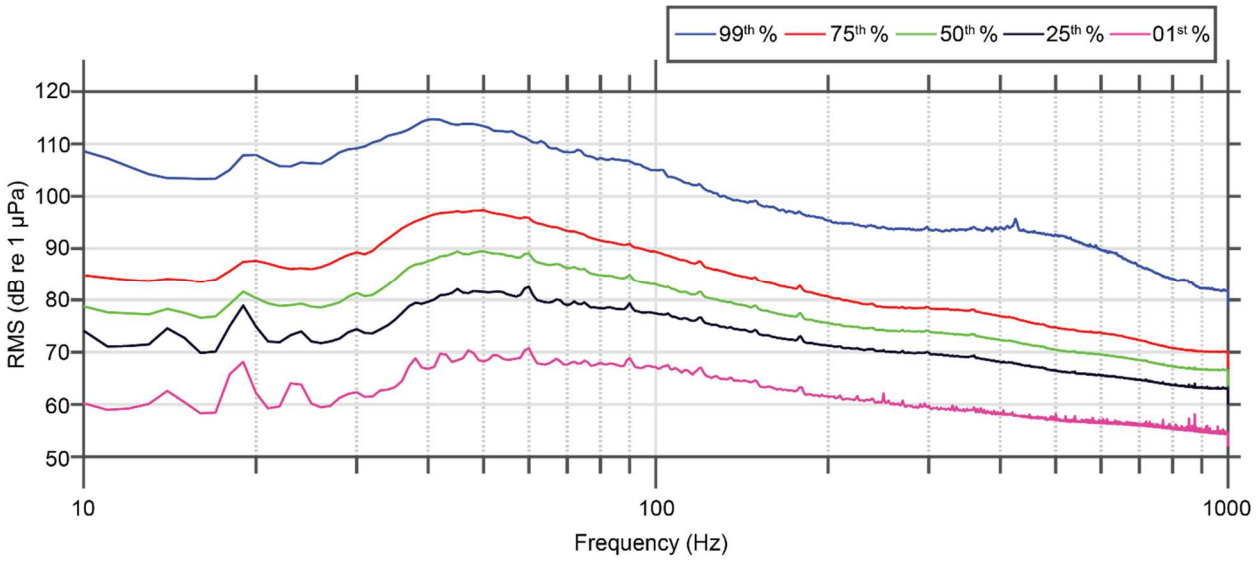

Figure 4.7.1g. Power spectral density for site A-5M
Frequency is represented on a log scale along the x-axis and sound level is represented along the y-axis on a linear scale. Each colored line represents the noise percentile for the site.

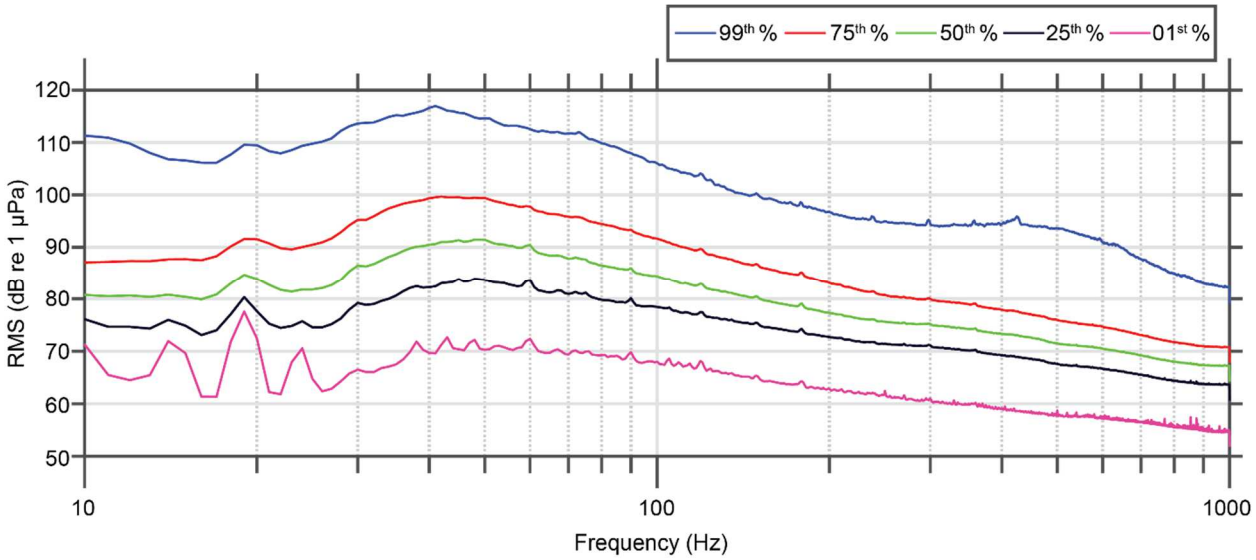

Figure 4.7.1h. Power spectral density for site A-7M
Frequency is represented on a log scale along the x-axis and sound level is represented along the y-axis on a linear scale. Each colored line represents the noise percentile for the site.

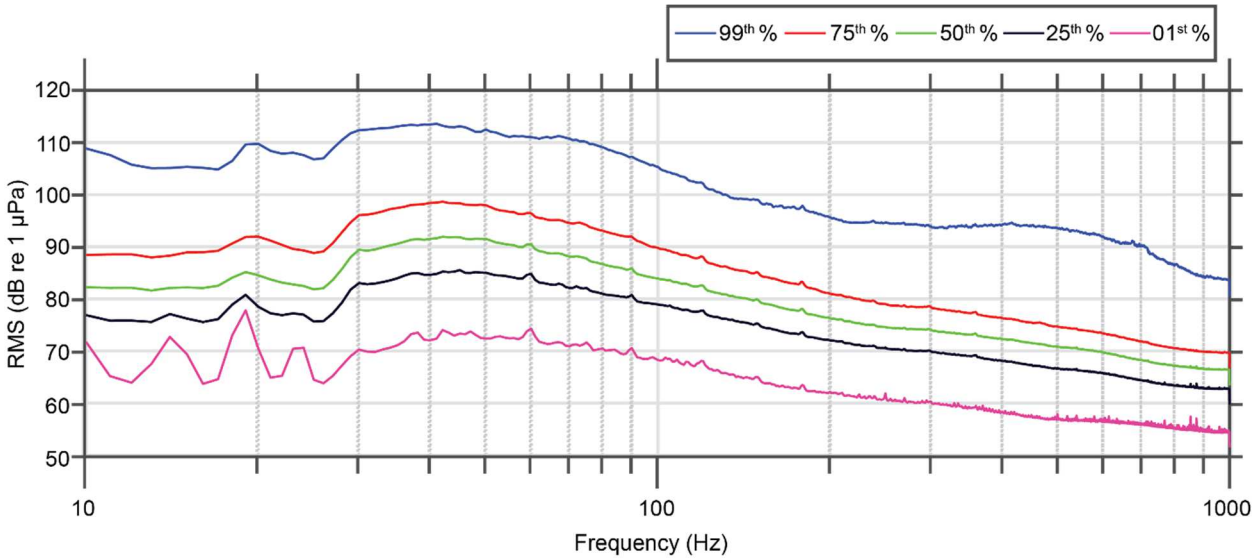

Figure 4.7.1i. Power spectral density for site T-2M
Frequency is represented on a log scale along the x-axis and sound level is represented along the y-axis on a linear scale. Each colored line represents the noise percentile for the site.

Cumulative percent distribution curves of sound levels show the cumulative percentage of time each survey site recorded sound at a specific L_{eq} value (dB re: 1µPa). Sound levels in the full frequency band (10 – 800 Hz 1/3rd octave center frequency) for each survey site varied between approximately 105 dB and 112 dB during 50% of the 3-year survey period (Figure 4.7.1j). Sites T-1M, A-2M, and A-3M had the lowest L_{eq} values, with sound pressure levels of approximately 107 dB or less 50% of the time (Figure 4.7.1j). Sites A-4M, A-7M, T-2M, and T-3*M consistently recorded the loudest L_{eq} values over the 3-year

survey period, with sound levels of approximately 110 dB and above 50% of the 3-year survey period (Figure 4.7.1j).

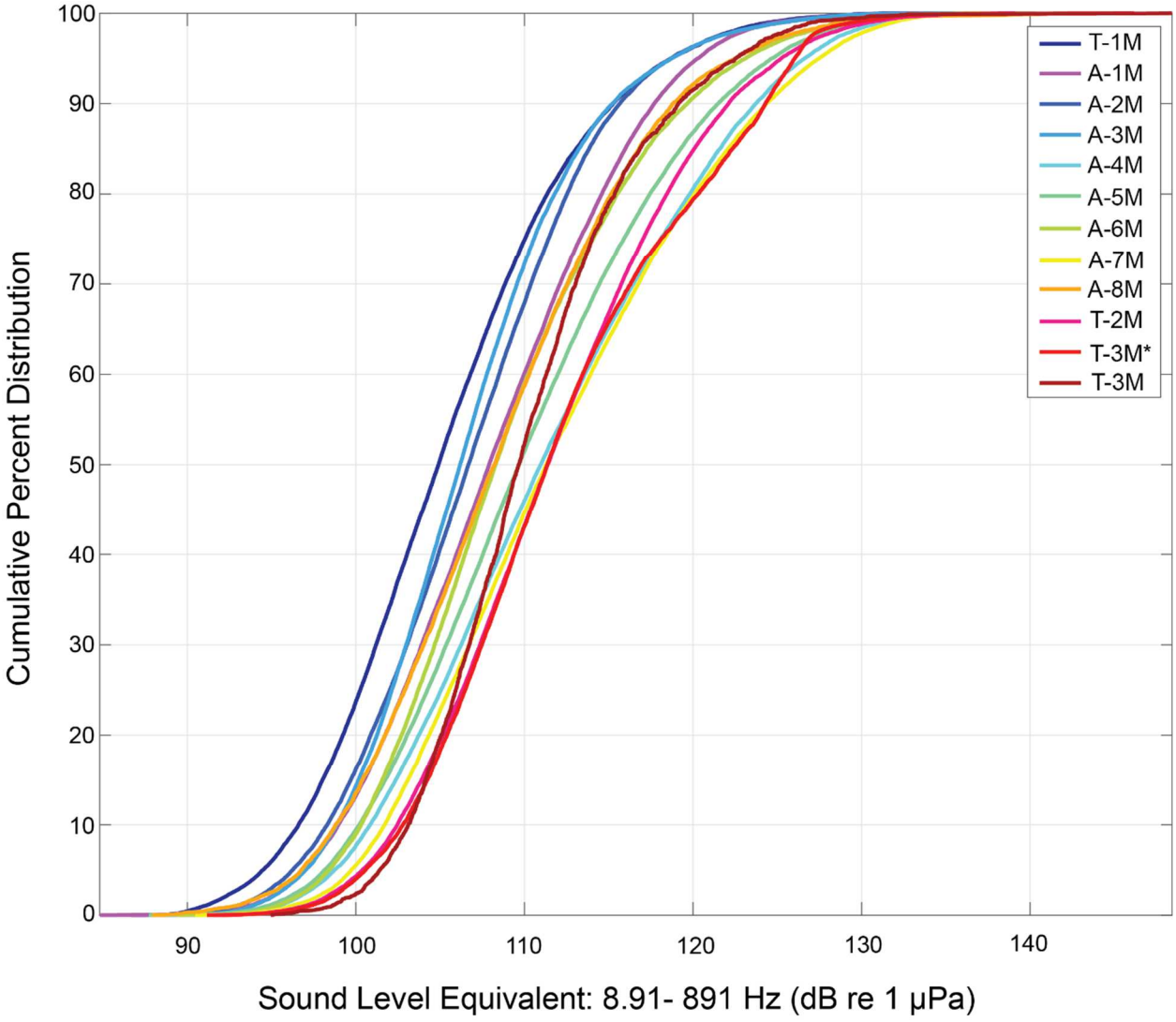

Figure 4.7.1j. Cumulative percent distribution plot for all marine autonomous recording unit (MARU) survey sites
Each colored line represents a specific recording site.

Median noise values calculated across the 3-year survey period in the full frequency band corroborated the same trend in noise levels, with sites along the eastern edge of the WEA (sites A-4M, A-7M) and sites just offshore of the WEA (site T-2M) being consistently louder than other sites located inshore the WEA and within the WEA (Table 4.7.1a). Given the proximity of the survey area to shipping lanes (see Figure 3.2a), shipping noise likely contributes to the relatively louder noise levels for sites along the eastern edge of the WEA and just offshore of the WEA.

Table 4.7.1a Average noise levels (dB re 1µPa) calculated each year of the survey period for each site, and the median noise levels calculated across the entire 3-year survey period for each site. No data were collected at site T-3*M during year 1 (4 November 2014 – 31 October 2015) and site A-8M and T-3M during year 3 (1 November 2016 – 31 October 2017).

Site	Average dB Year 1	Average dB Year 2	Average dB Year 3	Median dB
T-1M	109.8	108.7	108.2	107.2
A-1M	111.7	110.7	111.3	110.5
A-2M	110.1	109.8	109.8	108.5
A-3M	110.7	109.1	109.0	108.1
A-4M	116.3	116.0	116.1	115.6
A-5M	114.9	113.5	114.4	113.8
A-6M	113.2	113.3	112.4	112.1
A-7M	116.9	116.3	116.7	116.1
A-8M	112.4	113.0	NA	111.4
T-2M	115.4	115.8	115.0	115.3
T-3*M	NA	118.3	114.2	113.8
T-3M	113.8	112.0	NA	112.0

Additional cumulative percent distribution curves were plotted for whale 1/3rd octave frequency bands: fin whale (17.8 – 28.2 Hz), humpback whale (28.2 – 708 Hz), minke whale (44.7 – 355 Hz), and North Atlantic right whale (70.8 – 224 Hz) (Figure 4.7.1k). While sites T-1M, A-2M, and A-3M consistently had the lowest L_{eq} values across all whale frequency bands, a different pattern emerges for the loudest surveyed sites in the fin whale band: sound pressure levels recorded at sites T-3M and T-3*M were at or above 96 dB 50% of the time, while L_{eq} values for sites A-7M and T-2M were lower (95 dB) 50% of the time (Figure 4.7.1k). Most notably, site T-3M noise levels diverge from the trends of other sites, where 10% of the noise levels exceed 116 dB, whereas the next loudest site (A-7M) at that

percentage measured 110 dB. Overall, the humpback whale, minke whale, and North Atlantic right whale bands recorded higher noise levels than the fin whale band. (Figure 4.7.1k).

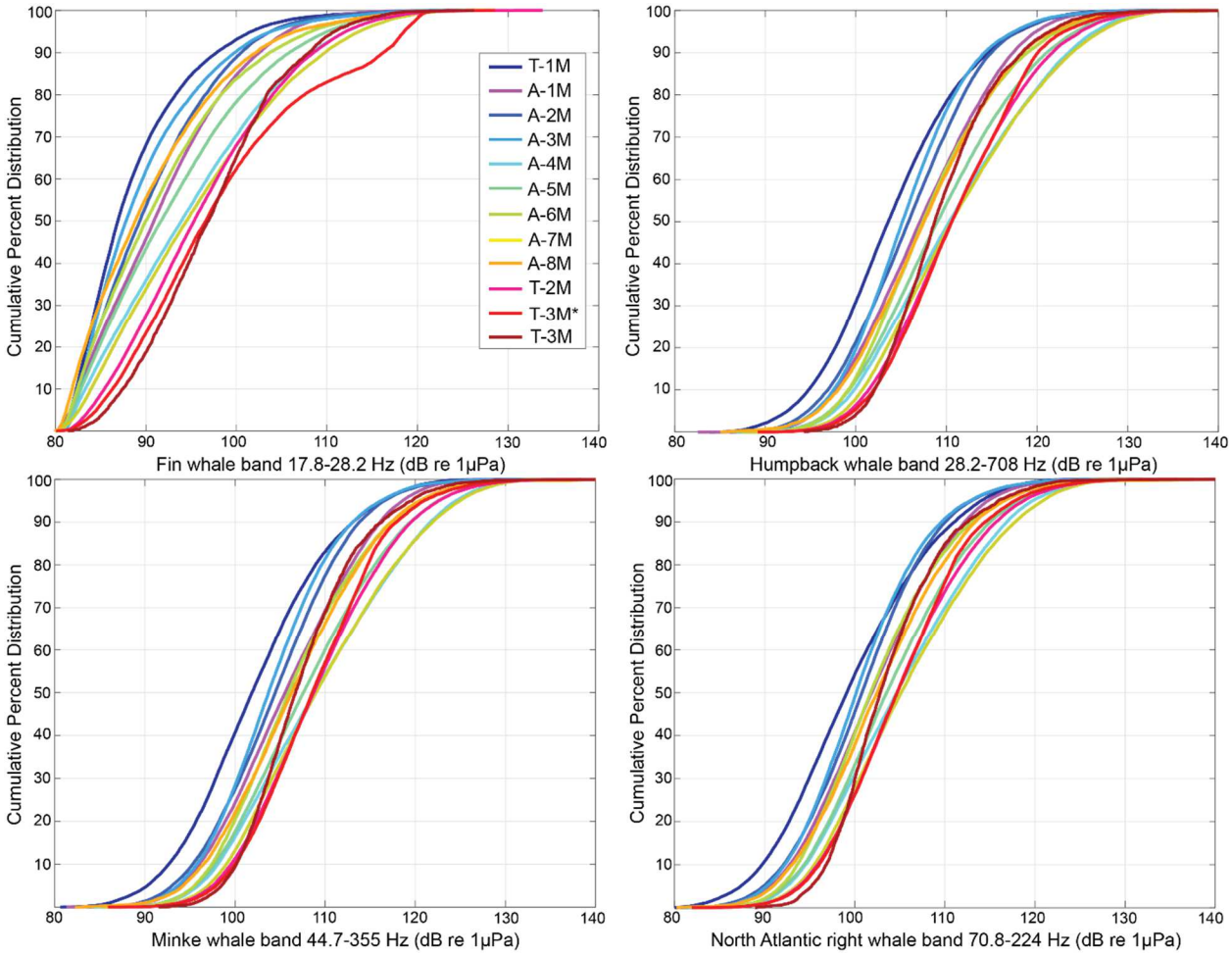

Figure 4.7.1k. Cumulative percent distribution plots in whale bands for all marine autonomous recording unit (MARU) survey sites
Each colored line represents a specific recording site.

The percentage of hours that each survey site exceeded 120 dB was plotted to represent chronic noise conditions at each site. Figure 4.7.1l illustrates that site A4-M and A-7M exceeded hourly noise levels of 120 dB for all species bands except the fin band, and the two sites exceeded 120 dB more than other site locations. The humpback whale species band encountered the highest percentage of time (18%) in which hourly noise levels exceeded 120 dB. In the full band, site A-4M and site A-7M exceeded 120 dB approximately 18-20% of hours recorded during the 3-year survey. Site T-3*M exceeded 120 dB in the fin whale band < 2% of hours recorded, and likely reflects the elevated low frequency noise that occurred between December 2015 and March 2016.

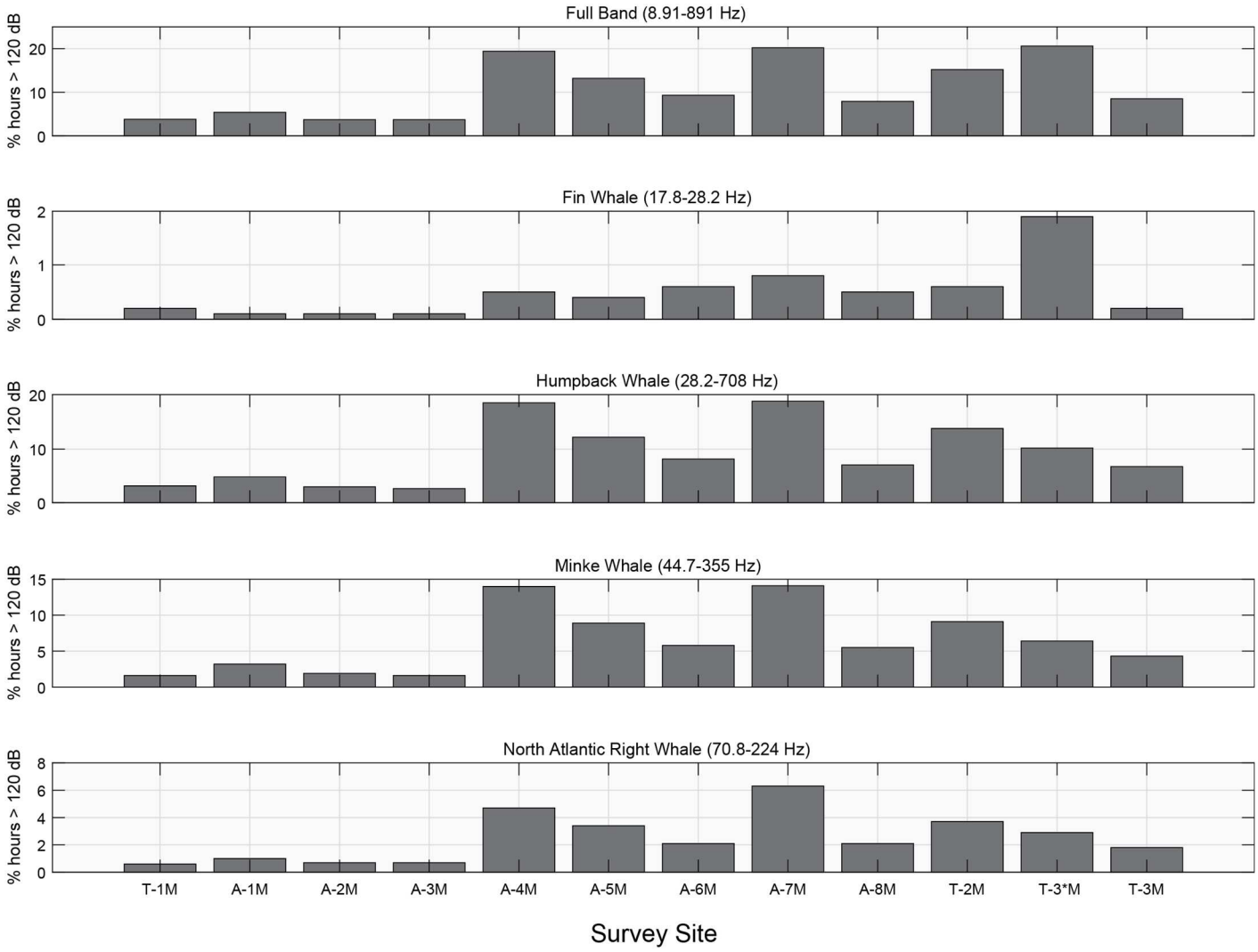

Figure 4.7.1l. Percent hours in which noise levels exceeded 120 dB for each survey site
Each plot represents noise in a specific frequency band. These values represent the entire survey period. Note the differences in y-axis scale between plots.

Figure 4.7.1m represents the percentage of time (10 s time bins per day) sound levels exceeded Marine Mammal Protection Act (MMPA) exposure thresholds for continuous noise sources. All of the surveyed sites had noise levels exceeding the regulatory threshold < 20% of the time during the 3-year survey. Based on the density of colored bars, site A-4M and site A-7M also had the greatest percentage of 10 s averages exceeding 120 dB. The noise event occurring at multiple survey sites during September 2015 that was visible in the spectrograms is also apparent in Figure 4.7.1m. Between December 2015 and March 2016 at site T-3M*, noise levels across the full band exceeded 120 dB nearly 100% of the time, due to an unidentified anthropogenic sound source.

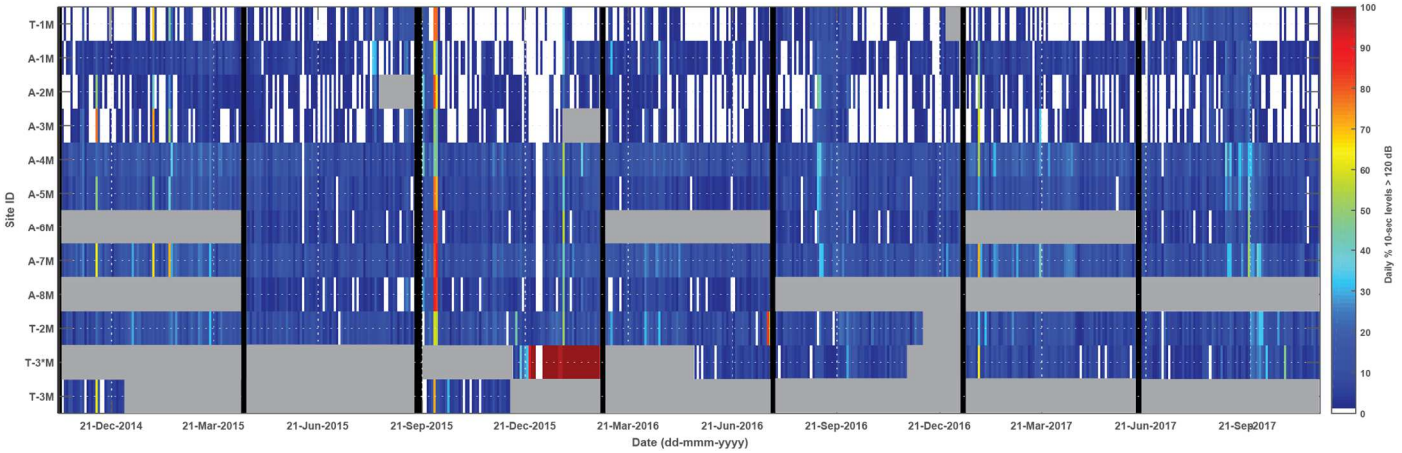

Figure 4.7.1m. Percent 10 s averages per day in which noise levels ≥ 120 dB for each marine autonomous recording unit (MARU) survey site
Each bar represents 1 day of time throughout the 3-year survey period in the full frequency band (10 – 800 Hz 1/3rd octave center frequency). The color scale represents the percentage of 10 s averages within the day noise levels exceeded 120 dB. The white bars represent days in which 10 s average noise levels did not exceed 120 dB. They gray boxes indicate time periods where no data were collected or analyzed. The black lines delineate the seven deployment periods of the 3-year survey period.

4.7.2 Dolphin Whistle Characteristics in Relation to Ambient Noise Levels

In total, 200 high-quality whistles from 16 encounters were used in the analysis. Whistles occurred in the frequency range 2.93 – 23.83 kHz with durations of 0.07 – 1.17 s (Table 4.7.2a; Figure 4.7.2a). Ambient broadband noise associated with these whistles was 108.1 – 134.2 dB re 1 µPa and had a significant effect on whistle characteristics (MANOVA: $F = 2.7$, $DF = 12$, $p < 0.01$). High levels of collinearity between TOLs were found when assessed using variance inflation factors (VIFs). Therefore, all TOLs with VIFs > 3 were removed. The bands centered on 40 Hz, 500 Hz, 2500 Hz, 10000 Hz, and 20000 Hz remained, and GEEs were fit incorporating these TOLs as explanatory variables. Increased noise in the 2.5 kHz TOL significantly affected the greatest number of characteristics, including reducing whistle length, delta frequency, and the number of steps while increasing the start and minimum frequency (Table 4.7.2b; Figure 4.7.2b). A significant reduction in the number of inflections and saddles occurred during increased ambient noise in the 20 kHz TOL. Increased noise in the 40 Hz, 400 Hz, and 10 kHz TOLs also had significant effects on dolphin whistle characteristics (Table 4.7.2b). Over the entire deployment period, relatively high ambient noise levels were mainly caused by vessel noise and were above 120 dB re 1 µPa 11% of the time (Figures 4.7.2c – d).

Table 4.7.2a A summary of the mean, minimum, and maximum values for whistle characteristics.

Whistle Characteristic	Mean	Minimum	Maximum
Length	0.40 s	0.07 s	1.17 s
Minimum frequency	6792 Hz	2929 Hz	18531 Hz
Maximum frequency	10075 Hz	5081 Hz	23826 Hz
Delta frequency	3282.3 Hz	310.5 Hz	15573.8 Hz
Start frequency	7808 Hz	3003 Hz	19478 Hz
End frequency	8958 Hz	2929 Hz	19074 Hz

Table 4.7.2b Statistically significant results from the generalized estimating equation (GEE) models. TOL refers to third octave band levels.

Frequency Band	Response Variable	Estimate	Standard Error	Wald	Pr (>|W|)
Broadband	Minimum frequency	94.80	20.10	22.30	< 0.01
	Maximum frequency	56.40	24.50	5.28	0.02
	Start frequency	91.50	24.00	14.54	< 0.01
40 Hz TOL	Extrema	-0.08	0.020	15.20	< 0.01
400 Hz TOL	Delta frequency	43.00	14.10	9.37	< 0.01
	Steps	0.07	0.02	8.14	< 0.01
	Saddles	-0.02	0.01	12.11	< 0.01
2.5 kHz TOL	Length	-0.005	0.001	14.14	< 0.01
	Minimum frequency	86.52	22.16	15.25	< 0.01
	Delta frequency	-67.20	24.10	7.75	< 0.01
	Start frequency	61.60	22.80	7.31	< 0.01
	Harmonics	-0.007	0.003	5.35	0.02
	Steps	-0.04	0.02	6.69	0.01
	Saddles	0.03	0.01	9.29	< 0.01
10 kHz TOL	Saddles	0.09	0.02	20.97	< 0.01
20 kHz TOL	Inflections	-0.10	0.05	4.32	0.04
	Saddles	-0.05	0.02	8.27	< 0.01

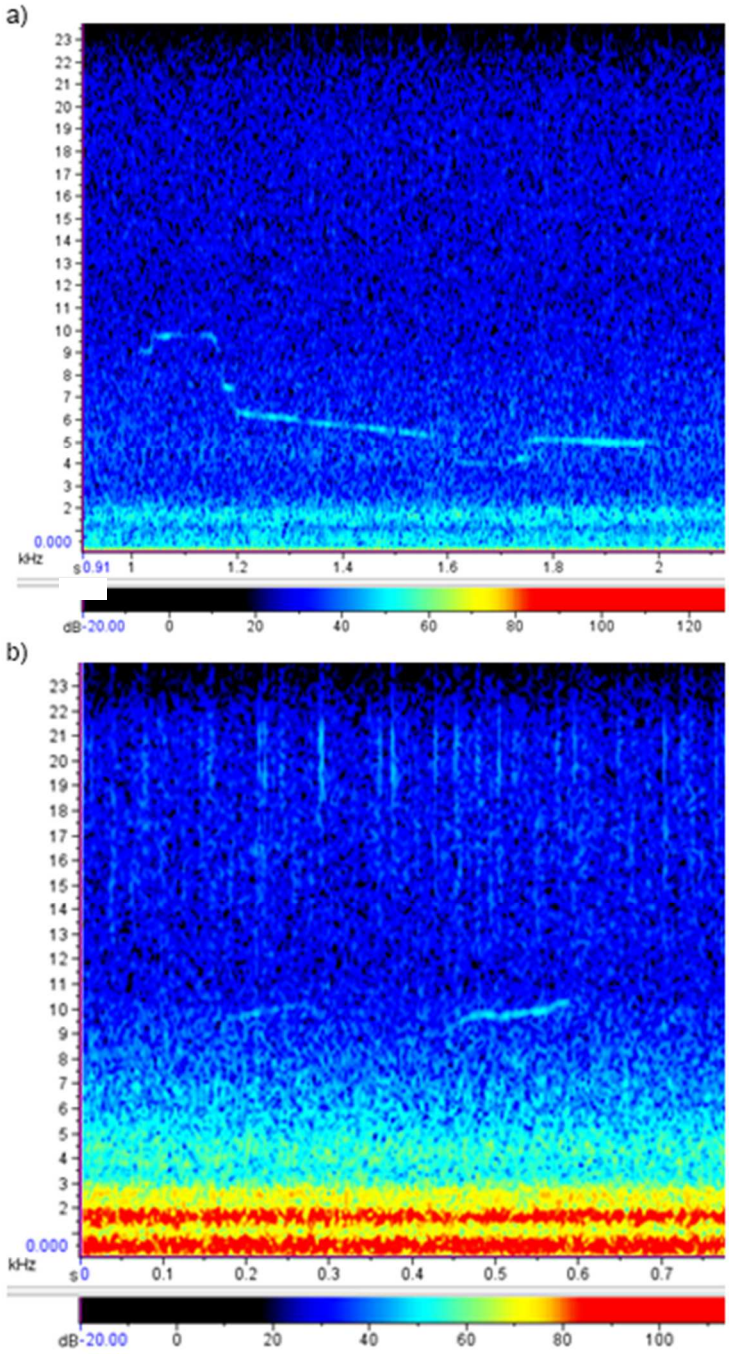

Figure 4.7.2a. Spectrograms of example whistles
Whistles during a) relatively low ambient noise (64.4 dB re 1 µPa^2/Hz) on 14 September 2016 and b) relatively high ambient noise (89.8 dB re 1 µPa^2/Hz) on 7 September 2016.

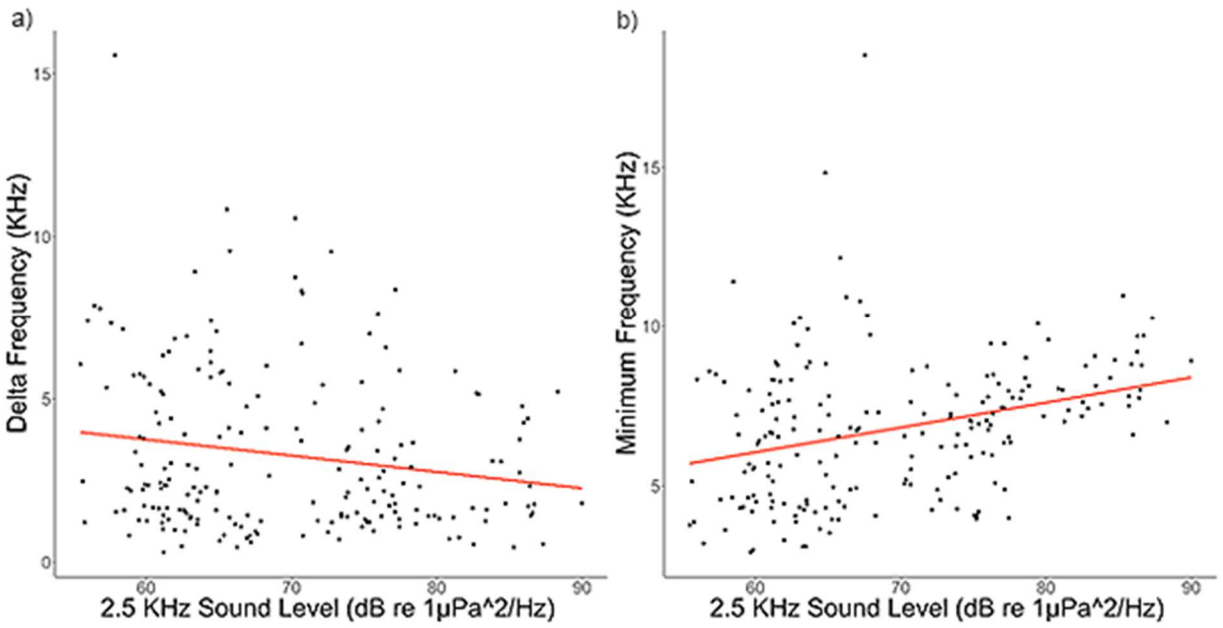

Figure 4.7.2b. Third octave level sound level variables
Effect of 2.5 kHz TOL on a) delta frequency and b) minimum frequency of dolphin whistles with linear regression lines.

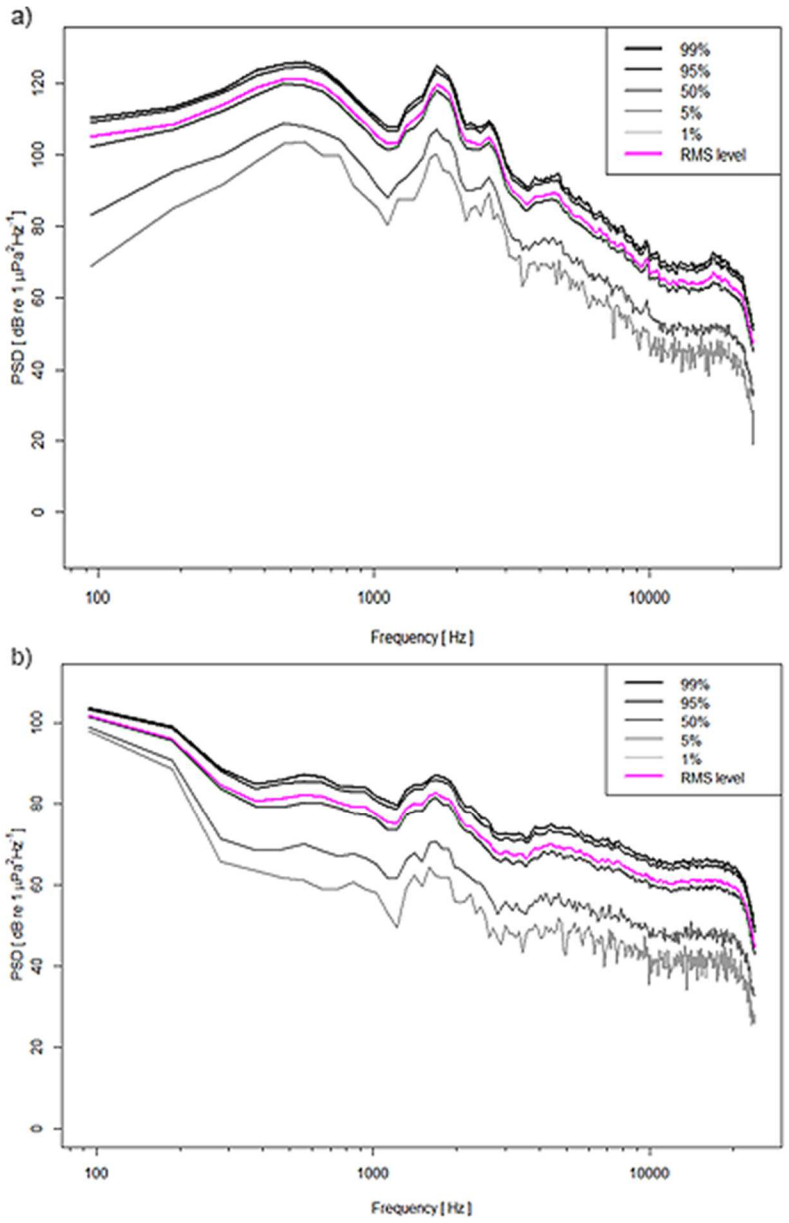

Figure 4.7.2c. Power spectral density plots
Power spectral density of the a) loudest (7 September 2016) and b) quietest (14 September 2016) ambient noise levels contemporaneous with selected high quality whistles with the percentiles and root-mean-square (RMS) sound pressure levels shown.

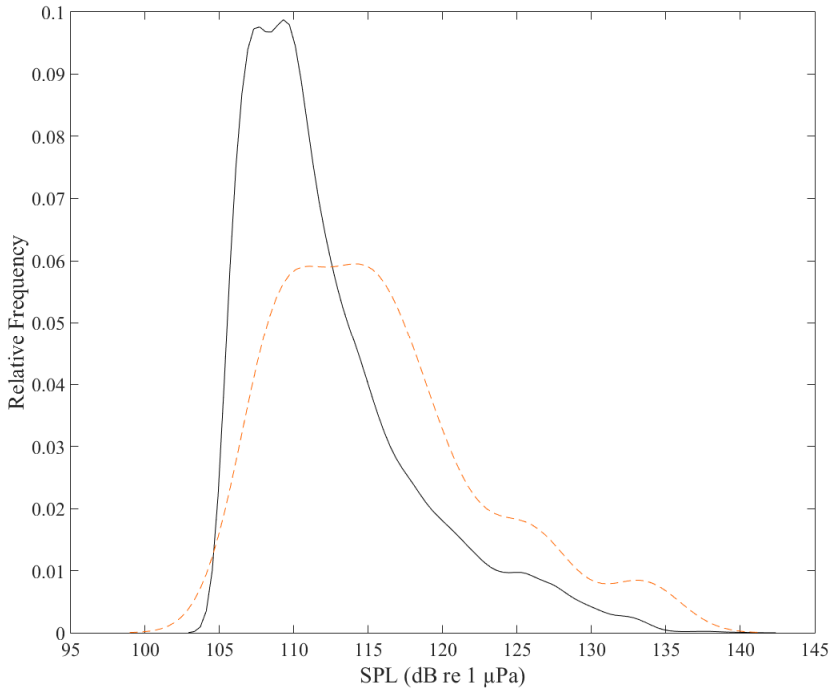

Figure 4.7.2d. Ambient noise levels during deployment
Ambient noise levels during the entire deployment period July-September 2016 (black line) and contemporaneous with selected high-quality whistles (dotted red line).

5 Discussion

5.1 Spatial and Temporal Use of Vocalizing Marine Mammals

5.1.1 Baleen Whales

Our 3-year acoustic survey is the first to systematically describe the seasonal acoustic occurrence and distribution patterns of fin whales, humpback whales, minke whales, and North Atlantic right whales in the coastal waters of Maryland, USA. Given the dearth of information regarding baleen whale ecology in the mid-Atlantic region, our study provides an important baseline understanding of the distribution and movements of baleen whales off the coast of Maryland, particularly in the context of ongoing wind energy development.

In our acoustic survey, fin whales were the most frequently detected baleen whale species, with peak occurrence during autumn and winter months inshore, offshore, and within the Maryland WEA. Fin whales acoustically occurred during all seasons within and offshore of the WEA; however, they occurred less frequently during the summer months. Our findings are consistent with previous studies suggesting a persistent occurrence of fin whales in the Western North Atlantic, north of Cape Hatteras (Webster et al. 1995; Nieukirk et al. 2004; Morano, Salisbury, et al. 2012; Roberts et al. 2016; Hayes et al. 2017). While fin whale detections significantly varied seasonally with peak presence during autumn and winter, we did not observe statistically significant variations in inter-annual occurrence. This suggests that how fin whales are using this particular area (migration, feeding, etc.) appears to be relatively stable across years

and less susceptible to influences of environmental variability than other species. Fin whales were detected at all survey sites inshore, offshore, and within the WEA, but had the greatest relative acoustic occurrence offshore of the WEA. This is consistent with previous studies suggesting fin whales are more common in deep water habitats (Clark and Gagnon 2002; Hayes et al. 2017). Since fin whales are so broadly distributed, and since the propagation distances of fin whale song under low ambient noise conditions and in deep water habitats can be extensive (Payne and Webb 1971; Širović et al. 2007), it is possible some of our detected fin whales were well offshore of our recording sites rather than within the WEA. However, fin whales likely occurred within the WEA as well, since fin whale pulses were detected at our inshore survey site during high (95th percentile) noise conditions when the estimated detection range was limited to a 40 km radius, and would exclude detection of fin whales off of the continental shelf. Since fin whale presence was not constant across seasons between inshore, offshore, and WEA survey sites, fin whales likely have seasonal movements occurring inshore/offshore of the survey area. Given our survey design, it is unclear if there are any seasonal movements of fin whales moving north/south of our study area. Although our findings are consistent with previous studies, it is important to note our findings exclusively describe the seasonal distribution and movement patterns of male whales, since only male singers produce 20 Hz pulses (Croll et al. 2002). Our results therefore should be considered a minimum estimate of fin whale seasonal presence within and surrounding the Maryland WEA; future passive acoustic or other survey efforts could be designed to elucidate fin whale ecology in this area.

Based on the GAM model results, acoustic occurrence of fin whales was most strongly related to sea surface temperature (SST) at site A-5M. This suggests SST is correlated with fin whale occurrence off the coast of Maryland. The smoothing curve suggests fin whales are more likely to occur in the survey area during periods of low water temperatures, with peak occurrence at approximately ≤ 10°C. This suggests fin whale presence may predictably be lower during the summer months along the coast of Maryland. Given the moderate level of deviance explained in our model (23.5%), SST may not be a strong predictor of fin whale acoustic occurrence. Including other environmental variables could potentially improve our model.

Humpback whale occurrence was significantly higher during non-summer months, with bimodal peaks of acoustic presence during late autumn (November, December) and early spring (April). Our findings are consistent with previous acoustic surveys, stranding records, and visual sightings within the coastal mid-Atlantic region (Webster et al. 1995; Barco et al. 2002; Hodge 2011) as well as humpback whale singer detections further offshore (Clark and Gagnon 2002). Humpback whales showed very little variation in seasonal patterns between years, and were detected most frequently within and offshore of the WEA. Given that survey sites within the WEA are approximately 20 km away from the closest offshore survey site (T-2M), it is plausible that detections found at survey sites in the WEA reflect whale occurrence within the WEA during median (50th percentile) and noisy (95th percentile) conditions. Peaks in humpback presence occurred consistently following North Atlantic right whale peak acoustic occurrence, suggesting a staggered timing of occurrence within the survey area. Humpback whales also showed a diel pattern at site T-2M, with peak detections occurring during late night hours (0:00 – 1:00 UTC and 4:00 – 6:00 UTC, or 20:00 - 21:00 EST and 00:00 – 02:00 EST); it is unclear if this diel pattern reflects a change in the number of vocalizing whales, a change in individual calling rates, or both. Given the timing of their annual migration (summarized in Hayes et al. 2017), it is plausible our study is capturing humpback whale movements along their migratory path between winter calving grounds in the West Indies and summer feeding grounds in the North Atlantic. However, since humpback whales were also detected during winter months, we are likely recording some individuals that remain in the mid-Atlantic and North Atlantic regions, as only a portion of the population make the annual migration (Clapham et al. 1993; Swingle et al. 1993). This is consistent with previous acoustic studies in North Atlantic feeding grounds (Vu et al. 2012; Murray et al. 2014). Similar to fin whales, humpback whale

song (and song fragments) are only produced by reproductive males, and our results therefore do not represent the acoustic occurrence of the entire demographic population. However, humpback song has been documented to persist outside of the winter breeding season (Vu et al. 2012), making song a reliable acoustic indicator of humpback whale occurrence.

Based on GAM model results, SST was also correlated with humpback whale acoustic occurrence at survey sites A-5M and T-2M. The smoothing curves suggest humpback whales are more likely to occur at both survey areas during periods of low water temperatures, with peak occurrence at 10°C. This is warmer than the temperature associated with peak North Atlantic right whale occurrence (≤ 5°C), and may correlate with the staggered timing of peak seasonal presence observed between these two species. Humpback whale acoustic presence was also associated with Chl-a concentration at site T-2M; the smoothing curve shows a positive relationship between humpback whale occurrence and Chl-a concentration. Chl-a concentration reflects primary productivity, and is considered a proxy for prey abundance (e.g. Wingfield et al. 2017), as high primary productivity often attracts prey. Although there is high primary productivity off Maryland between March and May (O'Reilly and Zetlin 1998; Xu et al. 2011; Wingfield et al. 2017) when humpback whale occurrence is at its peak, it is unclear if humpback whales are either traveling through productive Maryland waters on their way to northern feeding grounds, or possibly using the coastal waters off Maryland as a mid-Atlantic feeding area (Hayes et al. 2017). The percent deviance explained for our models at site A-5M and T-2M were moderate (31.6% and 36.1%, respectively) and therefore may only have moderate predictive ability; the inclusion of other environmental variables could potentially improve our models.

Minke whales were the least detected baleen whale species in our study, occurring sporadically during autumn, winter, and spring months in all three spatial regions of the survey area. No inter-annual variability was observed for minke whale seasonal occurrence, although it is unclear if this is due to low sample size. Given the short propagation distances estimated for minke whale pulse trains in our survey area (10.3 km during median noise conditions), our data suggest minke whales were likely present in or near the surveyed sites where they were detected. Spring detections were likely individuals traveling to their northern summer feeding grounds (Risch et al. 2014). Surprisingly, we acoustically detected minke whales during the winter when they are predicted to be in southern wintering grounds (Risch et al. 2014). It is unclear if our data indicate a rare winter occurrence or an unknown presence of non-migratory minke whales at this time of year. It is possible our 25% subsampled analysis may be underestimating the spatial and seasonal acoustic occurrence of minke whales within and surrounding the Maryland WEA (Thomisch et al. 2015). However, given their hypothesized migratory distribution along and east of the shelf break between northern feeding grounds and southern wintering grounds (Risch et al. 2014), we expect minke whales to rarely occur within our mid-Atlantic survey area. It is also unclear if all sexes and age classes produce minke whale pulse trains, or if it is only produced by a limited demographic (e.g. reproductive males). Ultimately, our findings should be considered a minimum presence of minke whales in the coastal waters of Maryland. Previous studies have elucidated minke whale distribution patterns in the Northeast, Southeast, and farther offshore at the mid-Atlantic ridge (Risch et al. 2013; Risch et al. 2014); however, these studies did not survey a large portion of the mid-Atlantic region between Onslow Bay and New York. To our knowledge, our survey is the first acoustic study to fill in the mid-Atlantic data gap for documenting minke whale occurrence.

North Atlantic right whales were detected during all seasons within and surrounding the Maryland WEA. Our finding is similar to other studies of North Atlantic right whale occurrence in areas typically viewed as their migration corridor (Morano, Rice, et al. 2012; Mussoline et al. 2012; Hodge et al. 2015; Kraus et al. 2016; Salisbury et al. 2016). While North Atlantic right whale up-calls were detected in a majority of the months sampled during this survey, they showed a distinct and significant seasonal pattern of acoustic presence with no significant inter-annual variability. North Atlantic right

whales occurred at moderate levels (21.4 – 57.7% monthly presence) during late autumn, and peaked during the winter months (43.8 – 93.9% monthly presence). These seasonal trends parallel previous studies describing North Atlantic right whale seasonal migratory patterns (Winn et al. 1986; Kenney et al. 2001). Up-calls were also detected at low levels of presence during the summer months, when whales are predicted to be in their northern feeding grounds, similar to other recent acoustic studies in the mid-Atlantic region (Hodge et al. 2015; Salisbury et al. 2016). North Atlantic right whales were most frequently detected within and offshore of the WEA; given our estimated detection ranges during varying noise conditions (2.9 – 80.7 km), our data suggest North Atlantic right whales are likely occurring within our survey areas during median (50^{th} percentile) and high (95^{th} percentile) noise conditions. North Atlantic right whales also showed a diel pattern at site A-5M, with peak detections occurring during late night hours (0:00 UTC and 23:00 UTC, or 20:00 EST and 19:00 EST); it is unclear if this diel pattern reflects a change in the number of vocalizing whales, a change in individual calling rates, or both. Given our findings, we are likely detecting migrating North Atlantic right whales during the autumn and winter, when they are traveling between southern winter calving grounds or towards northern summer feeding grounds. However, the year-round presence of North Atlantic right whales in Maryland corroborates the recent (since 2010) shift in North Atlantic right whale distribution, with increased presence in the mid-Atlantic region (Hodge et al. 2015; Salisbury et al. 2016; Davis et al. 2017). Our data, in addition to previous mid-Atlantic studies, suggests this region may become an increasingly important non-migratory habitat for North Atlantic right whales.

Based on the GAM model results, acoustic occurrence of North Atlantic right whales was most strongly related to sea surface temperature (SST) at all three of our subsampled sites (sites A-5M, T-1M, T-2M). These results suggest SST is correlated with North Atlantic right whale occurrence off the coast of Maryland. The smoothing curves suggest North Atlantic right whales are more likely to occur in the survey area during periods of low temperatures, with peak occurrence at approximately $\leq 5\,^{\circ}C$. This is colder than the temperature associated with peak humpback whale occurrence ($10\,^{\circ}C$), and may correlate with the consistent staggered timing of peak seasonal presence observed between these two species. Previous studies have found SST to be a reliable predictor of North Atlantic right whale distribution, showing a correlation between SST and whale spatial occurrence (Keller et al. 2006; Keller et al. 2012). Chl-a concentration was also significantly associated with North Atlantic right whale occurrence at site A-5M, but not in the other subsampled sites. The smoothing curve that described the relationship between North Atlantic right whale occurrence and Chl-a concentration showed a non-linear relationship; while Chl-a concentration was found to be significant in our model, the relationship between Chl-a concentration and North Atlantic right whale acoustic occurrence is unclear. Given the moderate level of deviance explained in each of our models (22.4 – 32.7%), SST and Chl-a are not likely to be strong predictors of North Atlantic right whale occurrence. The inclusion of other environmental variables may potentially improve our models.

Similar to our findings from the relative spatial occurrence analysis, acoustic localization analysis showed North Atlantic right whales most frequently occurred within and offshore of the Maryland WEA. Our empirical test of the location algorithm's accuracy and precision suggests our discernment of acceptable location estimates yielded reliable results, with location accuracy of approximately 300 meters and precision of approximately 100 meters. The relative distribution of first arrival up-calls also confirmed North Atlantic right whale occurrence within and offshore of the WEA, with the greatest percentage of occurrence at survey sites along the eastern edge of the WEA. Most locatable calls occurred during the January through March timeframe; this likely reflects the North Atlantic right whale peak occurrence we observed during the winter months. It is unclear if the greater number of seasonal detections indicates a greater number of North Atlantic right whales in the area, an increase in calling rates, or both. While we did find eight potentially locatable up-calls during the summer, we were unable to reliably locate North Atlantic right whales during this season. However, most of these up-calls were

detected offshore of the WEA, suggesting North Atlantic right whales may be distributed further offshore during the summer months. We also observed a seasonal change in distribution of up-call locations, with aggregates of locations occurring both offshore and along the eastern edge of the WEA during the winter, and aggregates of locations occurring both offshore and within the central-western region of the WEA during the autumn. This could suggest North Atlantic right whales are distributed differently during their northbound and southbound movements during their annual migration.

A total of five putative North Atlantic right whale up-call tracks were identified from the localized data, each occurring during the month of December. Each track varied in heading, speed, and distance covered. The majority of the putative call tracks occurred within the WEA, and showed overall movement in both the northeast and southwest directions; one track was identified offshore of the WEA, heading in an overall southeast direction. The movement patterns of these tracks, however, were not all unidirectional. Since the movement patterns are so variable, it is difficult to infer what behaviors the whales may be engaged in through passive acoustic data alone; observational data (e.g. visual or aerial surveys) in conjunction with passive acoustic data could provide a more comprehensive understanding North Atlantic right whale behavior in our survey area. Putative call tracks covered distance of 0.5 – 2.58 km, and average speeds of most of these tracks ranged from 2 – 6.38 km/h, which is well within the documented swim speed of North Atlantic right whales (Mate et al. 1997). One track, however, showed an average swim speed of 9 km/h; while this is a fast estimate, Mate et al. (1997) noted the majority of tagged whales from their study traveled less than 10 km/h between locations. These results corroborate previous studies suggesting small-scale North Atlantic right whale movement patterns can be variable within migration areas (Mate et al. 1997). Our findings have several limitations; it is important to note that the identified putative call tracks have not been verified by observational data, so it is unclear if the located up-calls in these tracks were produced by an individual whale or multiple whales. Additionally, while we calculated swim speeds using documented vocalization rates (0 – 10 per hour) for North Atlantic right whale aggregates in the northern feeding grounds (Matthews et al. 2001), there is no literature on North Atlantic right whale up-call rates, and no literature on migrating North Atlantic right whale call rates in general. Our results, therefore, should be interpreted cautiously. Future studies determining the mean up-call rates for migratory North Atlantic right whales would be beneficial for estimating small-scale movement patterns using passive acoustic data.

5.1.2 Odontocetes

5.1.2.1 Detectability

We detected odontocetes using a click detector device, the C-POD, which provided a highly time-efficient method for analyzing odontocete detections. Our findings comparing these detections with those from an independent acoustic recorder showed that the "High" and "Moderate" C-POD filtered results were conservative but reliable indicators of dolphin occurrence, consistent with previous studies on T-PODs (Philpott et al. 2007; Bailey et al. 2010) and C-PODs (Roberts and Read 2015) that had been conducted in more nearshore and estuarine waters. The C-PODs reliably and consistently detected dolphin click trains across deployments at different locations and seasons under different ambient noise conditions with extremely low rates of false positive detections. The C-POD was not as accurate at detecting dolphin absence at the hourly scale. Therefore, periods with no detections should be considered with caution as equating to absence.

Data from T-PODs and C-PODs have been used to understand odontocete ecology as well as responses to anthropogenic activities, such as pile driving of offshore wind energy facilities, marine seismic surveys, and deterrent devices used by fisheries (e.g. Leeney et al. 2007; Bailey et al. 2010; Dähne et al. 2013; Thompson et al. 2013). While these studies rely on the device's detection of echolocation click trains to indicate odontocete presence, the metric used to describe occurrence has

varied across studies. These metrics include detections per minute, hour, or day (Verfuß et al. 2007; Thompson et al. 2010; Elliott et al. 2011). Detections have also been described by the number of clicks, encounters (defined as detections separated by a threshold duration), and waiting times (the duration between encounters or between a chosen event and the subsequent encounter) (Hardy et al. 2012; Teilmann and Carstensen 2012; Thompson et al. 2013). Given the conservative nature of the C-POD detection algorithm, shorter time bins could result in underestimation of presence. Our analysis indicates that at the hourly scale or longer, the pattern of detections would be representative of the animals' relative occurrence. At these time scales, the potential for underestimation is reduced, and presence trends, including diel patterns, can be reliably determined.

Currently, a limitation in areas with multiple dolphin species is that they cannot be distinguished using the C-POD. Bottlenose and common dolphins are particularly difficult to distinguish acoustically, even from their whistles (Oswald et al. 2007; Azzolin et al. 2014). Techniques are now being developed that incorporate multiple call types to improve acoustic classification of dolphin species (Rankin et al. 2017). This would aid with dolphin species classification, although currently the approach requires a high sampling rate, which would greatly reduce the deployment time or require increased duty cycling for a moored acoustic recorder. Species classification can also be aided, as in our case, by combining acoustic detections with other sources of information, such as visual boat-based or aerial surveys.

5.1.2.2 Dolphins

Bottlenose dolphins were most common inshore and within the WEA during the summer with almost daily detections. The frequent occurrence of bottlenose dolphins coastally is consistent with previous visual sightings data (Barco et al. 2015; Williams et al. 2015) and our understanding of the movements of the Western North Atlantic Northern Coastal Migratory Stock (Hayes et al. 2018), although this extended further offshore into the WEA than expected. The seasonal pattern of detections was very similar across years inshore of the WEA. At the site within the WEA, bottlenose dolphin occurrence was significantly lower in Year 1 than in Years 2 and 3 of the study, which corresponds with the low number of dolphin sightings within the WEA during the aerial surveys in 2014-2015 (Barco et al. 2015). Our sites offshore of the WEA, T-2 and T-3C, are farther from shore than many aerial and boat-based coastal surveys whilst shallower than the NOAA Atlantic Marine Assessment Program for Protected Species (AMAPPS) surveys that occur along the shelf at the 100m isobath and deeper. At these sites, dolphins occurred year-round with detections peaking in the December to April timeframe when they were most likely common dolphins – although bottlenose and other dolphin species may also occur (Barco et al. 2015).

Bottlenose and common dolphins exhibited similar diel patterns that may be related to the availability of prey. There are few studies that have linked area-restricted search behavior with foraging success in free-ranging marine species (Bailey and Thompson 2006; Thums et al. 2011). We examined the fine-scale time series of dolphin foraging behavior to determine if foraging activity initiated and led to the persistence of intensive search effort within a localized area (considered as the detection range around each of our C-PODs). Generally, for both bottlenose and common dolphins, foraging activity did persist with the occurrence of foraging behavior being more likely when it had also occurred in the preceding minutes. This supports the hypothesis that the occurrence of feeding increases the likelihood of further feeding indicating there is a higher probability of encountering other prey items nearby. Similarly, for both dolphin species, longer periods spent within the detection range of each of our C-POD sites, indicating more intensive ARS behavior, were also more likely to occur when there was higher foraging activity during the beginning of the encounter. This suggests that finding prey had led to the initiation of ARS behavior and the continuation of more intensive searching for prey within the localized area. This provides support for our second hypothesis that dolphins remain longer in a patch when feeding occurs at the start of an encounter and is consistent with the predictions of ARS behavior.

The benefit of ARS behavior to predators is that it can lead to a greater effective detection distance than their direct detection distance (Tinbergen et al. 1967). Bottlenose dolphins have an estimated maximum echolocation detection range of 93 – 173 m for fish prey depending on the ambient sound levels (Au et al. 2007). The size of ARS areas that have been identified for bottlenose dolphins were larger than this distance (Bailey and Thompson 2006) and this has also been found in other species (Sims and Quayle 1998; Papastamatiou et al. 2012), which may reflect the larger effective detection distance resulting from the ARS behavior.

The foraging patterns observed were relatively consistent across species and sites providing support for our third hypothesis and indicating broader use of the ARS strategy. Foraging in an ARS pattern is expected to occur when prey are patchily distributed (Kareiva and Odell 1987; Hill et al. 2003). Common dolphins primarily prey on pelagic schooling fish and cephalopods (Young and Cockcroft 1994; Pusineri et al. 2007; Meynier et al. 2008). Schooling fish would occur in aggregations that could be responsible for the ARS behavior. Bottlenose dolphins feed on a wide variety of species, including fish, cephalopods and crustaceans. Significant seasonal variation in diet composition has been observed, but not in prey size (Gannon and Waples 2004). Although bottlenose dolphins exhibited longer encounter durations typical of ARS behavior in the summer and fall periods (May – September), the significantly shorter encounter durations in the winter and spring periods (October – April) may have resulted from prey being distributed in lower densities. Intensive searching has only been triggered in captive juvenile plaice (*Pleuronectes platessa*) by aggregations of prey at high local densities and not by isolated prey that were more widely dispersed (Hill et al. 2002). The bottlenose dolphins at sites T-1C and A-5C are also most likely to be from the Western North Atlantic Northern Migratory Coastal Stock whereas those at sites T-2C and T-3C are from the Western North Atlantic Offshore Stock. Relatively little is known about the movements and diet of the Offshore Stock and there was relatively little difference in the behavior patterns observed in this study. It should be noted that our detections of foraging activity are representative of the group behavior since we could not localize calls to individual dolphins, which meant we could not measure foraging success per capita.

Estimating abundance from call rates is challenging because they often do not directly correlate as dolphins may listen to the calls of others, particularly in larger groups (Jones and Sayigh 2002). The use of signature whistles to identify individual dolphins provides an alternative approach to estimate abundance from passive acoustic monitoring. We estimated that at least 700 dolphins passed through our study area (within and inshore of the WEA) between July 2016 and September 2017 based on the signature whistles identified. This serves as a minimum estimate of the number of dolphins occurring in the study area, although it is likely that this underestimates the total number of dolphins visiting this location. The detection of signature whistles is limited by the hydrophone's detection range, the amount of data analyzed, and the requirement that dolphins emit signature whistles when passing through our site. While it is unlikely that the entire Northern Migratory Coastal Stock of bottlenose dolphins (population estimate 6,639) migrates through our area, our study suggests the number of dolphins traveling through our detection area is at least 700 dolphins.

When analyzing dolphin occurrence within individual deployment periods, a much smaller number of dolphins were found at A-5C during the summer of 2017 than the summer of 2016. Our results even suggested a smaller number of dolphins in our study area during the summer of 2017 than the winter of 2017, which is surprising given that dolphin click trains were detected more frequently during the summer, and there was no significant difference in frequency of occurrence based on the C-POD detections. The reason for this is unclear and would benefit from further study as this indicates that rates of occurrence may not necessarily be related to abundance.

Analysis of recurrence of dolphins within our detection range showed that the majority (71%) of all recurrences within the Maryland WEA at A-5C happened during the winter 2017 deployment. This

finding suggests that the bottlenose dolphins appearing in this area in the winter may be returning more frequently and exhibiting higher fine-scale site fidelity than those in the summer. A much greater number of individual dolphins were identified at site T-1C (even accounting for the subsampling at A-5C) and there were more frequent reoccurrences. The Northern Migratory Coastal Stock of bottlenose dolphins are a highly mobile population of bottlenose dolphins that generally occur in shallow waters, and these results may reflect their movement behavior. More dolphins occurred closer inshore at T-1C and returned via this route than in the WEA further offshore at A-5C which may be more on the fringe of their range. The higher number of recurrences at T-1C than at A-5C indicated higher site fidelity inshore than within the Maryland WEA. All recurring bottlenose dolphins were detected within the same deployment. This could indicate that bottlenose dolphins have flexibility in the specific path they take during migration and may not always pass through our 7 km detection range. While our results reflect the mobility of this stock, it is also important to note that the amount of acoustic data analyzed did not include all of our acoustic recorder deployments, and that the whistle detection range of our acoustic recorder was limited to 7 km. Additional analysis of data at this site and data at surrounding sites may reveal more bottlenose dolphin recurrences.

5.1.2.3 Harbor Porpoise

Harbor porpoises were regularly detected offshore of Maryland during the winter and spring, particularly from January to May. This is in contrast to low sighting rates during many boat-based and aerial surveys conducted over many years (Garrison and Barry 2013; Connelly et al. 2015). Our study has shown that harbor porpoise occurrence is greatest during the winter and spring, and during hours of the day with reduced light or darkness. These are periods of time during which conditions for sighting this small species are generally poor, and visual surveys are expected to underestimate harbor porpoise occurrence.

The observed seasonal pattern in harbor porpoise occurrence is consistent with prior information on their general distribution (Gaskin 1977; Kraus et al. 1983; Palka 1995). Harbor porpoises move between their summer habitat in the Bay of Fundy and Gulf of Maine to as far south as North Carolina in the winter (Gaskin 1977; Kraus et al. 1983; Palka 1995). Harbor porpoises in this population have been found to travel a range of distances between productive habitats, where aggregations of prey may occur (Read and Westgate 1997). Our analysis of the surface chlorophyll-a (Chl-a) concentration suggested March to May is a period of high primary productivity offshore of Maryland, which is during the winter-spring phytoplankton bloom (O'Reilly and Zetlin 1998; Xu et al. 2011).

There was a high degree of inter-annual variation in the number of minutes per day that porpoises were detected. The maximum periods of time between the clicks of three free-ranging, tagged harbor porpoises in Danish waters were brief (1.6, 4, and 22 minutes), demonstrating that porpoises click regularly (Linnenschmidt et al. 2013). Because of this regularity in click production, patterns in the C-POD detection rates of clicks were assumed to reflect occurrence of harbor porpoises (Thompson et al. 2013). Inter-annual variability in occurrence is also reflected in the stranding record, as 22 strandings were recorded in 2005, and only two in 2011 and 2012 on the shorelines of Virginia (Swingle et al. 2016). The change in porpoise occurrence between years could be due to a number of biological and oceanographic factors affecting the environment offshore of Maryland and in more northern foraging grounds. For example, favorable conditions in more northern foraging grounds could delay porpoise movement southwards, leading to decreased or delayed occurrence offshore of Maryland. Chl-a concentration at T-2C was greater in 2015 compared to 2016, which is likely to have led to increased prey abundance and in turn, higher porpoise occurrence at this site in 2015. It is unclear what caused the shift in distribution to the inshore site in 2016 and 2017. Further investigation into the environmental conditions in areas beyond our study area would provide insight into which factors affect broader porpoise movement up and down the coastline from year to year.

In addition to seasonal variation in occurrence, a particularly strong diel pattern was observed at the site within the Maryland WEA (A-5C), where porpoises occurred most frequently in the evening to early morning hours. This is consistent with previous studies, in which diel patterns in porpoise echolocation rates were hypothesized to be linked to prey availability (Todd et al. 2009; Schaffeld et al. 2016). As visual surveys are not conducted during these hours because of reduced visibility, it is probable that porpoise occurrence at this site will be underestimated by visual surveys. It is thus recommended that future monitoring of harbor porpoise distribution in this area be conducted using passive acoustic monitoring with moored or towed hydrophones.

The increase in detections during nighttime hours is consistent with patterns observed in harbor porpoise populations around the world (Cox et al. 2001; Carlström 2005; Todd et al. 2009; Schaffeld et al. 2016). The diel pattern in foraging may reflect nighttime diving behavior or prey distribution. Porpoises occurring offshore of Maryland may increase their mean dive depth during nighttime hours, as was seen in the Bay of Fundy (Westgate et al. 1995), and are therefore more likely to have been detected by the bottom-moored C-POD at night. However, there was no diel pattern in dive-depth observed in Japanese waters (Otani et al. 1998). Herring (*Clupea harengus*), one of the main prey species for harbor porpoises in the Northwestern Atlantic, migrate vertically in the water column at night (Shotton and Randall 1982; Scott and Scott 1988). This behavior may make herring easier to prey upon at night, leading to an increase in porpoise foraging. Fine-scale data on prey abundance, for example using sonar-imaging technology (Boswell et al. 2008), could help to improve our understanding of factors driving porpoise occurrence and foraging behavior.

We used environmental variables as proxies for prey abundance because fine-scale data on prey were not available. Chl-a concentration, SST and fraction of the moon illuminated were readily available data sets. Despite being a significant factor influencing the echolocation of some dolphin species (Benoit-Bird et al. 2009), lunar illumination did not significantly affect harbor porpoise echolocation offshore of Maryland (Wingfield et al. 2017). SST significantly affected harbor porpoise occurrence at our sites. This result is consistent with Roberts et al.'s (2016) model, which predicted greater harbor porpoise presence at lower SSTs. Harbor porpoises were expected to be present at colder temperatures given their seasonal distribution pattern. The peak in harbor porpoise detection rate at 5°C at all sites may also relate to the presence of herring, as other studies have found that catches were greatest in waters of 7 – 8°C in winter and 5°C in spring (Reid et al. 1999). Summertime (June to October) concentrations of Chl-a in the mid-Atlantic Bight are typically below 1 mg m^{-3} (Xu et al. 2011), compared to values exceeding 3 mg m^{-3} in coastal areas during the winter-spring bloom, which begins as early as January and continues until March or April (O'Reilly and Zetlin 1998; Xu et al. 2011). It is during this winter-spring bloom that porpoise presence peaked at T-2C and T-3C in Year 1, at Chl-a concentrations of 4.5 to 7.4 mg m^{-3}. These values are particularly high, even for this productive period in the mid-Atlantic coastal waters. Peaks in porpoise occurrence at higher Chl-a concentrations may be linked to prey, as areas of higher primary productivity are likely to have greater numbers of forage fish (Johnston et al. 2005). Roberts et al.'s (2016) final models of summer and winter harbor porpoise density also retained productivity parameters, which had positive effects on porpoise density.

In our findings in Wingfield et al. (2017), all of the acoustic metrics for A-5C, T-2C, and T-3C were significantly correlated with monthly habitat-based predictions of harbor porpoises from sightings data recorded during aerial and boat-based surveys (Roberts et al. 2016). However, the monthly density predictions for T-1C did not correlate well with the acoustic data. Roberts et al. (2016) fit two separate models, one for the winter (November to May) and another for the summer (June to October) data, as it was assumed porpoises switch environmental preferences during different phases of their annual migratory cycle. Although this strategy worked well when modelling baleen whale occurrence, it resulted in a rise in porpoise density at the May to June transition and discontinuity at the October to November

transition, which was most evident at T-1C. The results from this study have been used to help refine and improve the density models. Although it is difficult to determine absolute densities of cetacean species using passive acoustic data (Kyhn et al. 2012; Marques et al. 2013), this type of data can be a useful, independent data source to validate relative patterns and improve habitat-based models.

This study provides insight into the previously poorly understood occurrence of harbor porpoises offshore of Maryland and indicates that it is underestimated when using boat-based and aerial survey methods. The diel pattern in detections can be used to improve estimates of the detection probability for harbor porpoises during line transect surveys. Harbor porpoises occurred frequently offshore of Maryland from January to May. Consistent with our findings on their seasonal occurrence in the southern part of their range, strandings of porpoises after entanglement in fishing nets occurred primarily from January to May along the shores of Maryland, Virginia, and North Carolina (Byrd et al. 2014; Swingle et al. 2016).

5.2 Ambient Noise Levels

5.2.1 Spatial and Temporal Variability of Ambient Noise

To our knowledge, our 3-year acoustic survey is the first to characterize spatial and temporal variability of ambient noise conditions in the coastal waters of Maryland, USA. Overall, our results confirm a high level of variation in noise levels both spatially and temporally. According to the long-term spectrograms and power spectral density plots, elevated noise levels predominately occurred in low frequency (< 200 Hz) bands, suggesting anthropogenic noise is a major contributor to the noise environment (Wenz 1972; Hildebrand 2009). These findings are consistent with previous research assessing noise levels in the northeast and southeast western North Atlantic (Rice, Tielens, et al. 2014). When comparing noise levels spatially, sites along the eastern edge of the WEA (A-4M, A-7M) and offshore of the WEA (T-2M) consistently had the highest sound levels in the survey area, with median noise values ranging between 115.3 – 116.1 dB across the 3-year survey period. A cumulative percent distribution plot confirmed the eastern edge of the WEA and offshore of the WEA are the noisiest regions of the survey area, with sound levels of approximately 110 dB and above 50% of the 3-year study. Given the proximity of these relatively noisy sites to the Delaware to Cape Henlopen Traffic Lanes, shipping noise is likely a dominant contributor to the ambient noise environment. Noise levels also varied seasonally, with elevated noise levels consistently occurring during winter months within and offshore of the WEA. Interestingly, the survey site inshore of the WEA had significantly highest noise levels during the winter. It is plausible the seasonal differences in noise intensity may reflect spatial and temporal changes in vessel activities off coastal Maryland; further research exploring noise sources and their relative contributions to the noise environment is needed to explain these seasonal changes in noise conditions.

The cumulative percent distribution plots in whale frequency bands showed a consistent spatial pattern of noise levels between survey sites, with relatively high noise levels in each whale band at survey sites along the eastern edge of the WEA and offshore of the WEA. These findings corroborate the eastern edge of the WEA and offshore of the WEA are the noisiest surveyed regions. The North Atlantic right whale band cumulative percent distribution plot confirmed the noisiest sites in our survey area reach sound levels of approximately 105 dB and above 50% of the 3-year study. These North Atlantic right whale band sound level measurements offshore of Maryland are comparable to the noisiest regions (NY and NJ) surveyed in a previous study along the western North Atlantic (Rice, Tielens, et al. 2014). The plots also showed the humpback (28.2 – 708 Hz), minke (44.7 – 355 Hz) and North Atlantic right whale (70.8 – 224 Hz) frequency bands recorded higher noise levels than the fin whale (17.8 – 28.2 Hz) band. This is likely due to restricted bandwidth of the fin whale frequency band, which did not capture noise occurring at higher frequencies.

Examining the percentage of time when each survey site exceeded 120 dB illustrates the potential exposure of baleen whale species to elevated noise levels. Our analysis explored noise exposure in two temporal resolutions (percent hours and percent 10 s averages per day) in order to assess both chronic and acute noise conditions that surpassed the take threshold (Southall et al. 2007; National Oceanic and Atmospheric Administration 2018). Sites inshore of the WEA and along the western edge of the WEA had the lowest percentage of hours exceeding 120 dB; conversely, sites along the eastern edge of the WEA exceeded 120 dB approximately 18 – 20% of hours recorded during the 3-year survey. Sites along the eastern edge of the WEA also had the highest overall density of colored bars, suggesting these sites had the greatest percentage of 10 s averages exceeding the take threshold. However, most surveyed sites exceeded 120 dB more than 50% of the sampling period, given the density of colored bars. These results suggest that baleen whales near surveyed sites along the eastern edge of the WEA and offshore of the WEA would be at greatest risk of exposure to both prolonged and acute durations of elevated noise.

Given the baseline ambient noise conditions of our survey area, it is important to assess the potential impacts of introduced noise from wind energy construction activities. Previous studies have shown pile driving sounds can reach a broadband peak to peak sound level of 205 dB re 1 µPa at close range (within 100 meters), and attenuated sounds can extend hundreds of meters from the immediate construction area (Bailey et al. 2010). Increased vessel activity and shipboard surveys would also likely increase ambient noise conditions. Anthropogenic noise is considered a stressor for marine mammal species (Southall et al. 2007; Ellison and Southall 2012), as it could potentially cause acoustic masking of calls, hearing impairment, avoidance behaviors, or physiological or behavioral stress (Madsen et al. 2006; Clark et al. 2007; Weilgart 2007; Rolland et al. 2012; Bailey et al. 2014). Since pile driving sounds overlap in frequency with baleen whale communication and inferred auditory frequency bands, baleen whales would likely be sensitive to low frequency pile driving noise in our survey area (Nowacek et al. 2007; Bailey et al. 2014). However, the type and level of response they may have to low frequency pile driving sounds remains unclear, as this has not largely been explored empirically in baleen whale species (Gordon et al. 2003).

5.2.2 Response of Marine Mammals in Relation to Ambient Noise

Bottlenose dolphins changed their vocalization characteristics during increased ambient noise. Such changes have also been observed in primates, birds, bats and other species to counteract masking effects (Barber et al. 2010), and this is emerging as a widespread response to elevated ambient noise. In our study, we specifically examined the ambient noise level immediately prior to the call and examined contour shape characteristics as well as frequency parameters of the dolphin whistles. The dolphin whistles had a less complex contour shape during increased ambient noise in the 2.5 kHz and 20 kHz TOLs. These changes may serve to simplify the call, thereby reducing the potential loss of information due to masking by ambient noise. Beluga whales (*Delphinapterus leucas*) in the St. Lawrence River similarly produced less frequency modulated calls when background noise became louder due to vessel noise (Lesage et al. 1999). Call duration compression may serve to fit calls into quieter intervals or due to calls being truncated by the onset of noise (Egnor et al. 2007). It is unknown what impact this shortening and simplification of calls may have on the information communicated. Vocal communication is important in dolphin mother-offspring interactions and social bonding (Connor et al. 1998). The frequency modulation pattern of calls carries identity (Janik et al. 2006), and other information, and consequently there could be changes to the level of information communicated if individuals respond to increased ambient noise by simplifying the features of their whistles. The ambient noise environment could also affect vocal learning, as young animals exposed to elevated noise may hear adjusted calls from conspecifics (Janik and Slater 2000).

In addition to modifying the shape, dolphin whistles were also higher in frequency during increased broadband and 2.5 kHz TOL ambient noise immediately prior to the call. Marine mammals

have been recorded increasing the amplitude (Holt et al. 2009; Parks et al. 2011) or altering the frequency parameters (Heiler et al. 2016; Marley et al. 2017) or call rate (Iorio and Clark 2010) of their calls in response to ambient noise. Masking occurs when ambient noise overlaps with the frequency band of the calls (energetic masking), but can also occur when signals cannot be perceptually distinguished from other noise (informational masking) (Clark et al. 2009). Dolphins adjusted their calls when noise levels were elevated at a range of frequencies, including below the frequencies of their whistle calls. Increased low frequency ambient noise may be causing dolphins to change their vocalisation behaviour to avoid or compensate for masking. These changes could be detrimental to conspecific communication and potentially reduce group cohesion as has been found in terrestrial species (Barber et al. 2010).

Although ambient noise may increase as a result of natural processes, such as wind and waves, elevated noise conditions in our study were primarily attributed to vessel noise. The study area is adjacent to the shipping lanes going into and out of Delaware Bay and had ambient noise levels comparable to other coastal areas with frequent vessel traffic (Merchant et al. 2014). If a vessel is located in a different direction than conspecifics, there may be a decrease in masking (spatial release from masking), but the observed changes in the whistle signals indicate that the dolphins simplified their calls to counter the masking effects of vessel noise. Although marine mammals demonstrate vocal plasticity, there may be constraints to their vocal compensatory capabilities and the sustainability of the accommodation over time. Ambient noise levels are likely to rise in the future as vessel traffic increases and offshore wind energy facilities are proposed or subsequently are constructed. Regulations and voluntary incentives to reduce the sound production of vessels – for example, with speed limits or quieter engines – could help to decrease the effects on dolphins and other species sensitive to sound.

6 Conclusions and Recommendations

6.1 Overview of Marine Mammals

We characterized the acoustic occurrence of four baleen whale species within and surrounding the Maryland WEA: fin whale, humpback whale, minke whale, and North Atlantic right whale. Key findings in relation to whale occurrence were:

- Fin whales were detected throughout the study, with peak presence during autumn and winter months.
- While fin whale detections were found at all survey sites, they had the greatest relative acoustic occurrence offshore of the WEA.
- Humpback whales had a significant seasonal occurrence pattern, and were detected predominately during the late winter and early spring months within and offshore of the WEA.
- Peaks in humpback whale occurrence were consistently following North Atlantic right whale peak acoustic occurrence, suggesting a staggered timing of whale occurrence within the survey area.
- Minke whales rarely occurred within the survey area, and were detected sporadically during autumn, winter, and spring months inshore, offshore, and within the WEA.
- North Atlantic right whales were detected during all seasons within and surrounding the WEA, with peak seasonal presence during the late autumn, winter, and early spring months.
- Acoustic localization of up-calls revealed North Atlantic right whales most frequently occurred within and offshore of the Maryland WEA, with aggregates of locations along the eastern edge of the WEA. While we were unable to reliably locate up-call detections

during the summer, first arrival distributions showed most of these calls were detected offshore of the WEA.
- No significant inter-annual variability was observed for any of the baleen whale species.

Occurrence of dolphins and porpoises were elucidated using C-POD click detectors that were supplemented at a few sites with broadband acoustic recorders in Years 2 and 3. Key findings relating to dolphins and porpoises were:

- Bottlenose dolphins were frequently detected year-round within and inshore of the WEA, except in February, whereas offshore sightings were limited to summer and fall.
- Common dolphins were detected offshore of the WEA from December to May.
- During the tropical storms in Fall 2017, there were significantly fewer visits by dolphins to the study area, and daily foraging activity levels were reduced.
- Detection durations were significantly longer during the May to September than the October to April time periods and were reduced during storm events. Detection of dolphin signature whistles indicated a minimum of 174 individual bottlenose dolphins occurred within the Maryland WEA during Summer 2016 to Summer 2017, but only 14 of these were detected subsequently. Inshore of the Maryland WEA, a minimum of 526 individual bottlenose dolphins were detected during Summer 2017 with 111 of these being detected on more than one day indicating relatively frequent reoccurrence at this site.
- The smallest cetacean species detected, the harbor porpoise, occurred during the November to June timeframe, with the peak in detections between January and May.
- During the first year of the study, harbor porpoises were most common within and offshore of the WEA, whereas in the second and third years, this shifted to within and inshore of the WEA.
- Harbor porpoises were frequently detected foraging, mainly in the evening to early morning hours.

This study described the seasonal occurrence of whales, dolphins and porpoises within and around the Maryland WEA. This information can be used to inform which species will be most at risk of disturbance by offshore wind energy construction and operation activities, as well as when and how those impacts can be most effectively mitigated. Our results indicate that critically endangered North Atlantic right whales would be most vulnerable to any disturbance caused by anthropogenic activities in the Maryland WEA from November to April. Our 3-year baseline data indicates this is relatively consistent across years. However, occasional presence during the summer months that is less predictable means that mitigating the risk of any harm or disturbance from anthropogenic activities would require real-time monitoring. Bottlenose dolphins are the most prevalent species during the summer and hence would be the marine mammal species most exposed to stressors, such as loud sounds, during this season.

6.2 Overview of Ambient Noise Levels

We characterized the ambient noise environment within and surrounding the Maryland WEA, and found a high level of variation in noise levels both spatially and temporally. Key findings on the ambient noise levels were:

- Elevated noise levels predominately occurred in low frequency bands, suggesting anthropogenic noise is a major contributor to the noise environment.
- Survey sites along the western edge of the WEA and inshore of the WEA were the quietest surveyed areas, with median noise values ranging between 107.2 – 110.5 dB.

- Sites along the eastern edge of the WEA and offshore of the WEA had consistently higher sound levels than other surveyed areas, with median noise values ranging between 115.3 – 116.1 dB. Given the proximity of these relatively noisy sites to the Delaware to Cape Henlopen Traffic Lane, shipping noise is likely a dominant contributor to the ambient noise environment.
- Sites along the eastern edge of the WEA exceeded the 120 dB take threshold approximately 18 – 20% of hours recorded during the 3-year survey, as well as the greatest percentage of 10 s averages exceeding the threshold.

These results suggest that baleen whales near surveyed sites along the eastern edge of the WEA and offshore of the WEA would be at greatest risk of exposure to both prolonged and acute durations of elevated noise. Changes in dolphin whistle characteristics in response to increased ambient noise levels indicate compensatory behavior although it is unknown whether this could lead to communication impairment and fitness consequences.

6.3 Recommendations for Future Studies

This study has provided important baseline information on the spatiotemporal occurrence of vocalizing marine mammals. While the survey was a success in terms of the findings on cetacean ecology in this area, a limitation of this particular study design was balancing the number of sensors and the resolution of the analysis (large-scale spatial extent versus fine-scale resolution of locating calls). As a result, we tried to achieve a balance across all of these goals, but there were trade-offs. Additionally, our findings revealed a number of important data gaps and lessons learned that could be addressed in future efforts in both the Maryland WEA as well as other WEAs. These results will help inform regulators, resource managers, and others operating off our Atlantic coast, so that appropriate protection and mitigation measures can be developed. Recommendations for future studies include:

Future Studies to Address Ecological Data Gaps

- North Atlantic right whale ecology: Despite the large amount of data collected on North Atlantic right whales, there remain data gaps in the current scientific understanding of North Atlantic right whale ecology. Overall, little is known about the behavior and ecology of North Atlantic right whales during their migration through the Mid-Atlantic Bight.
    - Do North Atlantic right whales have different calling behavior during the northwards versus southwards migration (e.g., call rates, call types, source levels)? Many of the northward-migrating whales may be mothers with calves, which may cause whale calling behavior to change during their northward versus southward migration. These questions could be addressed with focal follow recordings and/or visual observations in combination with more archival PAM recordings.
    - How many North Atlantic right whales are occurring in this area? This would require establishing call rate and detection probability; both parameters are currently not established in this area, and extrapolation based on North Atlantic right whale behavior from other areas (such as the feeding or calving grounds) may not be appropriate.
    - What is the optimal number and spacing of acoustic recorders to improve the detectability of locatable calls and whale tracks? The exact number and spacing of the sensors would depend on the specific questions to be addressed. However, a key factor in our study was the higher than expected ambient noise levels,

which could mask whale calls and reduce our detection area. In future efforts, we would recommend ambient noise levels be recorded and measured prior to designing the localization array so that these noise levels can be taken into account. An optimization modeling effort could then be conducted for the survey design to balance detection ranges and resolution under the noise environment within the specific study area with the available number of sensors within the scope of the budget. Within the Maryland WEA, the MARU sensors were approximately 7 km apart and we would recommend this distance be reduced in future studies to increase call detection on multiple sensors. In future studies focused on localizing calls, we would suggest a gridded-survey design with instruments distributed every 5 km. This would represent significantly increased cost in terms of equipment and analysis effort. However, if locating or tracking whales in the WEA is the requirement, higher sensor density with decreased spacing would be important. Additionally, we found error rates for whale locations increased with farther distances outside the sensor array. The localization array should therefore be extended beyond the WEA if it is required to know whether whales were inshore or offshore of the WEA. This survey configuration would be designed for right whales or humpback whale localization. If locating fin or blue whales was desired, the spacing could be increased, but you may also want to extend the survey area farther offshore.

- Ecology of other baleen whale species: As with North Atlantic right whales, there is important behavioral and ecological information missing from our knowledge on other baleen whale species occurring off of Maryland.
    - What is the function of this area for fin, humpback, and minke whales?
    - Are there other calls these species produce that may be conducive to acoustic localization?
    - An increase in the spatial extent of sensors could clarify whether fin whales are calling more frequently offshore compared to within our study area.
- Ecology of dolphin species: The use of passive acoustic monitoring to contribute to our understanding of the ecology of dolphin species could be improved by:
    - Distinguishing calls amongst dolphin species: Further research to improve the ability to discriminate dolphin species, particularly for species with overlapping distributions, such as bottlenose and common dolphins, would aid passive acoustic monitoring studies.
    - Evaluating the performance of signature whistle analysis to estimate abundance in relation to other methods, such as photo-identification or line-transect surveys.
- Storm events: Our study area experienced several storm events during the three-year period. During these events, there were changes in dolphin occurrence and foraging activity, which were most likely caused by alterations in their prey that were more sensitive to the environmental change. As changes in ocean conditions and extreme events intensify with climate change, it will be important to further understand the effect of these changes and disturbances on marine mammals.

Future Studies Related to Offshore Human Activities and Resource Management

- Offshore wind energy development: There are many marine mammal species on the Atlantic OCS, such as baleen whales, that have not been studied in relation to offshore renewable wind energy development. Continued passive acoustic monitoring during wind farm construction and operation would provide valuable information on the received

sound levels and response of marine mammals, which could be used to inform future environmental impact assessments and permitting for wind energy projects along the Atlantic coast. We would recommend that if a localization array is used in future studies that the design include closer spacing (5 km or less) between hydrophones to improve detectability of North Atlantic right whales, as well as that of dolphin species that may be prevalent during the summer construction period. Testing the effectiveness of real-time passive acoustic marine mammal detection systems in this area prior to construction activities would also be valuable to determine performance within this environment of relatively high ambient noise. Increased data collection on the distribution and abundance of prey species, such as forage fish, would help to distinguish between direct and indirect effects of offshore wind energy development on marine mammals.

- Shipping traffic: Our study highlighted the high ambient noise levels offshore of Maryland, mainly caused by boats. Our study could be used to promote the use and development of quieter ship engines to reduce underwater ambient noise levels and potential stress to species sensitive to sound. Further study on the impact of sound on marine species would also help to determine the population-level effects of elevated noise levels. Additionally, accounting for vessel-specific acoustic signatures and cross-referencing sounds with AIS shipping data could clarify how different ships or vessel classes contribute to the soundscape.
- Other human uses: Our baseline data on the seasonal and temporal occurrence of marine mammals and the ambient noise levels will improve the ability of state and federal agencies and stakeholders to assess how increased human use of our ocean, such as fishing, aquaculture, oil and gas energy exploration and development, and marine mineral extraction, could result in changes to the marine environment and potentially impact marine mammals. It also serves as a comparison data set so that any significant changes in marine mammal distribution and ambient noise levels in the future can be detected and can assist in designing appropriate mitigation action. Further research on baleen whale call rates and dolphin signature whistles would help to determine the abundance of animals offshore of Maryland and any subsequent changes.

7 Research Products

7.1 Presentations

Bailey, H. and Rice, A. (2015) Determining Offshore Use by Marine Mammals and Ambient Noise Levels Using Passive Acoustic Monitoring. Maryland Department of Natural Resources and Maryland Energy Administration meeting, Annapolis, MD, 12 February 2015.

Wingfield, J., O'Brien, M., Rice, A.N., Diamond, C., Michalec, J., Channell, F. and Bailey, H. (2015) Winter habitat use and temporal segregation by dolphins and porpoises off Maryland, USA. 2015 ESA Annual Meeting, Baltimore, MD. 9 – 14 August 2015.

Wingfield, J., O'Brien, M., Rice, A.N., Diamond, C., Michalec, J., Channell, F. and Bailey, H. (2015) Winter Occurrence of Small Cetaceans in and around the Offshore Maryland Wind Energy Area. AWEA Offshore Wind Power Conference, Baltimore, MD. 29 – 30 September 2015.

Bailey, H. and Rice, A. (2016) Determining Offshore Use by Marine Mammals and Ambient Noise Levels Using Passive Acoustic Monitoring. Maryland Coastal Bays program meeting, Cambridge, MD, 20 January 2016.

Bailey, H. and Rice, A. (2016) Determining Offshore Use by Marine Mammals and Ambient Noise Levels Using Passive Acoustic Monitoring offshore of Maryland. BOEM Atlantic Ocean Energy and Mineral Science Forum, Sterling, VA, 16 – 17 November 2016.

Wingfield, J., O'Brien, M., Hodge, K.B, Tielens, J.T., Rice, A.N., and Bailey, H. (2016) Identifying cetacean migratory routes, foraging areas, and ambient noise levels in the Maryland Offshore Wind Energy Area. 4th International Conference on the Effects of Noise on Aquatic Life, Dublin, Ireland, 10 – 16 July 2016.

Bailey, H. and Rice, A. (2017) Determining Offshore Use by Marine Mammals and Ambient Noise Levels Using Passive Acoustic Monitoring. Maryland Department of Natural Resources, 18 May 2017. Host: Gwynne Schultz.

Bailey, H., Wingfield, J., Rice, A.N., and Hodge, K. (2017) Determining Occurrence of Marine Mammals Off Maryland Using Passive Acoustic Monitoring. BOEM, Sterling, VA, 1 August 2017. Host: Erica Staaterman.

Bailey, H., Wingfield, J., Fandel, A., Garrod, A., Lyubchich, V. and Rice, A.N. (2017) Identification of bottlenose dolphin foraging behavior and search strategies using passive acoustic monitoring. 22nd Biennial Conference on the Biology of Marine Mammals in Halifax, Canada, 22 – 27 October 2017.

Bailey, H., Garrod, A., Fandel, A., Wingfield, J., Fouda, L., Hodge, K., and Rice, A.N. (2017) Passive acoustic monitoring of marine mammals in the Maryland Wind Energy Area. Maryland Department of Natural Resources, Oxford, MD, 2 November 2017. Host: Cindy Driscoll.

Fandel, A., Bailey, H., Rice, A. and Wingfield, J. (2017). Passive acoustic monitoring of marine mammals in and around the Maryland Wind Energy Area. National Offshore Wind Innovation Center meeting, College Park, MD, 10 August 2017.

Hodge, K.B., Wingfield, J.E., Bailey, H. and Rice, A.N. (2017) Occurrence of baleen whale species in the Maryland Wind Energy Area. 22nd Biennial Conference on the Biology of Marine Mammals in Halifax, Canada, 22 – 27 October 2017.

Wingfield, J.E., Bailey, H., Rice, A. and Hodge, K.B. (2017) Acoustic monitoring of marine mammals within and surrounding the Maryland Wind Energy Area. OneNOAA seminar, Silver Spring, MD, 21 June 2017.

Wingfield, J.E., Bailey, H., Rice, A. and Hodge, K.B. (2017) Year-round spatiotemporal distribution of harbor porpoises within and around the Maryland Wind Energy Area. 22nd Biennial Conference on the Biology of Marine Mammals in Halifax, Canada, 22 – 27 October 2017.

Bailey, H., Garrod, A., Fandel, A., Wingfield, J., Fouda, L., Hodge, K., and Rice, A.N. (2018) Listening for marine mammals off Maryland. Smithsonian Environmental Research Center, Edgewater, MD, 8 February 2018. Host: Matthew Ogburn.

Bailey, H. and Rice, A. (2018) Multi-year passive acoustic monitoring of marine mammals in the Mid-Atlantic. Maryland's Inaugural State of the Coast Conference, Cambridge, MD, 23 May 2018.

7.2 Publications Through 2018

Fouda, L., Wingfield, J., Fandel, A., Garrod, A., Hodge, K., Rice, A., Bailey, H. (2018). Dolphins simplify their vocal calls in response to increased ambient noise. *Biology Letters, 14*(10), 20180484.

Garrod, A., Fandel, A. D., Wingfield, J. E., Fouda, L., Rice, A. N., & Bailey, H. (2018). Validating automated click detector dolphin detection rates and investigating factors affecting performance. *The Journal of the Acoustical Society of America*, *144*(2), 931-939.

Wingfield, J. E., O'Brien, M., Lyubchich, V., Roberts, J. J., Halpin, P. N., Rice, A. N., & Bailey, H. (2017). Year-round spatiotemporal distribution of harbor porpoises within and around the Maryland wind energy area. *PloS one*, *12*(5), e0176653.

8 References

Amano T, Katayama N. 2009. Hierarchical movement decisions in predators: Effects of foraging experience at more than one spatial and temporal scale. Ecology. 90(12):3536–3545.

Anderson TW, Goodman LA. 1957. Statistical inference about Markov Chains. Ann Math Stat. 28:89–110.

Au WWL. 1993. Sonar of Dolphins. New York: Springer-Verlag.

Au WWL, Benoit-Bird KJ, Kastelein RA. 2007. Modeling the detection range of fish by echolocating bottlenose dolphins and harbor porpoises. J Acoust Soc Am. 121(6):3954. doi:10.1121/1.2734487.

Au WWL, Branstetter B, Moore PW, Finneran JJ. 2012. The biosonar field around an Atlantic bottlenose dolphin (*Tursiops truncatus*). J Acoust Soc Am. 131(1):569–576. doi:10.1121/1.3662077.

Au WWL, Floyd RW, Penner RH, Murchison AE. 1974. Measurement of echolocation signals of the Atlantic bottlenose dolphin, *Tursiops truncatus Montagu*, in open waters. J Acoust Soc Am. 56(4):1280–1290. doi:10.1121/1.1903419.

Au WWL, Pack AA, Lammers MO, Herman LM, Deakos MH, Andrews K. 2006. Acoustic properties of humpback whale songs. J Acoust Soc Am. 120(2):1103–1110. doi:10.1121/1.2211547.

Azzolin M, Gannier A, Lammers MO, Oswald JN, Papale E, Buscaino G, Buffa G, Mazzola S, Giacoma C. 2014. Combining whistle acoustic parameters to discriminate Mediterranean odontocetes during passive acoustic monitoring. J Acoust Soc Am. 135(1):502–512. doi:10.1121/1.4845275.

Bailey H, Brookes KL, Thompson PM. 2014. Assessing environmental impacts of offshore wind farms: Lessons learned and recommendations for the future. Aquat Biosyst. 10(1):1–13. doi:10.1186/2046-9063-10-8.

Bailey H, Senior B, Simmons D, Rusin J, Picken G, Thompson PM. 2010. Assessing underwater noise levels during pile-driving at an offshore windfarm and its potential effects on marine mammals. Mar Pollut Bull. 60(6):888–897. doi:10.1016/j.marpolbul.2010.01.003.

Bailey H, Thompson P. 2006. Quantitative analysis of bottlenose dolphin movement patterns and their relationship with foraging. J Anim Ecol. 75(2):456–465. doi:10.1111/j.1365-2656.2006.01066.x.

Barber JR, Crooks KR, Fristrup KM. 2010. The costs of chronic noise exposure for terrestrial organisms. Trends Ecol Evol. 25(3):180–189. doi:10.1016/j.tree.2009.08.002.

Barco S, Burt L, DePerte A, Digiovanni R. 2015. Marine mammal and sea turtle sightings in the vicinity of the Maryland Wind Energy Area July 2013-June 2015. Prepared for the Maryland Department of Natural Resources, VAQF Scientific Report # 2015-06.

Barco SG, Mclellan WA, Allen JM, Asmutis-Silvia RA, Meagher EM, Pabst DA, Robbins J, Seton RE, Swingle WM. 2002. Population identity of humpback whales (*Megaptera novaeangliae*) in the waters of the US mid-Atlantic states. J Cetacean Res Manag. 4(2):135–141.

Barco SG, Swingle WM, McLellan WA, Harris RN, Pabst DA. 1999. Local abundance and distribution of bottlenose dolphins (*Tursiops truncatus*) in the nearshore waters of Virginia Beach, Virginia. Mar Mammal Sci. 15(2):394–408. doi:10.1111/j.1748-7692.1999.tb00809.x.

Benaglia T, Chauveau D, Hunter DR, Young D. 2009. mixtools: An R Package for analysing finite mixture models. J Stat Softw. 32:1–29.

Benjamin MA, Rigby RA, Stasinopoulos DM. 2003. Generalized autoregressive moving average models. J Am Stat Assoc. 98(461):214–223. doi:10.1198/016214503388619238.

Benoit-Bird KJ, Dahood AD, Würsig B. 2009. Using active acoustics to compare lunar effects on predator-prey behavior in two marine mammal species. Mar Ecol Prog Ser. 395:119–135. doi:10.3354/meps07793.

Bioacoustics Research Program. 2011. Raven Pro 1.4: Interactive Sound Analysis Software. Ithaca, NY: Cornell Lab of Ornithology.

Bioacoustics Research Program. 2015. Raven Pro 1.5: Interactive Sound Analysis Software. Ithaca, NY: Cornell Lab of Ornithology.

Bioacoustics Research Program. 2018. Raven Pro 2.0: Interactive Sound Analysis Software. Ithaca, NY: Cornell Lab of Ornithology.

Blair HB, Merchant ND, Friedlaender AS, Wiley DN, Parks SE. 2016. Evidence for ship noise impacts on humpback whale foraging behaviour. Biol Lett. 12(8). doi:10.1098/rsbl.2016.0005.

Boehlert GW, Gill AB. 2010. Environmental and ecological effects of ocean renewable energy development: A current synthesis. Oceanography. 23(2):68–81. doi:10.5670/oceanog.2010.46.

BOEM Office of Renewable Energy Programs. 2012. Commercial wind lease issuance and site assessment activities on the Atlantic Outer Continental Shelf offshore New Jersey, Delaware, Maryland, and Virginia: Final Environmental Assessment.

Boswell KM, Wilson MP, Cowan JH. 2008. A semiautomated approach to estimating fish size, abundance, and behavior from dual-frequency identification sonar (DIDSON) data. North Am J Fish Manag. 28(3):799–807. doi:10.1577/M07-116.1.

Boyce MS, Vernier PR, Nielsen SE, Schmiegelow FKA. 2002. Evaluating resource selection functions. Ecol Modell. 157(2–3):281–300. doi:10.1016/S0304-3800(02)00200-4.

Brandt MJ, Diederichs A, Betke K, Nehls G. 2011. Responses of harbour porpoises to pile driving at the Horns Rev II offshore wind farm in the Danish North Sea. Mar Ecol Prog Ser. 421:205–216. doi:10.3354/meps08888.

Brieman L. 2001. Random forests. Mach Learn. 45:5–32.

Brookes KL, Bailey H, Thompson PM. 2013. Predictions from harbor porpoise habitat association models are confirmed by long-term passive acoustic monitoring. J Acoust Soc Am. 134(3):2523–2533. doi:10.1121/1.4816577.

Buckstaff KC. 2004. Effects of watercraft noise on the acoustic behavior of bottlenose dolphins, *Tursiops truncatus*, in Sarasota bay, Florida. Mar Mammal Sci. 20(4):709–725. doi:10.1111/j.1748-7692.2004.tb01189.x.

Byrd BL, Hohn AA, Lovewell GN, Altman KM, Barco SG, Friedlaender A, Harms CA, McLellan WA, Moore KT, Rosel PE, et al. 2014. Strandings as indicators of marine mammal biodiversity and human interactions off the coast of North Carolina. Fish Bull. 112(1):1–23. doi:10.7755/FB.112.1.1.

Calupca TA, Fristrup KM, Clark CW. 2000. A compact digital recording system for autonomous bioacoustic monitoring. J Acoust Soc Am. 108(5):2582–2582. doi:10.1121/1.4743595.

Carlström J. 2005. Diel variation in echolocation behavior of wild harbor porpoises. Mar Mammal Sci. 21(1):1–12. doi:10.1111/j.1748-7692.2005.tb01204.x.

Carstensen J, Henriksen OD, Teilmann J. 2006. Impacts of offshore wind farm construction on harbour porpoises: Acoustic monitoring of echolocation activity using porpoise detectors (T-PODs). Mar Ecol Prog Ser. 321(May 2016):295–308. doi:10.3354/meps321295.

Chabot D. 1988. A quantitative technique to compare and classify humpback whale (*Megaptera novaeangliae*) sounds. Ethology. 77(2):89–102. doi:10.1111/j.1439-0310.1988.tb00195.x.

Charnov EL. 1976. Optimal foraging, the marginal value theorem. Theor Popul Biol. 9:129–136.

Clapham PJ, Baraff LS, Carlson CA, Christian MA, Mattila DK, Mayo CA, Murphy MA, Pittman S. 1993. Seasonal occurrence and annual return of humpback whales, *Megaptera novaeangliae*, in the southern Gulf of Maine. Can J Zool. 71:440–443.

Clark CW. 1995. Application of US Navy underwater hydrophone arrays for scientific research on whales.

Clark CW, Clapham PJ. 2004. Acoustic monitoring on a humpback whale (*Megaptera novaeangliae*) feeding ground shows continual singing into late spring. Proc R Soc B Biol Sci. 271(1543):1051–1057. doi:10.1098/rspb.2004.2699.

Clark CW, Ellison WT, Southall BL, Hatch L, Van Parijs SM, Frankel A, Ponirakis D. 2009. Acoustic masking in marine ecosystems: Intuitions, analysis, and implication. Mar Ecol Prog Ser. 395:201–222. doi:10.3354/meps08402.

Clark CW, Gagnon G. 2002. Low-frequency vocal behaviors of baleen whales in the North Atlantic: Insights from integrated undersea surveillance system detections, locations, and tracking from 1992 to 1996. US Navy J Underw Acoust. 52(3):609–640.

Clark CW, Gillespie D, Nowacek DP, Parks SE. 2007. Listening to their world: Acoustics for monitoring and protecting right whales in an urbanized ocean. In: Kraus SD, Rolland RM, editors. The Urban Whale: North Atlantic Right Whales at the Crossroads. Cambridge, MA: Harvard University Press. p. 333–358.

Connelly EE, Duron M, Williams KA, Stenhouse JJ. 2015. Summary of high resolution digital video aerial survey data. Wildlife densities and habitat use across temporal and spatial scales on the mid-Atlantic outer continental shelf: Final report to the Department of Energy EERE Wind & Water Power Technologies Office. Portland, Maine.

Connor RC, Mann J, Tyack PL, Whitehead H. 1998. Social evolution in toothed whales. Trends Ecol Evol. 13(6):228–232. doi:10.1016/S0169-5347(98)01326-3.

Cox TM, Read AJ, Solow A, Tregenza N. 2001. Will harbour porpoises (*Phocoena phocoena*) habituate to pingers? J Cetacean Res Manag. 3(1):81–86.

Croll DA, Clark CW, Acevedo A, Tershy B, Flores S, Gedamke J, Urban J, Suki B. 2002. Only male fin whales sing loud songs. Nature. 417(6891):809. doi:10.1038/417809a.

Dähne M, Gilles A, Lucke K, Peschko V, Adler S, Krügel K, Sundermeyer J, Siebert U. 2013. Effects of

pile-driving on harbour porpoises (*Phocoena phocoena*) at the first offshore wind farm in Germany. Environ Res Lett. 8(2). doi:10.1088/1748-9326/8/2/025002.

Davis GE, Baumgartner MF, Bonnell JM, Bell J, Berchok C, Bort Thornton J, Brault S, Buchanan G, Charif RA, Cholewiak D, et al. 2017. Long-term passive acoustic recordings track the changing distribution of North Atlantic right whales (*Eubalaena glacialis*) from 2004 to 2014. Sci Rep. 7(1):1–12. doi:10.1038/s41598-017-13359-3.

Deecke VB, Janik VM. 2006. Automated categorization of bioacoustic signals: Avoiding perceptual pitfalls. J Acoust Soc Am. 119(1):645–653. doi:10.1121/1.2139067.

Digby A, Towsey M, Bell BD, Teal PD. 2013. A practical comparison of manual and autonomous methods for acoustic monitoring. Methods Ecol Evol. 4(7):675–683. doi:10.1111/2041-210X.12060.

Dugan P, Pourhomayoun M, Shiu Y, Paradis R, Rice A, Clark C. 2013. Using high performance computing to explore large complex bioacoustic soundscapes: Case study for right whale acoustics. Procedia Comput Sci. 20:156–162. doi:10.1016/j.procs.2013.09.254.

Dunlop RA, Cato DH, Noad MJ. 2008. Non-song acoustic communication in migrating humpback whales (*Megaptera novaeangliae*). Mar Mammal Sci. 24(3):613–629. doi:10.1111/j.1748-7692.2008.00208.x.

Dunlop RA, Noad MJ, Cato DH, Stokes D. 2007. The social vocalization repertoire of east Australian migrating humpback whales (*Megaptera novaeangliae*). J Acoust Soc Am. 122(5):2893. doi:10.1121/1.2783115.

Edwards EF, Hall C, Moore TJ, Sheredy C, Redfern J V. 2015. Global distribution of fin whales *Balaenoptera physalus* in the post-whaling era (1980-2012). Mamm Rev. 45(4):197–214. doi:10.1111/mam.12048.

Egnor SER, Wickelgren JG, Hauser MD. 2007. Tracking silence: Adjusting vocal production to avoid acoustic interference. J Comp Physiol A Neuroethol Sensory, Neural, Behav Physiol. 193(4):477–483. doi:10.1007/s00359-006-0205-7.

Elliott RG, Dawson SM, Henderson S. 2011. Acoustic monitoring of habitat use by bottlenose dolphins in Doubtful Sound, New Zealand. New Zeal J Mar Freshw Res. 45(4):637–649. doi:10.1080/00288330.2011.570351.

Ellison WT, Southall B. 2012. A new context-based approach to assess marine mammal behavioral responses to anthropogenic sounds. 26(1):21–28. doi:10.1111/j.1523-1739.2011.01803.x.

Evans HF. 1976. The searching behaviour of *Anthocoris confusus* (Reuter) in relation to prey density and plant surface topography. Ecol Entomol. 1:163–169.

Fielding AH, Bell JF. 1997. A review of methods for the assessment of prediction errors in conservation presence/absence models. Environ Conserv. 24(1):38–49. doi:10.1017/S0376892997000088.

Fox J. 2008. An R and S-PLUS companion to applied regression. Thousand Oaks, CA: Sage Publications, Inc.

Gannon DP, Waples DM. 2004. Diets of coastal bottlenose dolphins from the U.S. Mid-Atlantic coast differ by habitat. Mar Mammal Sci. 20:527–545.

Garrison LP, Barry KP. 2013. Appendix A: Aerial abundance survey data during February-March 2013:

Southeast Fisheries Science Center. Annual Report of a Comprehensive Assessment of Marine Mammal, Marine Turtle, and Seabird Abundance and Spatial Distribution in US Waters of the West.

Garrod A, Fandel AD, Wingfield JE, Fouda L, Rice AN, Bailey H. 2018. Validating automated click detector dolphin detection rates and investigating factors affecting performance. J Acoust Soc Am. 144(2):931–939. doi:10.1121/1.5049802.

Gaskin D. 1977. Harbour porpoise *Phocoena phocoena* (L.) in the western approaches to the Bay of Fundy 1969-75. Rep Int Whal Comm. 27:487–492.

Gillespie D, Mellinger DK, Gordon J, McLaren D, Redmond P, McHugh R, Trinder P, Deng X-Y, Thode A. 2009. PAMGUARD: Semiautomated, open source software for real-time acoustic detection and localization of cetaceans. J Acoust Soc Am. 125(4):2547–2547.

van Ginkel C, Becker DM, Gowans S, Simard P. 2017. Whistling in a noisy ocean: Bottlenose dolphins adjust whistle frequencies in response to real-time ambient noise levels. Bioacoustics.:1–15. doi:10.1080/09524622.2017.1359670.

Gordon JCD, Gillespie D, Potter J, Frantzis A, Simmonds MP, Swift R, Thompson D. 2003. A review of the effects of seismic survey on marine mammals. Mar Technol Soc J. 37:14–32. doi:10.4031/002533203787536998.

Gridley T, Cockcroft VG, Hawkins ER, Blewitt ML, Morisaka T, Janik VM. 2014. Signature whistles in free-ranging populations of Indo-Pacific bottlenose dolphins, *Tursiops aduncus*. Mar Mammal Sci. 30(2):512–527. doi:10.1111/mms.12054.

Hain J, Ratnaswamy M, Kenney RD, Winn HE. 1992. The fin whale, *Balaenoptera physalus*, in waters of the northeastern United States continental shelf.

Halekoh U, Højsgaard S, Yan J. 2006. The R Package geepack for generalized estimating equations. J Stat Softw. 15(2):1–11. doi:10.18637/jss.v015.i02.

Hardy T, Williams R, Caslake R, Tregenza N. 2012. An investigation of acoustic deterrent devices to reduce cetacean bycatch in an inshore set net fishery. J Cetacean Res Manag. 12(2):85–90.

Hatch LT, Clark CW, Van Parijs SM, Frankel AS, Ponirakis DW. 2012. Quantifying loss of acoustic communication space for right whales in and around a U.S. national marine sanctuary. Conserv Biol. 26(6):983–994.

Hayes SA, Josephson E, Maze-Foley K, Rosel PE. 2017. NOAA Technical Memorandum NMFS-NE-241 US Atlantic and Gulf of Mexico Marine Mammal Stock Assessments - 2016 US Atlantic and Gulf of Mexico Marine Mammal Stock Assessments - 2016. (June).

Hayes SA, Josephson E, Maze-Foley K, Rosel PE, Byrd B, Chavez-Rosales S, Col TVN, Engleby L, Garrison LP, Hatch J, et al. 2018. US Atlantic and Gulf of Mexico Marine Mammal Stock Assessments - 2017. NOAA Tech Memo NMFS NE-245.

Heiler J, Elwen SH, Kriesell HJ, Gridley T. 2016. Changes in bottlenose dolphin whistle parameters related to vessel presence, surface behaviour and group composition. Anim Behav. 117:167–177. doi:10.1016/j.anbehav.2016.04.014.

Hildebrand JA. 2009. Anthropogenic and natural sources of ambient noise in the ocean. Mar Ecol Prog Ser. 395:5–20. doi:10.3354/meps08353.

Hill S, Burrows MT, Hughes RN. 2002. Adaptive search in juvenile plaice foraging for aggregated and dispersed prey. J Fish Biol. 61(5):1255–1267. doi:10.1111/j.1095-8649.2002.tb02469.x.

Hill SL, Burrows MT, Hughes RN. 2003. The efficiency of adaptive search tactics for different prey distribution patterns: A simulation model based on the behaviour of juvenile plaice. J Fish Biol. 63(SUPPL. A):117–130. doi:10.1111/j.1095-8649.2003.00212.x.

Hodge KB, Muirhead CA, Morano JL, Clark CW, Rice AN. 2015. North Atlantic right whale occurrence near wind energy areas along the mid-Atlantic US coast: Implications for management. Endanger Species Res. 28(3):225–234. doi:10.3354/esr00683.

Hodge LEW. 2011. Marine Mammal Monitoring in Onslow Bay, North Carolina, Using Passive Acoustics. *Dissertation*. Duke Universty.

Holm S. 1979. A simple sequentially rejective multiple test procedure. Scand Jounral Stat. 6:65–70.

Holt MM, Noren DP, Veirs V, Emmons CK, Veirs S. 2009. Speaking up: Killer whales (*Orcinus orca*) increase their call amplitude in response to vessel noise. J Acoust Soc Am. 125(1):EL27-32. doi:10.1121/1.3040028.

Inger R, Attrill MJ, Bearhop S, Broderick AC, James Grecian W, Hodgson DJ, Mills C, Sheehan E, Votier SC, Witt MJ, et al. 2009. Marine renewable energy: Potential benefits to biodiversity? An urgent call for research. J Appl Ecol. 46(6):1145–1153. doi:10.1111/j.1365-2664.2009.01697.x.

Iorio L Di, Clark CW. 2010. Exposure to seismic survey alters blue whale acoustic communication. 6:51–54. doi:10.1098/rsbl.2009.0651.

Janik VM. 2009. Chapter 4 Acoustic Communication in Delphinids. In: Advances in the Study of Behavior. Vol. 40. Elsevier. p. 123–157.

Janik VM, King SL, Sayigh LS, Wells RS. 2013. Identifying signature whistles from recordings of groups of unrestrained bottlenose dolphins (*Tursiops truncatus*). Mar Mammal Sci. 29(1):109–122. doi:10.1111/j.1748-7692.2011.00549.x.

Janik VM, Sayigh LS, Wells RS. 2006. Signature whistle shape conveys identity information to bottlenose dolphins. Proc Natl Acad Sci. 103(21):8293–8297. doi:10.1073/pnas.0509918103.

Janik VM, Slater PJB. 2000. The different roles of social learning in vocal communication. Anim Behav. 60(1):1–11. doi:10.1006/anbe.2000.1410.

Janik VM, Todt D, Dehnhardt G. 1994. Signature whistle variations in a bottlenosed dolphin, *Tursiops truncatus*. Behav Ecol Sociobiol. 35(4):243–248. doi:10.1007/BF00170704.

Johnston DW, Westgate AJ, Read AJ. 2005. Effects of fine scale oceanographic features on the distribution and movements of harbour porpoises (*Phocoena phocoena*) in the Bay of Fundy. Mar Ecol Prog Ser. 295:279–293. doi:10.3354/meps295279.

Jones GJ, Sayigh LS. 2002. Geographic variation in rates of vocal production of free-ranging bottlenose dolphins. Mar Mammal Sci. 18:374–393.

Kareiva P, Odell G. 1987. Swarms of predators exhibit “preytaxis” if individual predators use area-restricted search. Am Nat. 130:233–270.

Keller CA, Garrison L, Baumstark R, Ward-Geiger LI, Hines E. 2012. Application of a habitat model to define calving habitat of the North Atlantic right whale in the southeastern United States. Endanger Species Res. 18(1):73–87. doi:10.3354/esr00413.

Keller CA, Ward-Geiger LI, Brooks WB, Slay CK, Taylor CR, Zoodsma BJ. 2006. North Atlantic right whale distribution in relation to sea-surface temperature in the southeastern United States calving grounds. Mar Mammal Sci. 22:426–445.

Kenney RD. 1990. Bottlenose dolphins off the northeastern United States. In: Leatherwood S, Reeves RR, editors. The Bottlenose Dolphin. San Diego, CA: Academic Press. p. 369–386.

Kenney RD, Mayo CA, Winn HE. 2001. Migration and foraging strategies at varying spatial scales in western North Atlantic right whales: A review of hypotheses. J Cetacean Res Manag. 2:251–260.

King SL, Schick RS, Donovan C, Booth CG, Burgman M, Thomas L, Harwood J. 2015. An interim framework for assessing the population consequences of disturbance. Methods Ecol Evol. 6:1150–1158.

Kraus SD, Mayo C, Kenney RD, Clark CW, Rice AN, Estabrook BJ, Tielens JT. 2016. Northeast large pelagic survey collaborative aerial and acoustic surveys for large whales and sea turtles final report. US Department of the Interior, Bureau of Ocean Energy Management, Sterling, Virginia. OCS Study BOEM 2016-054.

Kraus SD, Prescott JH, Knowlton AR, Stone GS. 1986. Migration and calving of right whales (*Eubalaena glacialis*) in the western North Atlantic.

Kraus SD, Prescott JH, Stone GS. 1983. Harbor porpoise, *Phocoena phocoena*, in the US coastal waters off the Gulf of Maine: A survey to determine seasonal distribution and abundance. Technical Report Submitted to National Marine Fisheries Service. Boston, MA.

Krebs JR, Ryan JC, Charnov EL. 1974. Hunting by expectation or optimal foraging? A study of patch use by chickadees. Anim Behav. 22:953–964.

Kullback S, Kupperman M, Ku HH. 1962. Tests for contingency tables and Markov Chains. Technometrics. 4:573–608.

Kyhn LA, Tougaard J, Thomas L, Duve LR, Stenback J, Amundin M, Desportes G, Teilmann J. 2012. From echolocation clicks to animal density—Acoustic sampling of harbor porpoises with static dataloggers. J Acoust Soc Am. 131(1):550–560. doi:10.1121/1.3662070.

Leatherwood S, Reeves RR. 1983. Abundance of bottlenose dolphins in Corpus Christi Bay and coastal southern Texas. Contrib Mar Sci. 26:179–199.

Leeney RH, Berrow S, McGrath D, O'Brien J, Cosgrove R, Godley BJ. 2007. Effects of pingers on the behaviour of bottlenose dolphins. J Mar Biol Assoc United Kingdom. 87(1):129–133. doi:10.1017/S0025315407054677.

Lesage V, Barrette C, Kingsley MCS, Sjare B. 1999. The effect of vessel noise on the vocal behavior of belugas in the St. Lawrence River estuary, Canada. Mar Mammal Sci. 15(1):65–84. doi:10.1111/j.1748-7692.1999.tb00782.x.

Liaw A, Wiener M. 2002. Classification and regression by randomForest. R News. 2(3):18–22.

Linnenschmidt M, Teilmann J, Akamatsu T, Dietz R, Miller LA. 2013. Biosonar, dive, and foraging

activity of satellite tracked harbor porpoises (*Phocoena phocoena*). Mar Mammal Sci. 29(2):77–97. doi:10.1111/j.1748-7692.2012.00592.x.

Madsen PT, Wahlberg M, Tougaard J, Lucke K, Tyack PL. 2006. Wind turbine underwater noise and marine mammals: Implications of current knowledge and data needs. Mar Ecol Prog Ser. 309(Tyack 1998):279–295. doi:10.3354/meps309279.

Marley SA, Salgado Kent CP, Erbe C, Parnum IM. 2017. Effects of vessel traffic and underwater noise on the movement, behaviour and vocalisations of bottlenose dolphins in an urbanised estuary. Sci Rep. 7(1):1–14. doi:10.1038/s41598-017-13252-z.

Marques TA, Thomas L, Martin SW, Mellinger DK, Ward JA, Moretti DJ, Harris D, Tyack PL. 2013. Estimating animal population density using passive acoustics. Biol Rev. 88(2):287–309. doi:10.1111/brv.12001.

Mate BR, Nieukirk SL, Kraus SD. 1997. Satellite-monitored movements of the northern right whale. J Wildl Manage. 61(4):1393–1405.

Matthews J, Brown S, Gillespie D, Johnson M, Mclanaghan R, Moscrop A, Nowacek DP. 2001. Vocalisation rates of the North Atlantic right whale (*Eubalaena glacialis*). J Cetacean Res Manag. 3(3):271–282.

McDonald MA, Hildebrand JA, Webb SC. 1995. Blue and fin whales observed on a seafloor array in the Northeast Pacific. J Acoust Soc Am. 98(2):712–721. doi:10.1121/1.413565.

Mellinger D, Stafford K, Moore S, Dziak R, Matsumoto H. 2007. An overview of fixed passive acoustic observation methods for cetaceans. Oceanography. 20(4):36–45. doi:10.5670/oceanog.2007.03.

Mellinger DK, Roch MA, Nasal E, Klink H. 2016. Signal Processing. In: Au WWL, Lammers MO, editors. Listening in the Ocean: New Discoveries and Insights on Marine Life from Autonomous Passive Acoustic Recorders. New York: Springer. p. 359–409.

Merchant ND, Barton TR, Thompson PM, Pirotta E, Dakin DT, Dorocicz J. 2013. Spectral probability density as a tool for ambient noise analysis. J Acoust Soc Am. 133(4):EL262-EL267. doi:10.1121/1.4794934.

Merchant ND, Pirotta E, Barton TR, Thompson PM. 2014. Monitoring ship noise to assess the impact of coastal developments on marine mammals. Mar Pollut Bull. 78(1–2):85–95. doi:10.1016/j.marpolbul.2013.10.058.

Meynier L, Stockin KA, Bando MKH, Duignan PJ. 2008. Stomach contents of common dolphin (*Delphinus sp.*) from New Zealand waters. New Zeal J Mar Freshw Res.(February):257–268. doi:10.1080/00288330809509952.

Morano JL, Rice AN, Tielens JT, Estabrook BJ, Murray A, Roberts BL, Clark CW. 2012. Acoustically detected year-round presence of right whales in an urbanized migration corridor. Conserv Biol. 26(4):698–707. doi:10.1111/j.1523-1739.2012.01866.x.

Morano JL, Salisbury DP, Rice AN, Conklin KL, Falk KL, Clark CW. 2012. Seasonal and geographical patterns of fin whale song in the western North Atlantic Ocean. J Acoust Soc Am. 132(2):1207–1212. doi:10.1121/1.4730890.

Morfey CL. 2001. Dictionary of acoustics. San Diego, CA: Academic Press.

Muirhead CA, Warde AM, Biedron IS, Nicole Mihnovets A, Clark CW, Rice AN. 2018. Seasonal acoustic occurrence of blue, fin, and North Atlantic right whales in the New York Bight. Aquat Conserv Mar Freshw Ecosyst. 28(3):744–753. doi:10.1002/aqc.2874.

Murray A, Rice AN, Clark CW. 2014. Extended seasonal occurrence of humpback whales in Massachusetts Bay. J Mar Biol Assoc United Kingdom. 94(6):1117–1125. doi:10.1017/S0025315412001968.

Mussoline SE, Risch D, Hatch LT, Weinrich MT, Wiley DN, Thompson MA, Corkeron PJ, Van Parijs SM. 2012. Seasonal and diel variation in North Atlantic right whale up-calls: Implications for management and conservation in the northwestern Atlantic ocean. Endanger Species Res. 17(1):17–26. doi:10.3354/esr00411.

National Academies of Sciences Engineering and Medicine. 2017. Approaches to understanding the cumulative effects of stressors on marine mammals. Washington, D.C.

Nieukirk SL, Stafford KM, Mellinger DK, Dziak RP, Fox CG. 2004. Low-frequency whale and seismic airgun sounds recorded in the mid-Atlantic Ocean. J Acoust Soc Am. 115(4):1832–1843. doi:10.1121/1.1675816.

National Oceanic and Atmospheric Administration. 2018. Revisions to technical guidance for assessing the effects of anthropogenic sound on marine mammal hearing – underwater acoustic thresholds for onset of permanent and temporary threshold shifts. Fed Reg 81:51693-51724

Nowacek DP, Thorne LH, Johnston DW, Tyack PL. 2007. Responses of cetaceans to anthropogenic noise. Mamm Rev. 37(2):81–115. doi:10.1111/j.1365-2907.2007.00104.x.

Nuuttila HK, Meier R, Evans PGH, Turner JR, Bennell JD, Hiddink JG. 2013. Identifying foraging behaviour of wild bottlenose dolphins (*Tursiops truncatus*) and harbour porpoises (*Phocoena phocoena*) with static acoustic dataloggers. Aquat Mamm. 39(2):147–161. doi:10.1578/AM.39.2.2013.147.

Nuuttila HK, Thomas L, Hiddink JG, Meier R, Turner JR, Bennell JD, Tregenza NJC, Evans PGH. 2013. Acoustic detection probability of bottlenose dolphins, Tursiops truncatus , with static acoustic dataloggers in Cardigan Bay, Wales. J Acoust Soc Am. 134(3):2596–2609. doi:10.1121/1.4816586.

O'Reilly JE, Zetlin C. 1998. Seasonal, horizontal, and vertical distribution of phytoplankton chlorophyll a in the Northeast U.S. continental shelf ecosystem. US Dep Commer NOAA Tech Rep NMFS. 139:119 p.

OSPAR Commission. 2009. Overview of the impacts of anthropogenic underwater sound in the marine environment. OSPAR Biodiversity Series 441: 1–134.

Oswald JN. 2013. Development of a classifier for the acoustic identification of Delphinid species in the Northwest Atlantic Ocean. Final Report. Prepared for Naval Facilities Engineering Command Atlantic, Norfolk, Virginia, under HDR Environmental, Operations and Construc. Encinitas, California.

Oswald JN, Rankin S, Barlow J, Lammers MO. 2007. A tool for real-time acoustic species identification of Delphinid whistles. J Acoust Soc Am. 122(1):587–595. doi:10.1121/1.2743157.

Otani S, Naito Y, Kawamura A, Kawasaki M, Nishiwaki S, Kato A. 1998. Diving behavior and performance of Harbor porpoises, *Phocoena phocoena*, in Funka Bay, Hokkaido, Japan. Mar Mammal Sci. 14(2):209–220. doi:10.1111/j.1748-7692.1998.tb00711.x.

Palka D. 1995. Influences on spatial patterns of Gulf of Maine habor porpoises. In: Blix AS, Walloe L,

Ultang O, editors. Whales, Seals, Fish, and Man. Developments in Marine Biology. Amsterdam: Elsevier Science. p. 69–75.

Papastamatiou YP, DeSalles PA, McCauley DJ. 2012. Area-restricted searching by manta rays and their response to spatial scale in lagoon habitats. Mar Ecol Prog Ser. 456:233–244.

Parks SE, Clark CW. 2007. Acoustic communication: Social sounds and the potential impacts of noise. In: The Urban Whale: North Atlantic Right Whales at the Crossroads. p. 310–332.

Parks SE, Johnson M, Nowacek D, Tyack PL, Parks SE, Johnson M. 2011. Individual right whales call louder in increased environmental noise Individual right whales call louder in increased environmental noise. 7:33–35. doi:10.1098/rsbl.2010.0451.

Parks SE, Tyack PL. 2005. Sound production by North Atlantic right whales (*Eubalaena glacialis*) in surface active groups. J Acoust Soc Am. 117(5):3297–3306. doi:10.1121/1.1882946.

Payne R, Webb D. 1971. Orientation by means of long range acoustic signaling in baleen whales. Ann N Y Acad Sci. 188:110–141.

Payne RS, McVay S. 1971. Songs of Humpback Whales. Science. 173(3997):585–597.

Philpott E, Englund A, Ingram S, Rogan E. 2007. Using T-PODs to investigate the echolocation of coastal bottlenose dolphins. J Mar Biol Assoc United Kingdom. 87(1):11–17. doi:10.1017/S002531540705494X.

Pirotta E, Merchant ND, Thompson PM, Barton TR, Lusseau D. 2015. Quantifying the effect of boat disturbance on bottlenose dolphin foraging activity. Biol Conserv. 181:82–89. doi:10.1016/j.biocon.2014.11.003.

Pirotta E, Thompson PM, Miller PI, Brookes KL, Cheney B, Barton TR, Graham IM, Lusseau D. 2014. Scale-dependent foraging ecology of a marine top predator modelled using passive acoustic data. Funct Ecol. 28(1):206–217. doi:10.1111/1365-2435.12146.

Popescu M, Dugan PJ, Pourhomayoun M, Risch D, Lewis III HW, Clark CW. 2013. Bioacoustical periodic pulse train signal detection and classification using spectrogram intensity binarization and energy projection. ICML 2013 Work Mach Learn Bioacoustics.(May 2013).

Pusineri C, Magnin V, Meynier L, Spitz J, Hassani S, Ridoux V. 2007. Food and feeding ecology of the common dolphin (*Delphinus delphis*) in the oceanic Northeast Atlantic and comparison with its diet in neritic areas. Mar Mammal Sci. 23:30–47.

Pyke GH. 1984. Optimal foraging theory: A critical review. Annu Rev Ecol Syst. 15:523–575.

Quick NJ, Janik VM. 2012. Bottlenose dolphins exchange signature whistles when meeting at sea. Proc R Soc B Biol Sci. 279(1738):2539–2545. doi:10.1098/rspb.2011.2537.

R Core Team. 2015. R: A language and environment for statistical computing.

R Core Team. 2017. R: A language and environment for statistical computing.

R Core Team. 2018. R: A language and environment for statistical computing.

Rankin S, Archer F, Keating JL, Oswald JN, Oswald M, Curtis A, Barlow J. 2017. Acoustic classification

of dolphins in the California Current using whistles, echolocation clicks, and burst pulses. Mar Mammal Sci. 33(2):520–540. doi:10.1111/mms.12381.

Read AJ, Westgate AJ. 1997. Monitoring the movements of harbour porpoises (*Phocoena phocoena*) with satellite telemetry. Mar Biol. 130(2):315–322. doi:10.1007/s002270050251.

Reid RN, Cargnelli LM, Griesbach SJ, Packer DB, Johnson DL, Zetlin CA, Morse WW, Berrien PL. 1999. Atlantic Herring, Clupea harengus, Life History and Habitat Characteristics. NOAA Tech Memo. NMFS-TM-12(September):1–48.

Rice AN, Palmer KJ, Tielens JT, Muirhead CA, Clark CW. 2014. Potential Bryde's whale (*Balaenoptera edeni*) calls recorded in the northern Gulf of Mexico. J Acoust Soc Am. 135(5):3066–3076. doi:10.1121/1.4870057.

Rice AN, Tielens JT, Estabrook BJ, Muirhead CA, Rahaman A, Guerra M, Clark CW. 2014. Variation of ocean acoustic environments along the western North Atlantic coast: A case study in context of the right whale migration route. Ecol Inform. 21:89–99. doi:10.1016/j.ecoinf.2014.01.005.

Richardson WJ, Greene CR, Malme CI, Thomson DH. 1995. Marine Mammals and Noise. 1st ed. San Diego: Academic Press.

Risch D, Castellote M, Clark CW, Davis GE, Dugan PJ, Hodge LEW, Kumar A, Lucke K, Mellinger DK, Nieukirk SL, et al. 2014. Seasonal migrations of North Atlantic minke whales: Novel insights from large-scale passive acoustic monitoring networks. Mov Ecol. 2(1):1–17. doi:10.1186/s40462-014-0024-3.

Risch D, Clark CW, Dugan PJ, Popescu M, Siebert U, Van Parijs SM. 2013. Minke whale acoustic behavior and multi-year seasonal and diel vocalization patterns in Massachusetts Bay, USA. Mar Ecol Prog Ser. 489:279–295. doi:10.3354/meps10426.

Robbins JR, Brandecker A, Cronin M, Jessopp M, McAllen R, Culloch R. 2016. Handling dolphin detections from C-PODs, with the development of acoustic parameters for verification and the exploration of species identification possibilities. Bioacoustics. 25(2):99–110. doi:10.1080/09524622.2015.1125789.

Roberts BL, Read AJ. 2015. Field assessment of C-POD performance in detecting echolocation click trains of bottlenose dolphins (*Tursiops truncatus*). Mar Mammal Sci. 31(1):169–190. doi:10.1111/mms.12146.

Roberts JJ, Best BD, Mannocci L, Fujioka E, Halpin PN, Palka DL, Garrison LP, Mullin KD, Cole TVN, Khan CB, et al. 2016. Habitat-based cetacean density models for the U.S. Atlantic and Gulf of Mexico. Sci Rep. 6. doi:10.1038/srep22615.

Rolland RM, Parks SE, Hunt KE, Castellote M, Corkeron PJ, Nowacek DP, Wasser SK, Kraus SD. 2012. Evidence that ship noise increases stress in right whales. Proc R Soc B Biol Sci. 279(1737):2363–2368. doi:10.1098/rspb.2011.2429.

Russell DJF, Brasseur SMJM, Thompson D, Hastie GD, Janik VM, Aarts G, McClintock BT, Matthiopoulos J, Moss SEW, McConnell B. 2014. Marine mammals trace anthropogenic structures at sea. Curr Biol. 24(14):638–639. doi:10.1016/j.cub.2014.06.033.

Russell DJF, Hastie GD, Thompson D, Janik VM, Hammond PS, Scott-Hayward LAS, Matthiopoulos J, Jones EL, McConnell BJ. 2016. Avoidance of wind farms by harbour seals is limited to pile driving activities. J Appl Ecol. 53(6):1642–1652. doi:10.1111/1365-2664.12678.

Salisbury DP, Clark CW, Rice AN. 2016. Right whale occurrence in the coastal waters of Virginia, U.S.A.: Endangered species presence in a rapidly developing energy market. Mar Mammal Sci. 32(2):508–519. doi:10.1111/mms.12276.

Sayigh LS, Tyack PL, Wells RS, Scott MD. 1990. Signature whistles of free-ranging bottlenose dolphins *Tursiops truncatus*: Stability and mother-offspring somparisons. Behav Ecol Sociobiol. 26(4):247–260.

Schaffeld T, Bräger S, Gallus A, Dähne M, Krügel K, Herrmann A, Jabbusch M, Ruf T, Verfuß UK, Benke H, et al. 2016. Diel and seasonal patterns in acoustic presence and foraging behaviour of free-ranging harbour porpoises. Mar Ecol Prog Ser. 547(Au 1993):257–272. doi:10.3354/meps11627.

Scheidat M, Tougaard J, Brasseur S, Carstensen J, Van Polanen Petel T, Teilmann J, Reijnders P. 2011. Harbour porpoises (*Phocoena phocoena*) and wind farms: A case study in the Dutch North Sea. Environ Res Lett. 6(2):025102. doi:10.1088/1748-9326/6/2/025102.

Schoener TW. 1971. Theory of feeding strategies. Annu Rev Ecol Syst. 2:369–404.

Scott WB, Scott MG. 1988. Atlantic Fishes of Canada. Toronto, Ontario: University of Toronto Press.

Selzer LA, Payne PM. 1988. The distribution of white-sided (*Lagenorynchus acutus*) and common dolphins (*Delphinus delphis*) vs. environmental features of the continental shelf of the northeastern United States. Mar Mammal Sci. 4:141–153.

Shotton R, Randall R. 1982. Results of acoustic surveys of the southwest Nova Scotia (NAFO Division 4WX) herring stock during February and July 1981. Can Atl Fish Sci Adv Comm Res Doc 82/441982.

Simard P, Hibbard AL, McCallister KA, Frankel AS, Zeddies DG, Sisson GM, Gowans S, Forys EA, Mann DA. 2010. Depth dependent variation of the echolocation pulse rate of bottlenose dolphins (*Tursiops truncatus*). J Acoust Soc Am. 127(1):568–578. doi:10.1121/1.3257202.

Sims DW, Quayle VA. 1998. Selective foraging behaviour of basking sharks on zooplankton in a small-scale front. Nature. 393:460–464.

Sing TO, Sander O, Beerenwinkel N, Lengauer T. 2005. ROCR: Visualizing classifier performance in R. Bioinformatics. 21:3940–3941.

Širović A, Hildebrand JA, Wiggins SM. 2007. Blue and fin whale call source levels and propagation range in the Southern Ocean. J Acoust Soc Am. 122(2):1208–1215. doi:10.1121/1.2749452.

Southall BL, Bowles AE, Ellison WT, Finneran JJ, Gentry RL, Greene CR, Kastak D, Ketten DR, Miller JH, Nachtigall PE, et al. 2007. Marine mammal noise exposure: Intitial scientific recommendations. Aquat Mamm. 33(4):411–520.

Stasinopoulos DM, Rigby B, Eilers P. 2016. gamlss.util: GAMLSS Utilities.

Stimpert AK, Au WWL, Parks SE, Hurst T, Wiley DN. 2011. Common humpback whale (*Megaptera novaeangliae*) sound types for passive acoustic monitoring. J Acoust Soc Am. 129(1):476–482. doi:10.1121/1.3504708.

Swingle WM, Barco S, Pitchford T, McLellan WA, Pabst D. 1993. Appearance of juvenile humpback whales feeding in the nearshore waters of Virginia. Mar Mammal Sci. 9:309–315.

Swingle WM, Lynott MC, Bates EB, D'Eri LR, Lockhart GG, Phillips KM, Thomas MD. 2016. Virginia

Sea Turtle and Marine Mammal Stranding Network 2015 Grant Report. Final Report to the Virginia Coastal Zone Management Program, NOAA CZM Grant #NA14NOS4190141, Task 49. VAQF Scientific Report 2016-01. 2016(01):47.

Teilmann J, Carstensen J. 2012. Negative long term effects on harbour porpoises from a large scale offshore wind farm in the Baltic - Evidence of slow recovery. Environ Res Lett. 7(4). doi:10.1088/1748-9326/7/4/045101.

Thomisch K, Boebel O, Zitterbart DP, Samaran F, Van Parijs S, Van Opzeeland I. 2015. Effects of subsampling of passive acoustic recordings on acoustic metrics. J Acoust Soc Am. 138(1):267–278. doi:10.1121/1.4922703.

Thompson PM, Brookes KL, Graham IM, Barton TR, Needham K, Bradbury G, Merchant ND. 2013. Short-term disturbance by a commercial two-dimensional seismic survey does not lead to long-term displacement of harbour porpoises. Proc R Soc B Biol Sci. 280(1771). doi:10.1098/rspb.2013.2001.

Thompson PM, Lusseau D, Barton T, Simmons D, Rusin J, Bailey H. 2010. Assessing the responses of coastal cetaceans to the construction of offshore wind turbines. Mar Pollut Bull. 60(8):1200–1208. doi:10.1016/j.marpolbul.2010.03.030.

Thompson PO, Findley LT, Vidal O. 1992. 20-Hz pulses and other vocalizations of fin whales, *Balaenoptera physalus*, in the Gulf of California, Mexico. J Acoust Soc Am. 92(6):3051–3057. doi:10.1121/1.404201.

Thums M, Bradshaw CJA, Hindell MA. 2011. In situ measures of foraging success and prey encounter reveal marine habitat-dependent search strategies. Ecology. 92(6):1258–1270.

Tinbergen N, Impekoven M, Franck D. 1967. An experiment on spacing-out as a defence against predation. Behaviour. 28:307–321.

Todd VLG, Pearse WD, Tregenza NC, Lepper PA, Todd IB. 2009. Diel echolocation activity of harbour porpoises (*Phocoena phocoena*) around North Sea offshore gas installations. ICES J Mar Sci. 66(4):734–745. doi:10.1093/icesjms/fsp035.

Toth JL, Hohn AA, Able KW, Gorgone AM. 2011. Patterns of seasonal occurrence, distribution, and site fidelity of coastal bottlenose dolphins (*Tursiops truncatus*) in southern New Jersey, U.S.A. Mar Mammal Sci. 27(1):94–110. doi:10.1111/j.1748-7692.2010.00396.x.

Tougaard J, Carstensen J, Teilmann J, Skov H, Rasmussen P. 2009. Pile driving zone of responsiveness extends beyond 20 km for harbor porpoises (*Phocoena phocoena* (L.)). J Acoust Soc Am. 126(1):11–14. doi:10.1121/1.3132523.

Tougaard J, Henriksen OD, Miller LA. 2009. Underwater noise from three types of offshore wind turbines: Estimation of impact zones for harbor porpoises and harbor seals. J Acoust Soc Am. 125(6):3766–3773. doi:10.1121/1.3117444.

Urazghildiiev IR, Clark CW. 2006. Acoustic detection of North Atlantic right whale contact calls using the generalized likelihood ratio test. J Acoust Soc Am. 120(4):1956–1963. doi:10.1121/1.2257385.

Urazghildiiev IR, Clark CW. 2013. Comparative analysis of localization algorithms with application to passive acoustic monitoring. J Acoust Soc Am. 134(6):4418–4426. doi:10.1121/1.4824683.

Urazghildiiev IR, Clark CW, Krein TP, Parks SE. 2009. Detection and recognition of North Atlantic right

whale contact calls in the presence of ambient noise. IEEE J Ocean Eng. 34(3):358–368. doi:10.1109/JOE.2009.2014931.

Verfuß UK, Honnef CG, Meding A, Dähne M, Mundry R, Benke H. 2007. Geographical and seasonal variation of harbour porpoise (*Phocoena phocoena*) presence in the German Baltic Sea revealed by passive acoustic monitoring. J Mar Biol Assoc United Kingdom. 87(1):165–176. doi:10.1017/S0025315407054938.

Vu E, Risch D, Clark C, Gaylord S, Hatch L, Thompson M, Wiley D, Van Parijs S. 2012. Humpback whale song occurs extensively on feeding grounds in the western North Atlantic Ocean. Aquat Biol. 14(2):175–183. doi:10.3354/ab00390.

Wahlberg M, Jensen FH, Aguilar Soto N, Beedholm K, Bejder L, Oliveira C, Rasmussen M, Simon M, Villadsgaard A, Madsen PT. 2011. Source parameters of echolocation clicks from wild bottlenose dolphins (*Tursiops aduncus* and *Tursiops truncatus*). J Acoust Soc Am. 130(4):2263–2274. doi:10.1121/1.3624822.

Wahlberg M, Westerberg H. 2005. Hearing in fish and their reactions to sounds from offshore wind farms. Mar Ecol Prog Ser. 288(2001):295–309. doi:10.3354/meps288295.

Watkins WA, Tyack PL, Moore KE, Bird JE. 1987. The 20-Hz signals of finback whales (*Balaenoptera physalus*). J Acoust Soc Am. 82(1901):1901–1912. doi:10.1121/1.397466.

Webster WD, Goley PD, Pustis J, Gouveia JF. 1995. Seasonality in cetacean strandings along the coast of North Carolina. Brimleyana. 0(23):41–51.

Weilgart LS. 2007. The impacts of anthropogenic ocean noise on cetaceans and implications for management. Can J Zool. 85(11):1091–1116. doi:10.1139/Z07-101.

Weirathmueller MJ, Wilcock WSD, Soule DC. 2013. Source levels of fin whale 20 Hz pulses measured in the Northeast Pacific Ocean. J Acoust Soc Am. 133(2):741–749. doi:10.1121/1.4773277.

Wenz GGM. 1972. Review of underwater acoustics research: Noise. J Acoust Soc Am. 51(3):1010–1024. doi:10.1121/1.1912921.

Westgate AJ, Read AJ, Berggren P, Koopman HN, Gaskin DE. 1995. Diving behaviour of harbour porpoises, *Phocoena phocoena*. Can J Fish Aquat Sci. 52(5):1064–1073. doi:10.1139/f95-104.

Whitt AD, Dudzinski K, Laliberté JR. 2013. North Atlantic right whale distribution and seasonal occurrence in nearshore waters off New Jersey, USA, and implications for management. Endanger Species Res. 20(1):59–69. doi:10.3354/esr00486.

Wiley D, Asmutis R, Pitchford T, Gannon D. 1995. Stranding and mortality of humpback whales, *Megaptera novaeangliae*, in the Mid-Atlantic and Southeast United-States, 1985-1992. Fish Bull. 93(1):196–205.

Williams KA, Connelly EE, Johnson SM, Stenhouse IJ. 2015. Baseline wildlife studies in Atlantic waters offshore of Maryland: Final report to the Maryland Department of Natural Resources and the Maryland Energy Administration. Portland, Maine.

Williamson CE. 1981. Foraging behavior of a freshwater copepod: Frequency changes in looping behavior at high and low prey densities. Oecologia. 50:332–336.

Williamson LD, Brookes KL, Scott BE, Graham IM, Bradbury G, Hammond PS, Thompson PM. 2016. Echolocation detections and digital video surveys provide reliable estimates of the relative density of harbour porpoises. Methods Ecol Evol. 7(7):762–769. doi:10.1111/2041-210X.12538.

Wingfield JE, O'Brien M, Lyubchich V, Roberts JJ, Halpin PN, Rice AN, Bailey H. 2017. Year-round spatiotemporal distribution of harbour porpoises within and around the Maryland wind energy area. PLoS One. 12(5):1–18. doi:10.1371/journal.pone.0176653.

Winn HE, Price CA, Sorensen PW. 1986. The distributional biology of the right whale (*Eubalaena glacialis*) in the Western North Atlantic.

Wisniewska DM, Jonson M, Tielmann J, Siebert U, Galatius A, Dietz R, Madsen PT. 2018. High rates of vessel noise exposure on wild harbour porpoises (*Phocoena phocoena*). Proc R Soc B. 285:20172314. doi:10.1098/rspb.2017.2314.

Wood SN. 2006. Generalized Additive Models: An Introduction with {R}. Boca Raton, FL: CRC Press.

Xu Y, Chant R, Gong D, Castelao R, Glenn S, Schofield O. 2011. Seasonal variability of chlorophyll a in the Mid-Atlantic Bight. Cont Shelf Res. 31(16):1640–1650. doi:10.1016/j.csr.2011.05.019.

Yack T, Barlow J, Rankin S, Gillespie D. 2009. Testing and validation of automated whistle and click detectors using PAMGUARD 1.0 NOAA Technical Memorandum NMFS National Oceanic and Atmospheric Administration. (April):1–63.

Young DD, Cockcroft VG. 1994. Diet of common dolphins (*Delphinus delphis*) off the south-east coast of southern Africa: Opportunism or specialization? J Zool. 234:41–53.

Zach R, Falls JB. 1977. Influence of capturing a prey on subsequent search in the ovenbird (Aves: Parulidae). Can J Zool. 55:1958–1969.

Zucchini W, MacDonald IL, Langrock R. 2016. Hidden markov models for time series: An introduction using R, monographs on statistics and applied probability. Second Edi. Boca Raton, FL: CRC Press.

Zuur AF, Ieno EN, Walker NJ, Saveliev AA, Smith GM. 2009. Mixed effects models and extensions in ecology with R. New York, New York, USA: Springer-Verlag.

Appendix A: Baleen Whale Occurrence

The generalized auto-regressive moving average (GARMA) model output for North Atlantic right whale at site A-5M is as follows:

```
Family: c("BI", "Binomial")
Fitting method: "nlminb"
Call: garmaFit(formula = RW_presence ~ coshour + sinday + cosday, order = c(1,0), data = A5M, family
= BI,
 control = list(maxit = 200))
Coefficient(s):
                Estimate  Std. Error  t value   Pr(>|t|)
beta.(Intercept) -13.6364684   1.8227614 -7.48121 7.3719e-14 ***
beta.coshour       0.8311047   0.3071358  2.70598  0.0068102 **
beta.sinday        5.3506748   0.9374218  5.70786 1.1440e-08 ***
beta.cosday        9.2588096   1.3872234  6.67435 2.4834e-11 ***
phi               0.7694012   0.0313272 24.56019 < 2.22e-16 ***
---
Signif. codes:  0 ‘***’ 0.001 ‘**’ 0.01 ‘*’ 0.05 ‘.’ 0.1 ‘ ’ 1
Degrees of Freedom for the fit: 5 Residual Deg. of Freedom   6547
Global Deviance:     1542.74
          AIC:     1552.74
          SBC:     1586.68
```

The generalized auto-regressive moving average (GARMA) model output for North Atlantic right whale at site T-1M is as follows:

```
Family:  c("BI", "Binomial")

Call:  gamlss(formula = formula, family = family, data = data, trace = FALSE)

Fitting method: RS()

------------------------------------------------------------------
Mu link function:  logit
Mu Coefficients:
          Estimate Std. Error t value Pr(>|t|)
(Intercept)  -5.3496     0.2556 -20.933  < 2e-16 ***
sinday        1.3433     0.2252   5.965 2.58e-09 ***
cosday        2.2077     0.2764   7.989 1.60e-15 ***
---
Signif. codes:  0 ‘***’ 0.001 ‘**’ 0.01 ‘*’ 0.05 ‘.’ 0.1 ‘ ’ 1
------------------------------------------------------------------
No. of observations in the fit:  6455
Degrees of Freedom for the fit:  3
      Residual Deg. of Freedom:  6452
                  at cycle:  2
Global Deviance:     900.8849
          AIC:     906.8849
          SBC:     927.2028
```

The generalized auto-regressive moving average (GARMA) model output for North Atlantic right whale at site T-2M is as follows:

Family: c("BI", "Binomial")
Fitting method: "nlminb"

Call: garmaFit(formula = RW_presence ~ sinday + cosday, order = c(1, 0), data = T2M, family = BI, control = list(maxit = 200))
Coefficient(s):

	Estimate	Std. Error	t value	Pr(>|t|)	
beta.(Intercept)	-10.8719606	1.4131485	-7.69343	1.4433e-14	***
beta.sinday	4.5031602	0.7660208	5.87864	4.1365e-09	***
beta.cosday	5.6688975	0.8727321	6.49558	8.2717e-11	***
phi	0.7624022	0.0329488	23.13898	< 2.22e-16	***

Signif. codes: 0 ‘***’ 0.001 ‘**’ 0.01 ‘*’ 0.05 ‘.’ 0.1 ‘ ’ 1
Degrees of Freedom for the fit: 4 Residual Deg. of Freedom 6284
Global Deviance: 1595.66
AIC: 1603.66
SBC: 1630.64

The generalized auto-regressive moving average (GARMA) model output for humpback whale at site A-5M is as follows:

Family: c("BI", "Binomial")
Fitting method: "nlminb"

Call: garmaFit(formula = HW_Presence ~ sinday + cosday, order = c(2, 0), data = A5M, family = BI, control = list(maxit = 200))
Coefficient(s):

	Estimate	Std. Error	t value	Pr(>|t|)	
beta.(Intercept)	-37.6909322	7.9166815	-4.76095	1.9268e-06	***
beta.sinday	22.0894284	4.7749732	4.62608	3.7264e-06	***
beta.cosday	7.0745476	2.0702300	3.41728	0.00063251	***
phi1	0.6875314	0.0409011	16.80960	< 2.22e-16	***
phi2	0.2507957	0.0408772	6.13534	8.4977e-10	***

Signif. codes: 0 ‘***’ 0.001 ‘**’ 0.01 ‘*’ 0.05 ‘.’ 0.1 ‘ ’ 1
Degrees of Freedom for the fit: 5 Residual Deg. of Freedom 6547
Global Deviance: 1313.66
AIC: 1323.66
SBC: 1357.6

The generalized auto-regressive moving average (GARMA) model output for humpback whale at site T-1M is as follows:

Family: c("BI", "Binomial")

Call: gamlss(formula = formula, family = family, data = data, trace = FALSE)

Fitting method: RS()

Mu link function: logit
Mu Coefficients:

	Estimate	Std. Error	t value	Pr(>|t|)	
(Intercept)	-6.4916	0.3804	-17.064	< 2e-16	***
sinhour	-0.5619	0.3686	-1.524	0.12753	
coshour	0.4700	0.3646	1.289	0.19741	
sinday	1.2273	0.4522	2.714	0.00667	**
cosday	0.6009	0.3959	1.518	0.12909	

Signif. codes: 0 '***' 0.001 '**' 0.01 '*' 0.05 '.' 0.1 ' ' 1

No. of observations in the fit: 6455
Degrees of Freedom for the fit: 5
Residual Deg. of Freedom: 6450
at cycle: 2
Global Deviance: 219.9691
AIC: 229.9691
SBC: 263.8322

The generalized auto-regressive moving average (GARMA) model output for humpback whale at site T-2M is as follows:

Family: c("BI", "Binomial")
Fitting method: "nlminb"

Call: garmaFit(formula = HW_Presence ~ sinhour + sinday, order = c(2,0), data = T2M, family = BI, control =
list(maxit = 200))
Coefficient(s):

	Estimate	Std. Error	t value	Pr(>|t|)	
beta.(Intercept)	-31.8158611	6.5429690	-4.86260	1.1585e-06	***
beta.sinhour	1.0628494	0.3281494	3.23892	0.0011998	**
beta.sinday	18.4760758	3.8704895	4.77358	1.8098e-06	***
phi1	0.7100076	0.0398652	17.81019	< 2.22e-16	***
phi2	0.2217778	0.0396953	5.58701	2.3101e-08	***

Signif. codes: 0 '***' 0.001 '**' 0.01 '*' 0.05 '.' 0.1 ' ' 1

Degrees of Freedom for the fit: 5 Residual Deg. of Freedom 6283
Global Deviance: 1379.08
AIC: 1389.08
SBC: 1422.81

The generalized auto-regressive moving average (GARMA) model output for fin whale at site A-5M is as follows:
Family: c("BI", "Binomial")
Fitting method: "nlminb"

```
Call:  garmaFit(formula = FW_Presence ~ cosday, order = c(2, 0), data = A5M, family = BI,
control = list(maxit = 200))
Coefficient(s):
                Estimate  Std. Error  t value   Pr(>|t|)
beta.(Intercept) -10.6353084   1.9798591 -5.37175 7.7976e-08 ***
beta.cosday       14.6886180   2.6686672  5.50410 3.7105e-08 ***
phi1               0.6690335   0.0231047 28.95660 < 2.22e-16 ***
phi2               0.2446367   0.0232896 10.50413 < 2.22e-16 ***
---
Signif. codes:  0 ‘***’ 0.001 ‘**’ 0.01 ‘*’ 0.05 ‘.’ 0.1 ‘ ’ 1
 Degrees of Freedom for the fit: 4 Residual Deg. of Freedom   6548
Global Deviance:     3320.97
         AIC:     3328.97
         SBC:     3356.12
```

Appendix B: Acoustic Localization of North Atlantic Right Whales

Location estimates for North Atlantic right whale up-calls were modeled using the correlation sum estimation (CSE) Locator Tool in Raven 2.0 (Cornell Lab of Ornithology Bioacoustics Research Program). The CSE localization algorithm functions by searching for a point in space which maximizes the output power of a simple delay-and-sum beamformer. The beamformer output is given by the expression

$$y(t) = \sum_{i=1}^{N} x_i\,(t - t_i)$$

Where $x_i(t)$ is the signal received by the i^{th} sensor at time t, and t_i is a delay parameter which is used to steer the output $y(t)$ to a particular point in space. The average power in the signal $y(t)$ is given by

$$P_{ave} = \frac{1}{T}\int_0^T y(t)y^*\,(t)dt$$

Which becomes

$$P_{ave} = \frac{1}{T}\sum_{i=1}^{N}\sum_{j=1}^{N}\int_0^T x_i(t - t_i)x_j^*\big(t - t_j\big)dt$$

$$P_{ave} = \frac{1}{T}\sum_{i=1}^{N}\sum_{j=1}^{N}\int_0^T x_i(t')x_j^*\big(t' + t_i - t_j\big)dt'$$

The term under the integral sign is exactly the correlation function $R_{ij}\big(\tau_{ij}\big)$, where $\tau_{ij} = t_i - t_j$. So the average power is equal to the pairwise sum of the cross correlation functions evaluated at the time difference of arrival (TDOAs). To relate the TDOAs to a position in space, we can write

$$\tau_{ij}(\boldsymbol{r}) = \frac{|\,\boldsymbol{r} - \boldsymbol{r_i}| - |\,\boldsymbol{r} - \boldsymbol{r_j}|}{c}$$

Where $\boldsymbol{r}$ is the location in space of the source, $\boldsymbol{r_i}$ is the location in space of the i^{th}sensor, and c is the speed of sound. The CSE algorithm proceeds as follows:

1) Compute the pairwise correlation functions for all channels.
2) Initialize the search area to encompass a 40 x 40 km square about the centroid of the array.
3) Randomly place 9000 trial locations within the search region.
4) At each point, compute the set of theoretical TDOAs $\{\ \tau_{ij}\}$.
5) Compute the average power P_{ave} as the sum of the correlation functions evaluated at the TDOAs $\{\ \tau_{ij}\}$.
6) Take the top 15% of the points and compute their centroid.

7) Check for convergence. If the search area radius has not converged to 5 meters or less, decrease the radius of the search area by 10%, center the new search area on the centroid computed in step 6, and repeat steps 3 through 7.

To estimate the standard deviation of the location, we proceed as follows:

1) Compute the average power at a set of 100 points uniformly placed around the location as determined above.
2) Fit a paraboloid to the 100 points such that we have an analytical expression for the local average power surface.
3) Estimate the variance σ^2 of the peak of the energy surface using Box's formula for the variance of a cross correlation.
4) Form a two dimensional cut parallel to the x-y plane 2σ down from the paraboloid peak. This cut will have the shape of an ellipse; find its major and minor axes, these are the 95% confidence limits.

In order to estimate the accuracy and precision of the CSE localization algorithm, we compared the known locations of empirical data (synthetic playback signals that were transmitted in the survey area) to the estimated locations of the empirical data produced by the Raven 2.0 CSE locator tool. The accuracy estimation procedure was as follows:

1) Open a Raven selection table containing the time-frequency bounds of the 300 to 600 Hz sweeps.

2) Add the "Begin Clock Time" measurement

2) Run the Raven 2.0 CSE locator using the following settings:

Correlations tab

- Threshold = 0.1
- Use GCC checked
- Min. Channels = 3
- Complex envelope unchecked

Optimization tab

- Algorithm = Stochastic Search
- Reduction Factor = 0.900
- Points per Dimension = 300
- Top Percentage = 15.0
- Stopping Centroid = 5.0
- Stopping Step Size = 5.00 meters
- Max Function Evaluations = 500000000

Scoring Tab

- Energy Fraction = not included
- Average Correlation = [0, 0.4]
- Number of Channels = [2, 6]
- Peak Deviation = [10, 1]

- Q Value = not included

Search Bounds Tab
- Coordinate System = Cartesian
- X = [-20000, 20000]
- Y =[-20000, 20000]

2) Save the locator results and arrivals tables to new tables

3) Run a custom data analysis program to compare the 'truth' locations and the CSE locator estimated locations

The custom data analysis program cycles through the selection table, first extracting the "Begin Clock Time" of the selection, which is then used to interpolate in time the position of the playback source; this position, latitude and longitude, becomes the 'truth' value. It then uses spherical geometry to compute the distance between the truth position and the estimated position by the locator. As a measure of the precision of the result, the standard deviation is computed to be the greater of the latitude and longitude standard deviations, converted into meters.

North Atlantic right whale up-call locations were estimated using the Raven 2.0 CSE locator tool using the following settings:

Correlations tab
- Threshold = 0.1
- Use GCC checked
- Min. Channels = 3
- Complex envelope unchecked

Optimization tab
- Algorithm = Stochastic Search
- Reduction Factor = 0.900
- Points per Dimension = 300
- Top Percentage = 15.0
- Stopping Centroid = 5.0
- Stopping Step Size = 5.00 meters
- Max Function Evaluations = 500000000

Scoring Tab
- Energy Fraction = not included
- Average Correlation = [0, 0.4]
- Number of Channels = [2, 6]
- Peak Deviation = [10, 1]
- Q Value = not included

Search Bounds Tab
- Coordinate System = Cartesian
- X = [-20000, 20000]

- Y =[-20000, 20000]

Appendix C: Ambient Noise Analysis

Long-term spectrograms for all MARU and AMAR survey sites over the 3-year survey period show a qualitative overview of baseline ambient noise within and surrounding the Maryland WEA and allow for quick visual comparisons of noise levels between sites. Below are the 3-year long-term spectrogram figures for sites inshore (T-1M), offshore (T-2M, T-3*M, T-3M), and within (A-1M through A-8M; AMAR) the WEA.

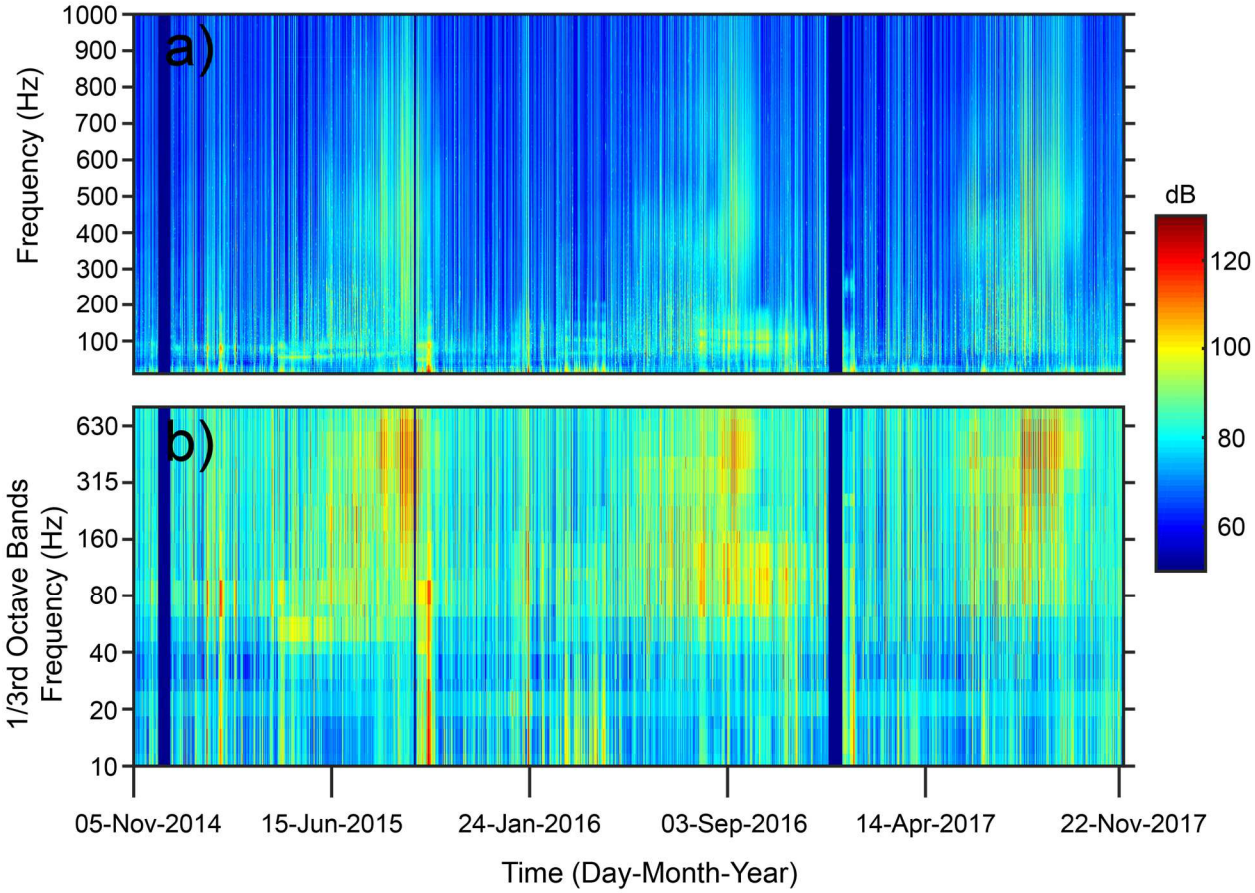

Figure C.1. 3-year long-term spectrograms for site T-1M
Panel a represents noise on a linear scale (Δ *time* = 1 h, Δ *frequency* = 1 Hz) along the Y-axis, while panel b represents noise on a 1/3rd octave scale (Δ *time* = 1 h). Dark blue sections indicate time periods with no sound data.

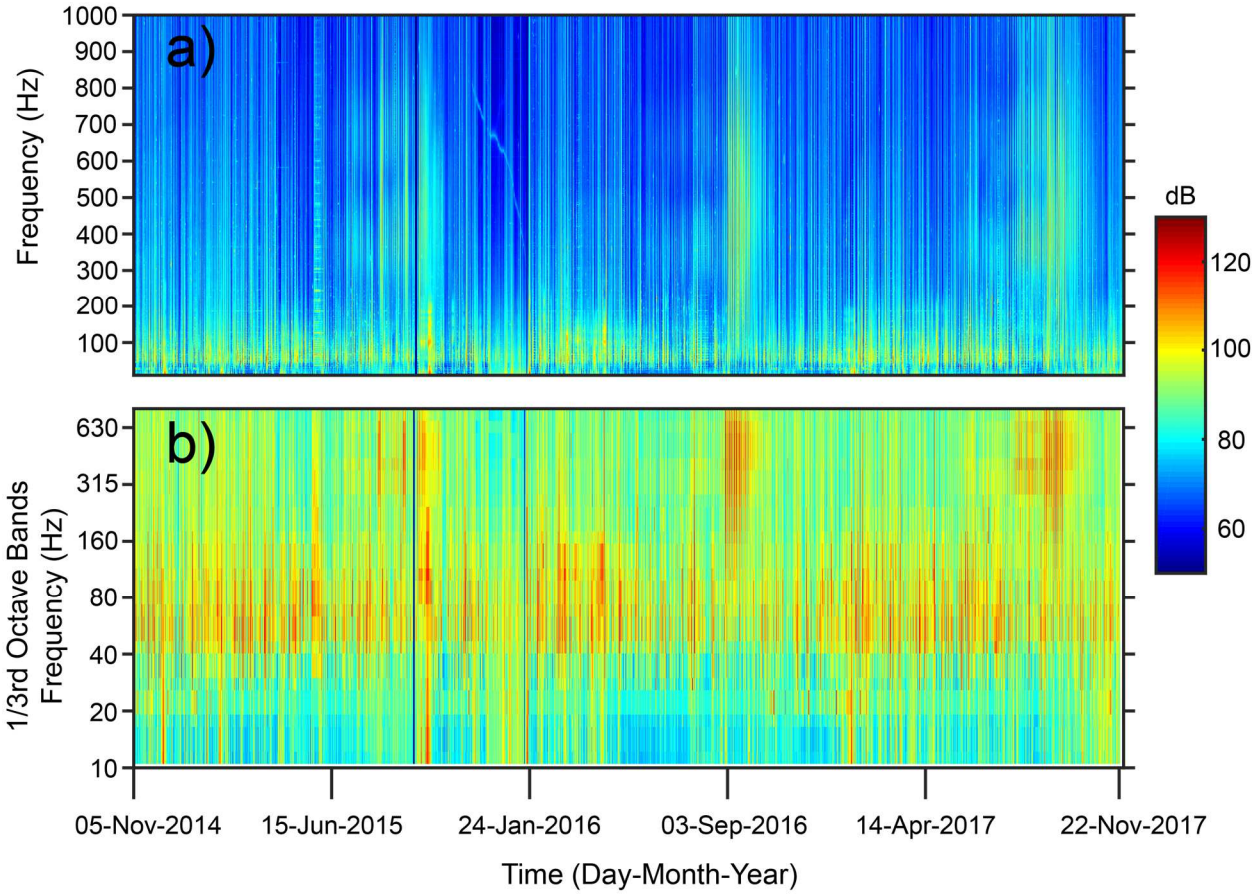

Figure C.2. 3-year long-term spectrograms for site A-1M
Panel a represents noise on a linear scale (Δ *time* = 1 h, Δ *frequency* = 1 Hz) along the Y-axis, while panel b represents noise on a 1/3rd octave scale (Δ *time* = 1 h). Dark blue sections indicate time periods with no sound data.

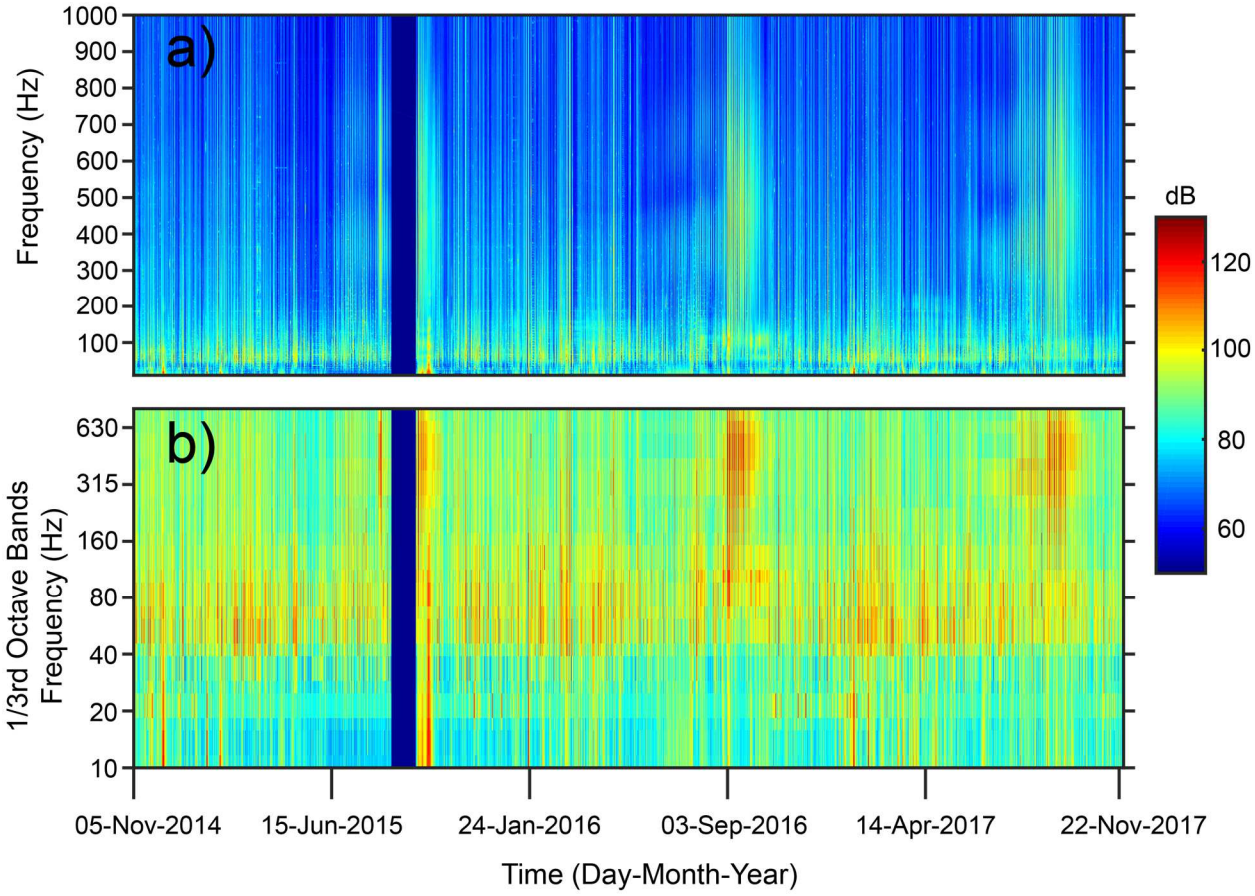

Figure C.3. 3-year long-term spectrograms for site A-2M
Panel a represents noise on a linear scale (Δ *time* = 1 h, Δ *frequency* = 1 Hz) along the Y-axis, while panel b represents noise on a 1/3rd octave scale (Δ *time* = 1 h). Dark blue sections indicate time periods with no sound data.

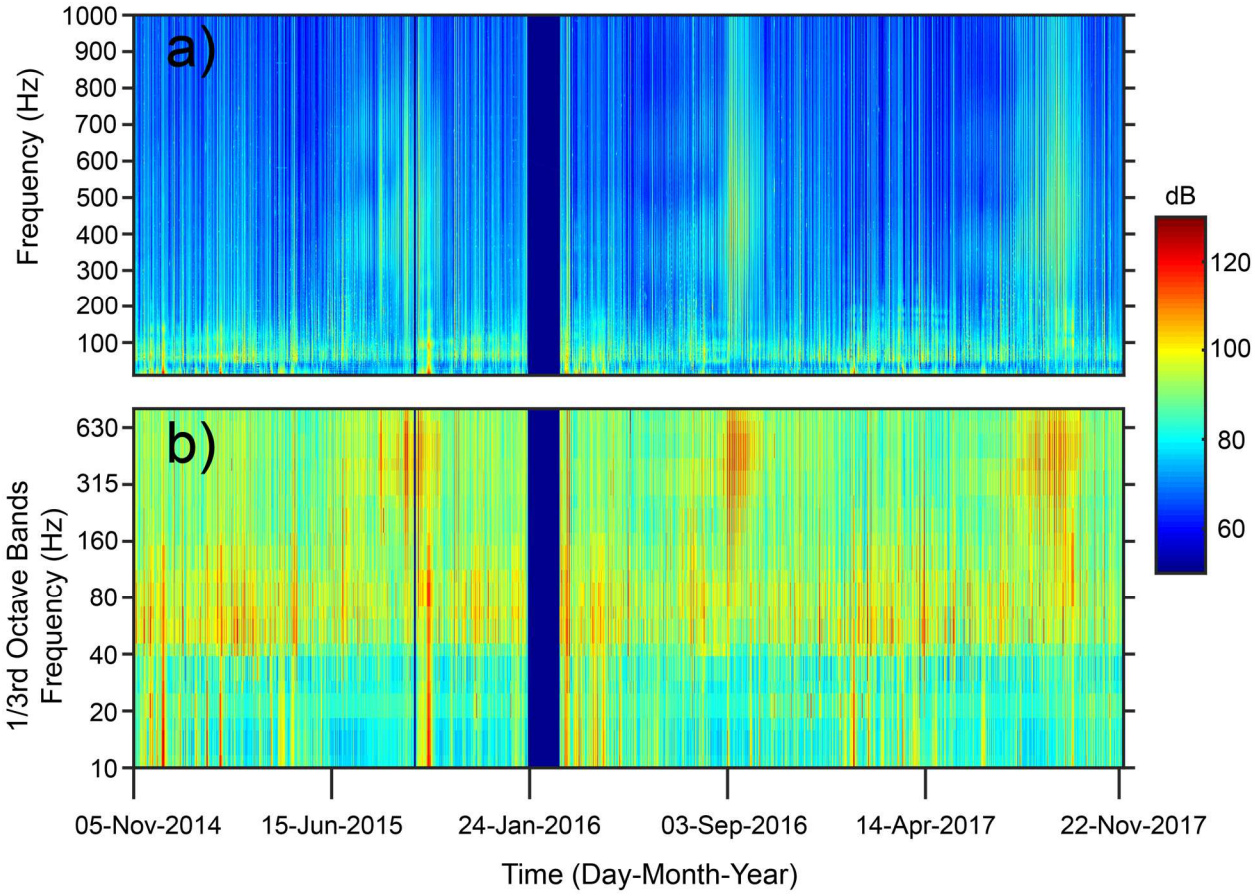

Figure C.4. 3-year long-term spectrograms for site A-3M
Panel a represents noise on a linear scale (Δ *time* = 1 h, Δ *frequency* = 1 Hz) along the Y-axis, while panel b represents noise on a 1/3rd octave scale (Δ *time* = 1 h). Dark blue sections indicate time periods with no sound data.

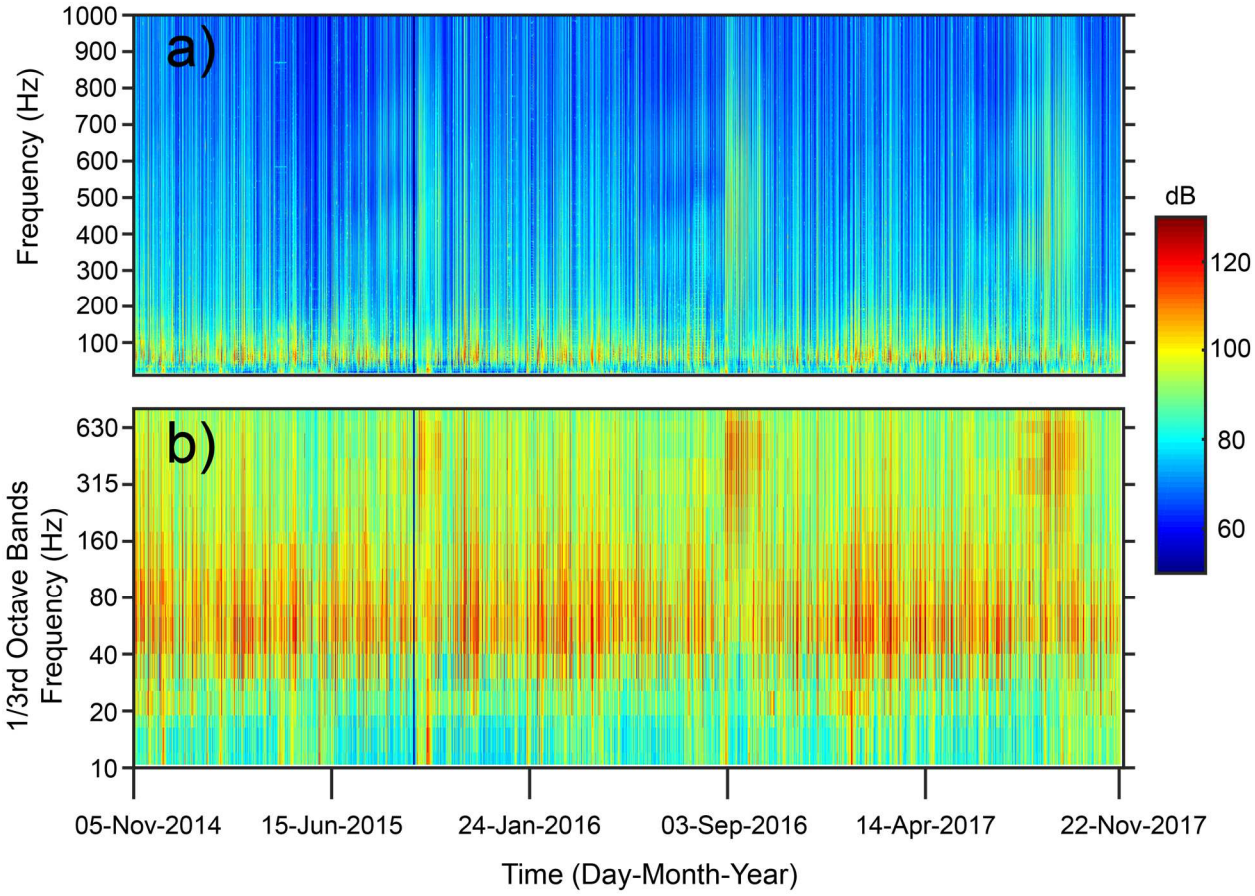

Figure C.5. 3-year long-term spectrograms for site A-4M
Panel a represents noise on a linear scale (Δ *time* = 1 h, Δ *frequency* = 1 Hz) along the Y-axis, while panel b represents noise on a 1/3rd octave scale (Δ *time* = 1 h). Dark blue sections indicate time periods with no sound data.

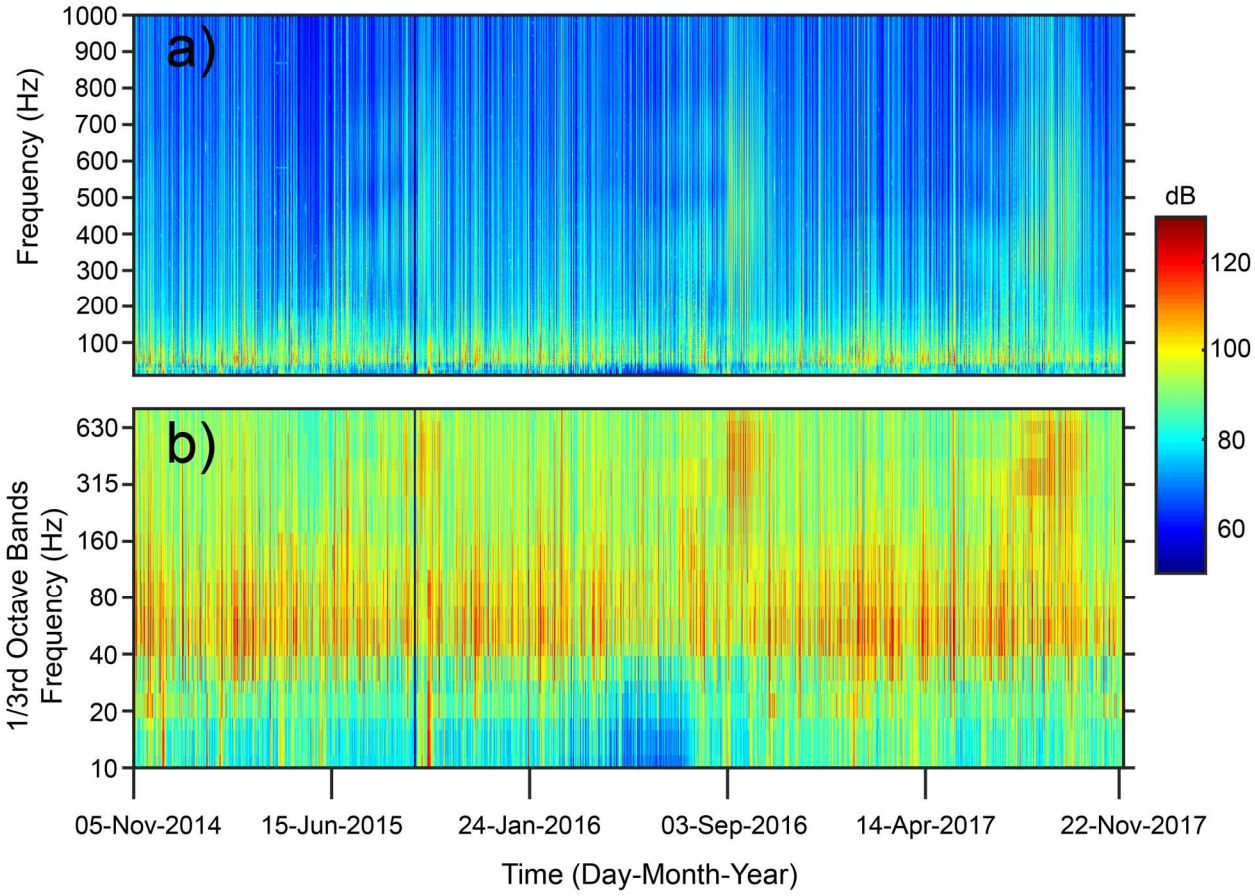

Figure C.6. 3-year long-term spectrograms for site A-5M
Panel a represents noise on a linear scale (Δ *time* = 1 h, Δ *frequency* = 1 Hz) along the Y-axis, while panel b represents noise on a 1/3rd octave scale (Δ *time* = 1 h). Dark blue sections indicate time periods with no sound data.

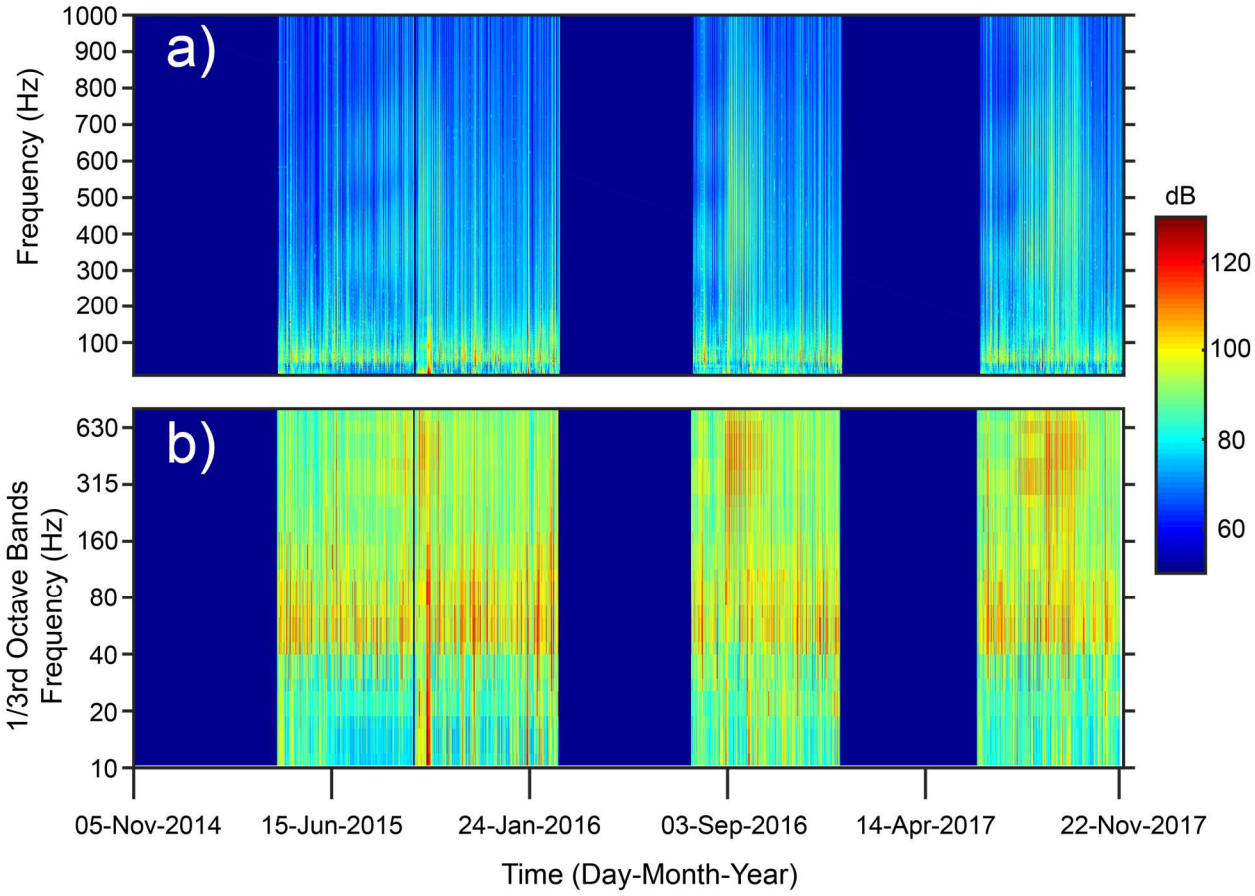

Figure C.7. 3-year long-term spectrograms for site A-6M
Panel a represents noise on a linear scale (Δ *time* = 1 h, Δ *frequency* = 1 Hz) along the Y-axis, while panel b represents noise on a 1/3rd octave scale (Δ *time* = 1 h). Dark blue sections indicate time periods with no sound data.

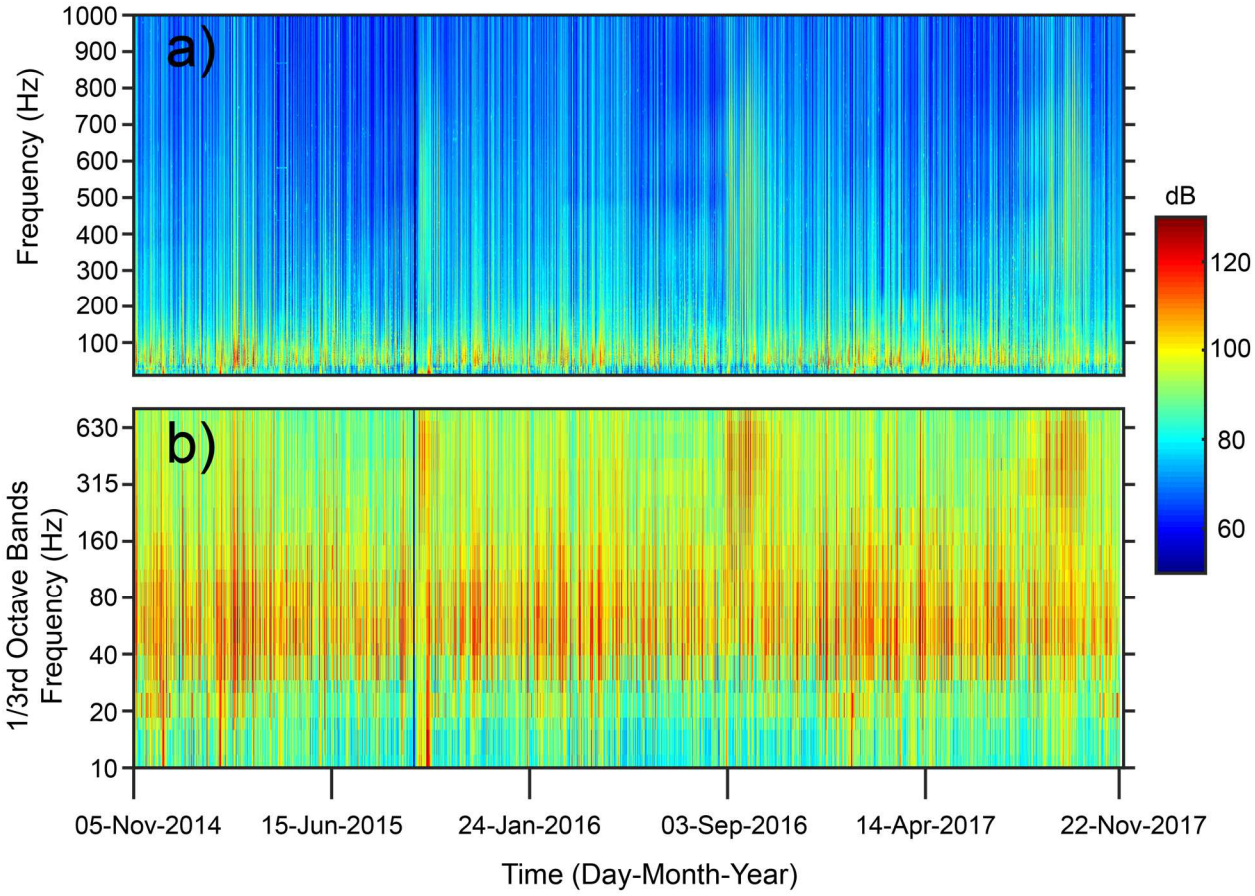

Figure C.8. 3-year long-term spectrograms for site A-7M
Panel a represents noise on a linear scale (Δ *time* = 1 h, Δ *frequency* = 1 Hz) along the Y-axis, while panel b represents noise on a 1/3rd octave scale (Δ *time* = 1 h). Dark blue sections indicate time periods with no sound data.

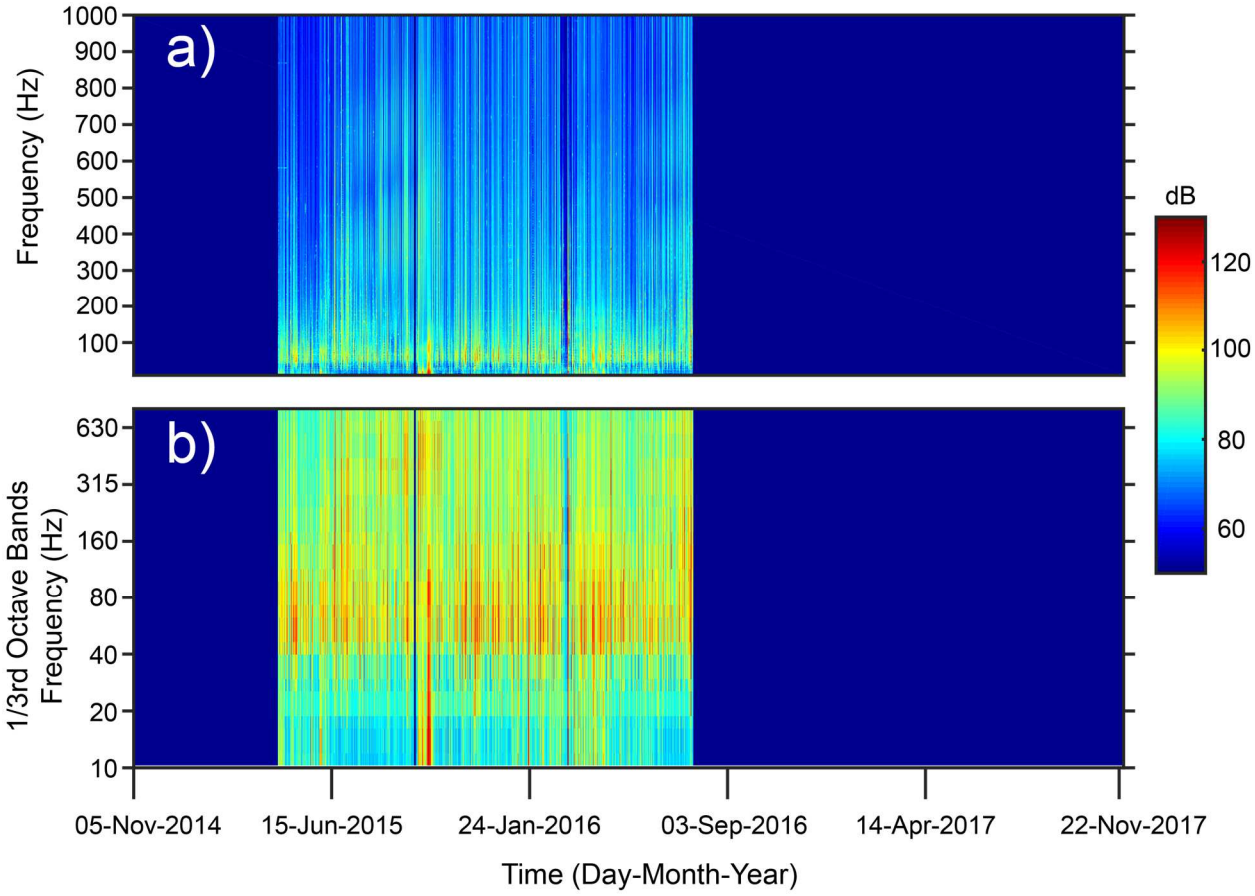

Figure C.9. 3-year long-term spectrograms for site A-8M
Panel a represents noise on a linear scale (Δ *time* = 1 h, Δ *frequency* = 1 Hz) along the Y-axis, while panel b represents noise on a 1/3rd octave scale (Δ *time* = 1 h). Dark blue sections indicate time periods with no sound data.

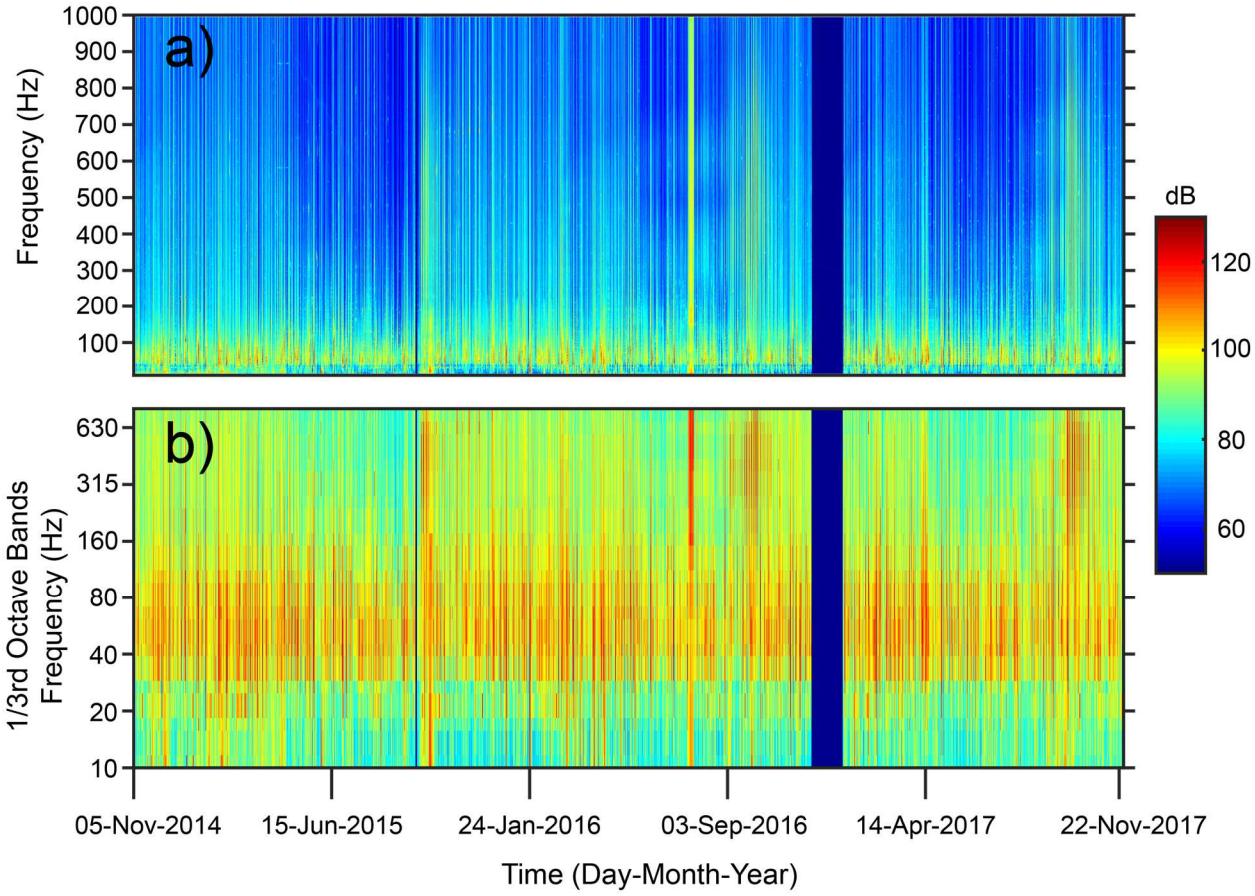

Figure C.10. 3-year long-term spectrograms for site T-2M
Panel a represents noise on a linear scale (Δ *time* = 1 h, Δ *frequency* = 1 Hz) along the Y-axis, while panel b represents noise on a 1/3rd octave scale (Δ *time* = 1 h). Dark blue sections indicate time periods with no sound data.

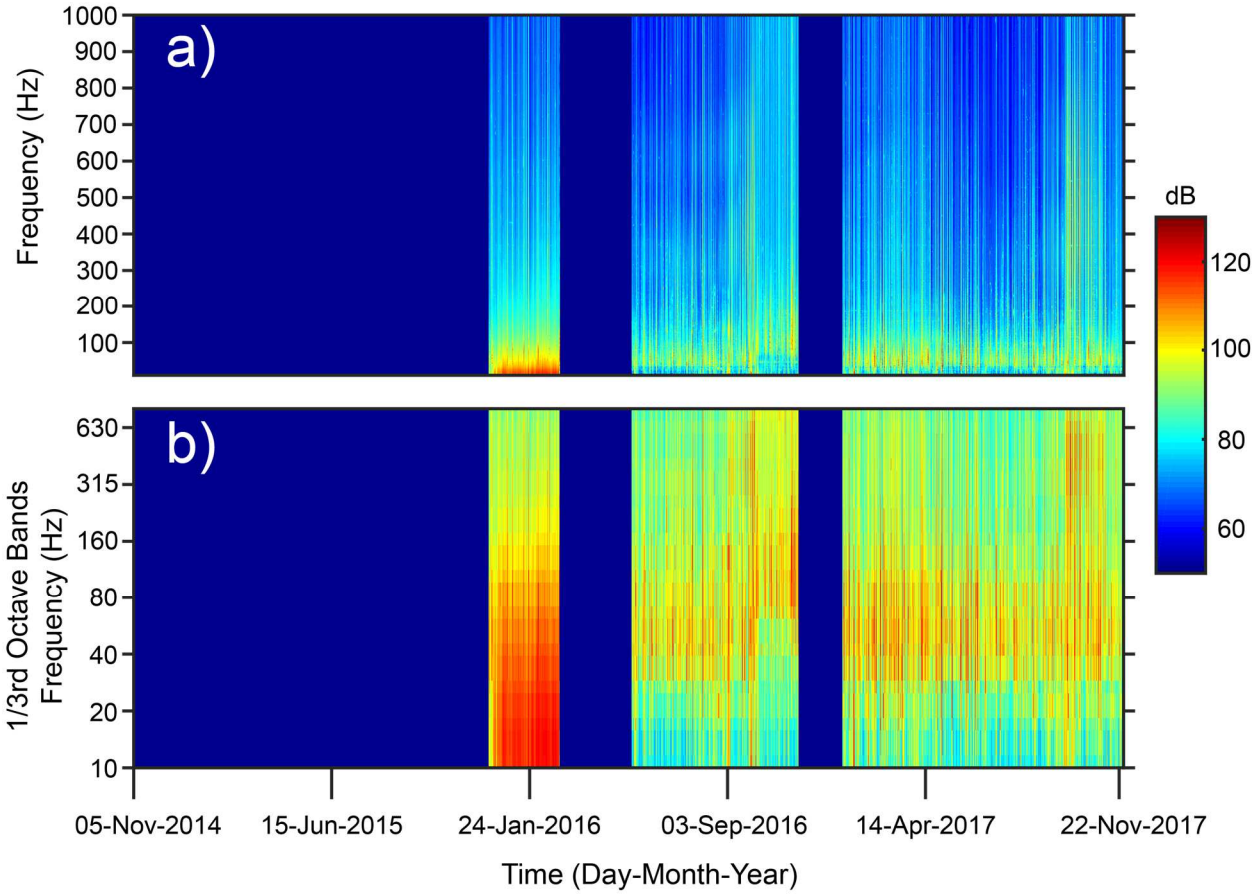

Figure C.11. 3-year long-term spectrograms for site T-3*M
Panel a represents noise on a linear scale (Δ *time* = 1 h, Δ *frequency* = 1 Hz) along the Y-axis, while panel b represents noise on a 1/3rd octave scale (Δ *time* = 1 h). Dark blue sections indicate time periods with no sound data.

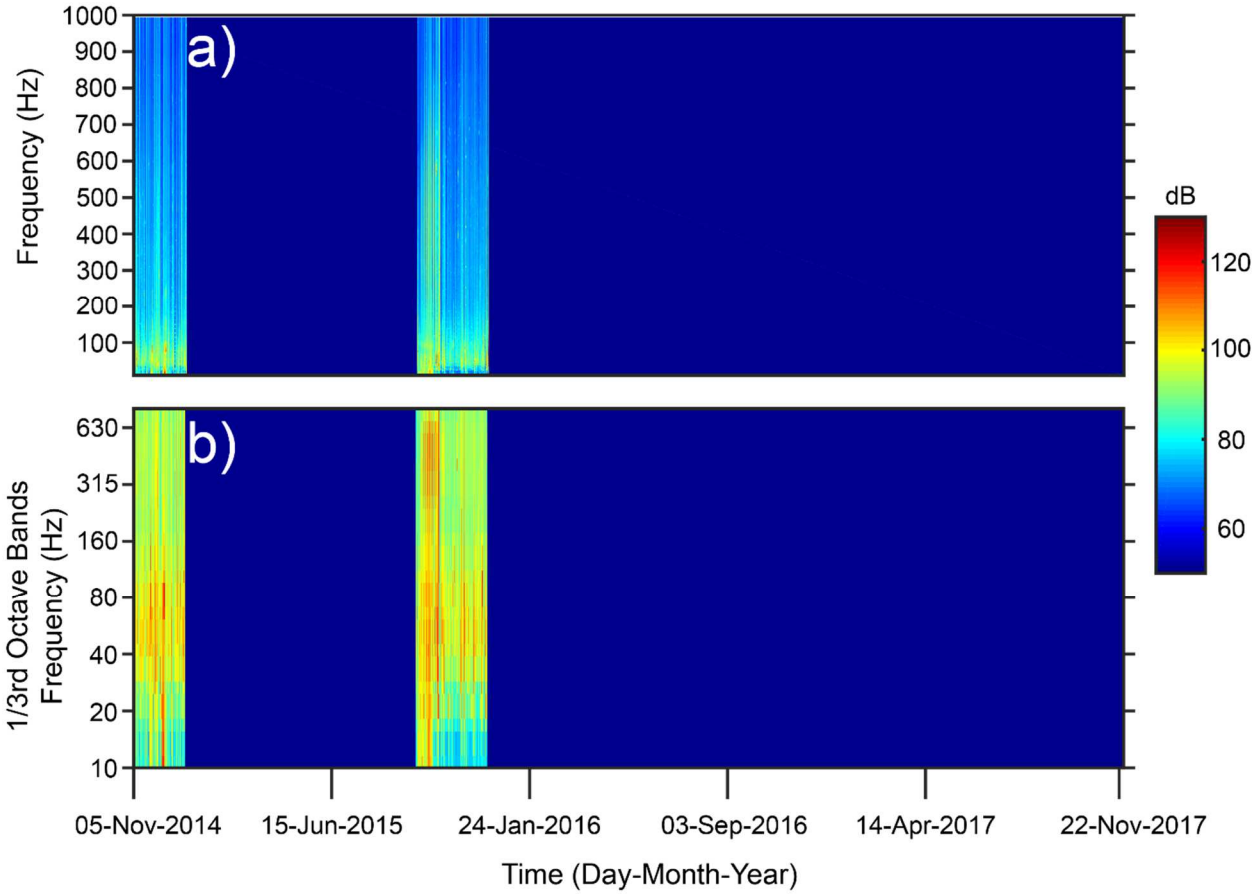

Figure C.12. 3-year long-term spectrograms for site T-3M
Panel a represents noise on a linear scale (Δ *time* = 1 h, Δ *frequency* = 1 Hz) along the Y-axis, while panel b represents noise on a 1/3rd octave scale (Δ *time* = 1 h). Dark blue sections indicate time periods with no sound data.

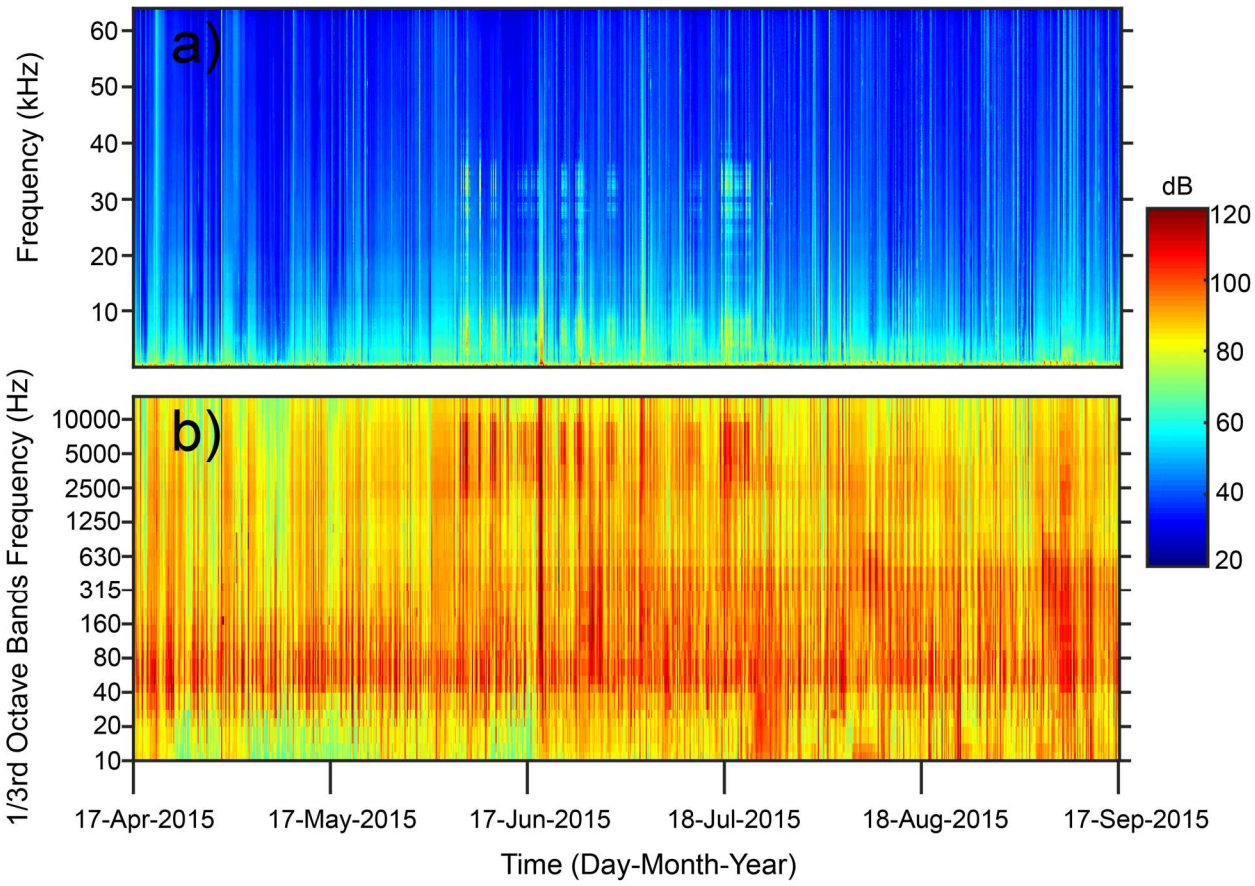

Figure C.13. Deployment 02 (17 April 2015 – 16 Sept 2015) long-term spectrograms for AMAR
Panel a represents noise on a linear scale (Δ *time* = 1 h, Δ *frequency* = 1 Hz) along the Y-axis, while panel b represents noise on a 1/3rd octave scale (Δ *time* = 1 h). Dark blue sections indicate time periods with no sound data.

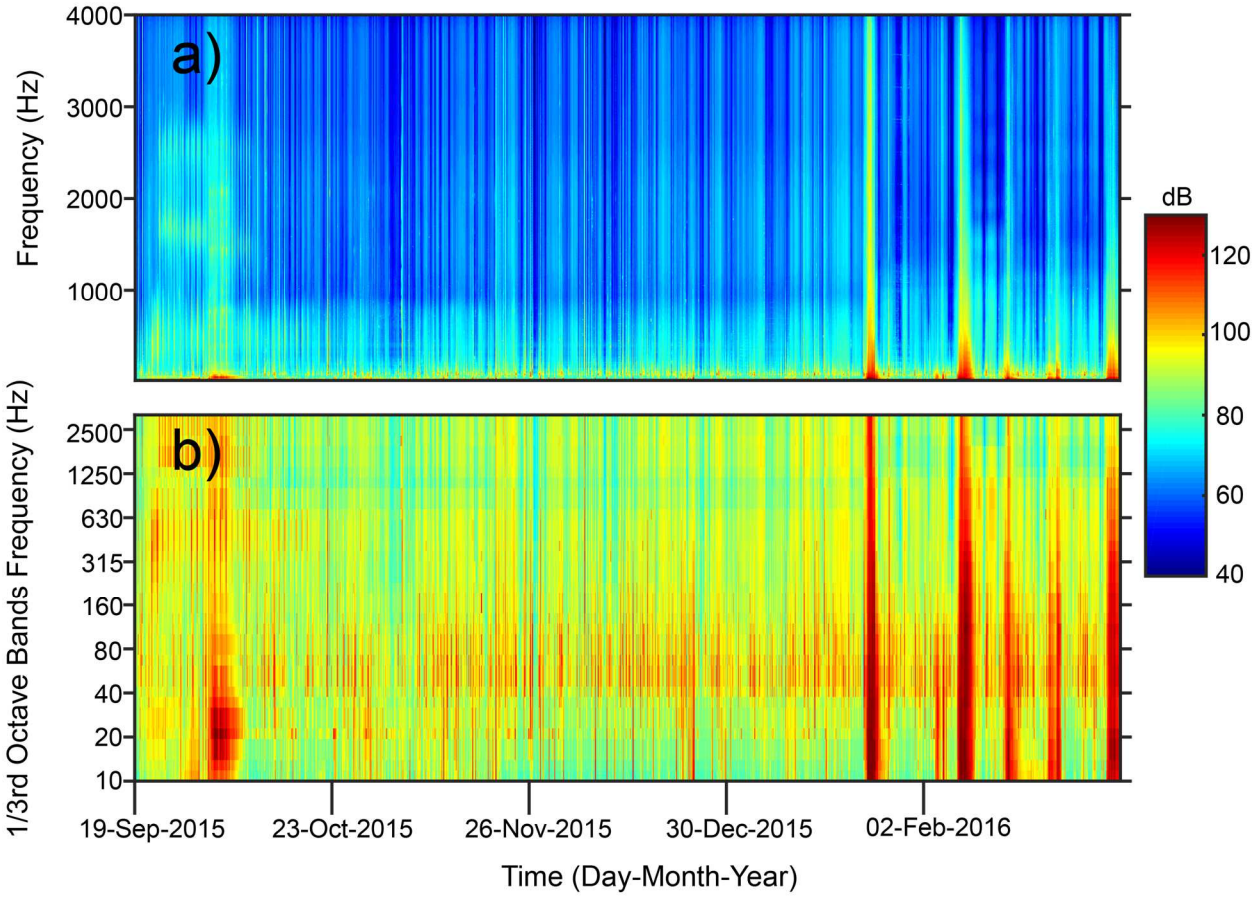

Figure C.14. Deployment 03 (19 Sept 2015 – 27 Feb 2016) long-term spectrograms for AMAR
Panel a represents noise on a linear scale (Δ *time* = 1 h, Δ *frequency* = 1 Hz) along the Y-axis, while panel b represents noise on a 1/3rd octave scale (Δ *time* = 1 h). Dark blue sections indicate time periods with no sound data.

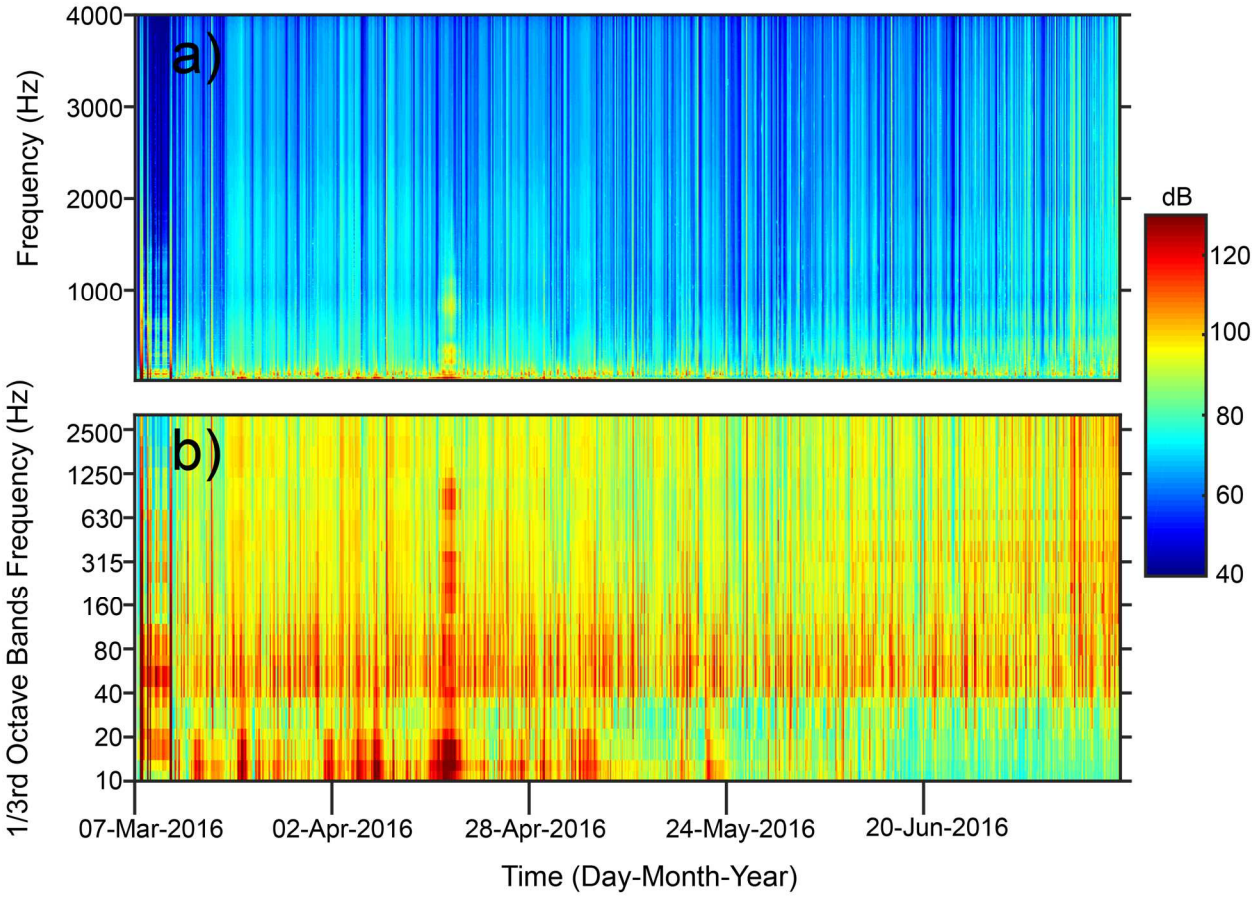

Figure C.15. Deployment 04 (28 Feb 2016 – 26 July 2016) long-term spectrograms for AMAR
Panel a represents noise on a linear scale (Δ *time* = 1 h, Δ *frequency* = 1 Hz) along the Y-axis, while panel b represents noise on a 1/3rd octave scale (Δ *time* = 1 h). Dark blue sections indicate time periods with no sound data.

Department of the Interior (DOI)

The Department of the Interior protects and manages the Nation's natural resources and cultural heritage; provides scientific and other information about those resources; and honors the Nation's trust responsibilities or special commitments to American Indians, Alaska Natives, and affiliated island communities.

BOEM
Bureau of Ocean Energy Management

Bureau of Ocean Energy Management (BOEM)

The mission of the Bureau of Ocean Energy Management is to manage development of U.S. Outer Continental Shelf energy and mineral resources in an environmentally and economically responsible way.

BOEM Environmental Studies Program

The mission of the Environmental Studies Program is to provide the information needed to predict, assess, and manage impacts from offshore energy and marine mineral exploration, development, and production activities on human, marine, and coastal environments. The proposal, selection, research, review, collaboration, production, and dissemination of each of BOEM's Environmental Studies follows the DOI Code of Scientific and Scholarly Conduct, in support of a culture of scientific and professional integrity, as set out in the DOI Departmental Manual (305 DM 3).